



BRNO UNIVERSITY OF TECHNOLOGY

VYSOKÉ UČENÍ TECHNICKÉ V BRNĚ

FACULTY OF CIVIL ENGINEERING

FAKULTA STAVEBNÍ

INSTITUTE OF STRUCTURAL MECHANICS

ÚSTAV STAVEBNÍ MECHANIKY

**SURROGATE MODELLING AND SAFETY
FORMATS IN PROBABILISTIC ANALYSIS OF
STRUCTURES**

VYUŽITÍ NÁHRADNÍ PLOCHY ODEZVY A FORMÁTŮ BEZPEČNOSTI V
PRAVDĚPODOBNOSTNÍ ANALÝZE KONSTRUKCÍ

DOCTORAL THESIS

DISERTAČNÍ PRÁCE

AUTHOR

AUTOR PRÁCE

Ing. Lukáš Novák

SUPERVISOR

VEDOUCÍ PRÁCE

prof. Ing. DRAHOMÍR NOVÁK, DrSc.

BRNO 2021

ABSTRACT

The presented doctoral thesis is focused on the development of theoretical methods for probabilistic design and assessment of structures. In order to reduce the computational burden of the probabilistic approach, the developed methods are based on surrogate models. Specifically, Taylor series expansion has been utilized for the derivation of a novel analytical method for a simplified semi-probabilistic design of structures represented by non-linear finite element models. The novel approach estimates a variance of quantity of interest and the influence of correlation among input random variables. The second part of the doctoral thesis aims at the development of efficient numerical algorithms for the construction of a surrogate model based on polynomial chaos expansion and its utilization for uncertainty quantification. Although the proposed algorithm is based on cutting edge techniques, it was beneficial to improve its accuracy and efficiency by advanced statistical sampling. Therefore, a novel technique for adaptive sequential statistical sampling, reflecting the exploration of the design domain, and exploitation of the surrogate model, is proposed specifically for polynomial chaos expansion.

KEYWORDS

Uncertainty quantification, semi-probabilistic approach, surrogate model, polynomial chaos expansion, Taylor series expansion.

ABSTRAKT

Předložená disertační práce je zaměřena na vývoj teoretických metod pro pravděpodobnostní návrh a posouzení konstrukcí. Za účelem snížení výpočetní náročnosti pravděpodobnostního přístupu jsou vytvořené metody založené na technikách náhradní plochy odezvy. Konkrétně byl využit Taylorův rozvoj k odvození originální analytické metody pro zjednodušený polo-pravděpodobnostní návrh a posouzení konstrukcí reprezentovaných nelineárním konečněprvkostním modelem. Nově navržený přístup je zaměřen na odhad rozptylu zájmové veličiny a vliv korelace mezi vstupními náhodnými veličinami. Druhá část disertační práce se zabývá vývojem efektivních numerických algoritmů pro tvorbu plochy odezvy založenou na rozvoji polynomiálního chaosu a její využití pro kvantifikaci nejistot. Ačkoli je představený algoritmus založen na aktuálních pokročilých technikách, bylo vhodné zvýšit jeho efektivitu také pokročilým statistickým vzorkováním. Tudíž byla konkrétně pro PCE vyvinuta technika adaptivního sekvenčního vzorkování, která zohledňuje jak průzkum návrhové domény, tak i využití informace o náhradní ploše odezvy.

KLÍČOVÁ SLOVA

Kvantifikace nejistot, polo-pravděpodobnostní přístup, náhradní plocha odezvy, rozvoj polynomiálního chaosu, Taylorův rozvoj.

NOVÁK, Lukáš. *Effective Probabilistic Design of Concrete Structures Using Safety Formats and Response Surface Methods*. Brno, 2021, 129 p. Doctoral thesis. Brno University of Technology, Faculty of Civil Engineering, Institute of Structural Mechanics. Advised by prof. Ing. Drahomír Novák, DrSc.

Copyright © 2021 Lukáš Novák. All rights reserved.

Institute of Structural Mechanics
Faculty of Civil Engineering
Brno University of Technology

Typeset by L^AT_EX

DECLARATION

I declare that I have written the Doctoral Thesis titled “Effective Probabilistic Design of Concrete Structures Using Safety Formats and Response Surface Methods” independently, under the guidance of the advisor and using exclusively the technical references and other sources of information cited in the thesis and listed in the comprehensive bibliography at the end of the thesis.

As the author I furthermore declare that, with respect to the creation of this Doctoral Thesis, I have not infringed any copyright or violated anyone’s personal and/or ownership rights. In this context, I am fully aware of the consequences of breaking Regulation § 11 of the Copyright Act No. 121/2000 Coll. of the Czech Republic, as amended, and of any breach of rights related to intellectual property or introduced within amendments to relevant Acts such as the Intellectual Property Act or the Criminal Code, Act No. 40/2009 Coll., Section 2, Head VI, Part 4.

Brno

.....

author’s signature

ACKNOWLEDGEMENT

First and foremost, I would like to express my deepest gratitude to my supervisor prof. Ing. Drahomír Novák, DrSc. This thesis would not exist without his professional guidance and relaxed, thoughtful insight. During our close and long lasting cooperation, he has always encouraged me to express and pursuit my own ideas. I could not have imagined having a better advisor and mentor.

I am also very grateful to the researchers of the Institute of Structural Mechanics. I especially appreciate our enthusiastic discussions with prof. Ing. Miroslav Vořechovský, Ph.D, about various aspects of structural reliability. I would also like to thank to my colleagues Petr Miarka and Lixia Pan with whom I shared the office and who always had time to chat during our coffee breaks.

My heartfelt gratitude goes to my family. I sincerely thank my parents for all the opportunities they gave me. This journey would not have been possible without their unconditional love and support. I also thank my brother for his great humour and levity, helping me to relieve stress. Finally, I wish to thank my wife Michaela for her continued and unfailing love, support and understanding during my pursuit of the Ph.D. degree. The last word goes to my son, Adam, who has been giving me unlimited happiness for the last four months. This thesis is dedicated to my family.

Brno

.....

author's signature

Contents

Motivation	8
1 Introduction	11
1.1 Semi-Probabilistic Approach and Safety Formats	12
1.2 Polynomial Chaos Expansion	16
2 Discussion and Further Work	20
3 Concluding Remarks	23
Bibliography	25
List of appendices	27
A Polynomial Chaos Expansion for Surrogate Modelling: Theory and Software	28
A.1 Description	28
A.2 Role of the Ph.D. Candidate	28
B On Taylor Series Expansion for Statistical Moments of Functions of Correlated Random Variables	35
B.1 Description	35
B.2 Role of the Ph.D. Candidate	35
C Neural network Ensemble-based Sensitivity Analysis in Structural Engineering: Comparison of Selected Methods and the Influence of Statistical Correlation	50
C.1 Description	50
C.2 Role of the Ph.D. Candidate	50
D Stochastic Modelling and Assessment of Long-span Precast Prestressed Concrete Elements Failing in Shear	70
D.1 Description	70
D.2 Role of the Ph.D. Candidate	70
E Estimation of Coefficient of Variation for Structural Analysis: The Correlation Interval Approach	87
E.1 Description	87
E.2 Role of the Ph.D. Candidate	87

F Variance-based Adaptive Sequential Sampling for Polynomial Chaos	
Expansion	99
F.1 Description	99
F.2 Role of the Ph.D. Candidate	99
Curriculum vitæ	126

Motivation

Uncertainties appear everywhere! When using a mathematical model, careful attention must be given to uncertainties in the model.

— Richard Feynman

The development of computational methods for civil engineering has become more important than ever, since it is often necessary to employ advanced numerical methods for the design of new structures in order to fulfil the significantly increasing economical and safety requirements in the last decades. Moreover, there are a lot of structures, especially bridges, built in the last century, which must often be enhanced for higher loads assuming actual conditions of the structures. As a result of these industrial needs, researchers and civil engineers are more interested in advanced numerical methods to solve the mathematical models of structures – typically non-linear finite element method (NLFEM). Although NLFEM is a very accurate numerical method for solving differential equations, there is still a lack of knowledge of material characteristics (e.g. fracture energy), actual geometrical properties (e.g. position of reinforcement) and even mathematical models of some physical phenomena (e.g. fracture mechanics of quasi-brittle materials) collectively called uncertainties. As can be seen from the given examples, uncertainties play an important role, especially in the case of concrete structures. This lack of knowledge may generally lead to inaccurate results and even fatal failures despite the advanced numerical analysis performed by NLFEM. In modern structural analysis, uncertainties are represented by random variables or vectors described by specific probability distribution, the structural system can then be seen as a mathematical function of a set of random parameters. Deterministic numerical analysis of structures must thus be enriched by stochastic analysis.

The elementary task of stochastic analysis is to propagate uncertainties through a mathematical model in order to obtain statistical and/or sensitivity information of outputs [1]. Such process is often called uncertainty quantification (UQ) and is schematically depicted in Fig. 1. UQ progressively grew to a mature general scientific area connecting engineers and mathematicians, since it represents a broad topic focused on practical stochastic analysis employed in almost every branch of engineering and science [2]. The necessity and popularity of UQ is clearly visible from the exponentially growing number of published journal papers in this field.

Nevertheless, the designer's greatest interest is structural reliability, which is assessed through the calculation of the probability of structural failure. The concept of failure probability was already implemented into the general design standards for structures, Eurocode 1990 [3], by semi-probabilistic approach. Instead of failure

probability, semi-probabilistic approach is focused on the estimation of design values of load effect and structural resistance, which satisfy the given safety requirements (target failure probability) assuming that both variables are independent and separated. Design values correspond to a specific quantile of probability distribution and thus it is necessary to utilize UQ methods for its identification.

The only generally applicable method for UQ is a Monte Carlo (MC) type sampling, which is based on a large number of deterministic simulations with randomly generated realizations of the input random vector according to its probability distribution. Unfortunately, it is not feasible in practical applications solved by NLFEM, since each calculation is highly computationally demanding, and MC typically works with millions of realizations. Naturally, it is possible to reduce the number of calculations by an assumption of several simplifications and the derivation of simplified formulas generally called safety formats. However, there is still a gap between a general MC analysis and significantly simplified approaches, which could lead to unrealistic results, especially in combination with NLFEM. This thesis is focused on the development of methods preserving a balance between accuracy and efficiency. Specifically, the task of the thesis is the development of methods based on surrogate models (in the context of structural reliability called response surface methods) for practical design, and the assessment of structures taking uncertainties into account.

Although there are many types of surrogate models, it is beneficial to use the techniques allowing for analytical statistical analysis of approximated quantity of interest (QoI). The obtained statistical information can be further utilized for semi-probabilistic design and the assessment of structures, or the surrogate model can be used for direct numerical integration. On the one hand, the classical technique utilized for derivation of simplifying formulas in codes is Taylor Series Expansion (TSE), which has been commonly used in engineering for decades. On the other hand, the advanced surrogate model in a form of Polynomial Chaos Expansion (PCE) has been getting a growing attention in the recent years. Both techniques can be used for a powerful analytical analysis of QoI resulting in statistical moments and

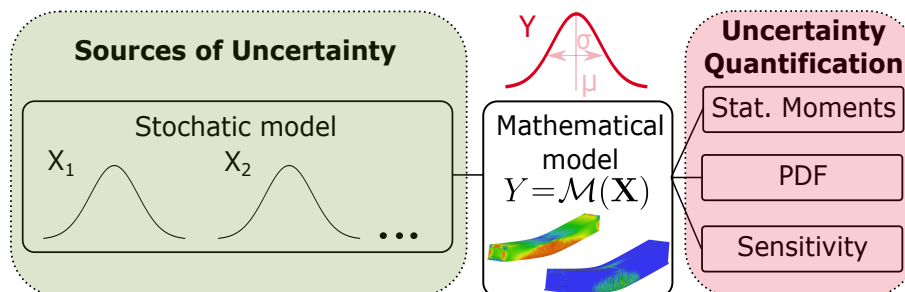


Fig. 1: The uncertainty quantification of a given mathematical model.

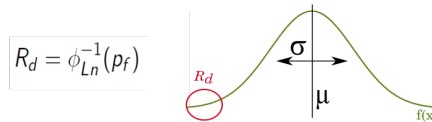
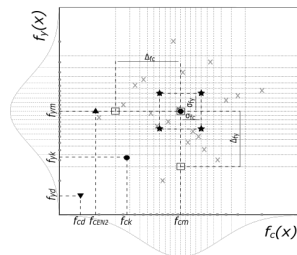
sensitivity indices. The main goal of this thesis is thus a development of theoretical methods based on the mentioned surrogate models – simplified analytical formulas derived from TSE applied in semi-probabilistic approach and efficient algorithms created specifically for PCE, which can be further used for direct MC simulation.

Aims and Objectives

The presented motivation is graphically interpreted together with aims and objectives in the following figures, which clearly divide the solution of the defined problem into two areas: simplified semi-probabilistic methods based on a limited number of samples and a development of a novel technique based on TSE, which can be employed in common applications; and advanced surrogate modeling utilizing PCE for more complicated examples (multiple failure modes, significant non-linearity etc.), optimization, or comprehensive stochastic analysis. The following aims and objectives were identified:

- Development of analytical ECoV method based on TSE:
 - review of existing methods and their comparison;
 - adaptation of TSE for civil engineering;
 - simplification of TSE in order to develop an analytical ECoV method.

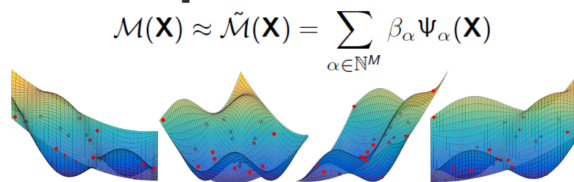
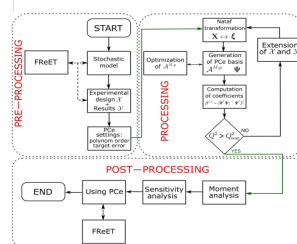
Semi-probabilistic approach Section 1.1



Negligible number of simulations
 Estimation of statistical moments
 Simplifying assumptions

- Development of efficient numerical algorithms for PCE:
 - construction of an efficient algorithm for the construction of PCE;
 - comparison with other existing surrogate models;
 - development of an innovative sampling scheme for PCE.

Polynomial Chaos Expansion Section 1.2



Negligible comp. req. per simulation
 Complex and robust analysis

1 Introduction

Assuming a probability space $(\Omega, \mathcal{F}, \mathcal{P})$ where Ω is an event space, \mathcal{F} is a σ -algebra on Ω (collection of subsets closed under complementation and countable unions) and \mathcal{P} is a probability measure on \mathcal{F} . If the input variable of a computationally demanding mathematical model representing a physical system, $Y = \mathcal{M}(X)$, is a random variable $X(\omega), \omega \in \Omega$, output QoI $Y(\omega)$ is also a random variable. Therefore, the deterministic analysis of $\mathcal{M}(X)$ is extended to stochastic analysis, which typically consists of an estimation of statistical moments, estimation of a probability distribution, sensitivity analysis, and ultimately reliability analysis. Note that, the input of a mathematical model is typically represented by a random vector \mathbf{X} consisting of M marginal random variables and described by a joint probability distribution function $p_{\mathbf{X}}$.

The reliability analysis represents a topic of great interest in engineering, and it is focused on the estimation of the safety margin Z given as a difference between structural resistance R and action effect E . The probability of a negative safety margin – probability of failure $p_f = P(Z < 0)$, is used in reliability analysis to prove the safety of structures. Nevertheless, the direct analytical calculation of the p_f is very complicated or impossible in most cases, thus the MC-type simulation techniques should be employed. MC techniques transform the stochastic problem into a set of deterministic calculations with randomly generated input variables according to their probability distribution law.

Although MC type techniques are the only generally usable tools for reliability problems, the main disadvantage of an MC simulation is the necessity of a large number of simulations to determine a low probability of failure. Moreover, civil engineering is a specific area with very low target p_f around 10^{-6} (depending on specific category of structure) and the fact that in practical applications, the accurate, but highly time-consuming, non-linear finite element analysis (NLFEM) is often employed nowadays. As a result, it is possible to conclude that it is not feasible to employ MC-type techniques for the practical design and assessment of structures. The solution of the defined problem can be, on one hand, an approximation of an original mathematical model by explicit function (typically called surrogate model in the context of UQ), which can be utilized for reliability analysis, or on the other hand, a reduction of the number of simulations as much as possible in simplified safety formats based on semi-probabilistic approach focused on the estimation of coefficient of variation (ECoV) as described in the following paragraphs.

1.1 Semi-Probabilistic Approach and Safety Formats

Semi-probabilistic methods were developed as a simplification of mathematical reliability methods, where R and E are separated and design values of structural resistance R_d and action effect E_d (satisfying the given safety requirements) are determined instead of the direct calculation of the failure probability p_f . The safety check is thus reformulated to a simple form $R_d \geq E_d$ often utilized in normative documents. The following text is focused only on the resistance side, since it represents the main interest of this thesis.

The design value of resistance R_d in Eurocode [3] is completely described by the sensitivity factor derived from First Order Reliability Method (usually simplified by the absolute value of $\alpha_R = 0.8$), the target reliability index β , and finally the first two central statistical moments together with the assumption of lognormal probability distribution of R . Obviously, for the determination of a design value by semi-probabilistic approach, it is crucial to correctly estimate the first two central statistical moments. In the context of semi-probabilistic approach, several methods were developed or adapted for this task: numerical quadrature [4, 5], ECoV methods [6, 7] or Latin Hypercube Sampling (LHS) [8, 9]. These methods differ in sampling of random variables, i.e. the number of realizations of input random vector and their positions in a probability space. For the sake of completeness, there are also two methods implemented in Eurocode: Partial Safety Factor (PSF) method generally used for structural design, and global safety factor method for a non-linear analysis of concrete structures according to EN 1992-2 (EN 1992-2). Note that methods implemented in Eurocode need only one calculation of the mathematical model in order to obtain R_d , and thus these methods are not focused on the estimation of statistical moments, but they try to directly estimate the design quantile of resistance. Despite the success of such approach in linear calculations, its utilization in NLFEM is questionable, since calculations with extremely low material characteristics may lead to unrealistic results (PSF), or implicit assumption for the value of CoV of R in set the global safety factor could lead to a significant deviation from the real values (EN 1992-2).

The very first study conducted during the author's Ph.D. research was focused on the semi-probabilistic assessment of precast prestressed concrete roof girders using LHS, which is an MC-type method achieving generally higher accuracy in the estimation of statistical moments. The stochastic analysis consists of sensitivity analysis via Spearman rank order correlation and statistical analysis. Since the stochastic analysis deals with a real structural element, it was also necessary to investigate the role of correlation among input random variables, which were obtained from laboratory experiments. More details can be found in *Stochastic Modelling*

and Assessment of Long-Span Precast Prestressed Concrete Elements Failing in Shear [Appendix D]. The obtained statistical moments were utilized for the determination of R_d by semi-probabilistic approach and compared to normative methods according to Eurocode. From the obtained results, it is clear that semi-probabilistic approach in combination with LHS leads to higher R_d in comparison to the standard approach implemented in Eurocode, and thus the employment of the advanced methods is generally beneficial. Unfortunately, the whole analysis was extremely time-consuming since 100 numerical simulations of NLFEM were performed in order to obtain a reliable estimation of the first two statistical moments, which is significantly limiting for the industrial application of such approach. This complication opens up the question of possibilities for the reduction of the number of numerical simulations maintaining the accuracy of the estimated statistical moments. Although there are several existing methods for simplified estimation of coefficient of variation of structural resistance, they are typically based on a vague theoretical background and cannot incorporate information about correlation structure of input random vector.

In order to derive a simplified method for statistical analysis based on a solid theoretical background, it was necessary to review the classic method for construction of surrogate model – Taylor Series Expansion (TSE). TSE is a very efficient technique widely accepted in civil engineering, since it was used for the derivation of First Order Reliability Method (FORM). Moreover, the significant advantages of TSE are its versatility and adaptivity via arbitrary truncation of infinite series and various schemes for numerical derivation. From a practical point of view, it is worth mentioning that TSE truncated to linear terms offers a simple analytical formula for the estimation of variance based on numerical results of the mathematical model utilized for numerical derivation. One of the possible formulas for numerical derivation was proposed by Schlune et. al [6], where derivatives are approximated by a simple one-sided differencing scheme, and TSE is truncated to linear terms. Despite the simplicity of this particular form of TSE and differencing scheme, this technique achieved interesting results in several numerical studies [10, 11, 12], and thus TSE became a topic of interest for this research. In order to reduce the number of samples as much as possible while maintaining the accuracy of the approximation, several differencing schemes adapted for semi-probabilistic approach were proposed in the paper ***On Taylor Series Expansion for Statistical Moments of Functions of Correlated Random Variables*** [Appendix B]. It is shown in the paper, that the proposed differencing schemes achieve a higher accuracy, especially in the case of correlated input random variables. Moreover, the proposed methodology of three levels of increasing complexity, accuracy, and computational cost can be employed in order to progressively increase the accuracy of TSE. Although the calculations of

the original mathematical model from one level of the methodology are also always used in the following level of the differencing schemes, it is still expensive for industrial applications since it represents general surrogate model without additional simplifying assumptions and thus its computational cost is highly dependent on the size of the stochastic model, i.e. number of input random variables.

The reduction of computational cost of TSE and derivation of simple analytical ECoV method was the last task of this research. The main drawback of TSE is the number of numerical simulations dependent on the size of the stochastic model, which can be circumvented by an additional strong assumption of fully correlated random variables. In this case, it was shown that TSE with simple differencing after Nataf transformation into correlated space coincides with the widely accepted and employed ECoV by Červenka in Gaussian space. Therefore, an identical process can be utilized for the transformation of the advanced differencing schemes in order to obtain analytical formulas for the estimation of mean and variance independent of the size of the stochastic model – Eigen ECoV method. Theoretical derivation and limitations of Eigen ECoV together with numerical examples are presented in *Estimation of Coefficient of Variation for Structural Analysis: The Correlation Interval Approach* [Appendix E]. The proposed Eigen ECoV fills the gap between the existing over-simplified methods implemented in codes commonly employed by civil engineers and the advanced techniques generally used by scientists such as LHS or TSE. It is based on the theoretical background of TSE, but its computational cost is dramatically reduced, thanks to strong assumptions, to 3 simulations (regardless of the size of the stochastic model). Naturally, it is necessary to carefully consider the applicability of these assumptions in industrial applications and their possible impact.

In order to present the synergy of TSE and the Eigen ECoV method, the correlation interval approach was proposed for industrial applications in the recent paper [Appendix E]. The estimated variance of QoI is significantly affected by the correlation among input random variables, though the definition of correlation among material characteristics is still challenging and there are no recommendations in codes. Therefore, it is beneficial to investigate two limit states: uncorrelated random variables and fully correlated random variables. Although both of the limit states are not physically acceptable, they define the interval of variance, which reflects vague or incomplete information about the correlation structure among input random variables. For practical application, it is suggested to start with the case of fully correlated random variables solved by computationally efficient Eigen ECoV, which typically leads to higher variance. If this estimation is too conservative, one should employ TSE for the estimation of variance in the case of uncorrelated random variables. Note that once the TSE is available, it is possible to analytically

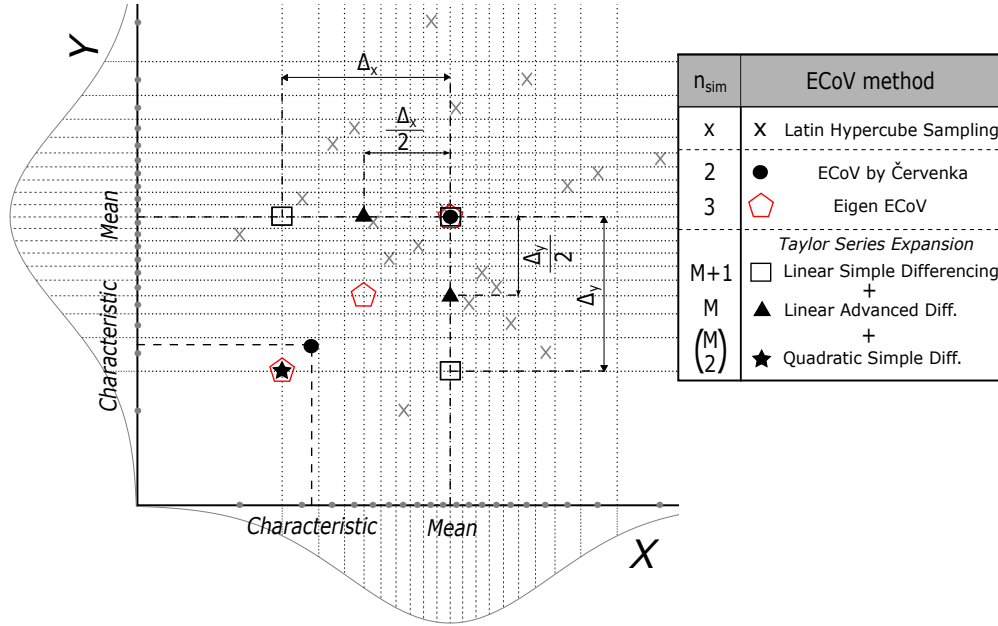


Fig. 1.1: Graphical interpretation of ECoV methods (adapted from Appendix E)

estimate variance for an arbitrary correlation structure, however its construction might bring high computational burden, and Eigen ECoV might then be the only feasible technique leading to a rough estimate on the safe side.

The comparison of the proposed techniques is schematically depicted in Fig.1.1 together with LHS and ECoV by Červenka. Note that the number of simulations for TSE is low in this 2-dimensional example, though it is highly dependent on M in contrast to Eigen ECoV. The illustration clearly presents an advantage of the proposed TSE methodology, that it is possible to progressively enrich the number of simulations in order to construct a more accurate (and expensive) form of TSE using also simulations from the previous level of approximation. Similar characteristic can be also seen in Eigen ECoV, which can be obtained directly from the simulations used by ECoV by Červenka extended by one intermediate simulation.

The SEMIP software

The proposed Eigen ECoV and adaptations of TSE were, together with the state-of-the-art methods, implemented into a standalone software tool [13]. SEMIP is created for practical advanced semi-probabilistic design and assessment of structures by ECoV methods together with normative methods implemented in Eurocode. The software contains three functionalities: the definition of stochastic model from experiments/normative documents, the estimation of coefficient of variation using probabilistic methods, and the graphical comparison of determined R_d obtained by selected techniques.

1.2 Polynomial Chaos Expansion

In the case of a comprehensive stochastic analysis or complicated examples, it is necessary to employ advanced and accurate methods for construction of the surrogate model. Naturally, it is necessary to perform a sufficiently large number of NLFEM calculations in order to obtain sufficient information about the investigated mathematical model. Moreover, a theoretical background of various types of surrogate models is usually complicated and their construction should be performed via efficient numerical algorithms. The combination of the above mentioned aspects clearly shifts the research from the field of structural safety and safety formats to computational sciences and applied mathematics, although such advanced computational methods represent a powerful tool in engineering applications. PCE as a surrogate model has got significant attention among researchers nowadays. Although a general theoretical background of this method (stochastic spectral approach) was proposed by a brilliant mathematician, Norbert Wiener, in 1938 already [14], surrogate model based on this idea was developed 60 years later [15]. Assuming that QoI has a finite variance, PCE represents the Y as a function of another random variable ξ called the germ with known probability distribution function p_ξ . The function is in the form of infinite series of the polynomial chaos expansion consisting of deterministic coefficients and basis functions orthogonal with respect to p_ξ . It is necessary to truncate the infinite series to a final number of terms for practical computation, which can be achieved by various methods. The standard approach is to select only those PCE terms whose total polynomial degree is less or equal than the given value. However, a truncated set of basis functions might be extremely high for practical computation, especially in the case of a large number of input random variables or high maximum total polynomial order, and thus there are methods for further reduction of the number of basis functions typically based on the limitation of interaction terms. This can be justified by the sparsity-of-effects principle, which states that most models describing physical phenomena are dominated by main effects and interactions of low order [16].

From the computational point of view, the calculation of PCE coefficients can be formulated in an intrusive or non-intrusive form. The intrusive approach is not widely used due to its implementation difficulties, since it reformulates the original deterministic model equations to obtain a system of equations for the PCE coefficients of the model outputs. This thesis is thus focused on a non-intrusive approach allowing for the use of third-party software as a black box within involving the calculation of PCE coefficients based on a set of model evaluations. Specifically, the regression-based non-intrusive approach is the main topic of this research, since it can be easily employed for practical UQ involving NLFEM. For the regression-

based non-intrusive PCE, it is also important to employ the best model selection algorithms in order to identify the sparse set of basis functions, which is ideal for the given information matrix and leads to the best possible approximation of the original mathematical model.

As can be seen in the previous paragraphs, there are various approaches in each step of the construction process of sparse PCE, and thus the first study was focused on the comparison of methods for a construction of the truncated set of basis functions and the existing sparsity solvers. The most efficient state-of-the-art methods were utilized for the construction of an efficient and fully automatic algorithm presented in *Polynomial Chaos Expansion for Surrogate Modelling: Theory and Software* [Appendix A]. The proposed algorithm and its later implementation into standalone software [17] can be easily coupled with any third-party software for NLFEM, and it can be employed by users without deep theoretical knowledge of PCE. The combination of the Least Angle Regression for the best model selection, maximal polynomial order adaptivity, and implemented Nataf transformation lead to the best possible approximation of the original mathematical model by PCE for the given experimental design. Thanks to a combination of simplicity for the user and accuracy achieved by advanced numerical methods, the algorithm represents an ideal solution for engineers dealing with UQ of computationally demanding mathematical models. Moreover, once this algorithm was created and validated on analytical examples, it was possible to employ it for further theoretical research and comparison with novel techniques.

The developed PCE algorithm was employed for a comparison with the artificial neural network (ANN), which represents another popular regression-based non-intrusive surrogate model. Although ANN is already well known in computational science, its specific form Neural Network Ensemble (NNE) is a new and promising technique improving the accuracy of ANN by the construction of several surrogates and the combination of their estimations. NNE thus might achieve higher accuracy of an approximation thanks to statistical processing of several single ANNs. The investigation of NNE in the context of sensitivity analysis is presented in *Neural Network Ensemble-based Sensitivity Analysis in Structural Engineering: Comparison of Selected Methods and the Influence of Statistical Correlation* [Appendix C]. The paper is focused on several methods of sensitivity analysis of both the local and global type. The reference solution are Sobol' indices and their generalization for correlated input random variables, which are obtained by PCE, and the algorithm presented in the previous paragraph. The PCE was employed since the orthogonality of basis functions allows for powerful and efficient post-processing. Once a PCE is created, it is possible to obtain statistical moments of function and Sobol' indices without any additional computational

demands. From the obtained results, it is clear that NNE achieves a high accuracy of an approximation (comparable to PCE), and it significantly outperforms a single ANN. However, NNE is still a black-box method, and thus its additional analysis during post-processing is limited, and its error estimation might be complicated.

In contrast to black-box methods, PCE is based on a strong theoretical background, which can be utilized for the derivation of interesting characteristics. Beside the error estimators, statistical moments and Sobol' indices of QoI, one might be interested in the local characteristics of the created PCE. This idea was recently presented in *Variance-Based Adaptive Sequential Sampling for Polynomial Chaos Expansion* [Appendix F] focused on local variance (variance density) of QoI. The idea of this approach is based on the definition of the m th statistical moment:

$$\begin{aligned} \langle y^m \rangle &= \int [\mathcal{M}(X)]^m p_X(x) dx = \int \left[\sum_{\alpha \in \mathbb{N}^M} \beta_\alpha \Psi_\alpha(\xi) \right]^m p_\xi(\xi) d\xi = \\ &= \sum_{\alpha_1 \in \mathbb{N}^M} \dots \sum_{\alpha_m \in \mathbb{N}^M} \beta_{\alpha_1} \dots \beta_{\alpha_m} \int \Psi_{\alpha_1}(\xi) \dots \Psi_{\alpha_m}(\xi) p_\xi(\xi) d\xi \end{aligned}$$

It can be seen in the last part of this formula that in the case of PCE it is necessary to integrate over basis functions Ψ (orthonormal polynomials), which leads to a dramatic simplification in comparison to the integration of $\mathcal{M}(\mathbf{X})$. In the case of variance, one can utilize the orthogonality properties of basis functions and obtain the second raw moment of QoI directly as a sum of squared deterministic coefficients β . However, one can also see this formula as an integration of local contributions to variance, which is called variance density in the paper. Variance density is a very interesting characteristic of the PCE, since it shows the local deviations of the mathematical model from its mean value. Such information can be beneficially incorporated into the criterion defining the best possible location of samples in experimental design based on rationale of Koksma-Hlawka inequality [18].

The proposed Θ criterion for sequential sampling consists of two parts: variance density and geometrical term assuring uniform coverage of the whole design domain. Both these terms taken together lead to an ideal coverage of the design domain with respect to local variance, and thus it leads to a dense sampling in locations with functional extrema. Such approach can be easily coupled with any existing sampling scheme and it leads to a higher accuracy of PCE in comparison to the non-sequential approach. This method represents the main advantage of PCE over ANN or NNE, since the explicit form of PCE allows for analytically deriving important information about the approximation and efficiently using it for further analysis. Moreover, PCE is specifically beneficial for UQ thanks to its basis functions orthogonal with respect to a probability distribution of input random vector, which allows for a simple analytical derivation of stochastic characteristics of QoI.

The PCE-UQ Software

The presented theoretical research was implemented into a standalone software tool for UQ of mathematical models of physical systems. PCE-UQ represents an efficient and easy-to-use tool for surrogate modeling of NLFEM, sensitivity analysis and statistical analysis, and it was already employed in several applications, e.g. [19]. The software can be virtually divided into three parts: pre-processing, processing and post-processing, as can be seen in Fig. 1.2. presenting a flow diagram.

In the *pre-processing* part, the users define the stochastic model of a problem and create an experimental design. This task can be done in cooperation with third party software. The very last step of pre-processing is a determination of the target accuracy of an approximation or maximum order of used polynomials. *Processing* is fully automatic and it contains several crucial steps. The core of processing is based on the iterative best-model selection algorithm based on adaptive polynomial order. Moreover, it is possible to employ the recently proposed sequential sampling. *Post-processing* is designed to be easy to understand and it contains sensitivity analysis of input random variables measured by Sobol indices', and statistical analysis (the first four statistical moments) of QoI. Moreover, it is also possible to use PCE as a computationally efficient approximation of the original mathematical model for additional analysis.

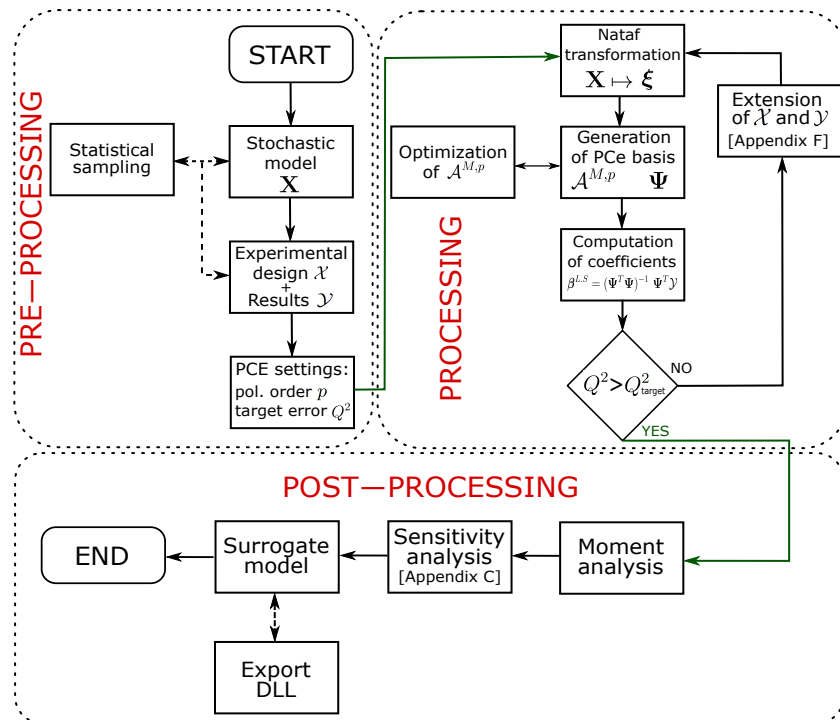


Fig. 1.2: Flow diagram of the PCE-UQ software (adapted from Appendix A)

2 Discussion and Further Work

The main goal of this thesis was the development of the theoretical methods based on surrogate models for probabilistic assessment of structures represented by mathematical models solved by NLFEM. Probabilistic approach is especially important in the case of concrete structures due to significant uncertainties in numerical models, since a concrete represents material with high variability of its material parameters with positive correlation among them, and thus it is necessary to employ advanced methods for UQ. Although it would be ideal to develop a single approach for general employment, the goal was thematically split into two parts, as was already rationalized and described together with the published results in the previous chapter. Surrogate modelling is getting increasing attention among engineers thanks to the exponential growth of computational power enabling calculation of enough samples in experimental design for construction of accurate approximation. The combination of the developed PCE algorithm and the proposed sequential sampling leads to a superior performance and can be easily used in combination with NLFEM. Naturally, the number of simulations must be significantly larger in comparison with ECoV methods, but it still represents highly efficient method for construction of the complete surrogate model, which can be further analyzed instead of original mathematical model. On the other hand, there are still highly computationally demanding industrial applications of NLFEM (complex structures) requiring the reduction of a number of numerical simulations as much as possible and thus Eigen ECoV and TSE should be employed for probabilistic design and assessment in this case.

The significant effort was made in the development of a simple analytical ECoV method, which can be used for practical design and assessment of structures in industrial applications. The estimation of the variance interval is based on adapted TSE and novel Eigen ECoV, proposed together as the correlation interval approach. Both methods are based on several simplifications, and so there are also limitations for their employment. TSE is typically truncated only to linear terms, which might lead to an inaccurate estimation of variance in the case of non-linear functions. Additionally, there is an assumption of fully correlated input random variables in Eigen ECoV, which is not physically correct, but it leads to a dramatic reduction of the number of NLFEM calculations. The justification of both simplifying assumptions can be found in ECoV by Červenka generally accepted in the civil engineering community. As was shown in the original paper [Appendix E], ECoV by Červenka in Gaussian space corresponds to Eigen ECoV based on linear TSE with simple backward differencing, and since this technique achieves satisfactory results in many practical comparative studies [10, 11, 12] and it is already implemented in *fib* Model Code 2010 [20], it is possible to justify the assumed simplifications.

The important question arising for discussion is the ideal step-size parameter used for TSE and Eigen ECoV, since it might significantly affect the accuracy of both methods. There are generally two possibilities: a step-size parameter dependent on the target reliability index, or a fixed step-size parameter. Although a step-size parameter dependent on the target reliability index might achieve a higher accuracy [6], it is computationally inefficient for a simultaneous analysis of several structural limit states. The computational burden is caused by the fact that the original mathematical model must be calculated for each limit state (and thus different target reliability index) separately with different values of input characteristics. Fixed step-size does not bring this additional computational burden and the user can obtain the results for all limit states from a single NLFEM. Moreover, if a fixed step-size parameter is set to $c = 1.645$, it is also beneficial from a practical point of view, since Eigen ECoV is then based on three typical calculations with input characteristics easily obtained from the tables in codes: mean values, characteristic values and intermediate values.

The remaining question is whether the Eigen ECoV can be used in the case of structures with multiple failure modes. From the theoretical point of view, the Eigen ECoV should actually achieve higher accuracy in comparison to the widely employed ECoV by Červenka, since the Eigen ECoV tries to linearize the response surface using three calculations and thus it is not as sensitive to the local extrema as other existing methods (including normative methods). However, this theoretical behaviour must be also verified in numerical examples, which is a task for future research.

The second part of the thesis deals with an efficient construction of surrogate models. The initial stage of the research consisted of the development of the state-of-the-art algorithm for automatic construction of PCE and its comparison with NNE. Although NNE is a very promising technique, it is still a black-box method in contrast to PCE. The advantage of explicit approximation and known theoretical characteristics of PCE was fully utilized in the final part of the research focused on the development of an innovative sequential sampling scheme created specifically for PCE.

Although the proposed criterion for sequential sampling can be coupled with any non-sequential sampling, it is clear from the obtained results that the final accuracy of PCE is highly dependent on the selected non-sequential technique, and thus this choice should be made carefully. Although the proposed sequential sampling leads to a significantly higher accuracy of PCE based on Latin Hypercube Sampling and Coherence D-optimal sampling, there is a potential of improvement by the employment of advanced sampling schemes generated from the target distribution that additionally avoids clustering or empty regions while maintaining true statistical

homogeneity via periodic distance-based criteria [21]. The significant drawback of the proposed sampling technique is its performance based on the size of the pool of candidates generated by arbitrary non-sequential sampling. It was shown that the related aspect is a maximum polynomial order of PCE, which might be the limiting aspect of the proposed approach, and thus further studies should work with the adaptive value as was shown in the first numerical example in [Appendix F]. However, the adaptivity of maximum polynomial order brings additional computational burden and non-trivial techniques might be necessary for the construction of the pool of candidates in the case of coherence D-optimal sampling. Further work will thus be focused on the comparison of the proposed sequential sampling coupled with advanced sampling schemes involving adaptive techniques such as adaptive coherence D-optimal sampling and induced sampling.

The utilization of a high polynomial degree could also be circumvented by a different philosophy: the division of the design domain into small sub-spaces approximated by low-order PCEs. Such algorithm could also be based on the identical Θ criterion, though for a different purpose. In this case, the suitable criterion is used for the detection of the most important strata associated with high local variance. The identified strata are further divided into smaller parts, and local PCE approximation is created for each of them. In order to achieve an approximation with continuous derivatives on boundaries of adjoining sub-spaces, it is also necessary to use interpolating PCE instead of regression-based PCE.

Although the theoretical development of the proposed methods was successful and they can be immediately employed for practical design or assessment of structures, these novel techniques also bring new challenges and reveal new research topics. Based on the presented discussion of the obtained results, the following specific tasks will be investigated in future research:

- a comparison of selected ECoV methods with TSE and Eigen ECoV in various practical examples represented by NLFEM including structures with multiple failure modes;
- a numerical study of the influence of the step-size parameter on accuracy of TSE and Eigen ECoV;
- an extensive numerical study focused on the combination of the proposed sequential sampling for PCE with advanced sampling schemes;
- a development of sequential sampling for local PCEs based on the division of the design domain into sub-spaces and the proposed Θ criterion.

3 Concluding Remarks

Obviously, the role of UQ is increasingly more important in the process of design and assessment of structures, and thus novel numerical methods for civil engineers should be created. Although the development of such techniques is a broad topic investigated by many researchers, there is still a gap between purely scientific methods and techniques for industrial applications. The results of this thesis have the potential to fill this gap, although the original task was divided into two parts and two separate techniques were investigated. Specifically, this thesis was focused on the development of novel theoretical methods for probabilistic design and assessment of structures via surrogate modeling. For the given task, the following two types of surrogate models were utilized: PCE and TSE, both employed in different contexts and for different types of applications.

The simplified safety formats can be easily used for industrial applications, although they have severe limitations. In order to develop a simple analytical theoretical method, the advanced differencing schemes adapted for civil engineering were proposed in order to create accurate TSE. The proposed advanced differencing schemes for TSE lead to a more accurate, but less efficient approximation of the original mathematical model in the case of functions of correlated input random variables, which is typical for NLFEM of concrete structures. Furthermore, TSE with the proposed differencing schemes was utilized for the development of a novel analytical method called Eigen ECoV, based on the theory of TSE and Nataf transformation. The Eigen ECoV represents the main result of this thesis for industrial applications, and it has the potential to significantly affect the semi-probabilistic design and assessment of structures. TSE and Eigen ECoV together form a correlation interval approach developed for industrial applications with a vague information about correlation structure among input random variables. A lack of knowledge on the joint probability distribution is typical for industrial applications, since only marginal probability distributions are usually known, although it is necessary to define a correlation structure of the input random variables in order to completely describe input random vector [22]. The proposed correlation interval approach might consequently reveal the impact of vague information about a correlation structure.

A complex stochastic analysis is typically based on an MC-type simulation and thus it is necessary to create an accurate surrogate model of the original function. The second part of the research was focused on PCE, which generally represents an efficient surrogate model for UQ. Since the construction of PCE is not simple task and there are various intrusive and non-intrusive approaches, the first step of the research was the construction of an automatic software algorithm based on the most efficient state-of-the-art methods. During the research, an efficient PCE

algorithm was also implemented into a stand-alone software tool. The software is fully automatic and can be generally coupled with any third-party NLFEM software, which allows for its employment by users without deep theoretical knowledge about PCE. The developed algorithm was further employed in comparison with NNE in the context of sensitivity analysis. Although NNE has a high potential for UQ, it is a black-box method, and its post-processing is complicated. On the other hand, the theoretical characteristics of PCE were utilized in the research task focused on the adaptive sequential sampling scheme developed specifically for PCE, which significantly reduces its computational cost. The sampling technique is based on a novel philosophy, which has the potential to affect the whole scientific field of UQ.

The developed theoretical methods are based on cutting-edge techniques of UQ for civil engineering and it can be concluded that all identified aims and objectives of this thesis were met. The developed theoretical methods also represent a significant progress beyond the state-of-the-art techniques and they have the potential to become efficient tools for industrial design and the assessment of structures as well as for further theoretical research in the field of computational science and applied mechanics. However, there still remain some open questions in both research areas briefly discussed in chapter 2 together with the directions of future research. The tasks of further work are clearly identified and ensure the continuity of this research.

As can be seen from the nature of the research topic, it was necessary to divide it into two parts and progressively build the theoretical background of the proposed methods almost independently in both scientific fields. Therefore, it was decided to create this thesis by publication (series of published journal papers), which represents an elegant way for the presentation of the obtained results. To sum up, this thesis consists of six journal papers listed in Tab. 3.1. As can be seen, the quality of the journals, measured by the traditional impact factor (IF) and also the novel article influence score (AIS), is increasing together with the progress of the research. The latest contributions (Appendices E and F) fall into the first decile according to AIS/IF, which confirms the significance of the obtained results.

	A	B	C	D	E	F
Year	2018	2020	2021	2021	2021	2021
IF	0.966	2.645	4.578	4.471	5.047	6.756
AIS	0.179	0.304	1.131	0.927	1.461	1.805
Quartile IF/AIS	Q3/Q4	Q2/Q3	Q1/ D1	Q1/Q1	Q1/ D1	D1/D1
Contribution [%]	90	90	40	30	90	60

Tab. 3.1: Journal metrics of the published papers included in this thesis. Note: the journal metrics from 2020 (latest) are used for the papers C,D,E and F.

Bibliography

- [1] T. J. Sullivan. *Introduction to Uncertainty Quantification*, volume 63. Springer International Publishing, 2015. doi:10.1007/978-3-319-23395-6.
- [2] Ralph C. Smith. *Uncertainty Quantification: Theory, Implementation, and Applications*. Society for Industrial and Applied Mathematics, USA, 2013.
- [3] Comité Européen de Normalisation (CEN), Brussels, Belgium. *EN 1990: Eurocode: Basis of Structural Design*, 2002.
- [4] Emilio Rosenblueth. Point estimates for probability moments. *Proceedings of the National Academy of Sciences*, 72(10):3812–3814, 1975.
- [5] John T. Christian and Gregory B. Baecher. Point-estimate method as numerical quadrature. *Journal of Geotechnical and Geoenvironmental Engineering*, 125(9):779–786, 1999.
- [6] Hendrik Schlune, Mario Plos, and Kent Gylltoft. Safety formats for nonlinear analysis tested on concrete beams subjected to shear forces and bending moments. *Engineering Structures*, 33(8):2350 – 2356, 2011.
- [7] Vladimír Červenka. Global safety format for nonlinear calculation of reinforced concrete. *Beton- und Stahlbetonbau*, 103(S1):37–42, 2008.
- [8] Michael D. McKay. Latin hypercube sampling as a tool in uncertainty analysis of computer models. In *Proceedings of the 24th Conference on Winter Simulation*, WSC '92, pages 557–564, New York, NY, USA, 1992.
- [9] Diego Lorenzo Allaix, Vincenzo Ilario Carbone, and Giuseppe Mancini. Global safety format for non-linear analysis of reinforced concrete structures. *Structural Concrete*, 14(1):29–42, 2013.
- [10] Lukáš Novák, Drahomír Novák, and Radomír Pukl. Probabilistic and semi-probabilistic design of large concrete beams failing in shear. In *Advances in Engineering Materials, Structures and Systems: Innovations, Mechanics and Applications*. Taylor and Francis Group CRC Press, 2019.
- [11] Drahomír Novák, Lukáš Novák, Ondřej Slowik, and Alfred Strauss. Prestressed concrete roof girders: Part III – semi-probabilistic design. In *Proceedings of the Sixth International Symposium on Life-Cycle Civil Engineering (IALCCE 2018)*, pages 510–517. CRC press, Taylor and Francis group, 2018.

- [12] M. Šomodíková, L. Novák, M. Lipowczan, M. Vyhliđal, J. Doležel, D. Lehký, D. Novák, and R. Pukl. Probabilistic analysis and safety formats approaches applied for czech bridge structures under the ATCZ190 SAFEBRIDGE project. In H. Yokota and D.M. Frangopol, editors, *Proceedings of the Tenth International Conference on Bridge Maintenance, Safety and Management (IABMAS 2020)*. CRC Press, June 2020.
- [13] Lukáš Novák and Drahomír Novák. SEMIP, 2020. Software. URL: <https://www.fce.vutbr.cz/STM/novak.l/semip/semip.html>.
- [14] Norbert Wiener. The homogeneous chaos. *American Journal of Mathematics*, 60(4):897–936, 1938. doi:10.2307/2371268.
- [15] Roger G. Ghanem and Pol D. Spanos. *Stochastic Finite Elements: A Spectral Approach*. Springer New York, 1991. doi:10.1007/978-1-4612-3094-6.
- [16] D.C. Montgomery. *Design and Analysis of Experiments*. John Wiley & Sons, 2008.
- [17] Lukáš Novák and Drahomír Novák. PCE-UQ, 2019. Software. URL: <https://www.fce.vutbr.cz/stm/novak.l/pce-uq/pce-uq.html>.
- [18] Michael D. Shields. Adaptive Monte Carlo analysis for strongly nonlinear stochastic systems. *Reliability Engineering & System Safety*, 175:207–224, July 2018. doi:10.1016/j.ress.2018.03.018.
- [19] Lukáš Novák and Drahomír Novák. Surrogate modelling in the stochastic analysis of concrete girders failing in shear. In *Proc. of the Fib Symposium 2019: Concrete - Innovations in Materials, Design and Structures*, pages 1741–1747, 2019.
- [20] fib federation internationale du beton. *fib Model Code for Concrete Structures 2010*. John Wiley & Sons, Berlin, Heidelberg, 2013.
- [21] Miroslav Vořechovský, Jan Mašek, and Jan Eliáš. Distance-based optimal sampling in a hypercube: Analogies to N-body systems. *Advances in Engineering Software*, 137:102709, 2019. doi:10.1016/j.advengsoft.2019.102709.
- [22] Armen Der Kiureghian and Pei-Ling Liu. Structural reliability under incomplete probability information. *Journal of Engineering Mechanics*, 112:85–104, 1986. doi:10.1061/(asce)0733-9399(1986)112:1(85).

List of appendices

A Polynomial Chaos Expansion for Surrogate Modelling: Theory and Software	28
A.1 Description	28
A.2 Role of the Ph.D. Candidate	28
B On Taylor Series Expansion for Statistical Moments of Functions of Correlated Random Variables	35
B.1 Description	35
B.2 Role of the Ph.D. Candidate	35
C Neural network Ensemble-based Sensitivity Analysis in Structural Engineering: Comparison of Selected Methods and the Influence of Statistical Correlation	50
C.1 Description	50
C.2 Role of the Ph.D. Candidate	50
D Stochastic Modelling and Assessment of Long-span Precast Prestressed Concrete Elements Failing in Shear	70
D.1 Description	70
D.2 Role of the Ph.D. Candidate	70
E Estimation of Coefficient of Variation for Structural Analysis: The Correlation Interval Approach	87
E.1 Description	87
E.2 Role of the Ph.D. Candidate	87
F Variance-based Adaptive Sequential Sampling for Polynomial Chaos Expansion	99
F.1 Description	99
F.2 Role of the Ph.D. Candidate	99

A Polynomial Chaos Expansion for Surrogate Modelling: Theory and Software

DOI: 10.1002/best.201800048

A.1 Description

The paper presents a novel algorithm for the construction of surrogate model in the form of Polynomial Chaos Expansion (PCE). Although there has been a significant theoretical development of PCE (especially in the recent decade), it is still challenging for the application in industrial problems. The selected, highly efficient algorithms for each sub-task of PCE construction were coupled in order to achieve the ultimate efficiency and accuracy. The significant advantage of the proposed algorithm is that it is possible to adaptively build PCE without extensive knowledge of the PCE theory. The paper presents an automatic software tool [17], which can be easily employed for uncertainty quantification of structures represented by non-linear finite element models. The developed software tool is directly connected to the commercial software FReET and ATENA Science developed by Červenka Consulting. However, it can be easily connected to any software tool via a specific format of input and output file.

A.2 Role of the Ph.D. Candidate

Percentage of contribution: 90%

Lukáš Novák is the main author of this paper responsible for the concept, the methodology and the numerical results of the presented research. Furthermore, he prepared the original draft of the paper which was later reviewed in cooperation with his supervisor, Drahomír Novák.

Polynomial chaos expansion for surrogate modelling: Theory and software

The paper is focused on the application of a surrogate model to reliability analysis. Despite recent advances in this field, the reliability analysis of complex non-linear finite element models is still highly time-consuming. Thus, the approximation of the non-linear finite element model by a surrogate meta-model is often the only choice if one wishes to perform a sufficient amount of simulations to enable reliability analysis. First, the basic theory of polynomial chaos expansion (PCE) is described, including the transformation of correlated random variables. The usage of the PCE for the estimation of statistical moments and sensitivity analysis is then presented. It can be done efficiently via the post-processing of the employed surrogate model in explicit form without any additional computational demands. The possibility of utilizing the adaptive algorithm Least Angle Regression is also discussed. The implementation of the discussed theory into a software tool, and its application, are presented in the last part of the paper.

1 Introduction

The mathematical model of a physical problem is represented by a function of a set of input variables $M(\mathbf{X})$. In practical applications, this function is often described in implicit form and solved via the non-linear finite element method (NLFEM), which is a very accurate method of solving mathematical models. However, to obtain realistic results, it is necessary to consider random input variables described by probability distribution functions as well. The combination of structural reliability methods and NLFEM is highly time-consuming, especially in the case of large mathematical models with many random input variables. One of the methods of reducing computational requirements is the approximation of NLFEM by an explicit function – a surrogate model. There are several types of surrogate models described in scientific papers which are used to solve practical problems: Polynomial chaos expansion, kriging, support vector machine and artificial neural networks. However, generally speaking the main steps are almost the same for all the methods.

First, several repetitive calculations of the original mathematical model are performed for the set of sample points, which is called the experimental design (ED). These points are usually generated by Monte Carlo type simulation techniques. Herein, the variance reduction method Latin Hypercube Sampling (LHS) [1] was used because the initial set of sample points should provide uniform coverage over the input space \mathbf{X} . A graphical interpretation of LHS can be seen in Fig. 1. The value of the

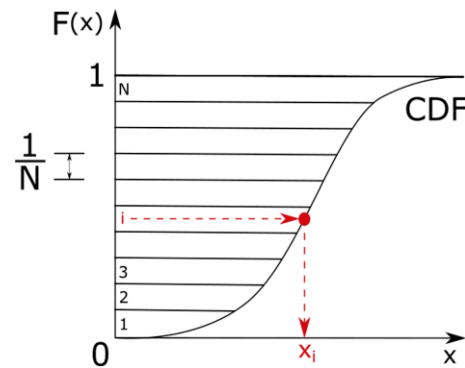


Fig. 1 Latin Hypercube Sampling methodology

i -th realization of random variable x_i is obtained from the cumulative distribution function (CDF) $F(x)$ of the input variable, which is divided into N intervals, where N is the number of simulations. Every value is chosen within each interval. There are several ways to choose probability in the interval: mean value/median of interval or random value. Once the realizations are chosen, random permutation is performed. The results of the simulations are used as a training set for the creation of an approximation function. The last and most important step is the estimation of the approximation error, which can be done by various methods, e.g. coefficient of determination or cross validation. The paper describes the surrogate model based on polynomial chaos expansion (PCE) [2].

2 PCE methodology

Assume a probability space $(\Omega, \mathcal{F}, \mathcal{P})$, where Ω is an event space, \mathcal{F} is a σ -algebra on Ω and \mathcal{P} is a probability measure on \mathcal{F} . If the input vector of mathematical model is random vector $\mathbf{X}(\omega)$, $\omega \in \Omega$, then random model response $Y(\omega)$ is a random variable. Considering $Y = \mathcal{M}(\mathbf{X})$ has the finite variance σ^2 , the polynomial chaos expansion according to SOIZE and GHANEM [3] is the following:

$$Y = \mathcal{M}(\mathbf{X}) = \sum_{\alpha \in \mathbb{N}^M} \beta_{\alpha} \psi_{\alpha}(\mathbf{X}) \quad (1)$$

where M is the number of input random variables, β_{α} are unknown deterministic coefficients and Ψ_{α} are multivariate basis functions orthonormal with respect to the joint probability density function of \mathbf{X} . Standard normal input variables ξ are assumed herein, thus normalized Hermite polynomials orthogonal with respect to the standard normal probability density function $f(x)$ (PDF) are used as

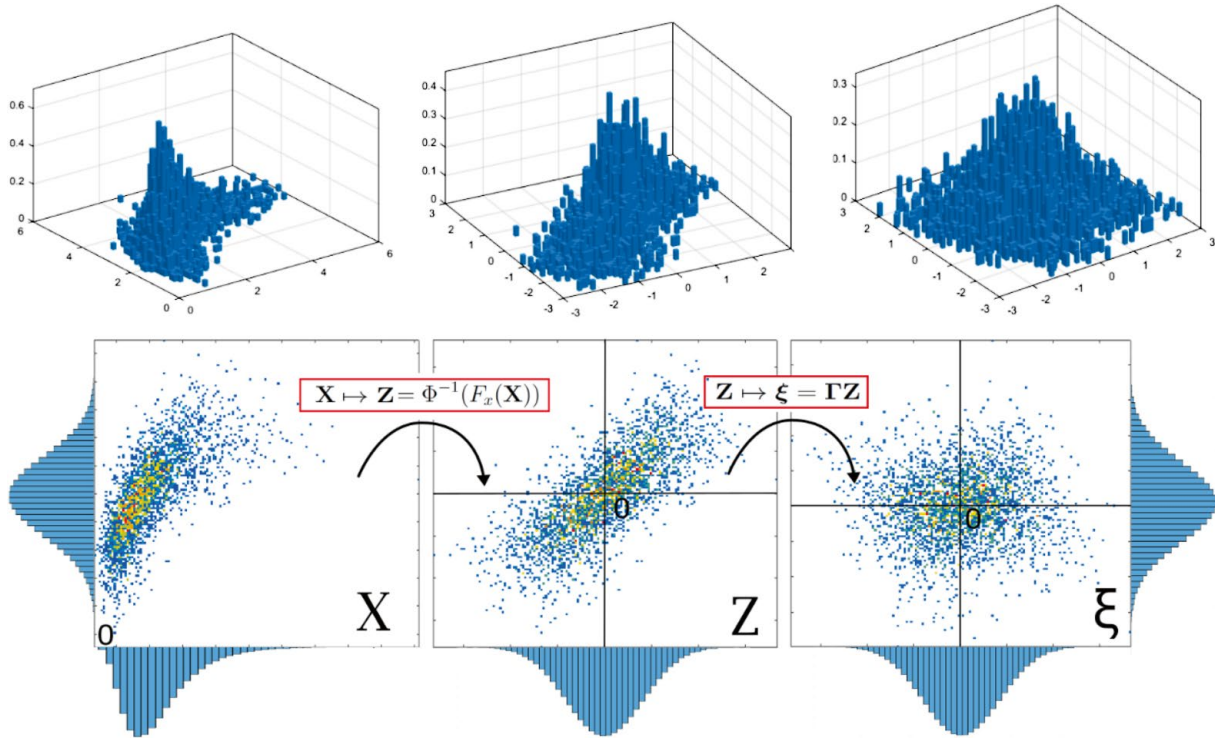


Fig. 2 Illustration of a Nataf transformation from original space X to uncorrelated standard normal space Z for a 2 dimensional case

basis functions. In the case of non-Gaussian or correlated input random variables, the Nataf transformation must be performed, Fig. 2. This approach is usually called the Wiener-Hermite polynomial chaos expansion. Alternatively, it is possible to use the Wiener-Askey generalized PCE, where different polynomials related to the PDF should be used according to the Wiener-Askey scheme [4] e.g. Legendre polynomials for uniform variables over $[-1,1]$.

2.1 Transformation of random variables

A standard iso-probabilistic transformation to uncorrelated standard normal space ξ can be used in the case of uncorrelated non-normal input variables as follows:

$$\xi = \Phi^{-1}(F_x(\mathbf{X})) \quad (2)$$

where Φ^{-1} is the inverse CDF of standard normal distribution. In the general case of non-normal correlated random variables, it is necessary to use more complicated transformation methods, e.g. Rosenblatt transformation [5].

The special case of Rosenblatt transformation with a normal copula is also known as Nataf transformation [6], which is usually utilized in reliability applications. Transformation to ξ space is composed of three steps:

$$\xi = T_{Nataf}(\mathbf{X}) = T_3 \cdot T_2 \cdot T_1(\mathbf{X}) \quad (3)$$

The first two steps represent iso-probabilistic transformation to standard normal space Z according to Eq. 2, i.e.:

$$T_1: \mathbf{X} \rightarrow \mathbf{W} = F_x(\mathbf{X}) \quad (4)$$

$$T_2: \mathbf{W} \rightarrow \mathbf{Z} = \Phi^{-1}(\mathbf{W}) \quad (5)$$

The last step contains a transformation to space ξ . For this procedure, Cholesky decomposition of the fictive correlation matrix R_Z must be performed:

$$R_Z = LL^T \quad (6)$$

where L is the lower triangular matrix and $L^{-1} = \Gamma$. The transformation is then defined by:

$$T_3: \mathbf{Z} \rightarrow \xi = \Gamma \mathbf{Z} \quad (7)$$

The critical task for Nataf transformation is finding the fictive correlation matrix R_Z . The following equation can be used to determine the fictive correlation coefficient $r_{z_{ij}}$ between two random variables:

$$r_{i,j} = \frac{1}{\sigma_i \sigma_j} \iint_{R^2} \left\{ \left(F_i^{-1}(\Phi(Z_i)) - \mu_i \right) \left(F_j^{-1}(\Phi(Z_j)) - \mu_j \right) \right\} dZ_i dZ_j \quad (8)$$

where μ is the mean and φ_2 is the bivariate standard normal PDF:

$$\varphi_2(Z_i, Z_j, r_{z_{i,j}}) = \frac{1}{2\pi\sqrt{1-r_{z_{i,j}}^2}} \exp\left(-\frac{Z_i^2 - 2r_{z_{i,j}}Z_iZ_j + Z_j^2}{2(1-r_{z_{i,j}}^2)}\right) \quad (9)$$

Note that Nataf transformation is not feasible for some marginal distributions and correlation matrices due to the Gaussian copula hypothesis [7].

2.2 Truncation of the PCE

The quantity of terms in the PCE is generally large and must be truncated to a finite number P for practical computation. Usually, terms whose total degree $|\alpha|$ is equal to or less than the given p are used, i.e. a truncated set of PCE terms dependent on the size of the stochastic model n is:

$$\mathcal{A}^{M,p} = \left\{ \alpha \in \mathbb{N}^M : |\alpha| = \sum_{i=1}^M \alpha_i \leq p \right\} \quad (10)$$

The cardinality of the truncated set is given by the number of permutations:

$$\text{card } \mathcal{A}^{M,p} \equiv P = \binom{M+p}{p} = \frac{(M+p)!}{M!p!} \quad (11)$$

The number of terms P , thus the size of the experimental design, is strongly dependent on the number of stochastic input variables. In the case of a large stochastic model, the advanced selection algorithm Least Angle Regression should be utilized in order to find the optimal set of PCE terms [8].

2.3 Estimation of PCE coefficients

There is an error ε due to missing terms in the definition of the truncated PCE:

$$Y = \mathcal{M}(\mathbf{X}) = \sum_{\alpha \in \mathcal{A}^{M,p}} \beta_\alpha \Psi_\alpha(\xi) + \varepsilon \quad (12)$$

The deterministic coefficients β_α are obtained by minimization of the ε . Herein, least-square regression (LSR) is utilized for the estimation of PCE coefficients. Thus, a sufficient amount of original mathematical model $\mathcal{M}(\mathbf{X})$ evaluations for sample points in experimental design \mathcal{X} are performed and the results are represented by vector \mathcal{Y} . The estimated coefficients $\hat{\beta}$ are obtained by minimizing L_2 -norm:

$$\hat{\beta} = \arg \min \frac{1}{N} \sum_{i=1}^N \left(\beta^T \Psi(\xi^i) - \mathcal{M}(x^i) \right)^2 \quad (13)$$

The solution of Eq. 13 is defined by:

$$\hat{\beta} = (\Psi^T \Psi)^{-1} \Psi^T \mathcal{Y} \quad (14)$$

where data matrix Ψ is:

$$\Psi = \left\{ \Psi_{i,j} = \Psi_j(\xi^i), i = 1, \dots, M; j = 0, \dots, P-1 \right\} \quad (15)$$

The information matrix $\Psi^T \Psi$ may be ill-conditioned in practical computation, thus singular value decomposition (SVD) or QR decomposition should be utilized in the algorithm, and the minimum size of the experimental design should be $2P$.

The approximation function in explicit form is fully defined after the estimation of deterministic coefficients, and it is not highly computationally demanding to perform reliability analysis. This approach is generally called response surface methodology.

2.4 Validation of the PCE

The crucial step in response surface methodology is the validation of the approximation. For this purpose, various methods have been developed. In general, the coefficient of determination R^2 between the original \mathcal{M} and the approximation \mathcal{M}^{PCE} is commonly used:

$$R^2 = 1 - \frac{\frac{1}{N} \sum (\mathcal{M}(\mathbf{x}) - \mathcal{M}^{PCE}(\mathbf{x}))^2}{\sigma_y^2} \quad (16)$$

However, R^2 may lead to overfitting in the case of small sample size experimental designs. Thus, more robust leave-one-out cross-validation Q^2 should be used. The core of the method is to use one set of sample points to build a PCE and another set to compute the error. Q^2 sets one point apart from the full ED and builds a PCE from the remaining points. This process is repeated for every point of the experimental design and is time-consuming in the case of a complex computational model. The advantage of the PCE is the possibility of analytical Q^2 determination without any additional computational demand:

$$Q^2 = 1 - \frac{\frac{1}{N} \sum \left(\frac{\mathcal{M}(x^{(i)}) - \mathcal{M}^{PCE}(x^{(i)})}{1 - h_i} \right)^2}{\sigma_y^2} \quad (17)$$

where h_i represents the i -th diagonal term of matrix $\Psi(\Psi^T \Psi)^{-1} \Psi^T$.

2.5 Post-processing of the PCE

Due to the orthonormality of the PCE basis, some information about the mathematical model can be computed just by post-processing the estimated coefficients, specifically the estimation of statistical moments and sensitivity analysis.

Due to the fact that $\Psi_0 \equiv 1$ and $E[\Psi_\alpha(\xi)] = 0 \forall \alpha \neq 0$, the mean value μ and variance σ^2 of the mathematical model can be easily derived:

$$\mu = E[Y^{PCE}] = E \left[\sum_{\alpha \in \mathcal{A}^{M,p}} \beta_\alpha \Psi_\alpha(\xi) \right] = \beta_0 \quad (18)$$

$$\sigma^2 = E \left[(Y^{PCE} - \beta_0)^2 \right] = \sum_{\substack{\alpha \in \mathcal{A}^{M,p} \\ \alpha \neq 0}} \beta_\alpha^2 \quad (19)$$

Variance-based sensitivity analysis can be computed in a similar way; more information can be found in SUDRET [9]. Briefly, Sobol' indices of any order for any variable are determined from deterministic coefficients β without additional computational demand, e.g. the total Sobol' indices are derived as follows:

$$S_i^T = \sum_{\alpha \in \mathcal{A}_i^T} \frac{\beta_\alpha^2}{\sigma^2} \mathcal{A}_i^T = \{\alpha \in \mathbb{N}^M : \alpha_i > 0\} \quad (20)$$

A generalization of variance-based sensitivity analysis called analysis of covariance for correlated variables can be found in [10].

3 PCE: Software

The presented PCE theory was implemented into a standalone software tool that cooperates with FReET (Feasible Reliability Engineering Tool), which is multi-purpose probabilistic software for the statistical, sensitivity and reliability analysis of engineering problems [11]. The software tool is able to automatically build the PCE for a target accuracy given by Q^2 , or the best possible variant for the initial ED. A surrogate model is used for statistical moments and sensitivity analyses or can be exported to FReET for advanced probabilistic and reliability analysis.

3.1 General information

A general flowchart of the software tool can be seen in Fig. 3 (left). The whole process can be divided to three basic imaginary blocks: pre-processing, processing and post-processing.

FReET should be utilized for the main part of pre-processing, i.e. the definition of the stochastic model, the generation of random vector realizations using Monte Carlo simulation techniques and the acquisition of the results of the original mathematical model. In the case of the finite element model, FReET is able to cooperate with ATENA non-linear finite element software. The last step of pre-processing is the definition of PCE attributes, including target accuracy Q^2 and the following optional settings: the maximal order of the polynomial basis and the optimization technique of the truncated set of PCE terms.

The processing part of the software tool contains the above-described PCE theory, including the transformation of random variables and an adaptive algorithm. Once the target accuracy is achieved, post-processing is performed. It is possible to export the PCE in Dynamic-link library (DLL) format.

3.2 Adaptive algorithm

The main advantage of the presented software is the possibility of the adaptive creation of a PCE surrogate model for a given ED and target accuracy. The adaptive algorithm, which is based on least angle regression, was originally described in [12].

A flowchart of the adaptive algorithm can be seen in Fig. 3 (right). If the accuracy of the PCE does not meet requirements, optimization of the truncated set by LARS is performed. Briefly, in each iteration of LARS one term which is most correlated to Y is added to the sparse set of basis functions. If the cardinality of the sparse set is equal to P , the maximal order of the used polynomials is increased and the process starts from the beginning again.

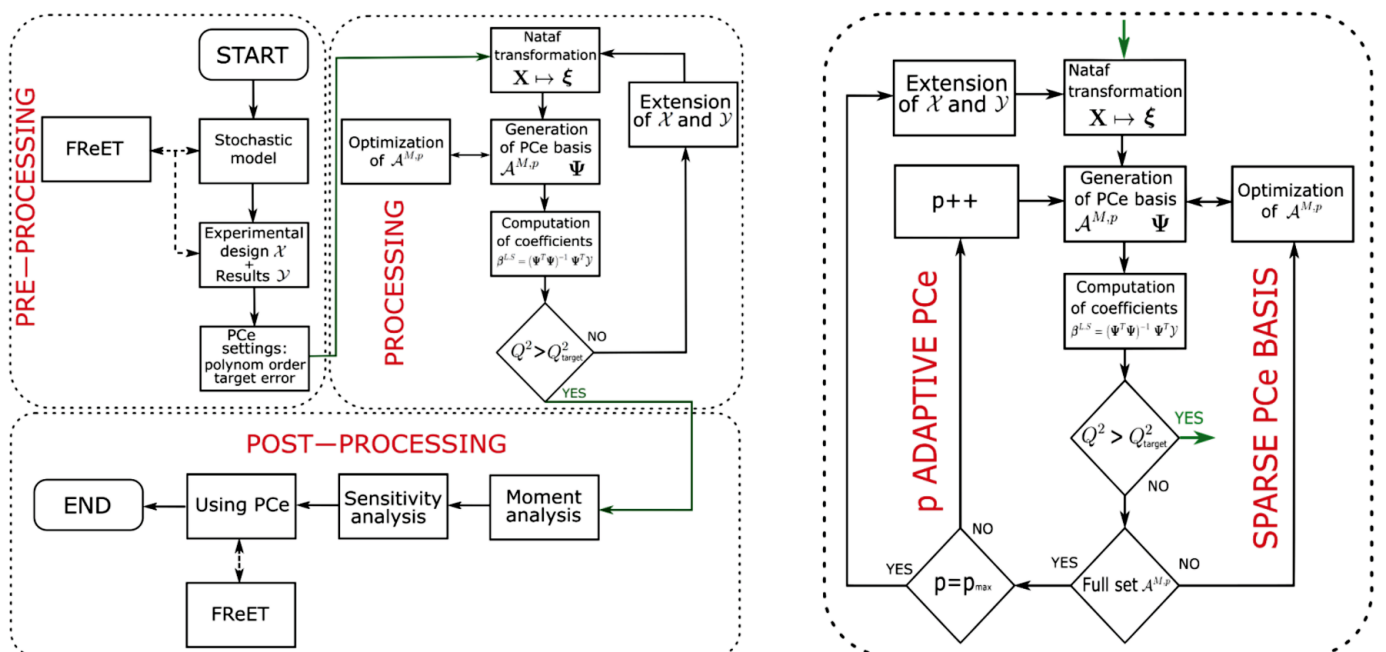


Fig. 3 A general flowchart of the developed software (left), and a detailed flowchart of the adaptive algorithm (right)

In the case of high target accuracy, extension of the experimental design is required.

It is clear that the described adaptive algorithm is able to find the best possible solution for a given target accuracy and ED without any user action. Thus, due to this adaptive feature, it is possible to recommend the software tool for users without deep knowledge regarding PCE.

3.3 Post-processing

Once the PCE approximation function is available, several important characteristics of model response Y can be obtained, as described in Ch. 2.5.

In structural reliability analysis, statistical moments and the influence of input variables on the behaviour of a given structure represent the most important information in many cases. Thus, the ability to provide this information without additional computational demand is a large advantage of PCE as regards its practical usage.

4 Application of the software tool

The algorithm used by the developed software was validated by the following academic example of the midspan deflection of a simply supported concrete beam with uniformly distributed load $v_{L/2}$. The stochastic model contains five random variables with lognormal distribution mentioned in Table 1, where b and H represent the width and height of the cross section, E is the Young's modulus of the concrete, q is the intensity of uniform load and L is the length of the beam, as is displayed in Fig. 4.

The mathematical model in explicit form is given by:

$$v_{L/2} = \frac{5}{32} \frac{qL^4}{EbH^3} \quad (21)$$

The example is focused on the quantification of statistical moments and failure probability p_f for a given threshold of deflection. The reference value was obtained via the Latin Hypercube Sampling method with 10^6 evaluations of the original mathematical model.

The target accuracy of PCE was set as $Q^2 = 1$, i.e. the best possible solution for the given ED containing 100 sample points generated by LHS. The LARS adaptive algorithm was employed and the maximal order of the polynomial basis was set as $p = 4$.

4.1 Results

The statistical moments of the model's response are shown in Table 2. As can be seen, the results obtained by the post-processing of the PCE are in good agreement with the reference values.

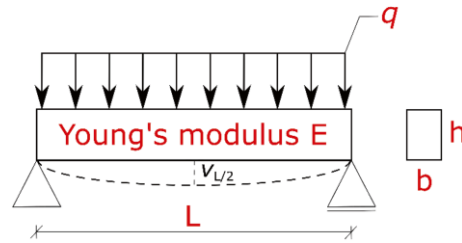


Fig. 4 Mathematical model: deflection of a simply supported beam

Tab. 1 Stochastic model of the example

Variable	μ	σ	Units
$b \sim LN$	0.15	0.075	[m]
$H \sim LN$	0.3	0.015	[m]
$E \sim LN$	30	4.5	[GPa]
$q \sim LN$	10	2	[kN/m]
$L \sim LN$	5	0.05	[m]

Tab. 2 Comparison of statistical moments obtained by PCE and LHS

Parameter	PCE (ED=100)	LHS (reference)
μ	8.366	8.368
σ	6.429	6.446

Tab. 3 Comparison of failure probability estimated for the original model and the PCE

Threshold	PCE	Original model
15 mm	1.716 e-2	1.719 e-2
20 mm	1.017 e-3	1.015 e-3
25 mm	6.250 e-5	6.180 e-5
30 mm	4.300 e-6	4.200 e-6

The second part of the example is the estimation of p_f for a given threshold. This task was performed utilizing FreET software. The PCE was exported in a dynamic library (DLL) and the failure probability was estimated via the Monte Carlo technique for several thresholds using FRReT. The reference value was estimated to be identical to that of the original mathematical model. The results are compared in Table 3.

5 Discussion

An academic example was employed for the validation of a software tool and the results were compared with those obtained via the fully probabilistic method. As can be seen, the software tool works correctly even with a small number (e.g. 100) of sample points in the ED.

Additionally, it was proved that the developed state-of-the-art software tool is able to create a PCE for surrogate modelling via an adaptive algorithm without any special inter-

active user actions. It can thus be used for complex implicit mathematical models, and especially for highly computationally demanding non-linear finite element analysis.

The software tool has already been employed in the complex, computationally demanding reliability analysis of prestressed concrete roof girders failing in shear and the results from the analysis described in [13] were also compared with those from an artificial neural network. A significant advantage of the PCE is the explicit form of the approximation function, which enables powerful post-processing without additional computational requirements.

6 Conclusion

The paper presented a recently developed state-of-the-art software tool for surrogate modelling using polynomial

chaos expansion. A necessary overview of PCE theory was given briefly in the first sections and the transformation of random variables to uncorrelated standard normal space was also discussed. The implementation of the theoretical methodology in a standalone software tool and an adaptive algorithm based on least angle regression was then presented. Finally, a simple numerical example was utilised for the validation of the software tool, and the excellent results were discussed.

Acknowledgement

The authors wish to express their thanks for the support provided by the Czech Science Foundation (GAČR) Project RESUS No. 18-13212S and project No. FAST-J-18-5309 provided by the Czech Ministry of Education, Youth and Sports.

Bibliography

- [1] MCKAY, M. D.; BECKMAN R. J.; CONOVER W. J.: *Comparison of three methods for selecting values of input variables in the analysis of output from a computer code*. Technometrics (1979), p. 239–245.
- [2] WIENER, N.: *The Homogeneous Chaos*. American Journal of Mathematics (1938), p. 897–936.
- [3] SOIZE, C.; GHANEM, R.: *Physical systems with random uncertainties: chaos representations with arbitrary probability measure*. Journal of Scientific Computing 26(2) (2004), p. 395–410.
- [4] XIU, D.; KARNIADAKIS, G.: *The Wiener-Askey polynomial chaos for stochastic differential equations*. Journal of Scientific Computing 24(2) (2002), p. 619–644.
- [5] ROSENBLATT, M.: *Remarks on a multivariate transformation*. The Annals of Mathematical Statistics 23 (1952), p. 470–472.
- [6] NATAF, A.: *Détermination des distributions de probabilité dont les marges sont données*. Comptes Rendus de l'Académie des Sciences (1962), p. 42–43
- [7] LEBRUN, R.; DUTFOY, A.: *An innovating analysis of the Nataf transformation from the copula viewpoint*. Probabilistic Engineering Mechanics 24 (2009), p. 312–320.
- [8] EFRON, B.; HASTIE, T.; JOHNSTONE, I.; TIBSHIRANI, R.: *Least angle regression*. The Annals of Statistics 32 (2004), p. 407–499.
- [9] SUDRET, B.: *Global sensitivity analysis using polynomial chaos expansions*. Reliability engineering and system safety 93 (2008). p. 964–979.
- [10] SUDRET, B.; CANIOU Y.: *Analysis of covariance (ANCOVA) using polynomial chaos expansions*. Safety, Reliability, Risk and Life-cycle Performance of Structures and Infrastructures (2013), p. 3275–3281.
- [11] NOVÁK, D.; VOŘECHOVSKÝ, M.; TEPLÝ, B.: *FReET: Software for the statistical and reliability analysis of engineering problems and FReET-D: Degradation module*. Advances in Engineering Software 72 (2014), p. 179–192
- [12] BLATMAN, G.; SUDRET, B.: *Adaptive sparse polynomial chaos expansion based on least angle regression*. Journal of Computational Physics (2011), ISSN: 0021-9991.
- [13] LEHKY, D., NOVAK, D., NOVAK L.; SOMODIKOVA M.: *Prestressed concrete roof girders: Part II – Surrogate modeling and sensitivity analysis*. Proceedings of IALCCE 2018 (2018). IN PRESS.

Authors

Dipl. Ing. Lukas Novak
Brno University of Technology
Faculty of Civil Engineering
Veveri 331/95
602 00, Brno, Czech Republic
novak.l@fce.vutbr.cz

Prof. Ing. Drahomir Novak, DrSc.
Brno University of Technology
Faculty of Civil Engineering
Veveri 331/95
602 00 Brno, Czech Republic
novak.d@fce.vutbr.cz

B On Taylor Series Expansion for Statistical Moments of Functions of Correlated Random Variables

DOI: 10.3390/sym12081379

B.1 Description

The paper is focused on a classic method for uncertainty quantification – Taylor Series Expansion (TSE). Unfortunately, the application of TSE in engineering is often limited to the simplest TSE truncated only to linear terms assuming independent random variables together with a simple differencing scheme. Therefore, the paper offers several modifications of TSE and differencing schemes suitable for semi-probabilistic design and assessment of structures. The main contribution of this paper is a methodology composed of three levels of approximation, in which each additional level of the methodology works with the information previously obtained from the calculations of the original mathematical model and thus it can progressively improve the accuracy of the estimated statistical moments in each level of the methodology. Moreover, it is shown that the simplest form of TSE is not suitable for functions of mutually dependent random variables, and the proposed advanced differencing schemes lead to more accurate results.

B.2 Role of the Ph.D. Candidate

Percentage of contribution: 90%

Lukáš Novák is the main author of this paper responsible for the concept, the methodology and the numerical results of the presented research. Furthermore, he prepared the original draft of the paper which was later reviewed in cooperation with his supervisor, Drahomír Novák.

Article

On Taylor Series Expansion for Statistical Moments of Functions of Correlated Random Variables [†]

Lukáš Novák *  and Drahomír Novák

Faculty of Civil Engineering, Brno University of Technology, 60200 Brno, Czech Republic; novak.d@fce.vutbr.cz

* Correspondence: novak.l@fce.vutbr.cz

† This paper is an extended version of our paper published in The 17th international Conference of Numerical Analysis and Applied Mathematics (ICNAAM 2019).

Received: 29 July 2020; Accepted: 17 August 2020; Published: 18 August 2020



Abstract: The paper is focused on Taylor series expansion for statistical analysis of functions of random variables with special attention to correlated input random variables. It is shown that the standard approach leads to significant deviations in estimated variance of non-linear functions. Moreover, input random variables are often correlated in industrial applications; thus, it is crucial to obtain accurate estimations of partial derivatives by a numerical differencing scheme. Therefore, a novel methodology for construction of Taylor series expansion of increasing complexity of differencing schemes is proposed and applied on several analytical examples. The methodology is adapted for engineering applications by proposed asymmetric difference quotients in combination with a specific step-size parameter. It is shown that proposed differencing schemes are suitable for functions of correlated random variables. Finally, the accuracy, efficiency, and limitations of the proposed methodology are discussed.

Keywords: Taylor series expansion; estimation of coefficient of variation; semi-probabilistic approach; structural reliability

1. Introduction

Mathematical modeling in civil engineering is often represented by the finite element method (FEM). Although FEM is an accurate and efficient technique, it is still highly time-consuming, particularly in the case of non-linear FEM including geometrical and material non-linearity. Therefore, from a practical point of view, it is necessary to decrease the number of FEM calculations as much as possible while satisfying the given safety requirements of the analyzed structure. A solution can be represented by a semi-probabilistic approach widely accepted in the engineering field [1] and implemented into the national codes such as Eurocode [2]. Such approach is able to greatly reduce the number of necessary calculations for the design and an assessment of structures. The basic reliability concept is given as $Z = R - E$, where Z is a safety margin, which is defined as the difference between the structural resistance R and the load effect E . The task of reliability analysis is the estimation of failure probability $p_f = P(Z < 0)$, which might be highly computationally demanding. According to the semi-probabilistic approach, the resistance of a structure R is separated, and the design value R_d satisfying given safety requirements is evaluated instead of calculating the failure probability. Such approach directly leads to the design value of resistance, which is obtained by the traditional Partial Safety Factor (PSF) approach, and thus can be easily used for a design and an assessment of structures. The PSF method is based on a simple assumption, that a calculation with design values of input random variables leads to the design value of resistance $R_d = r(\mathbf{x}_d)$, where design values of input random variables \mathbf{x}_d are derived under several simplifications, such as a linearization of a limit state function. In consequence, PSF works well for standard linear calculations, but there may

be a significant error for a non-linear analysis, which is far more popular nowadays. Therefore, it is necessary to develop new methods in compliance with the semi-probabilistic approach applicable for non-linear analysis. The semi-probabilistic approach is briefly presented in the following paragraph.

It is assumed that R and E are independent, and separated R is lognormally distributed; thus, the design value of resistance R_d is defined as

$$R_d = \mu_R \cdot \exp(-\alpha_R \beta v_R), \quad (1)$$

where v_R is the coefficient of variation (CoV) of resistance, and α_R represents the sensitivity factor associated with R derived from the First Order Reliability Method (FORM) [1,3]. FORM is commonly applied to linearization of limit state function at the most probable failure point by Taylor series expansion. FORM assumes the uncorrelated standardized Gaussian space ξ ; thus, all variables must be transformed by Rosenblatt transformation [4] from the original space. The coordinates of the most probable failure point, also called the design point, are thereafter described by the shortest distance β to the origin of the ξ space, direction cosines α_R associated with resistance and α_E associated with load. The shortest distance β is defined as the Hasofer–Lind reliability index, and its minimal value is given for various conditions in normative documents, in order to achieve the target safety of structures.

For industrial applications, FORM is simplified by the statistical estimation of fixed value $\alpha_R = 0.8$. Therefore, to determine the design value by a semi-probabilistic approach, it is crucial to correctly estimate the mean value and variance of structural resistance R , which can be seen as a function of multiple random variables. This task may be challenging due to the fact that input random variables can generally be non-Gaussian and correlated. There have been several methods proposed in last two decades to estimate the variation coefficient of R (ECoV methods) [5–10]; however, mathematical background and limitations of these methods are often missing, and there is no solution for correlated random variables, which is common for material characteristics.

The only general approach to estimate statistical moments is pseudo-random sampling by a Monte Carlo type algorithm such as Crude Monte Carlo or Latin Hypercube Sampling [11,12] employed in numerical examples as a reference solution. However, it is necessary to perform a high number of simulations of the original mathematical model, which is not feasible in industrial applications due to the enormous computational burden. On the other hand, it is possible to assume several simplifications and create an approximation of the original mathematical model of R .

The approximating function is called a surrogate model, or a metamodel, and it is a topic of great interest among researchers from various research fields. The Polynomial Chaos Expansion (PCE) is often used for uncertainty quantification [13,14]. The Gaussian process or Kriging has recently received significant attention in reliability analysis of systems with very low failure probabilities [15], and artificial neural networks are often utilized for reliability-based optimization [16]. Although PCE, Kriging, and ANN represent very powerful and efficient approaches with many advantages, these advanced techniques require deep knowledge of theoretical background, and it is necessary to use developed algorithms with great caution.

Another well-known approximation of functions is Taylor series expansion (TSE), which was also used for derivation of PSF and FORM as described, for example, in [17]. Although TSE is often used to estimate statistical moments of functions of random variables by mathematicians, it has not yet been well investigated in the context of non-linear FEM in civil engineering in order to adapt and directly use TSE for structural reliability and semi-probabilistic approaches. For industrial applications, it is crucial that the proposed methods are easy to implement and easy to use with the same level of knowledge about the mathematical model as in the case of PSF. Therefore, it makes perfect sense to generalize TSE, which is already utilized for the derivation of PSF implemented in codes, to directly use in combination with FEM and semi-probabilistic ECoV approach. Therefore, the ECoV method based on TSE adapted for civil engineers is discussed, and several modifications of this approach are proposed in the next section. Moreover, the whole methodology of increasing complexity and accuracy of TSE suitable for industrial applications is proposed in this paper.

2. Taylor Series Expansion

An original mathematical model is often highly time-consuming, and it is necessary to create an approximation—a simplified function in explicit form. Although there are several advanced types of surrogate models, it is still common to use the traditional approach, called Taylor series expansion, which can be truncated to arbitrary order and used with various differencing schemes. Although such adaptivity makes TSE a powerful technique, there are severe problems for practical computations in the case of non-linear functions with complex stochastic models containing a dependence structure. In the following paragraphs, let us assume an original mathematical model in form of software algorithm (e.g., FEM); thus, the derivatives must be calculated numerically.

Let $(\Omega, \mathcal{F}, \mathcal{P})$ be a probability space, where Ω is an event space, \mathcal{F} is Borel σ -algebra on Ω , and \mathcal{P} is a probability measure $\mathcal{P} : \mathcal{F} \rightarrow [0, 1]$. Let us assume a random vector $\mathbf{X} = (X_1, X_2, \dots, X_n)^T$ consisting of random variables $X(\omega), \omega \in \Omega$ with existing mean values $\mu_{X_1}, \mu_{X_2}, \dots, \mu_{X_n}$ and a mathematical model of this input random vector $r(\mathbf{X})$. The response of the mathematical model is thereafter a random variable R described by a specific probability distribution and statistical moments. Further, let us assume the mathematical model $r(\mathbf{X})$ to be infinitely differentiable in some open interval around the vector of mean values $\boldsymbol{\mu}_X = \mu_{X_1}, \mu_{X_2}, \dots, \mu_{X_n}$. Under this assumption, it is possible to expand the original model to the infinite Taylor series according to Taylor's theorem:

$$\begin{aligned} r(\mathbf{X}) &= r(\boldsymbol{\mu}_X) + \nabla r(\boldsymbol{\mu}_X) \cdot (\mathbf{X} - \boldsymbol{\mu}_X) + \frac{1}{2} (\mathbf{X} - \boldsymbol{\mu}_X) \cdot \nabla \nabla r(\boldsymbol{\mu}_X) \cdot (\mathbf{X} - \boldsymbol{\mu}_X) + \dots = \\ &= r(\mu_{X_1}, \mu_{X_2}, \dots, \mu_{X_n}) + \sum_{i=1}^n \frac{\partial r(\mathbf{X})}{\partial X_i} (X_i - \mu_{X_i}) + \frac{1}{2} \sum_{i=1}^n \sum_{j=1}^n \frac{\partial^2 r(\mathbf{X})}{\partial X_i \partial X_j} (X_i - \mu_{X_i}) (X_j - \mu_{X_j}) + \dots \quad (2) \end{aligned}$$

where the derivatives are evaluated at $\mu_{X_1}, \mu_{X_2}, \dots, \mu_{X_n}$. Note that TSE consists of a constant term, linear term, quadratic term, etc. For a practical computation, it is crucial to reduce Taylor series to a finite number of terms and to obtain derivatives by numerical differentiation. There are many possible differencing schemes, which are more or less suitable for specific applications. One of the possible formulas for numerical derivation was proposed by Schlune et al. [9], especially for civil engineers, where derivatives are approximated by the asymmetric difference quotient as follows:

$$\frac{\partial r(\mathbf{X})}{\partial X_i} = \frac{R_{X_m} - R_{X_{i\Delta}}}{\Delta X_i} \quad (3)$$

where the response of mathematical model R_{X_m} is a calculation with mean values of X , and $R_{X_{i\Delta}}$ is the result of the model using reduced mean values of the i -th input random variables by ΔX_i . This differencing scheme is adapted for a structural design and an assessment by the step-size parameter $c = (\alpha_R \beta) / \sqrt{2}$, and $X_{i\Delta}$ corresponds to quantile $F_i^{-1}(\Phi(-c))$, where F_i^{-1} is an inverse cumulative distribution function of the i -th variable, and Φ is the cumulative distribution function of standardized Gaussian distribution. For the sake of clarity, the difference is calculated as $\Delta X_i = X_{im} - X_{i\Delta}$. Note that the step-size parameter is a function of the reliability index; thus, it is in compliance with the philosophy of a semi-probabilistic approach implemented in civil engineering codes [1]. Following this idea, additional asymmetric differencing schemes adapted for civil engineering used in combination with TSE of the first and the second order are proposed in the following subsections.

2.1. Linear Terms of Taylor Series Expansion

In engineering applications, it is common to assume only linear terms of TSE and independent input random variables. Since a semi-probabilistic approach is focused on practical applications, the significant advantage of TSE reduced to linear terms is the possibility of analyzing expressions for an expected value and a variance, see e.g., [17].

Theorem 1. If an original mathematical function $r : \mathbb{R}^n \rightarrow \mathbb{R}$ of n independent random variables described by mean value μ_{X_i} and variance $\sigma_{X_i}^2$ is approximated by Taylor series expansion reduced to linear terms, the first two statistical moments of the response R_T of linear Taylor approximation are analytically obtained as follows:

$$\mathbb{E}_{R_T} \approx r(\boldsymbol{\mu}_X) \quad (4)$$

$$\text{Var}_{R_T} \approx \sum_{i=1}^n \left(\frac{\partial r(X)}{\partial X_i} \right)^2 \sigma_{X_i}^2 \quad (5)$$

Proof of Theorem 1. For the sake of clarity, the estimations of expected value E_{R_T} and variance Var_{R_T} for the function of n independent random variables are as follows:

$$\mathbb{E}_{R_T} \approx \mathbb{E} \left[r(\mu_{X_1}, \mu_{X_2}, \dots, \mu_{X_n}) \right] + \sum_{i=1}^n \mathbb{E} \left[\frac{\partial r(X)}{\partial X_i} (X_i - \mu_{X_i}) \right] \approx r(\mu_{X_1}, \mu_{X_2}, \dots, \mu_{X_n}) \quad (6)$$

and

$$\begin{aligned} \text{Var}_{R_T} \approx \text{Var} \left[r(\mu_{X_1}, \mu_{X_2}, \dots, \mu_{X_n}) + \sum_{i=1}^n \frac{\partial r(X)}{\partial X_i} (X_i - \mu_{X_i}) \right] &= \sum_{i=1}^n \text{Var} \left[\frac{\partial r(X)}{\partial X_i} (X_i - \mu_{X_i}) \right] + \\ &+ \sum_{\substack{i,j=1,\dots,N \\ i \neq j}} \text{Cov} \left[\frac{\partial r(X)}{\partial X_i} (X_i - \mu_{X_i}), \frac{\partial r(X)}{\partial X_j} (X_j - \mu_{X_j}) \right] = \sum_{i=1}^n \left(\frac{\partial r(X)}{\partial X_i} \right)^2 \sigma_{X_i}^2 \quad (7) \end{aligned}$$

where the final equation arises from the definition of variance $\text{Var}(X) = \sigma_X^2 = \mathbb{E}[(X - \mu)^2]$ and property of variance $\text{Var}(cX_i + dX_j) = c^2\text{Var}(X_i) + d^2\text{Var}(X_j) + 2cd\text{Cov}(X_i, X_j)$. Moreover, for independent variables, the covariance between variables is equal to zero, and thus the formula is reduced. \square

As can be seen from the proof above, there is a strict assumption of uncorrelated random variables for Equation (5). However, it is necessary to assume correlated random variables in some practical examples solved by FEM to represent realistic behaviors of structures. An extension of the method for dependent random variables can be obtained from the proof above using first-order Taylor series expansion assuming correlation among random variables represented by the correlation coefficient ρ in analytical form as

$$\text{Var}_{R_T} \approx \sum_{i=1}^n \left(\frac{\partial r(X)}{\partial X_i} \right)^2 \sigma_{X_i}^2 + \sum_{\substack{i,j=1,\dots,n \\ i \neq j}} \rho_{i,j} \sigma_{X_i} \sigma_{X_j} \frac{\partial r(X)}{\partial X_i} \frac{\partial r(X)}{\partial X_j}. \quad (8)$$

However, higher terms of TSE or more accurate approximation of derivatives should be considered for the correct estimation of variance in the case of dependent input random variables and non-linear functions. Otherwise, the correlation term may lead to significant inaccuracy of the resulting variance. We propose the second-order backward asymmetric differencing according to Equation (9), which is adapted for structural design utilizing the parameter $c = (\alpha_R \beta) / \sqrt{2}$ analogously to Equation (3) proposed by Schlune et al. The middle additional term $R_{X_i \frac{\Delta}{2}}$ is obtained by an evaluation of the original mathematical model with reduced i -th variable $X_{i \frac{\Delta}{2}} = X_{im} - \Delta_{X_i} / 2$. Note that the proposed approach needs $2n + 1$ evaluations of the original model, while the scheme proposed by Schlune needs $n + 1$ simulations. In practice, an analyst could use the derivative scheme according to Schlune and further compute additional n simulations in order to obtain $R_{X_i \frac{\Delta}{2}}$ and more accurate results.

$$\frac{\partial r(X)}{\partial X_i} = \frac{3R_{X_m} - 4R_{X_{i\frac{\Delta}{2}}} + R_{X_{i\Delta}}}{\Delta X_i}. \quad (9)$$

2.2. Higher-Order Taylor Series Expansion

If higher terms of TSE are considered, it is inefficient to derive analytical formulas for statistical moments [18], and thus mean and variance should be calculated numerically by simulation techniques directly from Equation (2) truncated to quadratic terms. Moreover, additional higher-order derivatives must be evaluated, which might not be feasible in computationally demanding practical examples. Therefore, linear TSE is preferred for practical computations. However, for specific cases with significant interaction of input variables, one may use second-order TSE for the estimation of coefficient of variation. In this case, it is necessary to compute all second-order partial derivatives. For numerical calculations of $\frac{\partial^2 r(X)}{\partial X_i^2}$, it is possible to use the already defined simulations R_{X_m} , $R_{X_{i\Delta}}$, $R_{X_{i\frac{\Delta}{2}}}$ in a standard asymmetric backward differencing scheme:

$$\frac{\partial^2 r(X)}{\partial X_i \partial X_i} = \frac{R_{X_m} - 2R_{X_{i\frac{\Delta}{2}}} + R_{X_{i\Delta}}}{\Delta X_i^2} \quad (10)$$

The only additional computations of the original mathematical model needed are for mixed partial derivatives $\frac{\partial^2 r(X)}{\partial X_i \partial X_j}$. Note that it is necessary to perform additional $\binom{n}{2}$ simulations in order to obtain all the mixed partial derivatives. In total, it is necessary to calculate $2n + \binom{n}{2} + 1$ simulations for second-order TSE using the proposed asymmetric differencing schemes.

Theorem 2. *Mixed partial derivatives can be approximated by the simple backward finite differencing as*

$$\frac{\partial^2 r(X)}{\partial X_i \partial X_j} = \frac{R_{X_m} - R_{X_{i\Delta}} - R_{X_{j\Delta}} + R_{X_{i\Delta}X_{j\Delta}}}{\Delta X_i \Delta X_j}, \quad (11)$$

where $R_{X_{i\Delta}X_{j\Delta}}$ represents the response of a mathematical model with reduced mean values of both i -th and j -th input random variables. All other variables were defined in the previous differencing schemes.

Proof of Theorem 2. Using the simple one-sided backward differencing defined by Equation (3), one can derive mixed partial derivatives as follows:

$$\frac{\partial^2 r}{\partial X_i \partial X_j} \approx \frac{\frac{\partial r(X)}{\partial X_j}(\mu_{X_i}, \mu_{X_j}) - \frac{\partial r(X)}{\partial X_j}(X_{i\Delta}, \mu_{X_j})}{\Delta X_i} \quad (12)$$

where $\frac{\partial r(X)}{\partial X_j}$ is computed for specific coordinates (μ_{X_i}, μ_{X_j}) and $(X_{i\Delta}, \mu_{X_j})$ as

$$\frac{\partial r(X)}{\partial X_j}(\mu_{X_i}, \mu_{X_j}) \approx \frac{R_{X_m} - R_{X_{j\Delta}}}{\Delta X_j} \quad (13)$$

and

$$\frac{\partial r(X)}{\partial X_j}(X_{i\Delta}, \mu_{X_j}) \approx \frac{R_{X_{i\Delta}} - R_{X_{i\Delta}X_{j\Delta}}}{\Delta X_j} \quad (14)$$

Therefore, the final derivative scheme for mixed second partial derivatives based on the simple backward differencing adapted for a semi-probabilistic approach is

$$\frac{\partial^2 r(X)}{\partial X_i \partial X_j} = \frac{R_{X_m} - R_{X_{i\Delta}} - R_{X_{j\Delta}} + R_{X_{i\Delta}X_{j\Delta}}}{\Delta X_i \Delta X_j} \quad (15)$$

□

3. Numerical Computation

3.1. Methodology of ECoV by TSE

Since TSE can be constructed in various forms, it is beneficial to create ECoV methodology using TSE, composed of the three levels of an approximation using asymmetric differencing schemes already described in the previous section in combination with linear and quadratic TSE as follows:

1. linear TSE with a simple differencing scheme using Equation (3)— $n_{sim} = n + 1$,
2. linear TSE with an advanced differencing scheme using Equation (9)— $n_{sim} = 2n + 1$,
3. TSE truncated to quadratic terms with a differencing scheme using Equation (9) for the first-order derivatives, Equation (10) for the second-order partial derivatives, and Equation (11) for the mixed derivatives—number of calculation is $n_{sim} = 2n + \binom{n}{2} + 1$ in total.

The first level was proposed by Schlune et al. [9] for uncorrelated random variables, and it was used in several practical studies [19–21]. However, its behavior for functions of correlated input random variables has not been investigated yet, though it is often necessary to assume correlated random material characteristics in industrial applications. It can be expected that the accuracy of the first level is not sufficient for dependent variables, which will be investigated in numerical examples.

The second level with the advanced differencing scheme still uses only linear terms of the TSE, and thus it is possible to calculate variance by the simple Equation (8), which might be important for easy applications in industry. The accuracy of the second level is significantly improved by additional simulations; however, interaction terms are missing due to a linear truncation of TSE.

The third level of approximation is especially suitable for mathematical models with strong interaction among random variables. However, it is also the most expensive approach, and statistical moments of the model response should be obtained numerically since an analytical calculation is inefficient. Therefore, it can be seen as a simple surrogate model that might be used in combination with Monte Carlo techniques.

Note that the calculations of the original mathematical model from one level are also always used in the following level of approximation. It represents the significant characteristic of the proposed approach, which is beneficial for industrial applications, where it is crucial to decrease the number of calculations as much as possible due to computational demands. Therefore, an analyst can start with the first level of an approximation and eventually increase the number of simulations only if it is necessary. The asymmetric differencing schemes for each level of approximation are depicted in Figure 1 together with iso-lines of bivariate standard Gaussian probability distribution in σ , 2σ , and 3σ distance, represented by dotted circles.

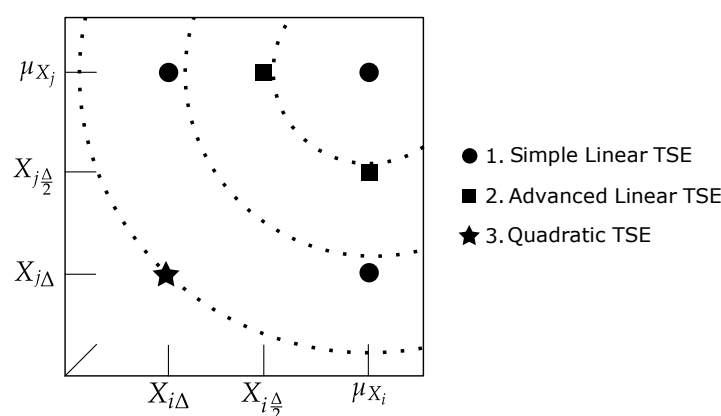


Figure 1. Proposed methodology composed of the three levels of Taylor series expansion (TSE) approximation using asymmetric differencing schemes adapted for civil engineering. Iso-lines of bivariate standard Gaussian probability distribution are represented by dotted circles.

3.2. Reference Solution

In industrial applications, only marginal distributions and a correlation matrix are usually known, which does not represent complete information about the joint probability distribution. Therefore, it is necessary to assume a specific copula [22]. A special case of Rosenblatt transformation assuming the Gaussian copula is also known as the Nataf transformation [23], which is usually utilized in reliability applications. The Nataf transformation is composed of three steps:

$$\boldsymbol{\xi} = T_{Nataf}(\boldsymbol{\xi}) = T_3 \circ T_2 \circ T_1(\boldsymbol{\xi}) \quad (16)$$

The first step represents a transformation from uncorrelated standard Gaussian space $\boldsymbol{\xi}$ to correlated standard normal space \mathbf{Z} using linear transformation.

$$T_1 : \boldsymbol{\xi} \mapsto \mathbf{Z} = \mathbf{L}\boldsymbol{\xi} \quad (17)$$

For this procedure, Cholesky decomposition of the fictive correlation matrix \mathbf{R}_Z must be performed:

$$\mathbf{R}_Z = \mathbf{L}\mathbf{L}^T \quad (18)$$

The following two steps are commonly known as an iso-probabilistic transformation by an inverse cumulative distribution function F_x^{-1} and the standard Gaussian cumulative distribution function Φ :

$$T_2 : \mathbf{Z} \mapsto \mathbf{W} = \Phi(\mathbf{Z}) \quad (19)$$

$$T_3 : \mathbf{W} \mapsto \mathbf{X} = F_x^{-1}(\mathbf{W}) \quad (20)$$

It is clear that the critical task of the Nataf transformation is to determine \mathbf{R}_Z . The relationship between the fictive correlation coefficients ρ_{zij} and ρ_{ij} between i -th and j -th variable is defined by the following integral equation:

$$\rho_{ij} = \frac{1}{\sigma_i \sigma_j} \iint_{\mathbb{R}^2} \{ F_i^{-1} [\Phi(z_i) - \mu_i] F_j^{-1} [\Phi(z_j) - \mu_j] \times \phi_2(z_i, z_j, \rho_{zij}) \} dz_i dz_j, \quad (21)$$

where μ is the mean value, σ is the standard deviation, and ϕ_2 is the bivariate standard normal probability density function parametrized by fictive correlation coefficients ρ_{zij} :

$$\phi_2(z_i, z_j, \rho_{zij}) = \frac{1}{2\pi\sqrt{1-\rho_{zij}^2}} \exp\left(-\frac{z_i^2 - 2\rho_{zij}z_iz_j + z_j^2}{2(1-\rho_{zij}^2)}\right). \quad (22)$$

Numerical examples are constructed in order to show the behavior of the presented differencing schemes and identify their limitations. For each example, the reference solution is obtained by numerical simulation with $n_{sim} = 10^5$ realizations of a given random vector generated by Latin Hypercube Sampling (LHS) in uncorrelated space $\boldsymbol{\xi}$ and transformed into the correlated space \mathbf{X} by the Nataf transformation. The reference solution by LHS is compared with the results obtained by TSE of increasing complexity using the proposed methodology.

Since this paper is focused on the potential of the presented differencing schemes for industrial applications, the input variables are assumed to be lognormally distributed with coefficient of variation $CoV = 0.1-0.2$, which is common for material characteristics. Specifically, all examples work with the following stochastic model of two input variables: vector of mean values $\boldsymbol{\mu} = [40, 300]$ and the corresponding vector of coefficients of variation $CoV = [0.1, 0.2]$. Moreover, Pearson's correlation coefficients (parameterizing Gaussian copula) are assumed to be positive in the range $(0, 0.9)$. The results of the numerical simulations are statistically processed in order to obtain the mean value, variance, and coefficient of variation of the model response.

3.3. Example 1: Simple Linear Model

The very first example represents the entire methodology. It is a simple linear model $R = r(\mathbf{X}) = X_1 + X_2$. The selected realizations generated by Latin Hypercube Sampling, which illustrate the uniform cover of the design domain, together with iso-lines of joint probability density of random vector in uncorrelated and correlated space (Gaussian copula parametrized by the correlation coefficient $\rho = 0.8$) are depicted in Figure 2. A reference solution based on a sample with $n_{sim} = 10^5$ is calculated for all examples.

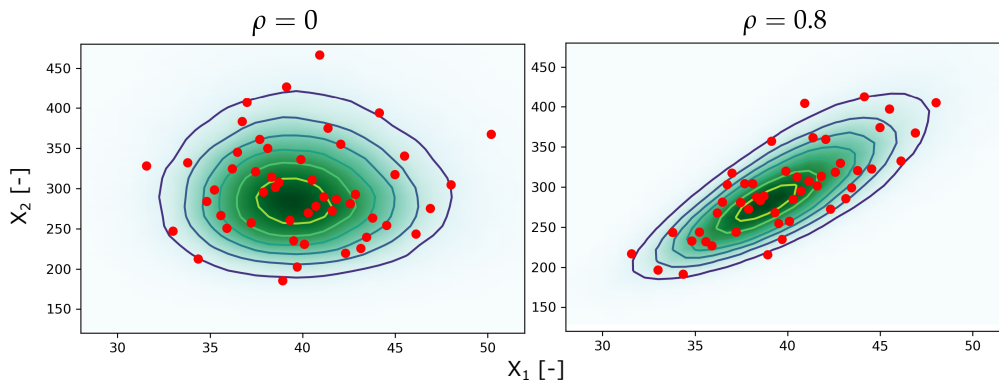


Figure 2. Realizations (red dots) generated by Latin Hypercube Sampling (LHS) and iso-lines of joint probability density of input random vector in uncorrelated (**left**) and correlated (**right**) space.

In this case, all the presented differencing schemes led to the exact solution, as can be seen in Figure 3, since a linear approximation fits the original model. For the sake of clarity, the figures in this section show estimation of CoV (top) and variance (bottom) as well, since CoV takes the estimation of mean value into account. The graphs in the right column represent CoV or variance for correlated variables with subtracted uncorrelated values, which represent pure influence of correlation estimated by the presented methods.

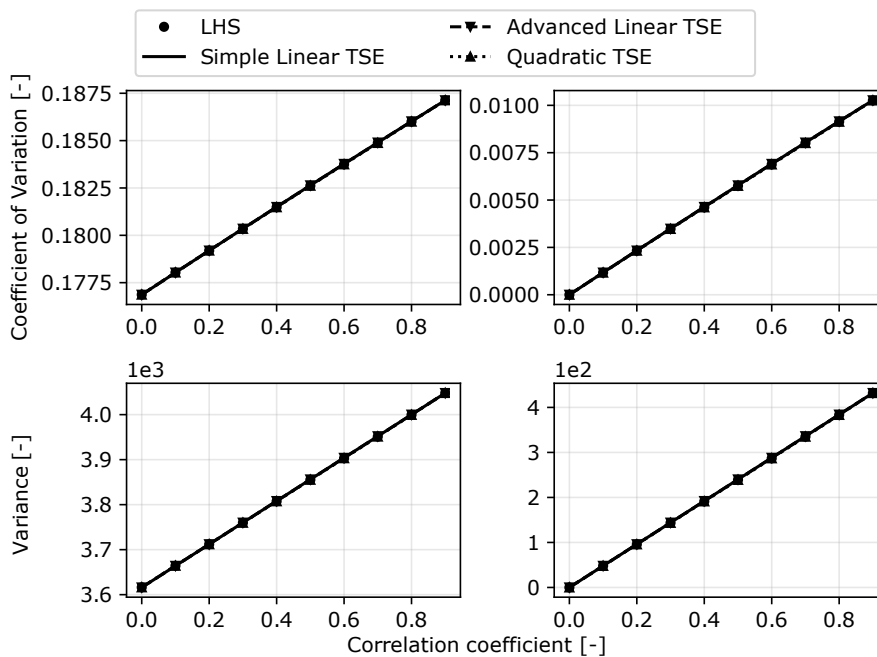


Figure 3. Estimation of coefficient of variance (CoV) (**top**) and variance (**bottom**) of the first example by the presented methods.

3.4. Example 2: Linear Model with Interactions

The second example is focused on the comparison of the first-order and the second-order Taylor series expansion. The first and the second level of approximation use the first-order Taylor expansion; thus, they are not recommended for mathematical models with significant interaction terms, since there are no mixed derivatives in the approximation, and the influence of the interaction is therefore underestimated. The quadratic TSE is the most computationally demanding and the only one reflecting the interaction terms. For the demonstration of this characteristic, the following adaptation of the previous simple mathematical model is assumed:

$$R = r(\mathbf{X}) = X_1 + X_2 + 5 (X_1 X_2) \tag{23}$$

The obtained results are depicted in Figure 4 in the same manner as in the previous example. The estimated mean value for the uncorrelated input random variable was accurate ($\mu_R = 260$). However, using only linear terms of Taylor expansion led to an identical mean value independent of the correlation among input variables. Therefore, the results of CoV are affected by this characteristic, and all methods seem comparable. The accuracy of the used approximations can be clearly seen on the estimation of variance, where the first two levels of an approximation led to identical results, with the error increasing together with the correlation between input random variables. Of course, the obtained results are exact only if the third-level approximation (quadratic Taylor expansion) is used for the estimation of variance, since Hessian of this function is not equal to the zero matrix $\mathbf{0}$. As can be seen, neglecting an interaction among random variables by the first-order Taylor expansion may lead to a significant error in the estimation of statistical moments even for simple linear functions; thus, an analyst should carefully choose the level of approximation in industrial applications considering the nature of the studied physical system.

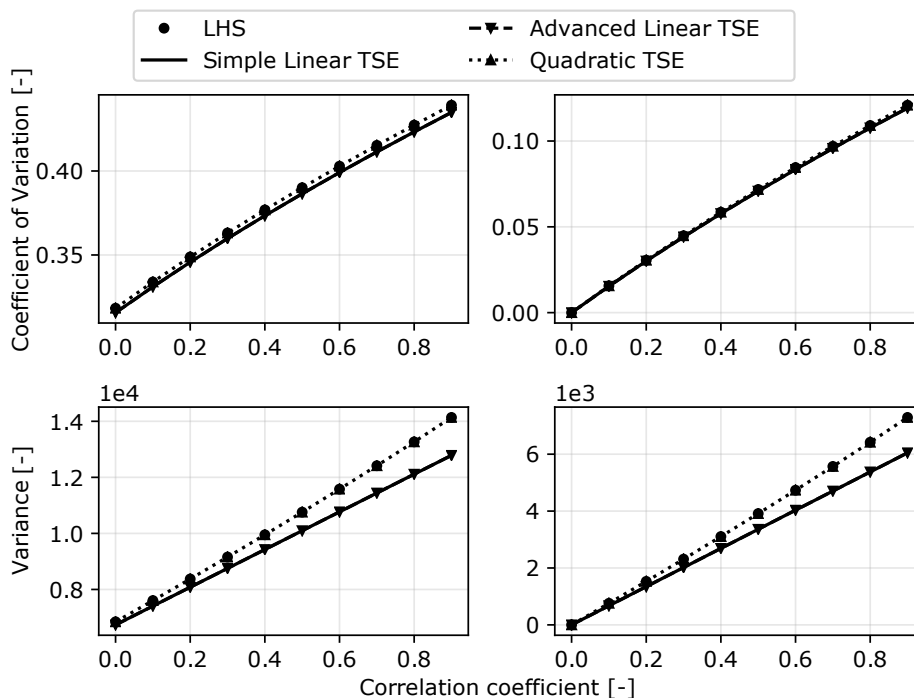


Figure 4. Estimation of CoV (top) and variance (bottom) of the second example by the presented methods.

3.5. Example 3: Approximation of Industrial Example

The third example is motivated by the industrial applications in civil engineering often represented by non-linear finite element models—typically ultimate resistance given by the peak of the load-deflection curve of concrete structural element. The behavior of such a physical system is often monotone with a slightly non-linear progress. A typical function solved by FEM can be found, for example, in [9], and due to the computational demands of FEM, its shape was replicated by the following artificial function:

$$R = r(\mathbf{X}) = X_1 X_2 - X_1^2 - \left(\frac{X_2^2}{30}\right) - (X_1 - 30)(X_2 - 200) \quad (24)$$

The exact mean value estimated by LHS was $\mu_R = 6264$ and by Taylor series $\mathbb{E}_{R_T} = 6400$, which leads to the difference between the estimation of CoV and variance depicted in Figure 5. However, the estimation of variance and CoV by linear TSE with advanced differencing together with quadratic TSE was accurate. On the other hand, linear Taylor expansion with simple one-sided backward differencing showed a significant error in estimation for all correlation coefficients. The results on the right-hand side of Figure 5 represent the pure influence of correlation, and as can be seen, the slope of the curve estimated by simple linear TSE was significantly different. Thus, this method is not able to correctly identify the role of correlation.

From the previous examples, it is clear that simple linear Taylor expansion as proposed by Schlune et al. is suitable only for functions of uncorrelated variables, which is not a typical industrial problem. However, it is possible to start with simple differencing for uncorrelated problem and add n additional simulations in order to adapt an approximation for correlated variables.

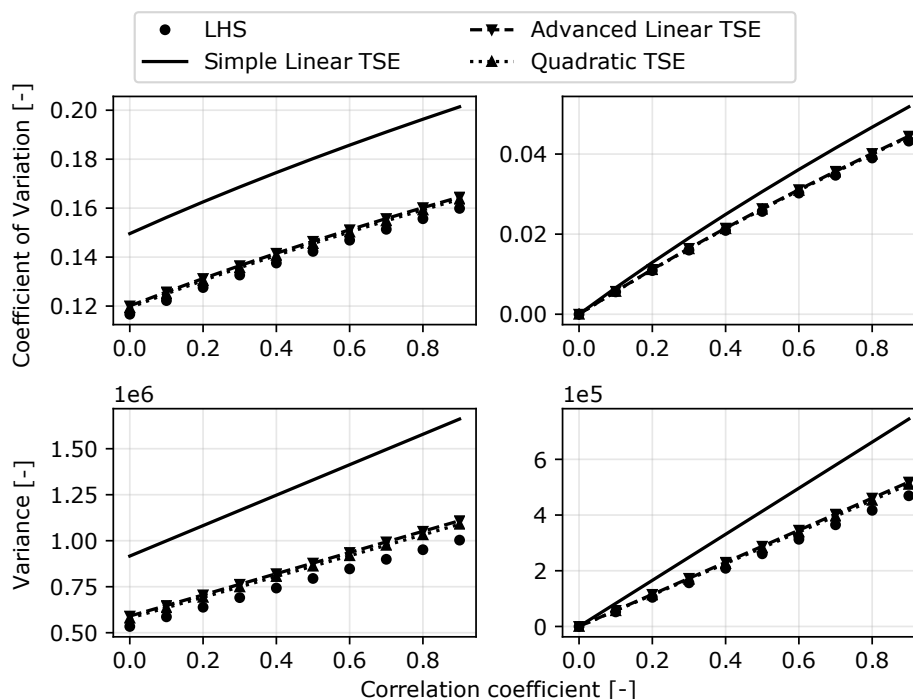


Figure 5. Estimation of CoV (top) and variance (bottom) of the third example by the presented methods.

3.6. Example 4: Non-Linear Function

The last example is created in order to show the limitations of all the presented methods with increasing non-linearity of the original mathematical model. The following function has a similar shape as the model in the previous example; however, it is significantly more non-linear:

$$R = r(\mathbf{X}) = X_1 X_2 \cos\left(\frac{\pi X_1}{200}\right) \cos\left(\frac{\pi X_2}{2000}\right) \quad (25)$$

The estimated mean value by TSE for the uncorrelated case was $\mathbb{E}_{R_T} = 8650$, and the exact value estimated by LHS was $\mu_R = 8468$. Variance and CoV of R estimated by the presented methods are summarized in Figure 6. As can be expected, with higher non-linearity of mathematical models, it was not suitable anymore to use TSE of lower orders as an approximation of the original model. Since computational requirements of higher-order Taylor series expansions are comparable to the commonly known surrogate models, and the estimation of statistical moments is inefficient, one should prefer more advanced surrogate models (e.g., Polynomial Chaos Expansion or Kriging) together with standard statistical methods.

Specifically in this example, the worst results were obtained by the linear TSE with simple differencing, which represents a poor approximation of the original function; thus, the estimation of variance was not satisfied as well. Similarly, a poor accuracy of the estimated influence of correlation can be clearly seen from the different trends of the curves in the column on the right-hand side in Figure 6. However, since there is no significant interaction between the input random variables, the results obtained by linear Taylor series with advanced differencing were almost identical to the more computationally demanding quadratic Taylor series, which might be a crucial advantage in high-dimensional industrial applications solved by FEM.

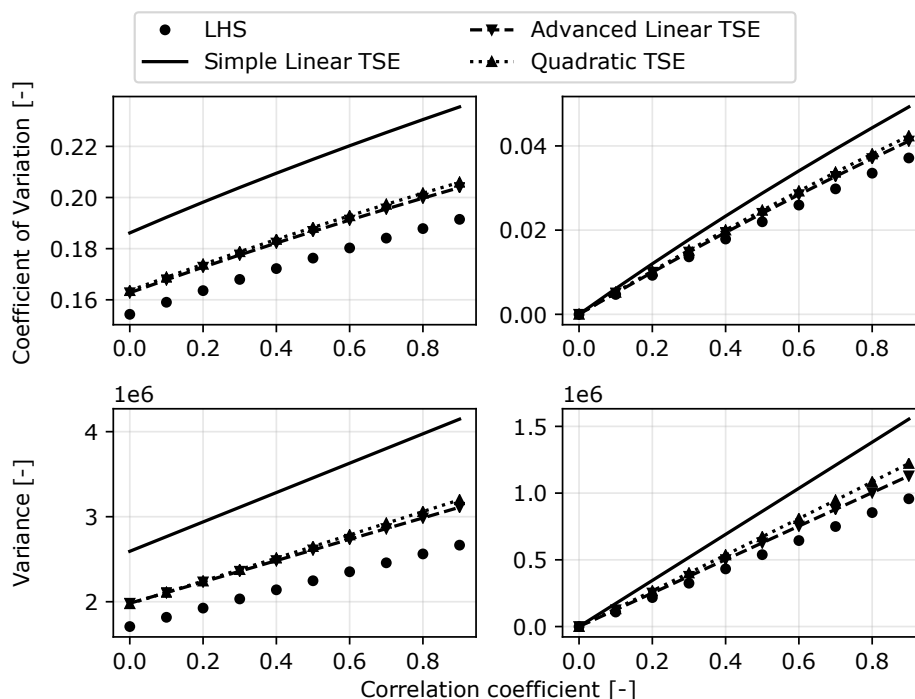


Figure 6. Estimation of CoV (**top**) and variance (**bottom**) of the fourth example by the presented methods.

4. Discussion

The TSE represents a powerful and accurate technique with a strong mathematical background. Unfortunately, it is usually truncated to linear terms in engineering applications, which may generally

lead to poor results in the case of non-linear functions and correlated random input variables. Although Schlune et al. proposed the ECoV method based on linear TSE with a simple asymmetric differencing, there are no studies on its limitations and possible generalizations, although TSE is a highly modifiable technique via differencing schemes and a truncation order of an approximation. Therefore, it was necessary to propose different variations of TSE for specific problems and create the novel methodology of three levels of TSE. The proposed methodology was applied on several analytical examples in order to show the limitations of each level. The variations of TSE were proposed with attention to the reduction of computational cost as much as possible, since derivations are computed by finite differencing of FEM in industrial applications. Therefore, each additional level of the methodology works with the information previously obtained from calculations of the original mathematical model; thus, an approximation can be sequentially made more accurate by calculating several additional simulations and combining them with the previous results used in the asymmetric differencing scheme of lower levels of the proposed methodology.

It can be seen from the presented results, that linear TSE fails in the case of significantly non-linear functions (the last example) and functions with important interaction terms (the second example). In such cases, it is necessary to use quadratic TSE (3rd level of proposed methodology) as an approximation. Moreover, the main motivation of this paper is dealing with correlation among random input variables, which has not been investigated yet in the context of ECoV methods. It is clear from the presented examples that the linear TSE with simple differencing (1st level of the proposed methodology) is not suitable for functions of correlated variables. However, once the differencing scheme according to Equation (9) is used in combination with linear TSE (2nd level of the proposed methodology), its accuracy is significantly improved. Thus, if there is not a strong interaction among input random variables, it is not necessary to use quadratic TSE (3rd level of the proposed methodology), which leads to additional computational requirements.

From the point of view of computational costs, it is possible to add higher terms of Taylor series, but it significantly increases the number of derivatives. Therefore, TSE above the second order is inefficient, and advanced surrogate models such as PCE, Krigging, or ANN should be used. On the other hand, a better accuracy of estimation of CoV and variance can be reached by the improved asymmetric differencing scheme as proposed in this paper. Computational requirements are slightly increased from $n + 1$, for the traditional scheme according to Equation (3), to $2n + 1$ for the proposed scheme according to Equation (9). It is obvious that variance estimation using Equation (9) is significantly improved in comparison to the traditional differencing scheme represented by Equation (3). However, the main advantage of the proposed method is the accuracy of variance estimation in the case of correlated random variables. It is obvious that there is a difference between the curves representing an increment of variance due to correlation (second part of Equation (8)) estimated by both approaches. The difference between both differencing schemes is proportional to a correlation among input random variables; thus, special attention should be given to functions with high correlation among input random variables.

Generally, the proposed methodology proved to be well-suited for typical industrial mathematical models in civil engineering. Moreover, the paper shows the influence of different variants of TSE and level of statistical correlation on estimated CoV, which is a base for semi-probabilistic approaches to determine design value in civil engineering. Such influence can be significant, for more basic random variables certainly amplified, which will be studied on practical examples represented by non-linear finite element models of structures in further research, and the obtained results will be compared to standard normative approaches as PSF and global safety factor method [24] designed specifically for civil engineering.

5. Conclusions

The non-linearity of functions and statistical correlation of input random variables represent crucial aspects in estimating statistical moments of industrial mathematical models. Unfortunately,

the accuracy of standard existing methods is not satisfying for such models. Therefore, this paper presents a novel methodology to estimate the coefficient of variation for functions of correlated input random variables. Since mathematical models in civil engineering are often functions of input correlated random variables, it is necessary to develop new and efficient methods based on a semi-probabilistic approach widely accepted for the design and assessment of structures satisfying given safety requirements. Therefore, the methodology of three levels of increasing complexity, accuracy, and computational cost based on Taylor series expansion is proposed and described. The methodology consists of three advanced differencing schemes adapted for civil engineering by step size parameter. The differencing schemes are based on the asymmetric quotient, which is typical for engineering applications, where one is interested in extreme structural behavior leading to failure. The proposed methodology is applied to four analytical examples, and the results are compared to reference solutions obtained by Latin Hypercube Sampling. The analytical examples are constructed in order to show the efficiency and limitations of each differencing scheme: simple linear function, linear function with strong interaction terms, and finally two non-linear functions. From the obtained results, extensively discussed in the previous section, it is clear that it is necessary to choose advanced asymmetric differencing schemes in the cases of correlated input random variables or increase the truncation order of Taylor series expansion. It was shown that its accuracy is significantly higher in comparison to the simple linear TSE (in absolute values but also in a relative trend of influence of correlation). The slight increment of computational demands of the proposed differencing schemes is a significant advantage in comparison to Taylor series of a higher order, where it is necessary to numerically evaluate a large number of additional derivatives. However, it was shown that quadratic TSE is necessary for mathematical models with strong interaction terms.

Author Contributions: Methodology, L.N.; validation, L.N.; formal analysis, L.N.; writing—original draft preparation, L.N.; writing—review and editing, D.N. and L.N.; visualization, L.N.; supervision, D.N.; funding acquisition, D.N. All authors have read and agreed to the published version of the manuscript.

Funding: This research was funded by by Czech Science Foundation under project No. 18-13212S and the support provided by the Czech Ministry of Education, Youth and Sports under project No. FAST-J-20-6417. The first author is Brno Ph.D. Talent Scholarship Holder—Funded by the Brno City Municipality.

Conflicts of Interest: The authors declare no conflicts of interest.

References

1. Cornell, C.A. A probability based structural code. *J. Am. Concr. Inst.* **1969**, *66*, 974–985.
2. Comité Européen de Normalisation (CEN). *EN 1990: Eurocode: Basis of Structural Design*; Comité Européen de Normalisation: Brussels, Belgium, 2002.
3. Hasofer, A.M.; Lind, N.C. Exact and Invariant Second-moment Code Format. *J. Eng. Mech. Div.* **1974**, *100*, 111–121.
4. Rosenblatt, M. Remarks on a multivariate transformation. *Ann. Math. Stat.* **1952**, *23*, 470–472. [[CrossRef](#)]
5. Pimentel, M.; Brühwiler, E.; Figueiras, J. Safety examination of existing concrete structures using the global resistance safety factor concept. *Eng. Struct.* **2014**, *70*, 130–143. [[CrossRef](#)]
6. Cervenka, V. Reliability-based non-linear analysis according to fib Model Code 2010. *Struct. Concr.* **2013**, *14*, 19–28. [[CrossRef](#)]
7. Val, D.; Bljucer, F.; Yankelevsky, D. Reliability evaluation in nonlinear analysis of reinforced concrete structures. *Struct. Saf.* **1997**, *19*, 203–217. [[CrossRef](#)]
8. Cervenka, V. Global Safety Format for Nonlinear Calculation of Reinforced Concrete. *Beton Und Stahlbetonbau* **2008**, *103*, 37–42. [[CrossRef](#)]
9. Schlune, H.; Plos, M.; Gylltoft, K. Safety formats for nonlinear analysis tested on concrete beams subjected to shear forces and bending moments. *Eng. Struct.* **2011**, *33*, 2350–2356. [[CrossRef](#)]
10. Bertagnoli, G.; Giordano, L.M.; Mancini, G.F. Safety format for the nonlinear analysis of concrete structures. *Studi e Ricerche- Politecnico di Milano. Scuola di Specializzazione in Costruzioni in Cemento Armato* **2004**, *25*, 31–56.

11. McKay, M.D. Latin Hypercube Sampling as a Tool in Uncertainty Analysis of Computer Models. In Proceedings of the 24th Conference on Winter Simulation, Arlington, VA, USA, 13–16 December 1992; pp. 557–564.
12. Iman, R.L.; Conover, W. Small sample sensitivity analysis techniques for computer models with an application to risk assessment. *Commun. Stat. Theory Methods* **1980**, *9*, 1749–1842. [[CrossRef](#)]
13. Sudret, B. Global sensitivity analysis using polynomial chaos expansions. *Reliab. Eng. Syst. Saf.* **2008**, *93*, 964–979. [[CrossRef](#)]
14. Blatman, G.; Sudret, B. An adaptive algorithm to build up sparse polynomial chaos expansions for stochastic finite element analysis. *Probabilistic Eng. Mech.* **2010**, *25*, 183–197. [[CrossRef](#)]
15. Echard, B.; Gayton, N.; Lemaire, M. AK-MCS: An active learning reliability method combining Kriging and Monte Carlo Simulation. *Struct. Saf.* **2011**, *33*, 145–154. [[CrossRef](#)]
16. Lehky, D.; Somodikova, M. Reliability calculation of time-consuming problems using a small-sample artificial neural network-based response surface method. *Neural Comput. Appl.* **2016**, *28*, 1249–1263. [[CrossRef](#)]
17. Melchers, R.E.; Beck, A.T. Second-Moment and Transformation Methods. In *Structural Reliability Analysis and Prediction*; John Wiley & Sons, Ltd: Hoboken, NJ, USA, 2017; Chapter 4, pp. 95–130, doi:10.1002/9781119266105.ch4. [[CrossRef](#)]
18. Paudel, A.; Thapa, M.; Gupta, S.; Mulani, S.B.; Walters, R.W. Higher-Order Taylor Series Expansion with Efficient Sensitivity Estimation for Uncertainty Analysis. In *AIAA Aviation 2020 Forum*; American Institute of Aeronautics and Astronautics: Reston, VA, USA, 2020.
19. Sykora, M.; Cervenka, J.; Cervenka, V.; Mlcoch, J.; Novak, D.; Novak, L. Pilot comparison of safety formats for reliability assessment of RC structures. In Proceedings of the fib Symposium 2019: Concrete—Innovations in Materials, Design and Structures, Kraków, Poland, 27–29 May 2019; pp. 2076–2083.
20. Novák, L.; Novák, D.; Pukl, R. Probabilistic and semi-probabilistic design of large concrete beams failing in shear. In *Advances in Engineering Materials, Structures and Systems: Innovations, Mechanics and Applications*; Taylor and Francis Group CRC Press: London, UK, 2019.
21. Novák, D.; Novák, L.; Slowik, O.; Strauss, A. Prestressed concrete roof girders: Part III—Semi-probabilistic design. In Proceedings of the Sixth International Symposium on Life-Cycle Civil Engineering (IALCCE 2018), Ghent, Belgium, 28–31 October 2018; pp. 510–517.
22. Lebrun, R.; Dutfoy, A. An innovating analysis of the Nataf transformation from the copula viewpoint. *Probabilistic Eng. Mech.* **2009**, *24*, 312–320. [[CrossRef](#)]
23. Lebrun, R.; Dutfoy, A. Do Rosenblatt and Nataf isoprobabilistic transformations really differ? *Probabilistic Eng. Mech.* **2009**, *24*, 577–584. [[CrossRef](#)]
24. Comité Européen de Normalisation (CEN). *EN 1992: Eurocode 2: Design of Concrete Structures*; Comité Européen de Normalisation: Brussels, Belgium, 2004.



© 2020 by the authors. Licensee MDPI, Basel, Switzerland. This article is an open access article distributed under the terms and conditions of the Creative Commons Attribution (CC BY) license (<http://creativecommons.org/licenses/by/4.0/>).

C Neural network Ensemble-based Sensitivity Analysis in Structural Engineering: Comparison of Selected Methods and the Influence of Statistical Correlation

DOI: 10.1016/j.compstruc.2020.106376

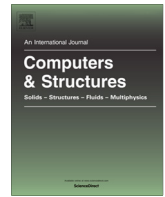
C.1 Description

The paper is focused on the comparison of selected methods for sensitivity analysis coupled with artificial neural network ensemble with a significant attention given to the influence of statistical correlation. In the first part of the paper, the theory of sensitivity techniques and interpretation of results is presented together with the theoretical background of the artificial neural network ensemble. Specifically, the following sensitivity methods were investigated: the input perturbation method, local analysis of variance, the connection weight method, non-parametric Spearman rank-order correlation and Sobol indices. The presented methods were applied to three examples: a simple analytical function, an analytical formula for deflection of the simply supported beam, and finally a non-linear finite element model of a real structure.

C.2 Role of the Ph.D. Candidate

Percentage of contribution: 40%

Lukáš Novák created the methodology and concept of this paper. The selected methods for sensitivity analysis were coupled with the artificial neural networks ensemble by Lixia Pan under the supervision of Lukáš Novák, and the obtained results were compared to the reference solution obtained by polynomial chaos expansion. Moreover, he prepared a significant part of the original draft, which was later reviewed in cooperation with Lixia Pan under the supervision of Drahomír Novák, David Lehký, and Maosen Cao.



Neural network ensemble-based sensitivity analysis in structural engineering: Comparison of selected methods and the influence of statistical correlation

Lixia Pan^{a,*}, Lukáš Novák^b, David Lehký^b, Drahomír Novák^b, Maosen Cao^a

^a College of Mechanics and Materials, Hohai University, No.8 Focheng West Road, 211100 Nanjing, China

^b Institute of Structural Mechanics, Faculty of Civil Engineering, Brno University of Technology, Veveří 95, 66237 Brno, Czech Republic

ARTICLE INFO

Article history:

Received 22 February 2020

Accepted 27 August 2020

Keywords:

Global sensitivity analysis

Local sensitivity

Statistical correlation

Neural network ensemble

ABSTRACT

Surrogate model-based sensitivity analysis, especially framed by neural network ensemble (NNE), is an attractive but unresolved issue in structural reliability assessment. In this paper, differing from existing studies, an overview and assessment of typical methods for surrogate model-based parameter sensitivity analysis, namely the input perturbation method, the local analysis of variance, the connection weight method, the non-parametric Spearman rank-order correlation method, and the Sobol indices method, are performed and demonstrated on three illustrative cases of increasing complexity: a simple theoretical instance, an engineering case of midspan deflection of a simply-supported beam, and a real-world practical application of shear failing in a precast concrete girder. Through comprehensive comparisons, several findings are obtained as follows: (i) the NNE is testified a superior surrogate model for sensitivity analysis to a single artificial neural network; (ii) robustness and accuracy of an NNE in sensitivity analysis are demonstrated; (iii) the properties of these parameter sensitivity analysis methods are fully clarified with distinguished merits and limitations; (iv) mechanism of local- and global- sensitivity analysis methods is revealed; and (v) the strategy for sensitivity analysis of correlated descriptive variables are elaborated to address the impact of correlation among random variables in engineering systems.

© 2020 Elsevier Ltd. All rights reserved.

1. Introduction

The consideration of uncertainties in computational mechanics for structural reliability assessment has been a topic of growing importance during the last few decades, as it can provide valuable information as to the reliability of engineering structures [1]. These uncertainties generally affect input variables such as geometry, materials, loads and environment-related properties. These random variables operate within several stages of computational modelling. Moreover, they are often statistically correlated. The main aim of stochastic computational modelling is to propagate uncertainties through a mathematical model in order to obtain statistical information on outputs, which are typically structural responses such as ultimate capacity, deflection, etc. This process is often called uncertainty propagation, or the statistical analysis of a computational model.

In computational mechanics, computational models (mathematical functions) are often defined using the finite element

method (FEM). This imposes a high computational burden, especially when calculating structures made of materials that exhibit nonlinear response and under nonlinear vibration [2]. The situation is even worse when the reliability analysis of structures is performed in a fully probabilistic manner. This means carrying out a large set of Monte Carlo-type numerical simulations, the number of which increases as the expected failure probability decreases. This process may be highly time-consuming without a surrogate model.

To overcome the above-mentioned high computational burden, it is desirable to employ methods which replace the initial computationally expensive model with a simpler model that can be evaluated more quickly. This approach is called surrogate modelling, meta-modelling or the response surface (RS) method in cases when the original function represents a limit state function. Together with sensitivity analysis (SA), it is a very important part of structural reliability assessment [3–5]. A great many improvements have been proposed since the first use of surrogate modelling in reliability analysis [6]. Recent contributions have been concerned with kriging [7,8], support vector machine algorithms [9,10] and polynomial chaos expansion [11–13]. Adaptive schemes are also

* Corresponding author.

E-mail address: plxxak@163.com (L. Pan).

of great interest since they allow more precise results to be obtained with a reduced number of simulations. Despite their differences, the main steps of these procedures are always the same: First, an initial experimental design is chosen – supporting points in a multi-dimensional space of random variables. Second, a specific type of RS is built. The idea was first introduced by Bucher and Bourgund [14], who used (in turn) double RS. They build supporting points using a star-shaped experimental design around the mean point. Rajashekhar and Ellingwood [15] suggested that this method could be improved by considering several iterations until a convergence criterion is satisfied. Once the surrogate model is available, it is feasible to perform a large number of evaluations in a matter of seconds. Note that it is of paramount importance for many types of sensitivity analysis to achieve such a drastic time reduction.

Sensitivity analysis (SA) is a crucial part of computational modelling and assessment [16]. It is an important step in every simulation and assessment, which is why it has received so much attention in the literature over the past decades. SA is important for the reduction of the space of random variables for stochastic calculations, the building of response surfaces, the training of neural networks, etc. Several interrogations are possible and several SA methods have been developed, giving rise to a vast and growing body of literature. An overview of the available methods is given in review papers such as those of Novák et al. [17], Kleijnen [18], Antucheviciene et al. [19] and Borgonovo and Plischke [20].

There are generally two types of sensitivity analysis. Local sensitivity analysis focuses on the behaviour of a function around a point of interest (e.g. one-at-a-time and screening). Global sensitivity analysis investigates the whole design domain, considering the probability distribution of input random variables. Local and global sensitivity analyses have different purposes and the interpretation of their results is frequently inaccurate or even erroneous. This is because the user often employs just one “available” method and states global conclusions without deeper knowledge of the problem.

Artificial neural networks (ANNs) are powerful, flexible, versatile techniques which are often employed as surrogate models in the solution of various types of engineering problem, including prediction, classification, approximation, etc. [21–27]. Apart from these prevailing applications, the use of ANNs to perform parameter sensitivity analysis for engineering systems is still uncommon, although the huge potential of ANNs has become evident in this area of research.

Many researchers currently engaged in the use of ANNs for parameter sensitivity analysis focus on the employment of a single ANN [28–36]. Compared to a single ANN, a neural network ensemble (NNE) is a construct made up of many neural networks which are jointly used to solve a particular task. The ensembling of multiple predictions is a widely used technique for improving the accuracy of various tasks. Due to its higher generalization ability, an NNE is more accurate than a single ANN, leading to more precise and reliable results [37–40]. Lehký et al. [41] compared an NNE with other two sensitivity analyses techniques applied to prestressed concrete girders. NNEs also have the potential to be used in efficient surrogate modelling in close connection with sensitivity analysis. This aspect has not been studied until now.

As already mentioned, statistical correlation among random variables plays an important role in statistical and reliability analyses and cannot generally be neglected. The probabilistic analysis of mathematical models of correlated random input variables is an important current research topic [42,43]. On the other hand, the role of statistical correlation in sensitivity analysis has seen less investigation in the literature since its effect is usually hard to interpret [44].

This paper serves to complement the parameter sensitivity analysis of NNE for engineering system and to exploit the potentiation of NNE as a powerful tool in engineering application. What is more, the unsolved issue of dependent input random variables, which is universally encountered in engineering, is addressed. We also provide guidance for an engineer to select the proper sensitivity analysis method. This paper is structured as follows. In Section 2, the element neural network of NNE applied in this paper and the general procedure of NNE are briefly described. Then five selected methods of parameter sensitivity analysis are introduced in Section 3. They are the input perturbation method, local analysis of variance, the connection weight method, non-parametric Spearman rank-order correlation and Sobol indices. To better understand the correlation among the inputs, the statistical correlation is presented in Section 4. In Section 5, comparisons are made among the five proposed methods in three examples of increasing complexity – a simple theoretical example, an engineering example and a complex application concerning a precast concrete girder failing in shear. Moreover, the role of statistical correlation among random variables is investigated in depth, as all examples are performed in both correlated and uncorrelated spaces of input random variables. The merits and limitations of the five selected sensitivity analysis methods are summarized. Section 6 shows the conclusions.

2. Framework of the neural network ensemble

2.1. Artificial neural network

It can be seen from the existing literature that surrogate models such as kriging, radial basis functions, artificial neural networks, etc. are widely used [45]. In this study, an NNE, which comprises a finite number of artificial neural networks, is applied as the surrogate model because of its ability to model complex systems accurately and stably. The artificial neural network that is used as the basic form/element of the NNE model applied in this study is represented by the following equation:

$$T = f_2 \left(\sum_j \mathbf{W}_2 f_1 \left(\sum_i \mathbf{W}_1 \mathbf{P} + \theta_1 \right) + \theta_2 \right) \quad (1)$$

where $\mathbf{P} = (p_1, \dots, p_m)$ are the independent variables (ANN inputs), $\mathbf{T} = (T_1, \dots, T_s)$ are the dependent variables (ANN outputs), \mathbf{W}_1 and θ_1 are the weights and biases between the input layer and hidden layer, \mathbf{W}_2 and θ_2 are the weights and biases between the hidden layer and output layer, and f_1 and f_2 are pre-defined activation functions, e.g. hyperbolic tangent, sigmoid function, softmax function, linear function. The neural network modelling starts with random initial weights and biases. A set of samples of independent variables are passed through the model and then the predictions are obtained. A comparison is made between the predictions and the desired results of the dependent variables, and the loss they incurred is calculated. Then the calculated loss is back propagated to every one of the parameters that make up the model of the neural network so that the weights and biases of the neural network are updated to reduce the loss. The step of updating weights and biases is based on some optimization, e.g. gradient descent, Levenberg-Marquardt algorithm, Newton etc. In this study, the Levenberg-Marquardt algorithm is applied with its fast and stable convergence [46]. To avoid the overfitting, the Bayesian regularization is used [47,48]. The above processing is iterated until good predictions are obtained. The criterion index used to evaluate the predictions is the mean square error (MSE), which is defined:

$$MSE = \frac{1}{N} \sqrt{\sum_{k=1}^N (h(k) - T(k))^2} \quad (2)$$

where MSE means the mean square error, N is the number of training samples; $h(k)$ are the real (desired) dependent variables, and $T(k)$ are the outputs calculated by the neural network.

The MSE is obtained after the training of each neural network. In step 3 (see the following subsection), the training of each neural network candidate, which is repeated t times, results in a statistical distribution (the mean value μ and the standard deviation σ) of the MSEs. This can be used as the criteria for the selection of a superior neural network. μ reflects the average accuracy of the neural network and σ shows the network's stability.

2.2. Concept and procedure

A neural network ensemble is a construct made up of many neural networks which are jointly used to solve a problem [37]. The fundamental mathematical idea of a neural network ensemble rationally originates from *the weak law of large numbers in probability* [49]. According to the law, the average of the results obtained from a large number of trials should be close to the expected value and will tend to become closer as more trials are performed. However, during the practical operation of neural network ensembles it is not possible to meet the requirement that the law only applies (as the name indicates) when a large number of observations is considered. In this situation, the mathematical optimization concept that *many could be better than all* [37] is a valuable means of gaining a better result. It entails picking out excellent neural networks and eliminating the poorer ones via a specific procedure.

The procedure of using the NNE to perform prediction, classification, and sensitivity analysis involves four basic steps:

Step 1: The creation of a basic neural network (called the seed) which correctly captures the intrinsic relationship between the explicative and dependent variables.

Step 2: The use of the seed network to produce a family of k candidate neural networks with dissimilar network structures.

Step 3: The repeated training of all candidate networks t times with different numbers of hidden layers or different numbers of hidden neurons. Subsequently, N ($N \leq k$) superior neural networks with better performance (see the statistical characteristics of MSEs) are selected to form an NNE.

Step 4: The repeated training of each superior neural network M times (here the topological structure of the neural network is fixed, while the synaptic weights and biases are adjusted during the training course). Then, the post-processing of the results including prediction/sensitivity can be carried out. The type of post-processing depends on its purpose: the validation of the neural network by verifying the accuracy of the predicted outputs, or the obtaining of sensitivity analysis results. In order to validate the neural network's performance, the average of $N \times M$ results is used. The particular steps to be taken during post-processing in order to obtain sensitivity measurements depending on the specific method of sensitivity analysis will be described in Section 3.

Through the four steps, the stability and robustness are improved. The selection of a superior neural network in step 3 and the repeated training of each superior neural network in step 4 lead to a decrease in the uncertainty of the neural structures. The integration of $N \times M$ results equalizes the different conditions to show a more general result.

Fig. 1 shows a schematic view of NNE-based parameter sensitivity analysis, including all of the above-mentioned components such as the seed, candidate networks, NNE and summary.

3. Selected methods of parameter sensitivity analysis

A number of parameter sensitivity analysis methods exist in the literature. They are classified into local and global sensitivity analysis methods. The methods selected among them for this study comprise the input perturbation algorithm, local sensitivity analysis of variance, the connection weight method, non-parametric Spearman rank-order correlation and global sensitivity analysis

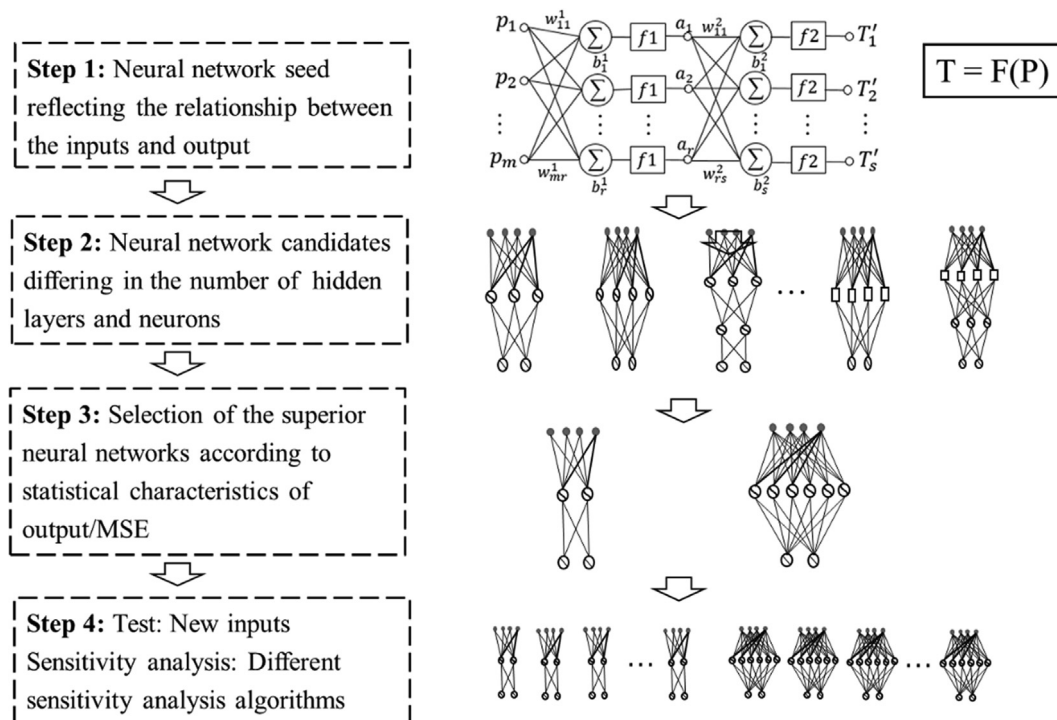


Fig. 1. Schematic view of neural network ensemble-based sensitivity analysis.

of variance (ANOVA) – Sobol indices. The basic concept and usage of these methods are briefly introduced in this section.

3.1. Input perturbation algorithm

The input perturbation algorithm [50] is the simplest way to interrogate a model. It produces sensitivity analysis results based on the assessment of the effect of input perturbation in each input on the neural network output [51]. The proper adjustment of the values of each explicative variable while keeping all the others unchanged allows the effect of the output variables corresponding to each perturbation in the input variable to be recorded. The result of sensitivity analysis is yielded by ranking the effect on neural network output induced by the same manner of perturbation in every input variable. The input variable whose perturbation influences the output most possesses the highest sensitivity or importance.

In principle, the MSE of a neural network’s output increases as the selected input variable increases. The changes to the input variable take the form of $x_i = x_i + \delta$, where x_i is the selected input variable and δ is the perturbation value. The input variables can be ranked according to the increasing magnitude of the MSE due to each input variable change. In other words, the result is a sensitivity analysis outcome.

It is common to choose a perturbation value δ as an increment or decrement in the percentage of the input variable. However, this approach fails to take into account the specific variance of random variables. Therefore, an alternative approach can be recommended where δ is represented by a standard deviation e.g. $\pm 3\sigma$. This alternative approach directly reflects the variability of every input random variable [52].

3.2. Local analysis of variance

The simple analysis of variance technique, which focuses on the area around mean values, can be seen as a study of the influence of the uncertainty of a given variable. Such a study may be desired in engineering practice for the identification of important variables and the improvement of quality control (e.g. of the quality of concrete mixture) in order to achieve lower uncertainty in the behaviour of a structure.

The idea behind the method is straightforward and simple: What is the influence of the variance of the i th random variable on the variance of the mathematical model result? Novak et al. [17] proposed a simple method within which it is necessary to generate n sets of realizations while assuming the i th variable to be random and keeping other variables at their mean values. This method can be easily improved in order to take interaction among random variables into account. In that case, the sensitivity indicator is obtained by estimating the variance of the given mathematical model while assuming the fixed i th variable is at its mean value μ and all other variables are free to vary. The sensitivity indicator can be then obtained as follows:

$$O_i = 1 - \frac{\sigma_i}{\sigma_{\text{original}}} \quad (3)$$

where σ_i is the standard deviation of the output if the i th input is fixed at μ and σ_{original} is the standard deviation of the output whose realizations are the original data (all random variables are free to vary). It is clear that the value O_i is close to one for the most important variables. In other words, $O_i = 1$ means that all of the variability in our mathematical model is caused only by the i th random variable and that the other variables do not have a significant influence on the variability of the result. Note that in some cases it is even possible to obtain indices with a negative value (especially in the case of correlated random variables), which

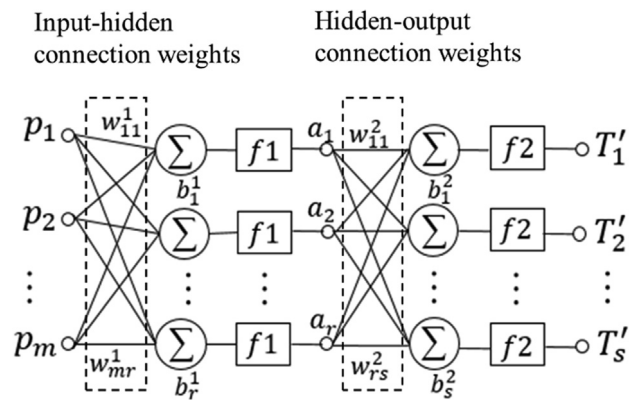


Fig. 2. The structure of a neural network with one hidden layer.

means that fixing the i th variable can actually increase the variability of a mathematical model. This result is surprising and reflects the significant role of statistical correlation and the weakness of the overly simple analysis of variance technique.

3.3. Connection weight method

The connection weight method [53], which is an evolution of Garson’s algorithm, calculates the importance values assigned to each input random variable by the summed product of raw input-hidden and hidden-output connection weights (shown in Fig. 2). The actual values should only be interpreted based on the relative sign and magnitude between explanatory variables. Explanatory variables with larger connection weights represent greater signal transfer intensities, and therefore are more important in the prediction process than variables with smaller weights. Negative connection weights represent inhibitory effects on neurons (reducing the intensity of the incoming signal) and decrease the value of the predicted response, whereas positive connection weights represent excitatory effects on neurons (increasing the intensity of the incoming signal) and increase the value of the predicted response. The importance value can be then obtained as follows:

$$R_{is} = \sum_{j=1}^r w_{ij} w_{js} \quad (4)$$

where R_{is} means the importance value of the i th input with respect to the output neuron s , w_{ij} represents the connection weight between the input neuron i and the hidden neuron j , and w_{js} stands for the connection weight between the hidden neuron j and the output neuron s .

In this study, based on the importance value, there are two evolution results: qualitative description by ordinal number and quantitative illumination by relative value. As for the qualitative description, in every training, the influence of the input is ranked according to the importance value, e.g. the most influential input whose ordinal number is 1. Through integration, there are $N \times M$ ordinal numbers of each input, then sum them up. Based on the sum, re-rank the inputs again; the smaller the sum, the more important the input is. As for the quantitative value, in every training, the important value needs to be normalized as follows,

$$RR_{is} = \frac{R_{is}}{\sum_{i=1}^m R_{is}} \quad (5)$$

RR_{is} is the relative importance value of the i th input to sth output among all the m inputs.

Through integration, there are $N \times M$ normalized importance values of each input, then make average of them. Based on the average value, the influence of the input could be illuminated by

the detail value. The larger the average value is, the more important the input is.

3.4. Non-parametric Spearman rank-order correlation

The traditional sensitivity analysis method in statistics is represented by the correlation between an input variable and the quantity of interest of mathematical model [54]. Although standard measurement via the Pearson correlation coefficient is simple and efficient enough for linear monotonic dependency, it is necessary to utilize a generalized measure for nonlinear monotonic relationships called the non-parametric Spearman rank-order correlation technique [52,55]. This method is used to determine the relationship between two variables. For example, \mathbf{X} and \mathbf{Y} are two sets of variables. Through being sorted in an ascending order, the corresponding ordinal numbers of $\mathbf{X} = (x_1, x_2, \dots, x_i, \dots, x_n)$ and $\mathbf{Y} = (y_1, y_2, \dots, y_i, \dots, y_n)$ are $\mathbf{U} = (u_1, u_2, \dots, u_i, \dots, u_n)$ and $\mathbf{V} = (v_1, v_2, \dots, v_i, \dots, v_n)$, respectively, where $1 \leq i \leq n$, $1 \leq u_i \leq n$ and $1 \leq v_i \leq n$. The biggest value in one set belongs to the ordinal number 1, while the ordinal number n will get the smallest value. This should be done for both sets of measurements. The non-parametric Spearman rank-order correlation ρ is calculated according to the following equation:

$$\rho = 1 - \frac{6 \sum d_i^2}{n(n^2 - 1)} \quad (6)$$

$$d_i = u_i - v_i \quad (7)$$

where n is the number of data in one set; d_i is the difference in paired ranks; ρ will always be a value between -1 and 1 . The higher absolute value of ρ corresponds to the stronger relationship between the two variables. If it is positive, then as one variable increases, the other tends to increase. If it is negative, then as one variable increases, the other tends to decrease.

3.5. Global sensitivity analysis of variance (ANOVA) – Sobol indices

One of the most important tasks in uncertainty quantification is the analysis of variance – the analysis of the influence of input variables on the variance of a mathematical model. Such information may be utilized to practically reduce the uncertainty of important input variables (material characteristics) used in mathematical model by experiments and measurements, which leads to a significant reduction in the uncertainty of the quantity of interest. Herein, the well-known ANOVA method represented by Sobol indices [56,57] is employed. The Sobol indices method is the most advanced and well developed method for sensitivity analysis and thus is considered as a reference solution herein. However, it is still highly computationally demanding to evaluate Sobol indices via the classical double loop Monte Carlo method, and thus efficient calculation via Polynomial Chaos Expansion in the manner proposed in [58] is used. A software tool for the automatic creation and post-processing of PCE is employed [59] for the practical computation tasks required.

Let $\mathbf{X}=(X_1, \dots, X_M)$ be a random vector with independent marginal distributions and joint probability distribution denoted by $p_{\mathbf{X}}(\mathbf{x}) = p_{x_1} \otimes \dots \otimes p_{x_M}$. For any $\mathbf{x} \in \mathbb{R}^M$ and any subset $\mathbf{u} \subseteq I = \{1, \dots, M\}$, $\mathbf{x}_{\mathbf{u}}$ concatenates the components of \mathbf{x} whose indices are included in \mathbf{u} . According to Hoeffding-Sobol decomposition, any square-integrable function $f(\mathbf{X})$ can be decomposed as:

$$\begin{aligned} f(\mathbf{x}) &= f_0 + \sum_{i=1}^M f_i(x_i) + \sum_{1 \leq i < j \leq M} f_{ij}(x_i, x_j) + \dots + f_{1,2,\dots,M}(\mathbf{x}) = \\ &= f_0 + \sum_{\substack{\mathbf{u} \subseteq \{1, \dots, M\} \\ \mathbf{u} \neq \emptyset}} f_{\mathbf{u}}(\mathbf{x}_{\mathbf{u}}). \end{aligned} \quad (8)$$

In consequence of the defined decomposition, the variance of Y can be decomposed as:

$$\sigma_Y^2 = \text{Var}[Y] = \sum_{\substack{\mathbf{u} \subseteq \{1, \dots, M\} \\ \mathbf{u} \neq \emptyset}} \text{Var}[f_{\mathbf{u}}(\mathbf{x}_{\mathbf{u}})], \quad (9)$$

where $\text{Var}[f_{\mathbf{u}}(\mathbf{x}_{\mathbf{u}})]$ are partial variances. The first Sobol' indices are obtained if \mathbf{u} contains a single i -th input variable, i.e.:

$$S_i = \frac{\text{Var}[f_i(X_i)]}{\text{Var}[Y]} \quad (10)$$

The second-order indices correspond to two input variables etc. Important information about the influence of input variables and all interactions can be expressed by total Sobol indices, which include all interactions, and thus may be computed as

$$S_i^T = \sum_{\mathbf{u} \in \mathbf{u}} S_{\mathbf{u}} \quad (11)$$

Due to the statistical dependence among input random variables, it is not possible to derive a unique decomposition in terms of orthogonal summands of increasing order. However, it is possible to cast the variance of Y as a covariance decomposition (ANCOVA). More theoretical details can be found in [60]. The estimation of covariance decomposition via PCE consists of two steps:

- building a PCE $f(\mathbf{X})$ approximation assuming uncorrelated random variables
- using the PCE as a surrogate model in order to evaluate the variance of output with the correlated input variables $f(\mathbf{X}_c)$

The variance of the model response, assuming correlated input random variables, is defined as

$$\text{Var}[f(\mathbf{X}_c)] = \sum_{\substack{\mathbf{u} \subseteq \{1, \dots, M\} \\ \mathbf{u} \neq \emptyset}} \text{Cov}[f_{\mathbf{u}}(\mathbf{X}), f(\mathbf{X}_c)] \quad (12)$$

The covariance-based total sensitivity index S_i^{cov} is then obtained as:

$$S_i^{\text{cov}} = \frac{\text{Cov}[f_{\mathbf{u}}(\mathbf{X}), f(\mathbf{X}_c)]}{\text{Var}[f(\mathbf{X}_c)]} \quad (13)$$

which can be further decomposed into the sum of a structural (uncorrelated) sensitivity index, S_i^u , and a correlative sensitivity index, S_i^c , defined as:

$$S_i^u = \frac{\text{Var}[f_{\mathbf{u}}(\mathbf{X})]}{\text{Var}[f(\mathbf{X}_c)]} \quad (14)$$

$$S_i^c = S_i^{\text{cov}} - S_i^u \quad (15)$$

The global ANCOVA method is a very powerful technique, though problems often occur when interpreting the results [44].

4. Statistical correlation

It is clear that sensitivity analysis plays an important role in the stochastic analysis of structures. Moreover, it is important to understand and clearly interpret the results obtained from different types of sensitivity analysis. Such information could be strongly influenced by statistical correlation among material characteristics. Therefore, it is important to understand the differences between results gained for correlated and uncorrelated random variables. Herein, the commonly known and widely used Nataf transformation technique is utilized for the transformation of realizations to correlated space, as will be briefly described in this section.

In the general case of non-normal correlated random variables, it is necessary to use a more complicated process for transformation, called Rosenblatt transformation [61]. However, in practical applications only the marginal distributions and correlation matrix are usually known, which does not represent a complete information about the joint probability distribution [62]. Therefore, it is necessary to assume a specific copula [63]. A special case of Rosenblatt transformation that assumes a Gaussian copula is also known as Nataf transformation [64], which is very often utilized in reliability applications. The Nataf transformation to uncorrelated standard normal space is composed of 3 steps and proceeds as follows (see Fig. 3):

$$\xi = T_{Nataf}(\mathbf{X}) = T_3^{\circ} T_2^{\circ} T_1(\mathbf{X}) \quad (16)$$

The first two steps represent an isoprobabilistic transformation to correlated standard normal space:

$$T_1 : \mathbf{X} \rightarrow \mathbf{W} = F_x(\mathbf{X}) \quad (17)$$

$$T_2 : \mathbf{W} \rightarrow \mathbf{Z} = \Phi^{-1}(\mathbf{W}) \quad (18)$$

The last step represents a transformation to uncorrelated space using linear transformation. For this procedure, Cholesky decomposition of the correlation matrix is commonly utilized:

$$\mathbf{R}_Z = \mathbf{L}\mathbf{L}^T \quad (19)$$

$$T_3 : \mathbf{Z} \rightarrow \xi = \mathbf{\Gamma}\mathbf{Z} \quad (20)$$

\mathbf{R}_Z is a fictive correlation matrix and $\mathbf{\Gamma}$ is the inverse of a lower triangular matrix, \mathbf{L} , obtained via Cholesky decomposition. The assumed Gaussian copula is parametrized by elements ρ_{zij} of \mathbf{R}_Z and the relationship between the fictive correlation coefficients ρ_{zij} and the linear correlation coefficients defined in physical space ρ_{xij} is defined by the following integral equation:

$$\rho_{xij} = \frac{1}{\sigma_i \sigma_j} \iint \{F_i^{-1}[\Phi(Z_i)] - \mu_i\} \cdot \{F_j^{-1}[\Phi(Z_j)] - \mu_j\} \times \varphi_2(Z_i, Z_j, \rho_{zij}) dz_i dz_j, \quad (21)$$

where μ is a mean value, σ is a standard deviation and φ_2 is the bivariate standard normal probability density function with the fictive correlation coefficients ρ_{zij} :

$$\varphi_2(Z_i, Z_j, \rho_{zij}) = \frac{1}{2\pi\sqrt{1-\rho_{zij}^2}} \exp\left(-\frac{Z_i^2 - 2\rho_{zij}Z_iZ_j + Z_j^2}{2(1-\rho_{zij}^2)}\right). \quad (22)$$

The whole process can be simply reversed to transform the realizations $\xi \rightarrow \mathbf{X}$. The reverse approach is employed for the generation of correlated realizations of a random vector in the following examples.

5. Numerical examples

The comparison of the methods is performed in a progressive order starting from a theoretical example, then progressing to a simple engineering example, and finally moving on to a more complex practical application. The theoretical example concerns an analytical function of only two input random variables, while the engineering example is a formula for the midspan deflection of a simply-supported beam and the practical application deals with a precast concrete girder failing in shear. The sensitivity analysis is performed in two scenarios – one where the correlation among the input variables is considered, and the other where it is not. Therefore, the examples are treated in both a correlated and an uncorrelated space of basic random variables. For each case, the selected methods are compared and evaluated, and their advantages and disadvantages are highlighted.

5.1. Theoretical example: Analytical function

The first theoretical example is a simple analytical function which defines the numerical relationship between a response variable and two input random variables with standard Gaussian distribution (with zero mean and unit standard deviation):

$$y = x_1 + x_2 + x_2^2 + x_1 \times x_2 + 3 \quad (23)$$

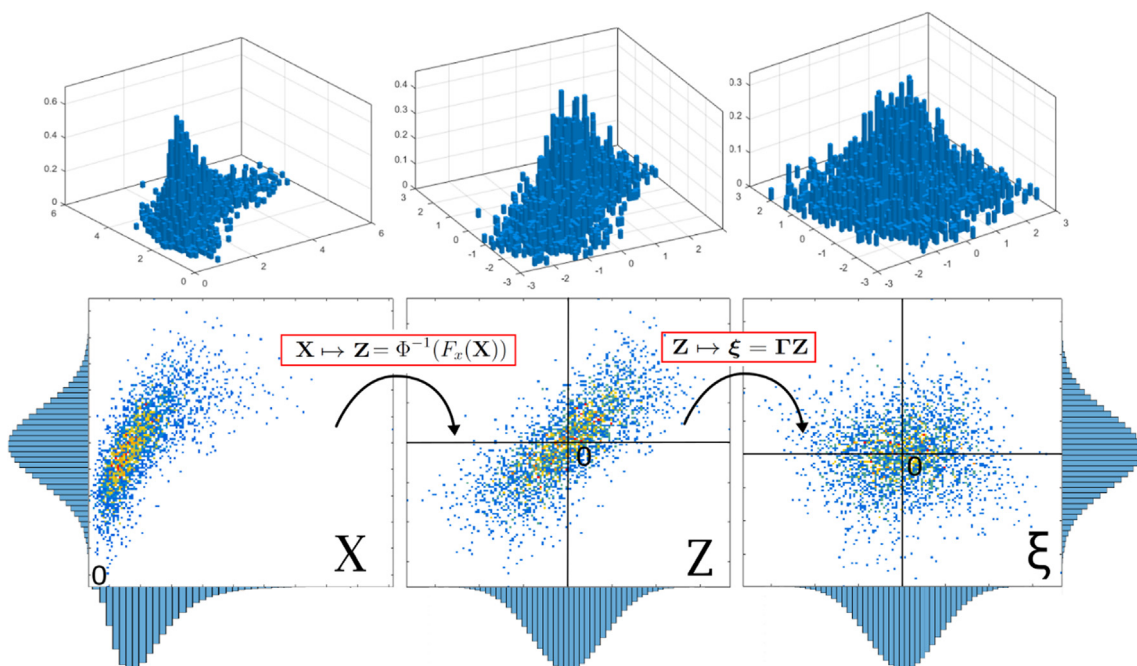


Fig. 3. Illustration of a Nataf transformation from an original space X to an uncorrelated standard normal space Z for a 2-dimensional case.

The realizations of the input random vector are generated by a Monte Carlo-type technique – the Latin Hypercube Sampling method [65], which is implemented in FReET software [66]. In this first example, it was decided that 10,000 simulations of the original model would be used as the training data set and 100 realizations as the testing data set for the validation of the approximation. The purpose of this example is to demonstrate the convergence of an approximation to an exact solution with a sufficient number of simulations. The evaluation of sensitivity indices is performed for both uncorrelated and correlated random variables, and the correlation coefficient used is 0.8. Therefore, it was necessary to perform the procedure described in Section 4 in order to generate correlated realizations assuming a Gaussian copula.

5.1.1. Sensitivity analysis with uncorrelated variables

A multilayer perceptron artificial neural network was selected as the seed, and it was utilized in the rest of the examples. 10 candidate neural networks with different numbers of hidden neurons were constructed as shown in Fig. 4. Each candidate neural network was repeated 15 times with 10,000 training realizations, which produced 15 sets of MSEs. The statistical characteristics of the MSEs are reference indices for the selection of the superior neural networks. The neural networks with low values for both the means and standard deviations of the MSEs are selected as neural networks with better performance. Here, neural networks with the structures 2-3-1 and 2-5-1 (i.e. the latter is a structure with two inputs, five hidden neurons and one output) were selected as the candidates for the neural network ensemble. To examine the robustness of the selected structures, comparisons were made between the real output of 100 new samples and the results calculated by the NNE, repeating each superior structure 15 times and calculating the average of 30 sets of results. Fig. 4 shows the good agreement between the exact results and the results calculated by the NNE (represented by the MSE which is close to zero, as can be seen in Fig. 4).

Once the neural network ensemble is available, it is possible to utilize it for sensitivity analysis. Herein, it was used in combination with several sensitivity analysis methods found in the literature and described in Section 3. First of all, the input per-

turbation method for local sensitivity analysis was performed. It is clear that the results of perturbation are strongly dependent on the perturbation parameter. Therefore, it was decided that sensitivity measurements would be determined in three locations of input space, as can be seen in Fig. 5 in the form of a bar diagram where the perturbation parameter varies by $\pm 10\%$, $\pm 30\%$ and ± 3 standard deviations of the input variable. As can be seen in Fig. 5, the MSE of x_2 is distinctly larger than that of x_1 . In other words, a change to the input parameter x_2 leads to a significantly higher change in the model output than in the case of input parameter x_1 .

The reference solution for global sensitivity analysis is to employ Sobol indices (ANOVA), which are computationally demanding even in combination with a surrogate model. Therefore, a simplified version of ANOVA was proposed in Section 3 under the name ‘local analysis of variance’. This approach may be of use to engineers and designers in the reduction of uncertainty. The idea behind this method can be seen in Fig. 6, where it is possible to see a comparison of the results of a mathematical model in which one variable is assumed to be a deterministic value and the variables of the original stochastic model are assumed to be free to vary. The method is based on the quantification of the reduction of output variability due to the reduction of input variability, which can be clearly seen in Fig. 6. If we assume x_2 is a mean value, the variability of the result drastically decreases. This means that x_2 is more important in the sense of variability reduction, as can be seen from the numerical results in Table 1, which are in agreement with the first order Sobol indices.

According to the connection weight method, after each importance value is obtained for the input, it is given an ordinal number as its rank. However, it is possible to observe that some variables have importance values that are very similar, thus making them difficult to differentiate. Consequently, the ranks determine whether one variable is more meaningful than another, but they do not specify by how much. The present study also used normalized importance values. In the ‘ANN weight’ column in Table 1, the number in bold script inside the brackets represents the sum of each input’s rank order, while the number in normal script means the normalized importance value. In this case, the sum of rank

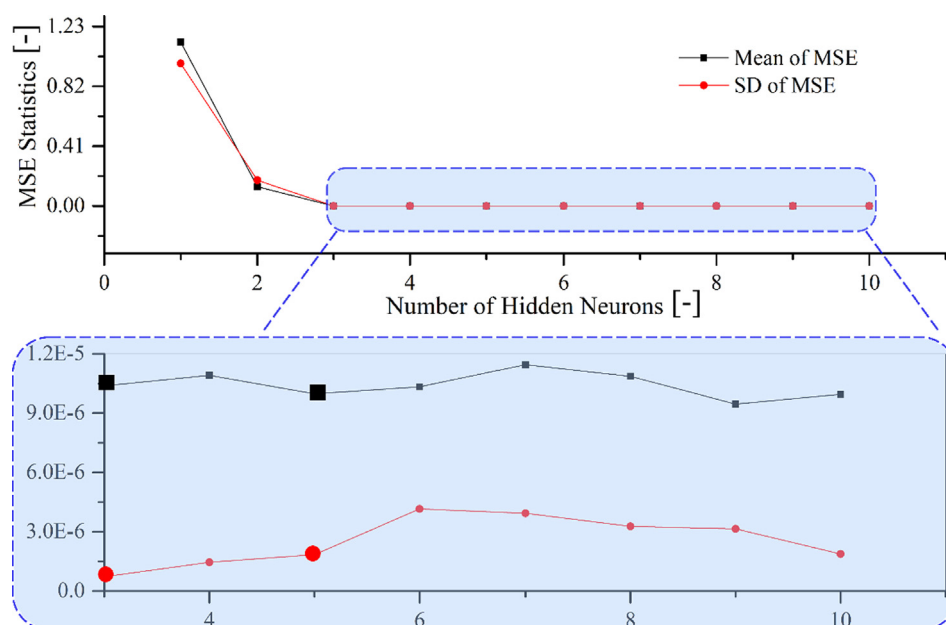


Fig. 4. The MSE information of different hidden neurons for a simple analytical function with uncorrelated variables.

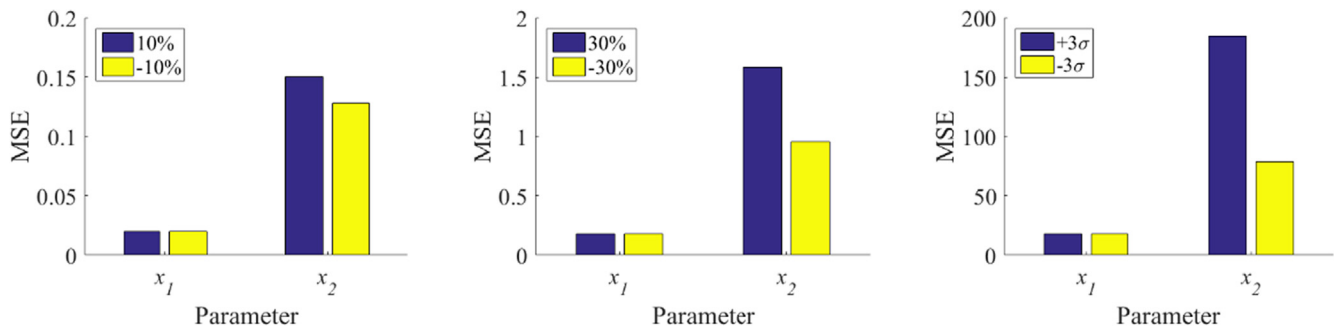


Fig. 5. The sensitivity results obtained by the input perturbation method for a simple analytical function with uncorrelated variables.

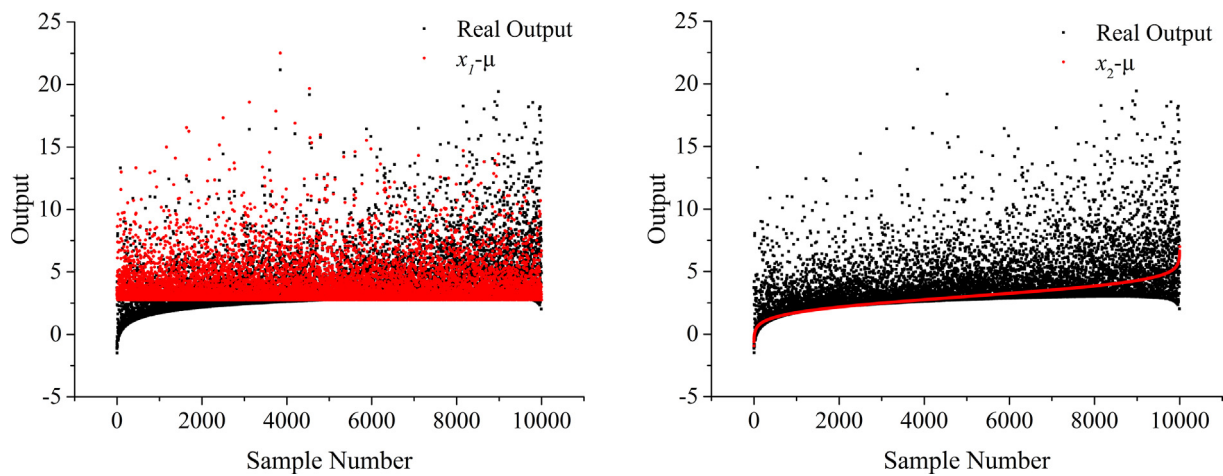


Fig. 6. The local analysis of variance for a simple analytical function with uncorrelated variables.

Table 1

The sensitivity results for a simple analytical function with uncorrelated variables.

Random variable	Non-parametric Spearman rank-order correlation	Sobol first order	Connection weight method	Local analysis of variance
x_1	1 (0.559)	2 (0.200)	2 (50/0.452)	2 (0.225)
x_2	2 (0.362)	1 (0.600)	1 (40/0.548)	1 (0.552)

(Note: the numbers outside the brackets are the rank order and those inside the brackets are the normalized sensitivities).

order shown in Table 1, x_1 is 50, and it is higher than x_2 . In other words, x_2 is more important than x_1 . As for the normalized importance value, x_1 is 0.452, while x_2 is 0.548. If the non-parametric Spearman rank-order correlation is excluded from Table 1, the ranks calculated by the proposed methods are identical.

5.1.2. Sensitivity analysis with correlated variables

It is necessary to assume statistical correlations among input random variables in many practical cases, and therefore the study of the influence of correlation is of high interest and represents a significant part of this study. In the first analytical example, an assumed correlation between two standard normal variables is given by the Pearson correlation coefficient as equal to 0.8. The whole process of ANN creation and sensitivity analysis was performed for correlated variables generated by Nataf transformation again, and the obtained results are presented in this subsection. The characteristics of the MSE were similar to those in the uncorrelated case in this very simple analytical function, as can be seen

in Fig. 7, and thus the complexity of the NNE was not increased – the selected structures were 2-3-1 and 2-4-1.

It is obvious that the correlation between input random variables can affect the results of sensitivity analysis, and therefore the results in the correlated space of this example are slightly different compared to those from the uncorrelated space. The results obtained from the input perturbation technique are depicted in Fig. 8.

In Table 2 the numerical results of global sensitivity methods are summarized. Please note that in correlated space it is possible to decompose Sobol first order indices into a correlative part and an uncorrelated part. Such information can play a significant role in the interpretation of obtained results, as will be described in the next subsection. From the connection weight method, the sum of rank order shown in Table 2, x_1 is 51, and it is higher than x_2 . In other words, x_2 is more important than x_1 . From the relative quantification of influence shown in Table 2, x_1 is 0.431 while x_2 is 0.569. This value is very similar to the results obtained for uncorrelated variables.

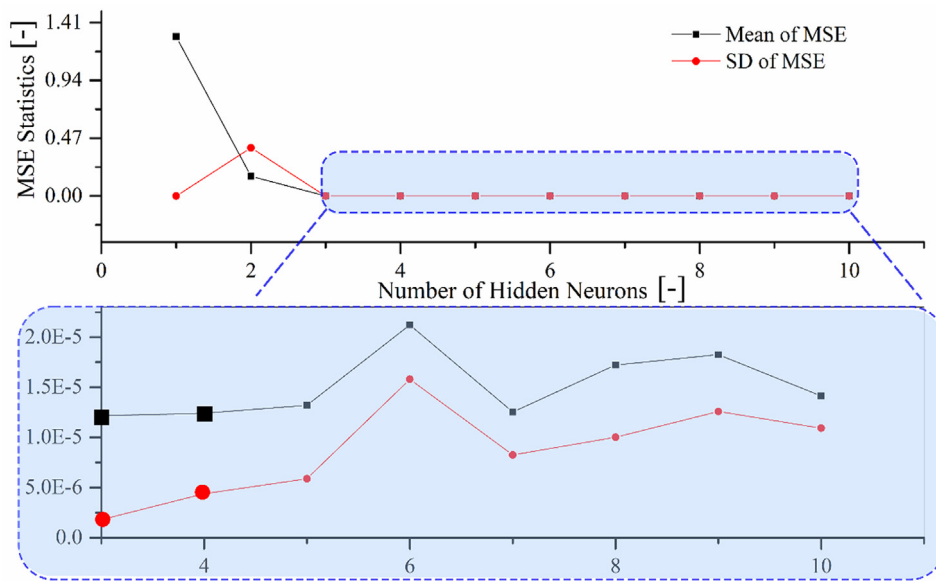


Fig. 7. The MSE information of different hidden neurons for a simple analytical function with correlated variables.

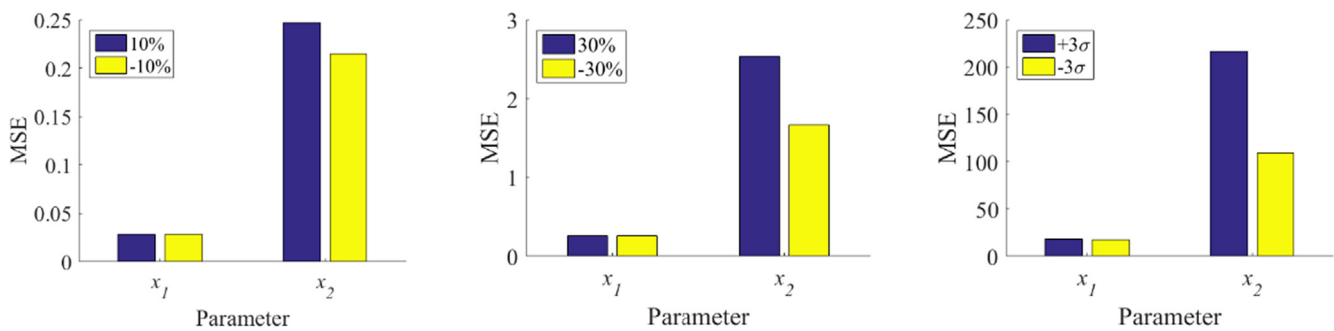


Fig. 8. The sensitivity results shown by the input perturbation method for a simple analytical function with correlated variables.

Table 2

The sensitivity results for a simple analytical function with correlated variables.

Random variable	Non-parametric Spearman rank-order correlation	Sobol first order	Sobol correlative part	Connection Weight method	Local analysis of variance
x_1	1 (0.640)	2 (0.190)	0.01	2 (51/0.431)	2 (0.432)
x_2	2 (0.566)	1 (0.540)	0.06	1 (39/0.569)	1 (0.671)

5.1.3. Comparison and remarks

In the case of the uncorrelated situation, the input perturbation method could exactly distinguish the most important/influential parameter: the MSE of x_2 is obviously larger than the MSE of x_1 . What is more, the differences between the yellow bar and blue bar in Fig. 5 show the linearity/nonlinearity of parameters. As for the nonlinear parameter, the output changes are different for the increased input and decreased input values with the same range (x_2 shows the nonlinearity). Global sensitivity methods examine the whole design space and thus can be represented by one specific value for the whole function in contrast to local sensitivity analysis methods such as input perturbation. Remember that the non-parametric Spearman rank-order correlation method gives us information about the strength and direction of the dependence between a specific input and output of a mathematical model, and thus represents an additional source of information together with variance based methods (Sobol indices and local analysis of variance).

As regards the correlated situation, input perturbation could also sort the parameters in terms of influence. With the presence of the correlation between x_1 and x_2 , the sensitivity gap between the parameters becomes smaller, which affects the results of the sensitivity analysis. This can be clearly seen in the results of the non-parametric Spearman rank-order correlation method, which naturally identified both input variables as being almost identically important for the mathematical model due to the fact that the higher values generated for one input variable correspond to the higher values obtained for the other input variables, which leads to higher results of mathematical model. Sobol first order and local analysis of variance are variance based methods, and thus the effect of correlation is not so significant. Although the connection weight method could quantify the influence of the parameters, it couldn't exactly distinguish the effect from the correlation among the input parameters. As the weights are parts of the neural network, the connection weight method ignores the influence of biases and the activation function.

5.2. Engineering example: Midspan deflection of a simply-supported beam

As a second, more complex example, the sensitivity analysis methods described above were applied to the following engineering example of the midspan elastic deflection of a simply-supported concrete beam with uniformly distributed load $v_{L/2}$. The stochastic model of the beam, which contains five random variables with lognormal distribution, is summarised in Table 3. b and H represent the width and height of the cross section, E is the Young's modulus of the concrete, q is the intensity of the uniformly distributed load and L is the length of the beam, as depicted in Fig. 9.

The mathematical model in explicit form is given by:

$$Y = v_{L/2} = \frac{5}{32} \frac{qL^4}{EbH^3} \quad (24)$$

5.2.1. Sensitivity analysis with uncorrelated variables

The 100 training realizations of a random vector were generated by the Latin Hypercube Sampling method. The same procedure was followed as in Section 2. After a trial run with 15 different neural network structures, shown in Fig. 10, the structures 5-12-1 and 5-14-1 were selected as the candidates for the neural network ensemble. Note that both structures have relatively low values for the mean and the standard deviation of the MSE.

The example was focused on the validation of the NNE approach via the quantification of statistical moments and failure probability for a given threshold of deflection by the NNE and the LHS technique. Note that once the NNE is available, it is possible to evaluate millions of simulations in a few seconds, and thus the approach can even be applied to highly time-consuming mathematical models. The reference value was obtained analytically in this simple equation and the results are compared in Tables 4 and 5. The statistical moments obtained by the NNE are in excellent agreement with those obtained analytically (see Table 4).

The accuracy of approximation can be validated clearly and in depth via the estimation of low probabilities, which is a challenging task for any type of surrogate model. In Table 5, there is a comparison between the results obtained by a single superior ANN and by an NNE. As can be seen, the NNE is able to estimate much lower probabilities (e.g. $10e-5$ or $10e-6$) even for a low number of training realizations. Note that the accuracy of a single ANN (which could not calculate failure probabilities at all for the thresholds of 25 and 30 mm in this case) can be improved for lower probabilities using the updating procedure proposed by Lehký and Šomodíková [67] in which a new set of training realizations are generated close to the design point. The updated surrogate model consequently fits the original function in the failure region better. Nevertheless, the NNE is able to provide more accurate results without the need to generate new training samples, which can certainly be considered as a significant advantage. Specific failure probabilities were calculated via the crude Monte Carlo simulation technique with 10^8 numerical simulations of the surrogate model.

Once the NNE was available, it was possible to perform sensitivity analysis for 5 input random variables in the same manner as in

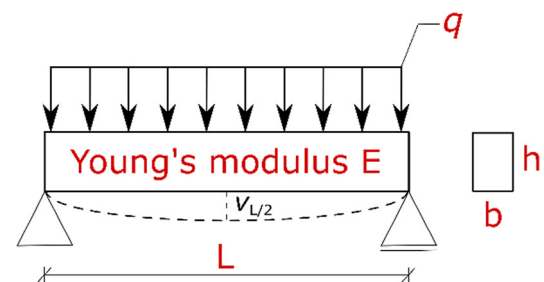


Fig. 9. The simple beam.

the previous example. The results obtained from the global sensitivity methods for uncorrelated space are summarized in Table 6, and it is clear that load intensity q is the most important variable from the global point of view. Nevertheless, the results of local sensitivity analysis via the perturbation method (see Fig. 11) do not correspond to that conclusion. According to the diagrams, it is clear that the results of local sensitivity analysis are highly dependent on the location of interest. This important characteristic can be beneficial in practical cases where one might be interested in a location that corresponds to one's practical possibilities, e.g. 10% increase of the compressive strength.

In the case of the connection weight method, the sum of the rank order could qualify the influence of the input shown in Table 6, where q , E and H are the three most important parameters, followed by b and L . On the other hand, normalization may be able to show more details about the percentage/difference among the inputs shown in Table 6 and Fig. 14. This could also be seen from the sign of the important value of each parameter: b , H and E are the same sign, while L and q are opposite. This phenomenon is in accordance with the mathematical model formula, where b , H and E have a negative influence on the deflection, while L and q have a positive influence. In other words, increasing the values of b , H and E decreases the deflection value. Otherwise, if the values of L and q are enlarged, the deflection increases.

It can be seen that the more complex example naturally requires a more complicated interpretation of the sensitivity analysis, e.g. the differences in the results obtained by the local and global sensitivity techniques. Moreover, the problem can be even more complicated in correlated space, as will be described in the next subsection.

5.2.2. Sensitivity analysis with correlated variables

The statistical correlation among random parameters should be considered in order to ensure the mathematical model behaves realistically for all realizations of a random vector. The correlation matrix shown in Table 7 is composed of Spearman correlation coefficients between each pair of random variables. In this example, it assumes correlation among geometrical parameters H , L and b due to the quality of fabrication.

From Fig. 12 it can be seen that even the creation of an NNE was affected significantly by correlation due to the complexity of correlated space. Consequently, it was necessary to use more neurons in the hidden layer to correctly represent the original mathematical model. Specifically, structures 5-13-1 and 5-15-1 were used for the NNE.

The results of the perturbation method shown in Fig. 13 are proportional to the results in uncorrelated space. However, the MSE is bigger in the absolute values for the uncorrelated variables.

On the other hand, the influence of correlation on sensitivity measurements can be clearly seen in the global sensitivity analysis results summarized in Table 8. Note that the influence of b and L is significantly higher due to its correlation with H , which is the

Table 3
Stochastic model of the beam.

Variable	μ	σ	Units
$b \sim \text{lognormal}$	0.15	0.0075	[m]
$H \sim \text{lognormal}$	0.3	0.015	[m]
$E \sim \text{lognormal}$	30	4.5	[GPa]
$q \sim \text{lognormal}$	10	2	[kN/m]
$L \sim \text{lognormal}$	5	0.05	[m]

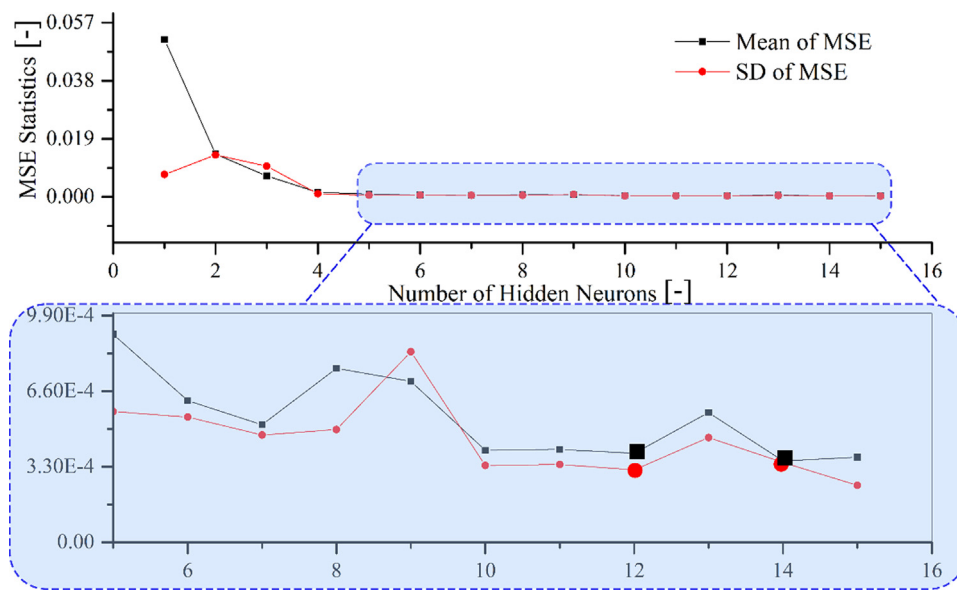


Fig. 10. The MSE information of different hidden neurons for a simple beam with uncorrelated variables.

Table 4
Statistical moments.

Parameter	NNE	Analytical solution	Units
μ	8.367	8.367	[mm]
σ	2.530	2.538	[mm]

Table 5
Failure probability of a given threshold of deflection.

Threshold	Single ANN	NNE	Analytical solution
15 mm	1.730e-2	1.709e-2	1.721e-2
20 mm	1.490e-4	8.027e-4	1.019e-3
25 mm	[-]	2.940e-5	6.232e-5
30 mm	[-]	1.000e-6	4.268e-6

second most important variable in uncorrelated space. Such phenomena can be seen significantly in the results from the non-parametric Spearman rank-order correlation method and from local analysis of variance, which are also depicted in Table 8.

Another very important result is the negative sign of the sensitivity indices for L obtained from Spearman's ρ , local analysis of variance and reference Sobol indices. Several authors have already discussed this possible negative value of Sobol indices [68] and, as can be seen, the same phenomena can also occur in other global sensitivity methods in correlated space.

According to the sum of rank order, E , q and H are the three most important parameters for the connection weight method, followed by b and L . On the other hand, normalization can sometimes show more details about the percentage/difference among the inputs shown in Table 8 and Fig. 14. The influence gap between the top three parameters and the last two parameters is large.

Table 6
The sensitivity results for a simple beam with uncorrelated variables.

Random variable	Non-parametric Spearman rank-order correlation	Sobol first order	Connection weight method	Local analysis of variance
b	4 (-0.16131)	4 (0.03)	4 (80/0.076)	4 (0.019)
H	2 (-0.4879)	3 (0.24)	3 (60/0.237)	3 (0.163)
L	5 (0.12912)	5 (0.02)	5 (100/0.056)	5 (0.002)
E	3 (-0.48497)	2 (0.25)	2 (37/0.294)	2 (0.177)
q	1 (0.6498)	1 (0.42)	1 (23/0.338)	1 (0.259)

5.2.3. Comparison and evaluation

It can be seen from Figs. 11 and 13 that the dominant parameters vary for different perturbations. The same trend exists in the results gained from perturbation by 10% and 30%. Of course, the most important variables are H and L because these values are raised to the 3rd and 4th power in the formula. However, in this second example the input variables have different variance (in contrast to the first example with standard Gaussian variables) and thus the results of the third perturbation, which takes variance into account, are significantly different in comparison to the results assuming a perturbation parameter in percentages. Note that the dependence of the perturbation parameter on variance increases the sensitivity measure for variables with higher uncertainty.

In the case of the global sensitivity methods, the results are similar to the form of the sensitivity rank for both uncorrelated and correlated conditions. However, there are still some different quantitative values. The results calculated via the connection weight method (shown in Tables 6 and 8) are normalized values which represent the relative influence. Actually, the contributions of the independent variables to the dependent variables depend primarily on the magnitude and direction of the connection weights. In this study, before normalization, the connection weight shows the positive/negative influence on the output through the sign: E , b and H have a “-”, while q and L have a “+”. This information is in agreement with the accurate relation between the independent variables and the dependent output.

The non-parametric Spearman rank-order correlation sensitivity method leads to interesting results for correlated variables, where the influence of b significantly increases in absolute value due to correlation among b , H and L . Moreover, the result of Spear-

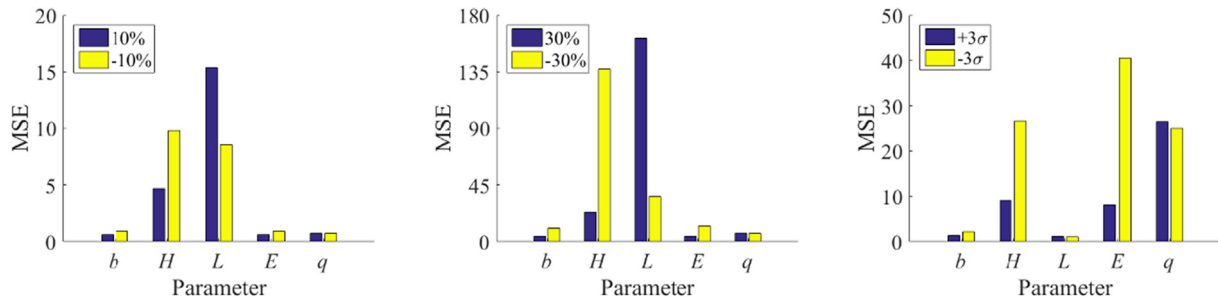


Fig. 11. The sensitivity results shown by the input perturbation method for a simple beam with uncorrelated variables.

Table 7

Correlation matrix.

	b	H	E	q	L
b	1	0.7	0	0	0.7
H	0.7	1	0	0	0.7
E	0	0	1	0	0
q	0	0	0	1	0
L	0.7	0.7	0	0	1

man correlation between L and Y is negative due to input correlation between L and H , which has a significant negative influence on deflection (higher H leads to lower deflection). Therefore, it is obvious that the results of Spearman's ρ in correlated space may lead to

the misunderstanding of the meaning of input variables, and this technique should be performed in uncorrelated space.

The negative sign of the first order Sobol index of L might be confusing to interpret. It reflects the fact that the correlative part of Sobol indices indicates the influence of the interaction between L and other input random variables, and that fixing L can actually increase the variance of the mathematical model output, which leads to negative covariance between L and Y . Note that in the case of uncorrelated random variables E and q , there is no correlative part in Sobol indices, and thus ANCOVA reduces to the ordinary ANOVA method in this case. Local analysis of variance is based on a simplified idea like ANCOVA and thus the negative value of index O_L is caused by correlation as well.

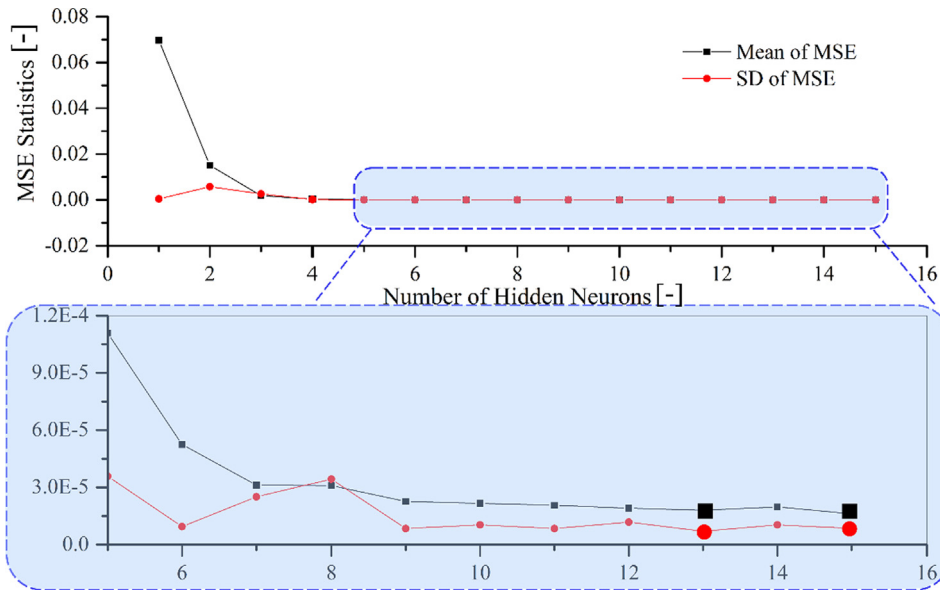


Fig. 12. The MSE information of different hidden neurons for a simple beam with correlated variables.

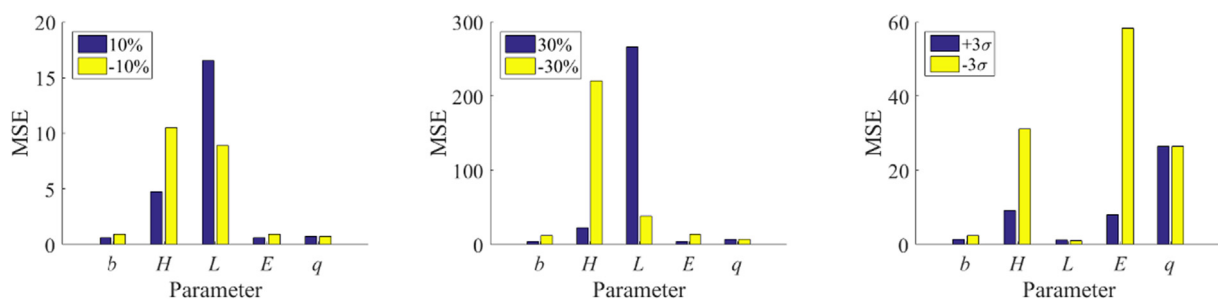


Fig. 13. The sensitivity results shown by the input perturbation method for a simple beam with correlated variables.

Table 8
The sensitivity results for a simple beam with correlated variables.

Random variable	Non-parametric Spearman rank-order correlation	Sobol first order	Sobol correlative part	Connection weight method	Local analysis of variance
<i>b</i>	4 (-0.39909)	4 (0.07)	0.04	4 (120 /0.081)	4 (0.072)
<i>H</i>	2 (-0.50286)	2 (0.26)	0.02	3 (89 /0.226)	2 (0.183)
<i>L</i>	5 (-0.31665)	5 (-0.04)	-0.06	5 (150 /0.052)	5 (-0.063)
<i>E</i>	3 (-0.48737)	3 (0.25)	0.00	1 (35 /0.347)	3 (0.176)
<i>q</i>	1 (0.66195)	1 (0.42)	0.00	2 (56 /0.294)	1 (0.277)

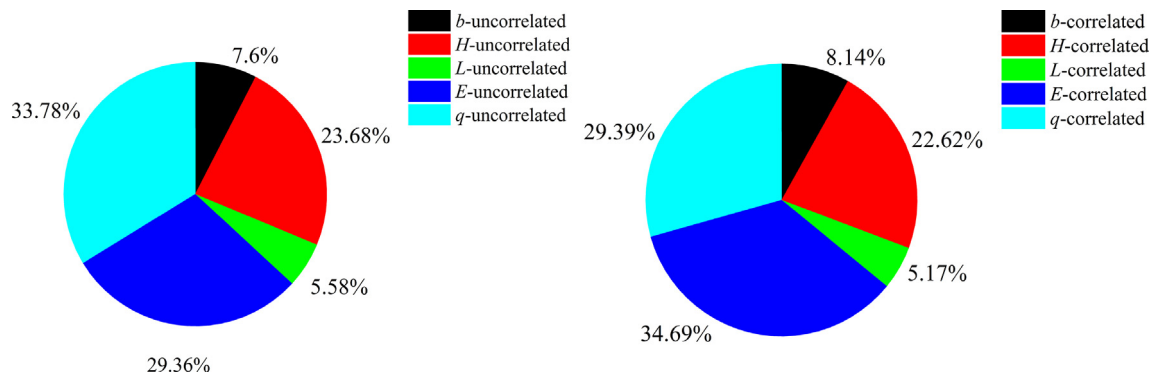


Fig. 14. The sensitivity results shown by the connection weight method for a simple beam with uncorrelated and correlated variables.

5.3. Practical application: a precast concrete girder failing in shear

The analyzed structure was a full-scale LDE7 precast prestressed roof girder produced by Franz Oberndorfer GmbH & Co KG in Austria. Details concerning the FEM and stochastic model are described in the following paragraphs. The surrogate modelling was carried out as part of a long-term research project that includes laboratory experiments [66], mathematical modelling [69], semi-probabilistic design [70] and stochastic analysis using a surrogate model [4].

The girder was made from C50/60 concrete and was prestressed by 2 × 8 strands in each web (cables - St 1570/1770 - F93). The strands are located at the following distances from the bottom: 70 and 7 × 40 mm. The girder had a TT-shaped cross-section, a total length of 30.00 m and a height of 0.50 m at the ends and 0.90 in the middle. The reinforcement and geometry of the beam was symmetrical along the middle cross-sectional and longitudinal plane. The load was applied at 4.125 m from the support above both webs and the ultimate limit state was represented by the critical value of the force applied during the simulation (the peak of the load-deflection diagram). The geometry of the girder, the cross-section and the place of applied load can be seen in Fig. 15.

5.3.1. Stochastic nonlinear finite element model

The finite element model was created in ATENA Science software, which is focused on the nonlinear fracture mechanics modelling of concrete structures [71]. The geometry of the beam, supports and reinforcement was created exactly according to drawings provided by the manufacturer. The ‘3D Nonlinear Cementitious 2’ material model was used for the concrete. The steel reinforcement and prestressing tendons were modelled using 1D elements with a multilinear stress vs. strain diagram with hardening. Prestressing was applied in the form of initial strain in the tendons. Prestress losses (immediate and long-term) were taken into account according to the fib Model Code (2012). The result of the FEM is the ultimate resistance of the prestressed concrete roof girder, i.e. maximal applied load leading to the failure of the structure, typically identified as a peak of loading-deflection curve.

Fig. 16 shows crack patterns captured via nonlinear simulation at peak load, documenting the complexity of the advanced computational FEM model. The FEM evaluation is highly time-consuming (one simulation takes approx. 8 h), so it is necessary to use a surrogate model to perform the stochastic analysis.

The original stochastic model contained 12 random variables, though a reduced stochastic model was utilized for the surrogate modelling. The reduced stochastic model was based on a sensitivity analysis of scaled girders performed during previous research [4]. The model contains 5 lognormally distributed random variables, as can be seen in Table 9: F_c stands for the compressive strength of concrete, E is Young’s modulus of concrete, F_t is the tensile strength of concrete, G_f is the fracture energy of concrete and P_Uncert stands for the uncertainty of calculated immediate prestressing losses, i.e. immediate prestressing losses are calculated according to fib Model Code and the resulting value is multiplied by P_Uncert in order to include the uncertainty of the used simplified analytical formula.

5.3.2. Sensitivity analysis with uncorrelated variables

This example can be seen as a highly non-linear mathematical model in implicit form, and therefore the most difficult and challenging model for an NNE. For the sake of clarity, this example was treated in the same way as the previous examples. First of all, Latin Hypercube Sampling was employed via FReET software to create a training data set containing 100 realizations in uncorrelated space. The best ANN structures 5-6-1, 5-8-1, and 5-9-1 were chosen for the NNE according to the study illustrated in Fig. 17. It is clear that the MSE is higher than in the previous analytical examples and thus such an approach was necessary to obtain an NNE with sufficient accuracy.

Once the NNE was ready, it was validated on 30 samples generated via LHS, and the result in terms of the prediction vs. the original model can be seen in Fig. 18. It is clear that the NNE’s predictions of the realizations are in very good agreement with those of the NLFEM, though some of the realizations have significant differences. The general behaviour of the surrogate model in the form of the NNE can be validated by estimating the statistical

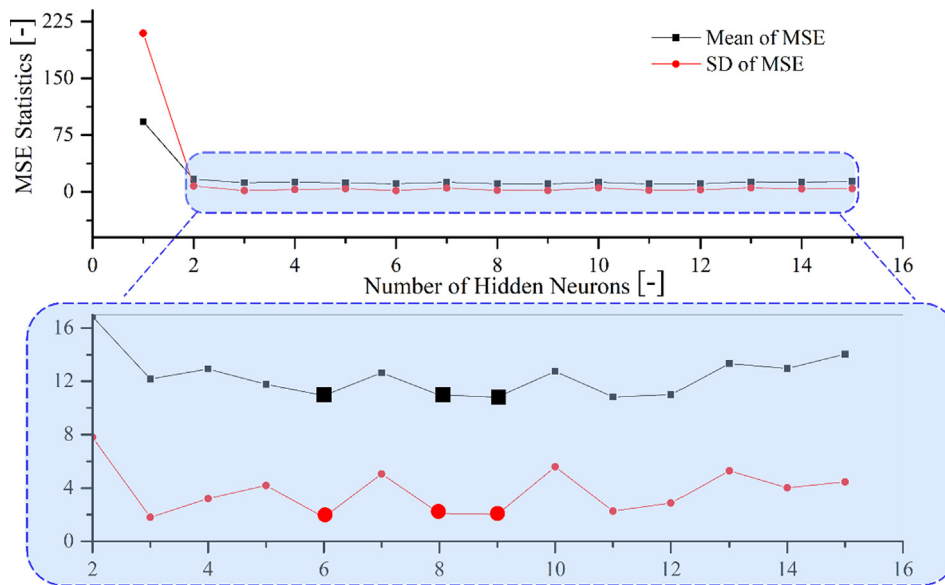


Fig. 17. The MSE information of different hidden neurons for a precast concrete girder with uncorrelated variables.

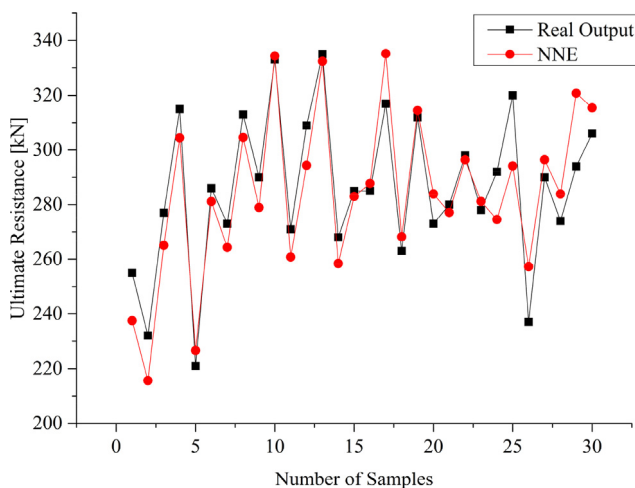


Fig.18. Comparison of the results gained from the original FEM output and those calculated by the NNE.

Table 10
Statistical moments of the ultimate resistance.

Parameter	NNE	LHS 100 samples	Units
μ	284.129	284.2	[kN]
σ	28.684	29.7	[kN]

However, the representation of the results is problematic due to the different nature of these methods. For example, non-parametric Spearman rank-order correlation is highly affected by correlation and it can be seen that all material parameters have similar coefficients due to the generated correlated values of random variables. On the other hand, Sobol indices are able to give us similar results as in the case of uncorrelated space. As for the connection weight method, P_{Uncert} , G_f and F_t are the three most important parameters, which is quite different from the results for the uncorrelated variables and other global sensitivity analysis methods.

5.3.4. Comparison and discussion

In this very last example, the presented methods were applied to the nonlinear finite element model of a real structure, which is the most challenging task for theoretical methods of sensitivity analysis. The strong nonlinearity of the mathematical model is clear from the results of the perturbation method, where the influence of variables is highly dependent on the location of interest of the design domain.

From the practical point of view, the results in uncorrelated space are important for the correct identification of the failure mode. According to the results of the global sensitivity analysis, the compressive strength and tensile strength of concrete have the greatest influence on the ultimate limit state of girders. The negligible influence of fracture energy can be explained by the fact that the modelled structure is at ultimate capacity. This is reflected by the well-known and widely used strut inclination method for shear capacity prediction, where shear is resisted by concrete struts acting in compression when cracks have already occurred, and thus fracture energy has no influence at that time. All of the global sensitivity analysis methods could identify the influential parameters, and they could even quantify the degree of the influence exactly. Compressive strength strongly affects the ultimate limit state of girders (see Table 11). Its sensitivity is significantly higher compared to other parameters – compressive strength is 0.743, while the second most important parameter, tensile strength, is 0.418 with the non-parametric Spearman rank-order correlation method.

Correlation among random variables leads to significantly different results from all of the performed sensitivity methods in comparison to uncorrelated space. The differences among random variables are not very clear from the results of the perturbation technique for correlated variables, except for the reduction in the influence of F_c , which is caused by the high influence of the correlated group of variables F_t , G_f and E . The influence of P_{Uncert} is more or less the same as for uncorrelated variables.

Spearman's ρ is highly affected by correlation as in the previous examples, and thus all the correlated concrete material parameters have a high positive influence on the ultimate limit state. Although it can still be identified that the most important variables for ultimate shear capacity are F_t and F_c , the influence of G_f and E is over-estimated due to imposed correlation. This phenomenon is in

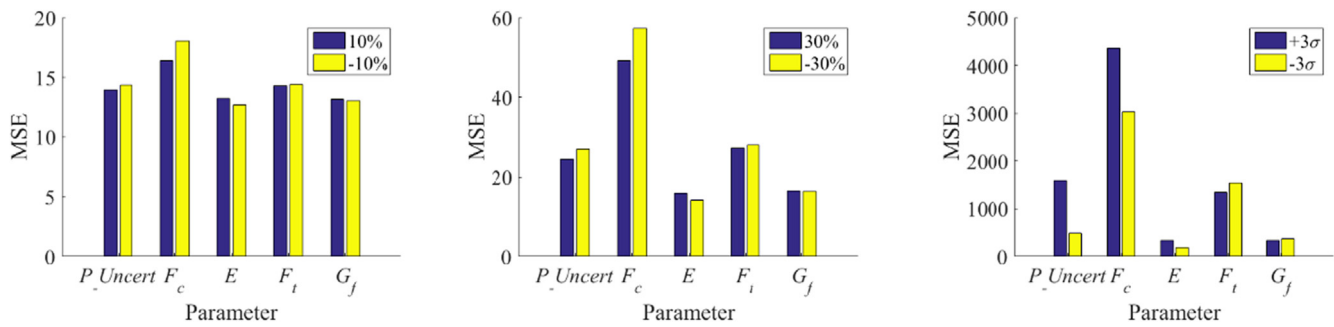


Fig. 19. The sensitivity results shown by the input perturbation method for a precast concrete girder with uncorrelated variables.

Table 11

The sensitivity results for a precast concrete girder with uncorrelated variables.

Random variable	Non-parametric Spearman rank-order correlation	Sobol first order	Connection weight method	Local analysis of variance
P_Uncert	3(0.264)	3(0.08)	3(89 /0.189)	3(0.098)
F_c	1(0.743)	1(0.28)	1(30 /0.377)	1(0.334)
E	5(0.147)	5(0.01)	5(147 /0.083)	5(0.008)
F_t	2(0.418)	2(0.09)	2(64 /0.231)	2(0.101)
G_f	4(0.202)	4(0.02)	4(120 /0.121)	4(0.023)

Table 12

Correlation matrix.

	F_c	E	F_t	G_f
F_c	1	0.8	0.7	0.6
E	0.8	1	0.5	0.5
F_t	0.7	0.5	1	0.8
G_f	0.6	0.5	0.8	1

compliance with ANOVA, as can be seen from the correlative parts of the Sobol indices. It can be seen that the results of the local analysis of the variance method are different, which is caused by the nonlinearity of the mathematical model and the nature of the method, where the location of interest is near the mean value of the random variables. As for the connection weight method, the sensitivity analysis results are totally different. Such results may be caused by the mechanism of the artificial neural network and

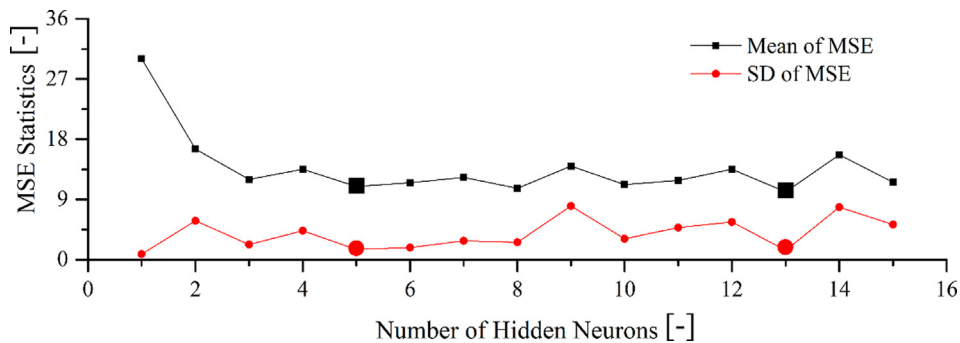


Fig. 20. The MSE information of different hidden neurons for a precast concrete girder with correlated variables.

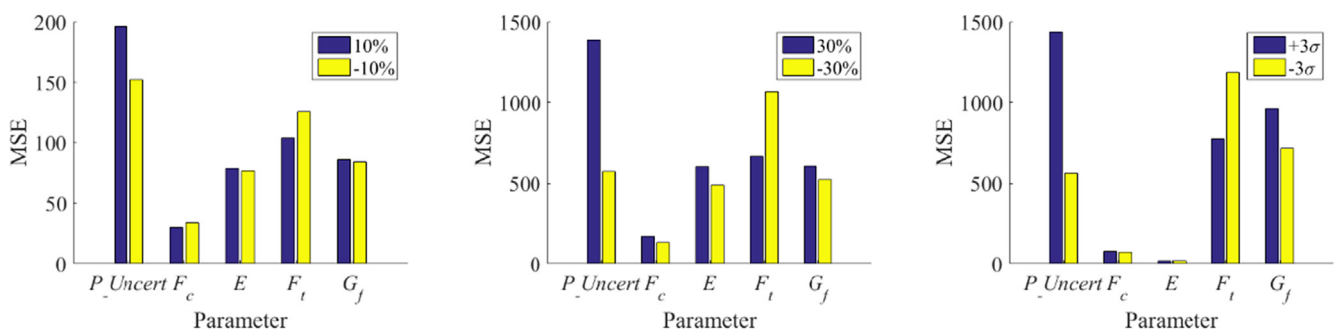


Fig. 21. The sensitivity results shown by the input perturbation method for a precast concrete girder with correlated variables.

Table 13
The sensitivity results for a precast concrete girder with correlated input variables.

Random variable	Non-parametric Spearman rank-order correlation	Sobol first order	Sobol correlative part	Connection weight method	Local analysis of variance
P_{Uncert}	5(0.264)	4/5(0.08)	0.00	1(57 /0.269)	4(0.098)
F_c	1(0.991)	1(0.48)	0.20	5(149 /0.026)	5(0.049)
E	4(0.766)	4/5(0.08)	0.07	4(113 /0.182)	3(0.165)
F_t	2(0.849)	2(0.25)	0.16	3(71 /0.250)	2(0.247)
G_r	3(0.774)	3(0.11)	0.09	2(60 /0.273)	1(0.286)

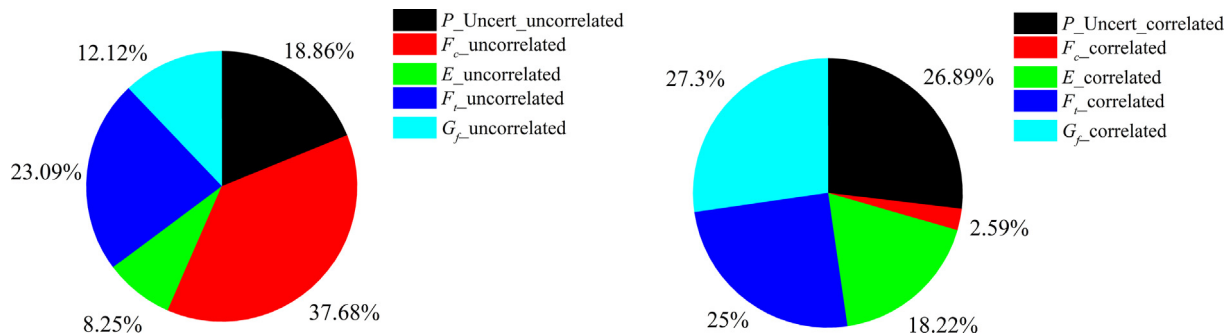


Fig. 22. The sensitivity results shown by the connection weight method for a precast concrete beam with uncorrelated and correlated variables.

its ability to establish the relation between the independent variables and the dependent variables. This relation is not dependent only on weights, but also on ANN structure, activation functions, and neuron biases. Note that the nonlinear relations in the presented example are complicated even with correlated input quantities.

6. Conclusions

The paper shows the possibility of utilizing a neural network ensemble for sensitivity analyses of different types. The efficiency of an NNE as a surrogate model coupled with the sensitivity analysis method is verified.

Several sensitivity analysis methods are compared: the input perturbation method, local analysis of variance, the connection weight method, non-parametric Spearman rank-order correlation and Sobol indices. They are applied to three examples of increasing complexity – a simple function, an analytical formula for the deflection of a simple beam, and a nonlinear finite element model of a real structure. The results are discussed in depth for each example. The general conclusions can be highlighted as follows:

- Local and global sensitivity analyses have different purposes and interpretations. It is necessary to distinguish clearly between these two types of sensitivity. This is demonstrated by the three cases in this paper. The input perturbation algorithm is a straightforward sensitivity analysis method which is easy to apply, but it is local and pays no attention to joint probability and correlation among the inputs. Nonetheless, such a sensitivity study can give us a first insight into a mathematical problem of interest, especially if one is interested in a special location in the design domain. The connection weight method is a global sensitivity analysis method and could serve as a measure of both relative qualitative ranks and quantitative specific values. However, it is sensitive to initial weights and fails to take into account the influence of the activation function and biases. Local analysis of variance is visual and quantitative, but it only works properly for nearly linear cases. Non-parametric

Spearman rank-order correlation is easy to apply even for correlated inputs, while the relation between the input and output is linear and monotonic, but it is necessary to perform a large number of numerical simulations to obtain accurate results. Sobol indices are a typical global sensitivity analysis method and are able to clearly quantify the influence of the correlations among the inputs, but they need more computations. Moreover, it may be complicated to interpret the obtained results.

- As regards robustness, the employed NNE could perform the calculations needed to approximate the desired output in the two applications of failure probability evaluation and test ultimate limit state prediction. Specifically, it has better performance in comparison to a single ANN, as was shown in the analytical formula for the deflection of a simple beam. This means that the NNE could be used efficiently as a surrogate model.
- NNE-based sensitivity analysis methods, such as the input perturbation algorithm, connection weight method and local analysis of variance, could be used for different levels of sensitivity analysis tasks ranging from local to global and from qualitative to quantitative in nature. What is more, the accuracy of such methods was verified herein. Therefore, the NNE has high potential for use in surrogate modelling in close connection with sensitivity and reliability analysis.
- Statistical correlation among material characteristics should be considered when attempting to perform the realistic modelling of structures. It is necessary to perform sensitivity analysis in both correlated and uncorrelated space in order to correctly identify the roles of input variables. In this study, the Sobol indices are able to shed light on the difference between uncorrelated and correlated cases, and to identify the influences caused by the correlation clearly. However, it is usually computationally demanding to obtain all Sobol indices. Therefore, the obtained Sobol indices were compared to other sensitivity measurements and the influence of correlation was explained.
- The potential of NNE for surrogate modelling and sensitivity analysis has been verified, and good performance has been obtained. In some cases, the NNE-based sensitivity analysis

method is still not precise enough – as with the shear failure of precast concrete girders with correlated variables. The method will be improved so that it is not only sensitive to weights but also reflects other network parameters.

Declaration of Competing Interest

The authors declare that they have no known competing financial interests or personal relationships that could have appeared to influence the work reported in this paper.

Acknowledgement

The first author is grateful for the support from the Fundamental Research Funds for the Central Universities, China (Grant No. 2017B659X14); the Postgraduate Research & Practice Innovation Program of Jiangsu Province (Grant No. KYCX17_0492) and the China Scholarship Council (Grant No. 201706710090). The authors acknowledge the financial support provided by the Czech Science Foundation under project RESUS No. 18-13212S, and by the Ministry of Education, Youth and Sports of the Czech Republic under mobility project No. 8JCH1074.

References

- Bayat M, Pakar I, Ahmadi HR, Cao M, Alavi AH. Structural health monitoring through nonlinear frequency-based approaches for conservative vibratory systems. *Struct Eng Mech* 2020;73(3):331–7.
- Bayat M, Kia M, Soltangharai V, Ahmadi HR, Ziehl P. Bayesian demand model based seismic vulnerability assessment of a concrete girder bridge. *Adv Concr Constr* 2020;9(4):337–43.
- Saltelli A. Sensitivity analysis for importance assessment. *Risk Anal* 2002;22(3):579–90.
- Lehký D, Novák D, Novák L, Šomodíková M. Prestressed concrete roof girders: Part II – Surrogate modeling and sensitivity analysis. In: *Proceedings of IALCCE 2018*. ISBN: 978-1-138-62633-1; 2018.
- Iooss B, Marrel A. Advanced methodology for uncertainty propagation in computer experiments with large number of inputs. *Nucl Technol* 2019:1–19.
- Faravelli L. Response-surface approach for reliability analysis. *J Eng Mech* 1989;115(12):2763–81.
- Bichon BJ, Eldred MS, Swiler LP, Mahadevan S, McFarland JM. Efficient global reliability analysis for nonlinear implicit performance functions. *AIAA J* 2008;46(10):2459–68.
- Picheny V, Ginsbourger D, Roustant O, Haftka RT, Kim NH. Adaptive designs of experiments for accurate approximation of a target region. *J Mech Des* 2010;132(7):071008.
- Deheeger F, Lemaire M. Support vector machine for efficient subset simulations: 2SMART method. In: *Proc 10th int conf on applications of stat Prob in Civil Engineering (ICASP10)*, Tokyo, Japan; 2007.
- Bourinet JM, Deheeger F, Lemaire M. Assessing small failure probabilities by combined subset simulation and support vector machines. *Struct Saf* 2011;33(6):343–53.
- Ghanem RG, Spanos PD. *Stochastic finite elements: a spectral approach*. Courier Corporation; 2003.
- Blatman G, Sudret B. Adaptive sparse polynomial chaos expansion based on least angle regression. *J Comput Phys* 2011;230(6):2345–67.
- Novák L, Novák D. Surrogate modelling in the stochastic analysis of concrete girders failing in shear. *Proceedings of the fib Symposium 2019: Concrete - Innovations in Materials, Design and Structures*, International Federation for Structural Concrete. ISBN 9782940643004, 2019.
- Bucher CG, Bourgund U. A fast and efficient response surface approach for structural reliability problems. *Struct Saf* 1990;7(1):57–66.
- Rajashekhar MR, Ellingwood BR. A new look at the response surface approach for reliability analysis. *Struct Saf* 1993;12(3):205–20.
- Bayat M, Daneshjoo F, Nisticò N. Probabilistic sensitivity analysis of multi-span highway bridges. *Steel Compos Struct* 2015;19(1):237–62.
- Novák D, Teplý B, Shiraiishi N. Sensitivity analysis of structures: a review. In: *Proceedings of the 5th international conference on civil and structural engineering computing*, Edinburgh, Scotland. p. 201–7.
- Kleijnen JPC. Sensitivity analysis of simulation models: An overview. *Proc – Soc Behav Sci* 2010;2(6):7585–6.
- Antucheviciene J, Kala Z, Marzouk M, Vaidogas ER. Solving civil engineering problems by means of fuzzy and stochastic MCDM methods: Current state and future research. *Math Probl Eng*, (Article ID362579) 2015:1–16.
- Borgonovo E, Plischke E. Sensitivity analysis: a review of recent advances. *Eur J Oper Res* 2016;248(3):869–87.
- Asteris PG, Tsaris AK, Cavaleri L, Repapis CC, Papalou A, Di Trapani F, et al. Prediction of the fundamental period of infilled RC frame structures using artificial neural networks. *Comput Intell Neurosci* 2016;2016:20.
- Hore S, Chatterjee S, Sarkar S, Dey N, Ashour AS, Balas-Timar D, et al. Neural-based prediction of structural failure of multistoried RC buildings. *Struct Eng Mech* 2016;58(3):459–73.
- Gopalakrishnan K, Khaitan SK, Choudhary A, Agrawal A. Deep Convolutional Neural Networks with transfer learning for computer vision-based data-driven pavement distress detection. *Constr Build Mater* 2017;157:322–30.
- Chatterjee S, Sarkar S, Hore S, Dey N, Ashour AS, Balas VE. Particle swarm optimization trained neural network for structural failure prediction of multistoried RC buildings. *Neural Comput Appl* 2017;28(8):2005–16.
- Chatterjee S, Sarkar S, Hore S, Dey N, Ashour AS, Shi F, et al. Structural failure classification for reinforced concrete buildings using trained neural network based multi-objective genetic algorithm. *Struct Eng Mech* 2017;63(4):429–38.
- Cha YJ, Choi W, Büyüköztürk O. Deep learning-based crack damage detection using convolutional neural networks. *Comput-Aided Civ Infrastruct Eng* 2017;32(5):361–78.
- Khademi F, Akbari M, Jamal SM, Nikoo M. Multiple linear regression, artificial neural network, and fuzzy logic prediction of 28 days compressive strength of concrete. *Front Struct Civil Eng* 2017;11(1):90–9.
- Jain A, Jha SK, Misra S. Modeling and analysis of concrete slump using artificial neural networks. *J Mater Civ Eng* 2008;20(9):628–33.
- Beiki M, Bashari A, Majidi A. Genetic programming approach for estimating the deformation modulus of rock mass using sensitivity analysis by neural network. *Int J Rock Mech Min Sci* 2010;47(7):1091–103.
- Das SK, Biswal RK, Sivakugan N, Das B. Classification of slopes and prediction of factor of safety using differential evolution neural networks. *Environ Earth Sci* 2011;64(1):201–10.
- Hadzima-Nyarko M, Nyarko EK, Morić D. A neural network based modelling and sensitivity analysis of damage ratio coefficient. *Expert Syst Appl* 2011;38(10):13405–13.
- Hao J, Wang B. Parameter sensitivity analysis on deformation of composite soil-nailed wall using artificial neural networks and orthogonal experiment. *Math Probl Eng*; 2014.
- Mozumder RA, Laskar AI. Prediction of unconfined compressive strength of geopolymer stabilized clayey soil using artificial neural network. *Comput Geotech* 2015;69:291–300.
- Shafabakhsh G, Naderpour H, Noroozi R. Determining the relative importance of parameters affecting concrete pavement thickness. *J Rehabil Civil Eng* 2015;3(1):61–73.
- Cidade RA, Castro DS, Castrodeza EM, Kuhn P, Catalanotti G, Xavier J, et al. Determination of mode I dynamic fracture toughness of IM7-8552 composites by digital image correlation and machine learning. *Compos Struct* 2019;210:707–14.
- Pires dos Santos R, Dean DL, Weaver JM, Hovanski Y. Identifying the relative importance of predictive variables in artificial neural networks based on data produced through a discrete event simulation of a manufacturing environment. *Int J Model Simul* 2019;39(4):234–45.
- Zhou ZH, Wu J, Tang W. Ensembling neural networks: many could be better than all. *Artif Intell* 2002;137(1–2):239–63.
- Cao M, Qiao P. Neural network committee-based sensitivity analysis strategy for geotechnical engineering problems. *Neural Comput Appl* 2008;17(5–6):509–19.
- De Oña J, Garrido C. Extracting the contribution of independent variables in neural network models: a new approach to handle instability. *Neural Comput Appl* 2014;25(3–4):859–69.
- Cao MS, Pan LX, Gao YF, Novák D, Ding ZC, Lehký D, et al. Neural network ensemble-based parameter sensitivity analysis in civil engineering systems. *Neural Comput Appl* 2017;28(7):1583–90.
- Lehký D, Pan L, Novák D, Cao M, Šomodíková M, Slowik O. A comparison of sensitivity analyses for selected prestressed concrete structures. *Struct Concr* 2019;20(1):38–51.
- Wang F, Li H. Towards reliability evaluation involving correlated multivariates under incomplete probability information: A reconstructed joint probability distribution for isoprobabilistic transformation. *Struct Saf* 2017;69:1–10.
- Wang P, Lu Z, Zhang K, Xiao S, Yue Z. Copula-based decomposition approach for the derivative-based sensitivity of variance contributions with dependent variables. *Reliab Eng Syst Saf* 2018;169:437–50.
- Da Veiga S, Wahl F, Gamboa F. Local polynomial estimation for sensitivity analysis on models with correlated inputs. *Technometrics* 2009;51(4):452–63.
- Luo J, Lu W. Sobol' sensitivity analysis of NAPL-contaminated aquifer remediation process based on multiple surrogates. *Comput Geosci* 2014;67:110–6.
- Yu H, Wilamowski BM. Levenberg-marquardt training. *Industr Electron Handbook* 2011;5(12):1.
- Burden F, Winkler D. Bayesian regularization of neural networks. In: *Artificial neural networks*. Humana Press; 2008. p. 23–42.
- Kayri M. Predictive abilities of bayesian regularization and Levenberg-Marquardt algorithms in artificial neural networks: a comparative empirical study on social data. *Math Comput Appl* 2016;21(2):20.
- Durrett R. *Probability: theory and examples (Vol. 49)*. Cambridge university press; 2019.
- Scardi M, Harding Jr LW. Developing an empirical model of phytoplankton primary production: a neural network case study. *Ecol Model* 1999;120(2–3):213–23.

- [51] Gevrey M, Dimopoulos I, Lek S. Review and comparison of methods to study the contribution of variables in artificial neural network models. *Ecol Model* 2003;160(3):249–64.
- [52] Downing DJ, Gardner RH, Hoffman FO. An examination of response-surface methodologies for uncertainty analysis in assessment models. *Technometrics* 1985;27(2):151–63.
- [53] Olden JD, Jackson DA. Illuminating the “black box”: a randomization approach for understanding variable contributions in artificial neural networks. *Ecol Model* 2002;154(1–2):135–50.
- [54] Iooss B, Lemaître P. A review on global sensitivity analysis methods. In *Uncertainty management in simulation-optimization of complex systems*. Boston, MA: Springer; 2015. p. 101–22.
- [55] Gauthier TD. Detecting trends using Spearman’s rank correlation coefficient. *Environ Forensics* 2001;2(4):359–62.
- [56] Sobol IM. Sensitivity estimates for nonlinear mathematical models. *Math Model Comput Exp* 1993;1(4):407–14.
- [57] Sobol IM. Global sensitivity indices for nonlinear mathematical models and their Monte Carlo estimates. *Math Comput Simul* 2001;55(1–3):271–80.
- [58] Sudret B. Global sensitivity analysis using polynomial chaos expansions. *Reliab Eng Syst Saf* 2008;93(7):964–79.
- [59] Novak L, Novak D. Polynomial chaos expansion for surrogate modelling: Theory and software. *Beton-und Stahlbetonbau* 2018;113:27–32.
- [60] Caniou Y. Global sensitivity analysis for nested and multiscale modelling (Doctoral dissertation); 2012.
- [61] Rosenblatt M. Remarks on a multivariate transformation. *Ann Math Stat* 1952;23(3):470–2.
- [62] Der Kiureghian A, Liu PL. Structural reliability under incomplete probability information. *J Eng Mech* 1986;112(1):85–104.
- [63] Lebrun R, Dutfoy A. An innovating analysis of the Nataf transformation from the copula viewpoint. *Probab Eng Mech* 2009;24(3):312–20.
- [64] Nataf A. Détermination des distributions de probabilité dont les marges sont données. *Comptes Rendus de l’Académie des Sciences* 1962;225:42–3.
- [65] McKay MD, Beckman RJ, Conover WJ. Comparison of three methods for selecting values of input variables in the analysis of output from a computer code. *Technometrics* 1979;21(2):239–45.
- [66] Novák D, Řoutil L, Novák L, Slowik O, Strauss A, Krug B. Database of fracture-mechanical concrete parameters and its implementation into reliability software free. In: *Proc of the 13th international probabilistic workshop (IPW 2015)*. ISBN 978-981-09-7963-8.
- [67] Lehký D, Šomodíková M. Reliability calculation of time-consuming problems using a small-sample artificial neural network-based response surface method. *Neural Comput Appl* 2017;28(6):1249–63.
- [68] Li G, Rabitz H, Yelvington PE, Oluwole OO, Bacon F, Kolb CE, et al. Global sensitivity analysis for systems with independent and/or correlated inputs. *J Phys Chem A* 2010;114(19):6022–32.
- [69] Strauss A, Krug B, Novák D, Slowik O. Prestressed concrete roof girders: Part I: deterministic and stochastic model. In: *Proceedings of IALCCE 2018*. ISBN: 978-1-138-62633-1; 2018.
- [70] Novák D, Novák L, Slowik O, Strauss A. Prestressed concrete roof girders: Part III – Semi-probabilistic design. In: *Proceedings of IALCCE 2018*. ISBN: 978-1-138-62633-1; 2018.
- [71] Červenka V, Jendele L, Červenka J. ATENA program documentation – Part 1: Theory. Prague, Czech Republic: Červenka Consulting; 2016.
- [72] Zimmermann T, Lehký D, Strauss A. Correlation among selected fracture-mechanical parameters of concrete obtained from experiments and inverse analyses. *Struct Concr* 2016;17(6):1094–103.

D Stochastic Modelling and Assessment of Long-span Precast Prestressed Concrete Elements Failing in Shear

DOI: 10.1016/j.engstruct.2020.111500

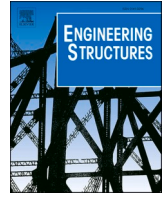
D.1 Description

The paper is focused on the stochastic analysis of the long-span prestressed concrete roof girders failing in shear. Note that, the paper is a continuation of the previous research focused on laboratory experiments and deterministic modeling performed by the first author Ondřej Slowik. Stochastic analysis consists of sensitivity and statistical analysis using Latin Hypercube Sampling and Nataf transformation in order to respect the described correlation matrix of the input random vector. The obtained statistical moments are utilized for the estimation of the design value of resistance by semi-probabilistic approach. Additionally, the interesting results of sensitivity analysis clearly show the role of statistical correlation.

D.2 Role of the Ph.D. Candidate

Percentage of contribution: 30%

Lukáš Novák wrote several parts of this paper and performed advanced stochastic analysis of the described numerical model, i.e. sensitivity and statistical analysis reflecting the influence of the statistical correlation among input random variables. Contribution of Lukáš Novák is confirmed directly in the paper (section Author Contributions).



Stochastic modelling and assessment of long-span precast prestressed concrete elements failing in shear

Ondřej Slowik^{a,*}, Drahomír Novák^a, Lukáš Novák^a, Alfred Strauss^b

^a Institute of Structural Mechanics, Faculty of Civil Engineering, Brno University of Technology, Brno, Czech Republic

^b Institute of Structural Engineering, Department of Civil Engineering and Natural Hazards, University of Natural Resources and Life Sciences, Vienna, Austria

ARTICLE INFO

Keywords:

Stochastic modelling
Fully probabilistic analysis
Shear capacity
Prestressed beam elements
Nonlinear numerical modelling
Experimental testing
Nonlinear finite element analysis

ABSTRACT

The shear behaviour of reinforced and prestressed concrete structures has been extensively studied over the last decades. However, there are still numerous open questions, concerning, e.g. the effects of normal-shear force interaction and material properties on shear performance. While the elastic behaviour of structures can be accurately captured by existing analytical approximations available within code standards, the description of the plastic behaviour of prestressed concrete elements occurring before typically quasi-brittle shear failure requires nonlinear analysis. Therefore, most prestressed concrete structures are designed to utilise only the elastic capacity of the material to avoid the performance of a complex nonlinear finite element analysis (hereinafter NLFEA) of pre-failure behaviour. In the case of mass-produced precast elements, however, the higher cost of performing NLFEA to provide valuable information on the complete loading of such element's history might be justified and economically beneficial. NLFEA can give much more objective information on a structure's performance and ultimate capacity, its cracking behaviour and failure indicators which can be utilised for the optimisation of the design, maintenance and inspection of produced structural elements. However, deterministic NLFEA cannot capture the naturally uncertain character of structural response. Current code standards provide a framework for NLFEA using several safety formats. The fully probabilistic approach remains the most general, straightforward and least conservative way of considering uncertainties, however. The stochastic modelling of a precast element's shear response requires the performance of a series of fracture-mechanical experiments with material samples, the evaluation of stochastic features of material parameters, and the use of identified random parameters as inputs for highly accurate nonlinear finite element models of destructive experiments. The information on material uncertainty is then used for the virtual statistical simulation of Monte Carlo type to obtain the probability distribution of structural resistance. This paper aims to describe the application of stochastic NLFEA to the shear behaviour simulation of a for wide-span prestressed reinforced concrete lightweight roof element. Extensive experimental studies on small specimens and scaled and full-scale girders have been performed to acquire the required information for the implementation of complex material laws in advanced probabilistic nonlinear numerical analyses. This information is used together with advanced monitoring systems to investigate stochastic features of shear structural response, the probabilistic safety level in terms of code-based design levels, and the experimental findings.

1. Introduction

The shear strength of prestressed reinforced concrete girders has been extensively studied over the last five decades, (e.g. [1–6]). The complex mutual influences of multi-axial states of stress, the anisotropy of composite materials caused by diagonal cracking, the interactions between concrete and steel reinforcement or tendons, and the brittle failure mode of prestressed concrete beams, all act together to render the

existence of a generally applicable analytical approximation of shear ultimate capacity unlikely (if not impossible) to achieve. Despite the significant progress made in understanding shear failure mechanisms [7], and the many shear tests conducted over the last decades [8], NLFEA remains the most accurate and only generally applicable approach for modelling shear structural behaviour. Most structural designs produced in engineering practice aim to utilise the strictly elastic shear capacity of prestressed structures to avoid the performance of complicated and computationally demanding NLFEA analysis. While

* Corresponding author at: Veveri 331/95, 602 00 Brno, Czech Republic.
E-mail address: slowik.o@fce.vutbr.cz (O. Slowik).

Notations			
<i>Variables and functions</i>		v_x	Coefficient of variation of variable X
Z	Safety margin	α	Coefficient of thermal expansion
T	Correlation matrix	E	Young's modulus
N_{var}	Number of variables	f_t	Tensile strength
μ_g	Mean value	f_c	Compressive strength
P_f	Probability of failure	G_f	Fracture energy
R	Structural response	ρ	Density of concrete mixture
E	Load actions	f_y	Yield strength of steel
N_{sim}	Number of simulations	IL	Uncertainty for immediate losses of prestress
s	Standard deviation	LTL	Uncertainty for long term losses of prestress
X	Vector of random input variables	ρ_s	Spearman rank-order correlation index
E	Error matrix	<i>Abbreviations</i>	
X_d	Design values of random variables	NLFEA	Nonlinear finite element analysis
β	Reliability index	CoV	Coefficient of Variation
α_x	Directional cosines derived from First Order Reliability Method	FORM	First Order Reliability Method
		LHS	Latin hypercube sampling
		LD	Load vs. displacement curve

earlier obstacles to the widespread use of NLFEA, such as its computational and algorithmic complexity, have slowly been removed by the development of information technology and dedicated advanced software tools ([9,10]), other barriers remain to be overcome. Complex NLFEA models require precise knowledge of material parameters, production processes and storage conditions in order to capture structural behaviour accurately. Such information is often unavailable before a design process starts, and a series of expensive fracture experiments need to be performed to obtain it. While linear elastic analysis is well established within design codes ([11,12]), the usage limitations and recommendations regarding NLFEA that are currently implemented within codes [12] are too general and require further specification. Users often need to rely (in specific cases) on various guidelines developed by researchers ([13,14]) instead of legally acceptable code frameworks. The available software solutions are still quite expensive, and the engineering time necessary for NLFEA is considerably higher compared to classical linear analysis. These obstacles render NLFEA a rather costly tool in spite of the existence of efficient software. The higher cost of NLFEA might very well be justified in the case of mass-produced precast elements, however. It provides objective information on a structure's ultimate capacity, its cracking behaviour and failure indicators which can be utilised for the optimisation of design and maintenance, and for the inspection of a produced structural element.

Moreover, simple deterministic NLFEA does not capture the uncertain nature of material properties, production deviations and other random effects resulting in variability of structural response. The probabilistic assessment of structural response represents the most accurate way to evaluate structural reliability using NLFEA. However, this procedure involves significant computational burden due to the many NLFEA runs necessary to assess the required (typically very low) probabilities of structural failure [15]. Since even a single NLFEA run can be computationally demanding, many advanced procedures have been suggested with the aim of reducing the significant computational burden of the probabilistic approach. Stratified simulation techniques such as Latin Hypercube Sampling (hereinafter LHS) [16] help to reduce the variance in statistical moment estimates that occurs compared to crude Monte Carlo sampling for the same sample size (see [17]). Importance sampling techniques ([18,19]) aim the course of the simulation so that it is close to the border of the failure domain using adjusted distribution functions of input random variables (known as weight functions). Such methods are often employed within design point search algorithms [20] involved in 2nd level reliability approaches such as the FORM and SORM approximation techniques ([21,22]). Also, other advanced simulation techniques such as asymptotic, adaptive or directional

sampling ([23,24,25]) can be utilised for efficient reliability evaluation. While FORM and SORM techniques approximate failure surfaces with multidimensional planes or parabola, response surface methods perform reliability analysis with simplified surrogate models represented by polynomial or polynomial chaos-based expressions or artificial neural networks ([26–28]). Despite the significant reduction of simulations necessary for the proper estimation of structural reliability compared to Crude Monte Carlo integration, most of the approaches mentioned above still need hundreds or thousands of simulations to be sufficiently accurate. Promising results have been obtained via the use of some advanced response surface methods combined with LHS-type simulations ([29–31]). However, the necessary computational burden combined with the lack of process automation remains a significant obstacle for the widespread application of the fully probabilistic approach within engineering practice. Despite its complexity, the fully probabilistic approach is necessary for the verification of developed simplified models and their overall safety level and becomes more attractive in the industry. Stochastic NLFEA modelling can also be utilised to virtually extend the number of performed destructive experiments, which are usually expensive or even impossible to conduct. It is possible to perform several destructive experiments and subsequently set up and verify deterministic models which can be utilised for stochastic analysis, significantly extending the number of observed tests.

This paper describes the stochastic modelling of long-span precast concrete roof girders failing in shear, built on the accurate deterministic modelling procedure summarised within [13]. The primary motivation for the conducted research was to obtain detailed information on the nonlinear behaviour of the shear structural response of prestressed T-shaped LDE7 roof girders produced by Franz Oberndorfer GmbH & Co KG, Austria. The studied structural member typically fails in shear. This fact can be proven via NLFE analysis using a three-point bending (hereinafter 3 PB) loading configuration. Fig. 1 captures the crack pattern and relative bending deformation of the investigated girder at ultimate limit state under 3 PB loading.

The conducted analysis, therefore, focuses on the shear behaviour of the studied girder under a complex combination of internal forces (shear force (V), the normal force (N), and bending moment (M)). Different alternative approaches for V models can be found in the literature, e.g. [32–34] and [35]. Such approaches and historical numerical models mainly deal with the combination of shear force and/or torsion ($V + T$), or combinations of the moment and/or normal force ($M + N$) together with $V + T$, or occur in partial combinations. The traditional approaches and models only enable limited consideration of the combinations $V + N$, $V + M$ and $V + N + M$ within limit states. Nonlinear numerical

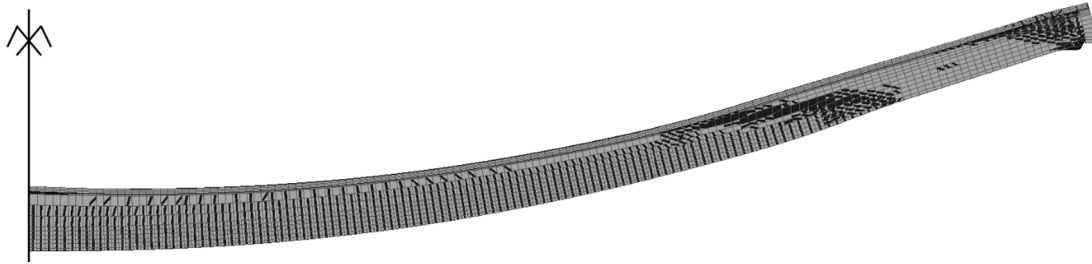


Fig. 1. Shear failure of an LDE7 roof girder in the 3 PB loading configuration.

approaches and appropriate material models are well suited for calculating stress and strain states and for the verification of the complex shear capacity of prestressed concrete components. Regardless of the calculation or simulation models used, the properties of the materials (reinforcing steel and prestressing steel) and of the composite material of the prestressed concrete form an essential basis for capturing load-bearing behaviour under mutual shear and normal force loads realistically. Due to the very high stresses which occur very early (usually at ages < 24 h) as a result of the prestressing procedure in the pre-tensioning bed, there is a great need for research on the time-dependent behaviour of concrete (creep, shrinkage and relaxation), bond stresses (the influence of the Hoyer effect), tension-stiffening and tension-softening, the dowel effect, and crack friction. Even though these individual properties and behaviours have been investigated in several scientific articles [36], in-depth research on their interaction and mutual influence is still required. Consequently, the simulation strategies and methods presented below were chosen so as to condense what limited information there is about V + N + M interaction in shear fields.

The producer followed multiple interests such as the development of structural design and monitoring systems, crack propagation analysis, the analysis of time-dependent behaviour, the evaluation of the fracture-mechanical properties of materials, and the estimation of shear structural response, and its stochastic features. A keystone of the conducted

research is the use of NLFEA based on the well-identified fracture parameters of the utilised concrete mixture combined with the stochastic modelling of destructive shear experiments.

Extensive experimental studies were performed on small specimens and small- and full-scale beams to obtain the required information for the implementation of complex material laws in advanced probabilistic nonlinear numerical analyses. It was understood from the early beginning that developing an excellent numerical model for comparison with experiments conducted on real structures would be impossible without proper knowledge of fracture-mechanical parameters. Therefore, a comprehensive experimental study of material parameters was performed first [37,38]. The aim was to expand the database of results for specified types of concretes by including the mean values, the standard deviations, the time of testing of the fracture mechanical concrete parameters and the most suitable mathematical model for probability distribution functions [37].

The fracture experiments were followed by destructive experiments with scaled precast elements and proof loading tests with full-scale TT roof girders [39]. The obtained information was utilised for the nonlinear deterministic modelling of the conducted destructive experiments and subsequent model updating connected with the development of the proper modelling procedure itself [13]. The resulting accurate numerical models were consequently utilised for the stochastic analysis

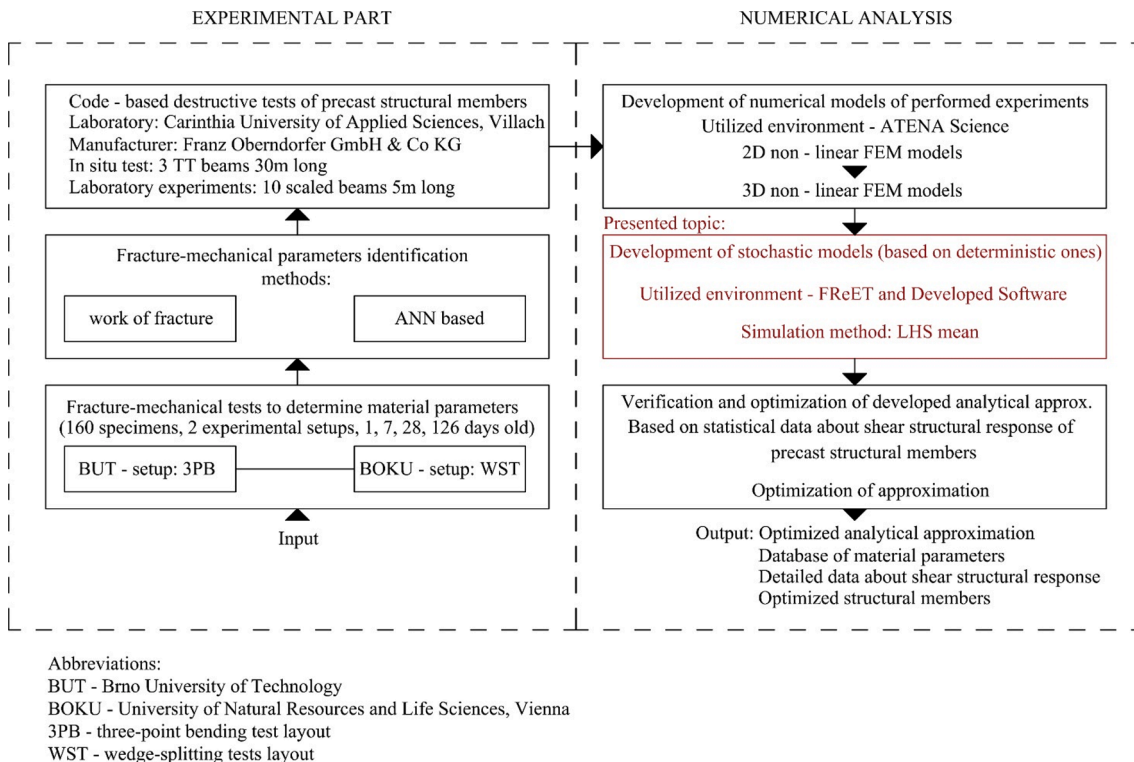


Fig. 2. The presented work within the broader context of conducted research.

presented within this paper.

The whole research program is summarised within the flow chart depicted in Fig. 2. Further efforts will be focused on the reliability-based optimisation of LDE7 girder's reinforcement layout. Since a specific load action system cannot be determined at the time a precast element is designed, conducted evaluations of failure probabilities can only be based on the separation of load actions and structural response allowed by [11]. The aim of the research is to assess the statistical moments of the ultimate shear strength of girders using the statistical simulation and to identify dominant random variables by the sensitivity analysis.

The complex methodology utilised for deterministic modelling and the experimental campaign necessary to obtain the used numerical models and the information on input random quantities was described in detail within the referenced papers ([13,37–41]). The other procedures necessary to complete the steps before stochastic analysis was performed (see Fig. 2.) will just be briefly mentioned/reviewed in Section 3 - experimental program and in Section 4 - development of the deterministic computational model.

2. Methodology

The most important efficient methods used for stochastic modelling are described here. Software tools combining existing software solutions for nonlinear modelling and stochastic simulation are briefly mentioned.

2.1. Statistical analysis and probability of failure

The following is a common definition of an engineering problem involving uncertainty and randomness, which is to be numerically analysed. A random variable, Z , represents a limit state of the studied engineering system (e.g. a structure and corresponding loading situation). In statistical analyses, Z may represent the random response of a system (e.g. limit deflection, limit stress, ultimate capacity, etc.), while during reliability determination, Z is referred to as a safety margin. Random variable Z is a function of random variables $X = X_1, X_2, \dots, X_{N_{var}}$ (or random fields):

$$Z = g(X) \quad (1)$$

where the function $g(X)$, a computational model, is a function of a random vector X (and of other, deterministic quantities). Random vector X follows a joint probability distribution function (PDF) $f_X(X)$. In general, its marginal variables can exhibit a statistical correlation. The paper focuses on situations when the information about $f_X(X)$ is limited to knowledge regarding univariate marginal distributions $f_1(x), \dots, f_{N_{var}}(x)$ and a correlation matrix, T (a symmetric square matrix of order N_{var} corresponding to the number of random inputs), which does not constitute complete information about the joint PDF. The aim is to perform sensitivity, statistical and reliability analysis upon the output quantity (generally a vector) Z representing a transformed variable. In the case of nonlinear analysis, the direct analytical description of the transformation of input variables to Z is not possible. It is typically performed in a numerical way by Monte Carlo type simulation.

The approach focused on the estimation of statistical moments of response quantities, such as means or variances, is commonly called statistical analysis, i.e. the estimate of the mean value of Z approximates the integral:

$$\mu_g = \int g(X)f(X)dX \quad (2)$$

Higher statistical moments of the response might be obtained by integrating polynomials of $g(X)$.

If $g(X)$ represents a failure condition, it is called the limit state function, and Z is referred to as the safety margin. Usually, the convention is that it takes a negative value if a failure event occurs; $Z \leq 0$, and a survival event is defined as $Z = g(X) > 0$. The limit state

function can reach various complexity an explicit or implicit function of basic random variables (e.g. in the form of a computer program). The aim of reliability analysis is to estimate unreliability using a probability measure called the theoretical failure probability $p_f = P(Z \leq 0)$.

The standard definition of a reliability indicator in the form of the probability of failure requires knowledge of load actions, and their statistics since safety margin Z is expressed as:

$$Z = R - E = g(X) \quad (3)$$

where R represents a selected quantity of structural response and E a benchmark quantity caused by load actions. The value of E cannot be known in the case of precast element design since environmental conditions and loads imposed during the lifetime of a structure rely on case-specific design situations concerning structures built from precast elements. It is, therefore, crucial to provide statistical data on the structural response of precast elements as an output from statistical analysis, according to Eq. (2).

The analytical calculation of the integral in Eq. (2) is generally impossible. Many efficient stochastic analysis methods have, therefore, been developed over the last seven decades (see Introduction). A straightforward solution to these tasks is numerical simulation. The principle behind the method is to introduce an analytical model – a computer-based response or limit state function (Eq. (1)) that predicts the behaviour of the studied system and repeat analysis many times under randomly generated conditions according to their probability distribution law. This simulation principle has remained formally the same up until the present day, and it was utilised for this study. The statistical analysis described below thus estimates the mean value of shear structural response (ultimate capacity) utilising the best linear unbiased estimator (the arithmetical mean), which is defined as:

$$\bar{\mu}_g \approx \frac{1}{N_{sim}} \sum_{i=1}^{N_{sim}} g(X_i) \quad (4)$$

The N_{sim} samples X_i (realisations, integration points) of the primary random vector X are selected to have an identical probability $1/N_{sim}$ (as in Eq. (2)). The corresponding standard deviation is then estimated as:

$$s = \sqrt{\frac{1}{N_{sim} - 1} \sum_{i=1}^N (X_i - \bar{\mu}_g)^2} \quad (5)$$

In the case studies described below functions $g(X)$ (see Eq. (1)) were represented by a complex NLFEA computational model developed according to the procedure described within [13]. Since one single simulation with NLFEA model took hours to complete, the LHS mean simulation technique was utilised in order to reduce the number of necessary simulations. LHS yields lower variance in statistical moment estimates compared to crude Monte Carlo sampling at the same sample size [17]. Thus, the technique has become very attractive for dealing with computationally intensive problems like, e.g. complex finite element simulations.

It has been shown that a preferable LHS strategy is the approach where the representative value of each interval corresponds to the mean value of interval. The sample averages equal the mean values of variables exactly, and the variances of the sample sets are much closer to the target values than those provided by other selection schemes; see [43] for details.

2.2. Statistical correlation among random variables

The required correlation among design variables can be introduced using traditional approaches such as Nataf's or Rosenblatt's transformations [44], or via the combinatorial optimisation of random permutations within generated design vectors minimising the error between desired and generated correlation matrixes [43]. The correlation among simulated variables is a research topic that lies beyond the

scope of this paper. Thus, only a brief description of the practical approach is given in the following subsections.

2.2.1. Nataf's transformation

In the general case of non-normal correlated random variables, it is necessary to use a more complicated process for transformation called Rosenblatt transformation [45]. However, in practical applications, only marginal distributions and the correlation matrix are usually known, meaning that the information about a joint probability distribution is incomplete [46]. Therefore, it is necessary to assume a specific copula [47]. A case of Rosenblatt transformation, which assumes a Gaussian copula, is also known as Nataf's transformation [48], which is very often utilised in reliability applications. Nataf's transformation, to uncorrelated standard normal space, is composed of 3 steps, which are as follows:

$$\xi = T_{Nataf}(X) = T_3^o T_2^o T_1(X) \quad (6)$$

The first two steps represent an isoprobabilistic transformation to correlated standard normal space:

$$T_1 : X \rightarrow W = F_x(X) \quad (7)$$

$$T_2 : W \rightarrow Z = \phi^{-1}(W) \quad (8)$$

The last step represents a transformation to uncorrelated space using a linear transformation. For this procedure, Cholesky decomposition of the correlation matrix is commonly utilised:

$$R_z = LL^T \quad (9)$$

$$T_3 : Z \rightarrow \xi = \Gamma Z \quad (10)$$

The R_z is a fictive correlation matrix and Γ is the inverse of a lower triangular matrix, L , obtained via Cholesky decomposition. The assumed Gaussian copula is parametrised by elements ρ_{zij} of R_z and the relationship between the fictive correlation coefficients ρ_{zij} and the linear correlation coefficients defined in physical space ρ_{xij} is defined by the following integral equation:

$$\rho_{xij} = \frac{1}{\sigma_i \sigma_j} \iint \left\{ F_i^{-1}[\Phi(z_i)] - \mu_i \right\} \cdot \left\{ F_j^{-1}[\Phi(z_j)] - \mu_j \right\} \times \varphi_2(z_i, z_j, \rho_{zij}) dz_i dz_j \quad (11)$$

where μ is the mean value, σ is the standard deviation, and φ_2 is the bivariate standard normal probability density function with fictive correlation coefficients ρ_{zij} :

$$\varphi_2(z_i, z_j, \rho_{zij}) = \frac{1}{2\pi\sqrt{1-\rho_{zij}^2}} \exp\left(-\frac{z_i^2 - 2\rho_{zij}z_i z_j + z_j^2}{2(1-\rho_{zij}^2)}\right) \quad (12)$$

The whole process can be reversed to transform realisations $\xi \rightarrow X$. Unfortunately, there is no guaranteed solution for specific combinations of input parameters and correlation coefficients. More details about the limitations of Nataf's transformation can be found in [43].

2.2.2. Combinatorial optimisation

A robust technique to impose statistical correlation based on the stochastic method of optimisation called simulated annealing has been proposed by Vořechovský and Novák [43]. The imposition of the prescribed correlation matrix on the sampling scheme can be understood as a combinatorial optimisation problem: The difference between the specified (target) T and the generated (actual) A correlation matrices must be as small as possible. Let us denote the difference matrix (error-matrix) E :

$$E = T - A \quad (13)$$

A suitable norm of the matrix E is introduced to obtain a scalar measure of the error. Two different norms have been defined in [43],

denoted as ρ_{max} and ρ_{ms} . These norms have to be minimised. The objective function for optimisation is the error norm. The design variables are related to the ordering in the sampling scheme. We want to find an efficient near-optimal solution. It can be achieved, e.g. by applying the Simulated Annealing optimisation algorithm.

The mutation by a transition called a swap from the parent configuration to the offspring configuration s performed at each step of the combinatorial optimisation algorithm. A swap (or a trial) is a small change to the arrangement of the sampling table. It is done by randomly interchanging a pair of values, x_{ij} and x_{ik} . In other words, one needs to generate i (select the variable) randomly, and a couple, j, k , (choose the pair of realisations to interchange); One swap may or may not lead to a decrease (improvement) in the error norm. Immediately, one configuration between the parent and offspring is selected to survive. The Simulated Annealing algorithm is employed for the selection step. Details on the algorithm and the implementation can be found in [43].

Extensive studies on the performance of the algorithm [43] show that it performs considerably better than other widely used algorithms for correlation control, namely both Iman and Conover's Cholesky decomposition and Owen's Gram-Schmidt orthogonalisation. Its performance for an extremely small number of simulations should mainly be highlighted here, along with the possibility to add additional samples correctly, as is described in [49].

2.3. Probabilistic design

The description above demonstrates that the probabilistic approach that directly evaluates failure probability is too complicated and time consuming for practical design and assessment of structures. Therefore, the semi-probabilistic approach was developed to reduce the high number of simulations necessary for traditional probabilistic analysis while ensuring the acceptable reliability of structures designed using NLFEA tools. Such procedures evaluate design values of action E_d and resistance R_d satisfying the given safety requirements instead of the direct calculation of the probability of failure p_f . If both R and E are lognormally distributed independent random variables, their design values are defined as:

$$X_d = \mu_X \exp(-\alpha_X \beta_n v_X) \quad (14)$$

where v_X is the coefficient of variation (CoV of X), α_X represents the directional cosines derived from First Order Reliability Method (FORM), and the recommended values are $\alpha_R = 0.8$ and $\alpha_E = -0.7$ according to [11]. β_n represents the required (target) reliability index prescribed by normative standards [11]. The aim is limited to the estimation of R_d , which is crucial, especially in case of design and assessment of precast structural members.

The target reliability index for the ultimate limit state, moderate consequences of failure and reference period of 50 years is set at $\beta_n = 3.8$ according to [50], and corresponding target failure probability in semi-probabilistic design and assessment of structures is $p_f = \Phi_N^{-1}(-\beta^* \alpha_R) = \Phi_N^{-1}(-3.8 * 0.8) = 0.0012$. Obviously, for the determination of a design value via the semi-probabilistic approach, it is crucial to correctly estimate the basic statistical moments. This can be done using various statistical methods or Monte Carlo simulation techniques in combination with statistical analysis.

3. Software tools

It was necessary to combine existing software solutions for nonlinear modelling and stochastic simulation in order to perform the analysis described below. The ATENA Science [9] software environment was utilised for the creation of numerical models. This solution allows the definition of model geometry, materials and solution parameters within the GID preprocessor [9], and the subsequent performance of calculations via an automatically generated input file in the ATENA Studio

processor. ATENA software provides a state-of-the-art environment [51] for NLFEA evaluations of concrete structures. It offers advanced material models for the accurate description of concrete behaviour [9] and allows input files to be easily manipulated by third-party applications. The utilisation of the ATENA environment was also supported by the strong connection and close cooperation between the authors of this paper and the developers of ATENA software [13,52].

The ATENA environment can be seamlessly connected with FReET software for simulation and reliability analysis [52] (see the brief description below) using the SARA software shell [53]. However, the SARA environment does not provide all of the functionality necessary for the stochastic analysis of prestressed structures. Prestressing losses calculated according to [12] are dependent on concrete material parameters and the applied prestressing force, which are represented by random quantities. The losses themselves must be defined at the beginning of each analysis. It was, therefore, necessary to create a dynamic library (hereinafter dll) for the evaluation of losses and plug this routine into the task solution procedure between the simulations (conducted in FReET) and the NLFEA performed within ATENA. A new ATENA-FReET interface was developed in order to automate the solution procedure. The following paragraphs briefly describe FReET and the new interface. This approach allowed the applicability of current software tools to be extended, and enabled the use of some previously developed routines and scripts with a relatively low programming cost compared to the development of interfaces for ATENA from scratch using different software and programming tools.

3.1. FReET

FReET multipurpose probabilistic software for the statistical, sensitivity and reliability analysis of engineering problems [46] is based on the efficient reliability techniques described in [16,17]. The software allows the definition of a stochastic model of the given problem along with the performance of advanced simulation within the design space, and the calculation of reliability using one of the built-in methods. FReET enables the probability distribution function to be defined for each random variable (via the selection of predefined functions and their parameters based on raw data, etc.). For simulation, FReET offers the simple Monte Carlo method or the above-described LHS methods (in random, median or mean form). It is also possible to prescribe a correlation matrix for random variables.

Simulated annealing approach defined in [43] is utilised to achieve the required correlation structure among generated simulations. For reliability calculations, FReET enables the use of simple Cornell index calculations, the Curve fitting technique or FORM. Other useful features of FReET are described fully in detail in [52].

3.2. The ATENA-FReET interface

The ATENA-FReET interface is a simple software environment developed in order to connect the finite element-based software package ATENA Science with FReET reliability software in a way that is both general and user-friendly. The environment mimics the basic concept of SARA software shell but adds some the functionality necessary to perform the stochastic analysis of complex prestressed structures. The software allows a task to be defined, the loading of a prepared ATENA input file containing a defined numerical model, the marking of quantities to be randomised, the calling of FReET to prepare a stochastic model (or utilise a predefined one), the generation of numerical model realisations based on simulated values, the connection of user-defined dll routines between simulation and analysis within ATENA, the running of simulations (also multiple in parallel) and management of computation resources, the postprocessing of output files and the extraction of defined quantities to be processed in FReET or any table processor. The current plan is to integrate the developed interface into a general software solution for reliability-based optimisation, which is

currently under development [54].

4. Experimental programme

The stochastic modelling of shear structural response using NLFEA requires solid knowledge of the utilised material model's fracture-mechanical parameters and their statistics. The required information must be obtained by an experimental study performed using concrete mixtures used for the casting of modelled structural members.

NLFEA can be carried out by many software solutions with generally different material models and solution procedures using a wide range of parameter sets. It also allows the modelling of detailed aspects of structural behaviour such as bond behaviour, the cracking of material and its plastic behaviour without any strictly defined "level of detail" required to achieve sufficient accuracy in solving the given task. It is up to the user's "expert guess" as to which model simplifications are acceptable. In the case of mass-produced precast elements, it is therefore beneficial to perform a set of destructive experiments to verify the utilised modelling procedure and its outcomes.

The following paragraphs will briefly describe an experimental campaign performed before the numerical and stochastic modelling of LDE7 roof girders took place (see the research workflow in Fig. 2). The results and findings acquired during the experiments have already been published ([13,37,38,39]). This section is therefore included to improve the readability of the paper and to provide context. Detailed information about the experimental phase of the research can be found within the papers mentioned above.

4.1. Fracture-mechanical quantities

A broad sampling and testing program has been conducted by the Institute of Structural Mechanics, Faculty of Civil Engineering at Brno University of Technology (BUT), Czech Republic, and the Institute for Structural Engineering at the University of Natural Resources and Life Sciences (BOKU) in Vienna in collaboration with the Austrian firm Franz Oberndorfer GmbH & Co KG. The program was performed to ensure the database for specified types of concrete including the mean values, the standard deviations, the time of testing of the fracture-mechanical concrete parameters and the most suitable models of probability distribution functions. The three-point bending (3 PB) and wedge-splitting tests were conducted on C50/60 and C40/50 concrete specimens (see [37]) with a central edge notch, and their results were assessed using the effective crack and work-of-fracture methods [40]. Through the advanced identification approach based on artificial neural network (ANN) modelling [41], the following essential material parameters of the utilised 3D Nonlinear Cementitious 2 material model of concrete (see Section 5.2) were identified: tensile strength f_{ct} , modulus of elasticity E_c , and specific fracture energy G_f . The compressive strength f_c was measured using standard cubic compression tests. The identification of the below-mentioned material parameters was carried out using FraMePID-3 PB software, which was developed in order to automate the time-consuming process of ANN-based inverse analysis. The lynchpin of the method is an AAN which transfers the input data obtained from the fracture test to the desired material parameters. For theoretical details on ANN-based inverse analysis, which lie beyond the scope of the present paper, we refer the interested reader to [55]. The FraMePID-3 PB software itself is described in depth in [41].

Table 1
Adjusted stochastic parameters of C50/60 concrete (age 28 days).

Parameter	Mean	COV	PDF
Compressive strength	77 MPa	6.4%	Lognormal
Tensile strength	3.9 MPa	10.6%	Lognormal
Modulus of elasticity	34.8 GPa	10.6%	Lognormal
Fracture energy	219.8 Jm ⁻²	12.8%	Lognormal

In total, 134 concrete conformity specimens made from two concrete mixtures commonly used within the industry were tested at hardening times of 1, 7, 28 and 126 days to estimate the stochastic attributes (E_c , f_{ct} , G_f and f_c) of the concrete mixtures material parameters. At the time of the destructive beam experiments (see Section 3.2), small-scale samples prepared according to EN 206 were also tested in order to characterise the fracture-mechanical parameters f_c and E_c directly. The parameters displayed in Tab. 1 were derived using an ANN-based approach for a grade of concrete C50/60 at the age of 28 days of hardening rapt from the 134 specimens [37].

Since the number of tested specimens is not high enough to disprove the prevailing opinion on the typical PDF for mentioned parameters [58] it was decided that lognormal distributions would be used instead of those identified using curve fitting and experimental realisations. Table 1 displays the adjusted (utilised) stochastic model of concrete. Note that values of material parameters summarised within Table 1 represent input parameters of CC3DNonLinCementitious2 material model [9] corresponding to virtual models of conducted 3 PB experiments [41].

4.2. Experiments conducted on prestressed full- and reduced-scale concrete girders

The primary area of interest is the normal-shear force interaction of long-span TT concrete roof elements made of C50/60 concrete (see Section 5). Proof loading tests carried out according to CEB-FIP Model Code 2010: Design Code to define the shear performance within linear brunch of the working diagram have been performed on three of these TT concrete roof girders. More details on testing and monitoring of the TT concrete roof elements are given in [39]. Note that due to the relatively large size of the full-scale precast elements, destructive experiments would be expensive and complicated. Thus, the performed proof loading tests cannot provide information about the plastic and pre-peak behaviour of the tested elements. Therefore, NLFEA was used to characterise the geometric and mechanical properties of the laboratory tested beams concerning their shear resistance performance. In particular, NLFEA was used to verify the layout of reinforcement, to choose suitable monitoring systems and to define the testing and loading procedures for scaled models of prestressed girders. Subsequently, destructive experiments were performed with scaled precast beams.

The ten laboratory tested beams were continuously prestressed at

449 MPa to 1105 MPa by four to eight strands (St 1570/1770). A span length of 5.00 m characterises the ten laboratory beams, a web width of 0.14 m and a height of 0.30/0.45/0.60 m. The slabs of the T shaped elements have a width of 1.50 m and a thickness of 0.07 m. The primary interest in testing the ten laboratory beams lies, just as with the TT roof elements, in the normal force-shear interaction. The performed destructive experiments helped to establish the NLFEA modelling procedure using the ATENA Science software environment [9]. The development of the NLFEA computational model mentioned above was summarised and demonstrated at the benchmark of the scaled T-shaped girder T30150 V2 in [13]. Material parameter calibration was performed based on experimental testing and a complex updating simulation. The below-described numerical model of full-size LDE7 girder was developed using this methodology and experience from scaled girder testing and simulation. The charts in Fig. 3 can demonstrate the resulting NLFEA accuracy. These charts display a comparison between the experimentally obtained and numerically derived load vs deflection (hereinafter LD) diagram for beams T30 150 V2 and R45 V2 (scaled experimentally tested girders).

Note that standard cubic specimens for compression tests were cast along with each girder. Those specimens were utilised to determine the material properties of the concrete employed for the casting of the beams.

5. The numerical model of an LDE7 roof girder

The numerical model was created using the ATENA Science software environment [9] and the modelling procedure described in [13]. Since losses of prestressing are dependent on random inputs such as f_c , E_c , prestressing force, etc. it was necessary to evaluate prestressing losses (according to [12]) before the NLFEA of each simulation in order to conduct stochastic simulation above the developed numerical model. The tools currently available within the ATENA Science environment do not allow the evaluation of quantities based on random inputs before the randomisation of the NLFEA input data itself. It was, therefore, necessary to develop a simple software shell (briefly described within Section 3.2) to perform the presented stochastic analysis.

The loading procedure is defined in the ATENA Science [9] environment using “intervals”. Specified loads and constraint conditions are applied within a specified number of load steps utilised in each interval. The employed software solution combined with the given NLFEA input

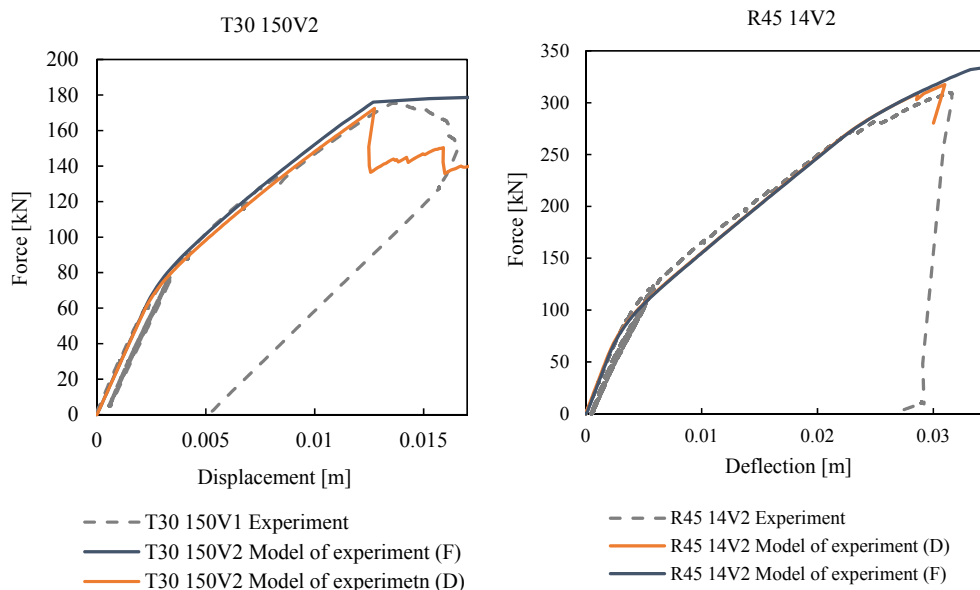


Fig. 3. Comparison between experimentally and numerically derived LD diagrams for beams T30 150V2 and R45 14 V2; (D) denotes displacement-controlled loading and (F) force-controlled loading of the numerical model [13].

file structure requires the application of prestressing force and live load within separate intervals. This separation can only be used without complications for the numerical models of scaled girders [13]. In case of the full-size LDE7 roof girder, it was necessary to introduce ten load intervals for live load application and ten intervals for prestressing. During the solution, one interval with 1/10 of prestressing was always followed by one interval with 1/10 of live load. The adjusted load application scheme was the only difference compared to the modelling procedure presented within [13].

Prestressing using initial strain was applied for the pretensioning wires. This application ensures that any loss of prestressing due to the elastic deformation of concrete is calculated directly. However, the prestressing force was applied to concrete with an age of only 14 h during the production process. It means that Young's modulus of the concrete was different (approximately half) from the value of elastic modulus after 28 days of hardening. The initial strain for the reinforcement should be reduced by the difference between the strain of prestressed concrete at 14 h and the strain of prestressed concrete at 28 days of hardening. The corresponding strains were calculated as ratios of stress within the cross-section of the beam caused by the application of prestressing normal force and the corresponding Young's modulus value. The second loss of prestressing, which was applied by the reduction of initial strain for the reinforcement line, occurred due to the relaxation of the tendons. This was evaluated according to [12].

Temperature loading was utilised to simulate the rheological behaviour of the precast concrete elements. Creep and shrinkage deformations also lead to losses of prestressing. MC 2010 was utilised for the calculation of creep and shrinkage strains after 28 days of hardening. The uniform temperature gradient to be applied in order to invoke equivalent strains was calculated with the assumption of a thermal expansion coefficient of $\alpha = 1.00e-05 \text{ K}^{-1}$. The creep and shrinkage affect the concrete throughout its volume. A temperature gradient can be utilised in order to mimic creep and shrinkage strains in all directions. This allows them to affect the whole structure, including the reinforcement.

5.1. Geometry and numerical model of an LDE7 roof girder

The beam has a TT-shaped cross-section, a total length of 30.00 m and a height of 0.50 m at the ends and 0.90 m in the middle of the beam. The width webs are 0.14 m (note that 0.14 m is the bottom dimension – the web a little conical). The slab has a dimension b/h of 3.00 m/0.07 m. The reinforcement and geometry of the beam are symmetrical along the middle cross-sectional and longitudinal plane. The girder is continuously prestressed to 1107.53 MPa via 32 (16 in each web) \times 7-wire 1/2-inch strands with a wire quality of ST 1570/1770. The prestressing reinforcement is divided into four layers depending on the length of the isolated part of the cables (the part where the wires have no bond to the concrete). The lowest six cables in each web are connected to the concrete along the whole length of the beam. The four wires in the second layer of each web are isolated 2.00 m from both sides of the beam. The four cables in the third layer of each web are isolated 4.00 m from both sides of the girder. The two cables in the fourth layer of each web are isolated 5.60 m from both sides of the beam. In addition to the pretensioning wires, two reinforcement bars with a diameter of 0.02 m are located at the bottom of webs, and six reinforcement bars with a diameter of 0.014 m are located in the upper reinforcement layer of each web. The areas at the ends of girder are reinforced using four horizontal rebars in a U-bolt shape with a diameter of 0.012 m. Despite the fact that basically no stirrup reinforcement was planned according to the reinforcement layout, 13 stirrups with a diameter of 0.006 m at a distance of 0.50 m from each other at the ends of the beam. Another 16 rebars with a diameter of 0.006 m were mounted in the middle of the girder. The plate of the girder was equipped with orthogonal reinforcement composed of 0.008 m diameter rebars at a distance of 0.20 m from each other in the longitudinal and transverse directions. Fig. 4 shows the reinforcement of

the area of expected shear failure (side view). Fig. 5 (left) shows a cross-sectional detail of the position of the reinforcement within the webs.

The modelled girder was loaded by displacement applied 4.125 m from the support above both webs. Loading was applied via steel plates ($0.50 \times 0.50 \times 0.05 \text{ m}$). The webs of the beam were supported by four steel plates ($0.14 \times 0.14 \times 0.05 \text{ m}$). Fig. 4 (right) displays the layout of the numerical simulation.

A regular hexagonal FE mesh of 61,784 finite elements was generated using GID software. The final 3D geometry of the model is shown in Fig. 6, along with the support conditions. The utilised model of reinforcement (including tendons) is visible in Fig. 7. The edge size of the elements in the area with condensed mesh was approximately 20 mm. Elements with edge size of roughly 35 mm were utilised for the rest of the beam. The ratio between the edge sizes of a single element never exceeded 3:1. The finite element mesh was condensed in the region of expected shear failure. The region of shear failure was estimated based on data obtained from performed experiments and numerical simulations (see description above). It was located at the web of the beam between the support and the point of loading.

Note that the numerical model can be reduced due to the longitudinal symmetry of the beam and low deformations in the direction perpendicular to the plane defined by the load vector and the longitudinal axis of the beam. This reduction was utilised for the below-mentioned stochastic simulations to decrease computational demand.

The element type of the concrete volume and steel plates was set to hexahedral linear eight nodal brick elements (CCIsoBrick [9]). These are isoparametric elements integrated by Gauss integration at defined integration points. The same elements were used for the web as well as for the flange of the beam (shell elements were not utilised). The reinforcement was modelled using two-nodal linear truss elements (CCIso-Truss [9]). The bond properties of the reinforcement were not investigated and thus kept at the default setting (perfect bond) [9].

Loading force was distributed via a $0.50 \times 0.50 \times 0.05 \text{ m}$ steel plate (shown in Fig. 5). The Steel VonMises 3D material model (in its default setting within the ATENA – GID environment) was utilised for the steel plates. The plates are connected to the beam using a master/slave-type contact with a rigid connection definition. The loading in the numerical model was applied using controlled displacement. The Newton-Raphson solution algorithm was utilised for the described NLFEA.

5.2. Materials

The steel reinforcement and tendons were modelled using the 1D Reinforcement material. The utilised stress–strain diagrams are presented in Fig. 8. The material of tendons was modelled using a bilinear diagram with hardening. This simplification was possible since modelled girders typically fail due to brittle shear failure of concrete.

The value of elastic modulus used for steel reinforcement was 200 GPa. The density of the reinforcement steel was considered to be 7850 kg/m³. The coefficient of thermal expansion (α - necessary due to the applied temperature load in order to simulate long-term losses of prestressing) was set to be $1.2 \text{ e}^{-5} \text{ C}^{-1}$.

The geometrical nonlinearity of material was neglected. The prestressing reinforcement was considered to have a perfect bond. The bilinear diagram with hardening utilised for the tendons is shown in Fig. 8. Young's modulus for the tendons was set to 195 GPa. The cross-section area was considered to be $9.3 \text{ e}^{-5} \text{ m}^2$. The density and α coefficient values for tendons were the same as for steel reinforcement.

The “3D Nonlinear Cementitious 2” material model was used to govern the gradual evolution of localised damage. The model is formulated in the total format assuming additive decomposition of small strains and initial isotropy of the material. The tensile behaviour is governed by the Rankine-type criterion with exponential softening according to Hordijk [56], while the Menétrey–Willam yield surface with hardening and softening phases is used for the behaviour in compression [57]. The fracture model employs the orthotropic smeared crack

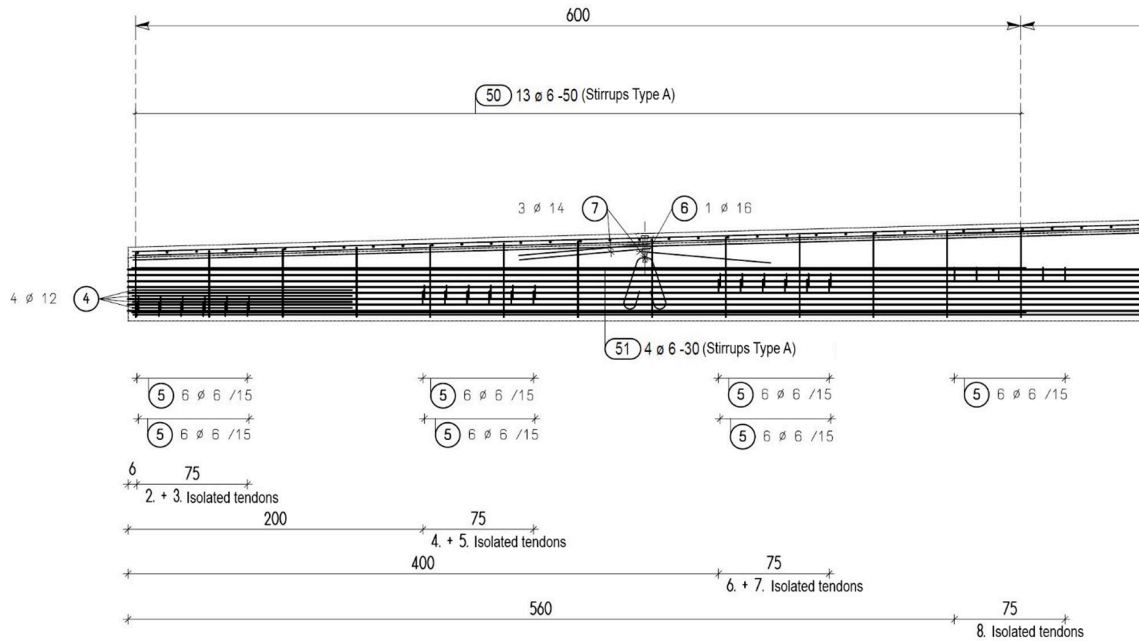


Fig. 4. Reinforcement of the area of expected shear failure.

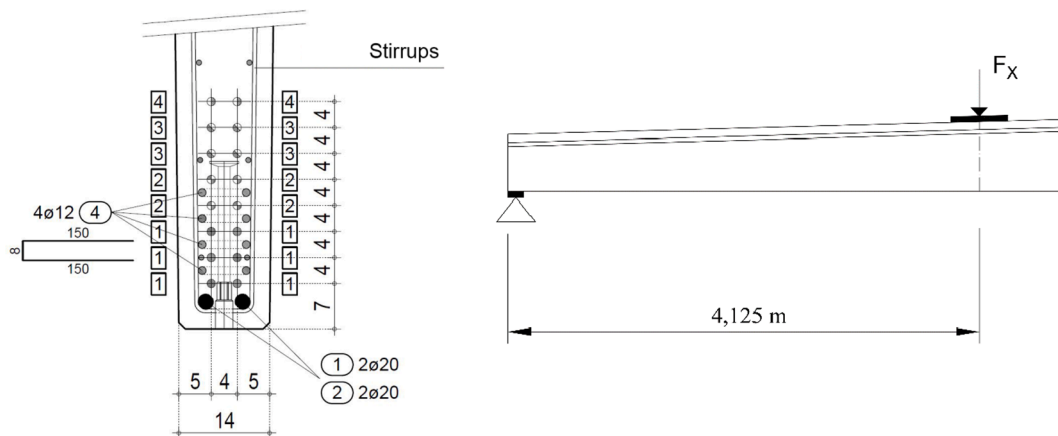


Fig. 5. Detail of the reinforcement position within the webs (left), and the layout of the numerical simulation (right).

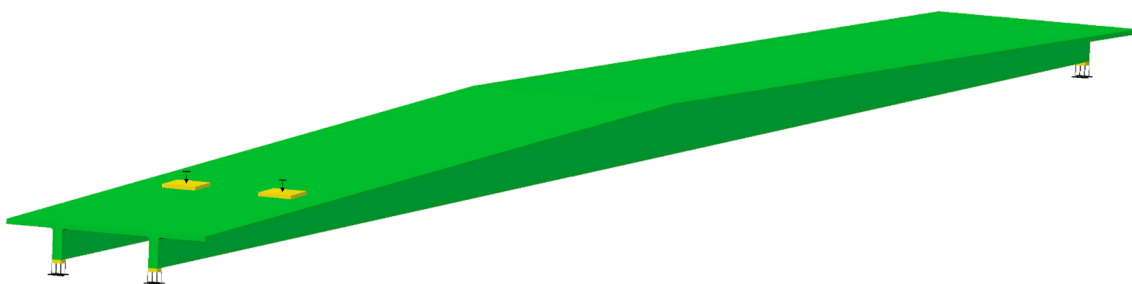


Fig. 6. 3D geometry of the model along with support conditions and loading.

formulation and the rotational crack model with the mesh-adjusted softening modulus. This model is defined based on characteristic element dimensions in tension and compression to ensure objectivity in the strain-softening regime; see [9] for details.

6. Stochastic modelling

The study aimed to estimate the statistical variability of the shear capacity of prestressed girders, to propose probabilistic design resistances and to establish a stochastic modelling procedure applicable within a reliability-based optimisation algorithm. For stochastic analysis, the ATENA-FReET interface (see Section 3.2) connecting the

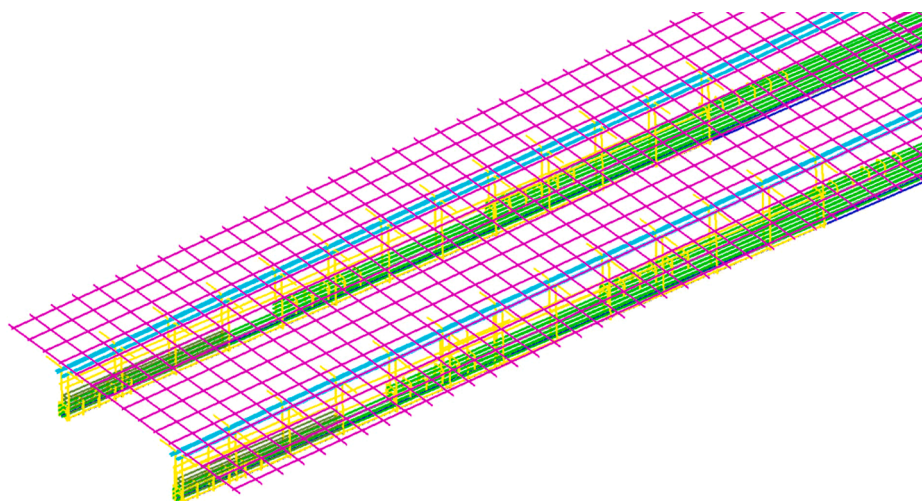


Fig. 7. 3D geometry of the modelled reinforcement.

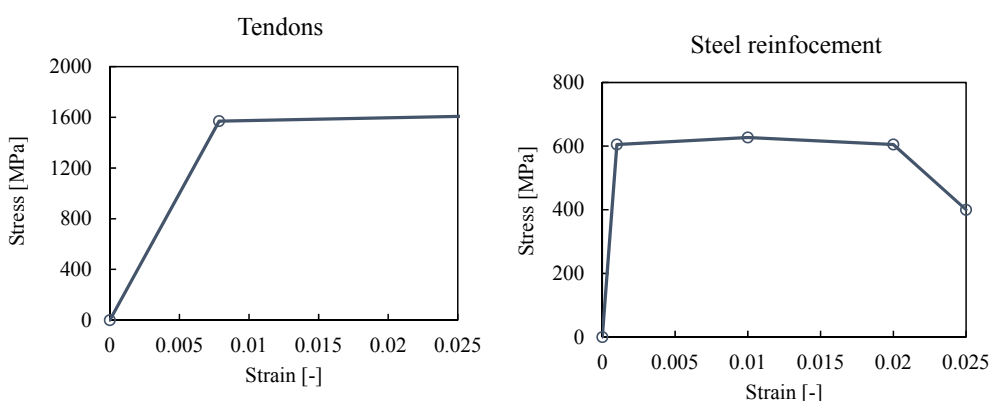


Fig. 8. Idealised stress–strain diagram of steel reinforcement (right) and tendons (left).

ATENA solver and the FReET reliability tool were utilised. A set of 12 parameters was used for the stochastic evaluation of structural response variability. The stochastic model of the concrete (probability distribution functions of concrete parameters) was defined according to Table 1. The value of load actions cannot be known in the case of precast element design since environmental conditions and the loads imposed during the lifetime of a structure rely on case-specific design situations concerning structures built from precast elements. It is, therefore, crucial (from the manufacturer’s point of view) to provide statistical data on the structural response of precast elements as an output from statistical analysis, conducted using Eq. (2).

The stochastic models of the steel reinforcement (Bst 550B) and the tendons (cables - ST 1570/1770) were based on JCSS recommendations [45] (variability) and information from the manufacturer (mean value). The prestressing force was randomised according to the recommendation of the JCSS [50]. Prestressing losses were also calculated for each realisation according to the FIB model code 2010 [12]. Ideally, model uncertainties should be obtained from a set of representative laboratory experiments and measurements conducted on real structures where all input values are measured or controlled. In such cases, model uncertainty has the nature of intrinsic uncertainty. If the number of measurements is small, the statistical uncertainty may be large. In addition, there may be uncertainty due to measurement errors both in the input and in the modelled output. Bayesian regression analysis is usually the appropriate tool to deal with the above situation. In many cases, however, a good and consistent set of experiments is lacking, and the statistical properties of the model uncertainties are purely based on

Table 2
The utilised stochastic model.

Parameter	Mean	COV	PDF
E	34.8 GPa	10.6%	Lognormal
f_t	3.9 MPa	10.6%	Lognormal
f_c	77 MPa	6.4%	Lognormal
G_f	219.8 J.m ⁻²	12.8%	Lognormal
ρ	0.0023 kton/m ³	4%	Normal
E_s	200 GPa	2%	Normal
f_{ys}	610 MPa	4%	Normal
E_t	195 GPa	2%	Normal
f_{yt}	1387.88 MPa	2.5%	Normal
P	0.0835 MN	6%	Normal
$I. L.$	1	10%	Lognormal
$L. T. L.$	1	10%	Lognormal

engineering judgement [50]. The most common way of introducing the model uncertainty into the calculation model is as follows:

$$Y' = \theta_l \times f(X_1 \dots X_n) \tag{15}$$

where Y' is a new model response including model uncertainty, the variables θ_l are referred to as parameters which contain the model uncertainties and are treated as random variables, and $f(X_1 \dots X_n)$ is the original response of the model. The model uncertainties were introduced only for the calculation of losses of prestressing [12]. It was decided that the uncertainty of calculated losses would be introduced with a variability corresponding to COV 10%. This value is lower compared to the

Table 3
The utilised correlation matrix.

	E	f_t	f_c	G_f	ρ	E_s	f_{ys}	E_t	f_{yt}	P	$I.L.$	$L.T.L.$
E	1	0.5	0.8	0.5	0	0	0	0	0	0	0	0
f_t	0.5	1	0.7	0.8	0	0	0	0	0	0	0	0
f_c	0.8	0.7	1	0.6	0	0	0	0	0	0	0	0
G_f	0.5	0.8	0.6	1	0	0	0	0	0	0	0	0
ρ	0	0	0	0	1	0	0	0	0	0	0	0
E_s	0	0	0	0	0	1	0.6	0	0	0	0	0
f_{ys}	0	0	0	0	0	0.6	1	0	0	0	0	0
E_t	0	0	0	0	0	0	0	1	0.6	0	0	0
f_{yt}	0	0	0	0	0	0	0	0.6	1	0	0	0
P	0	0	0	0	0	0	0	0	0	1	0	0
$I.L.$	0	0	0	0	0	0	0	0	0	0	1	0.5
$L.T.L.$	0	0	0	0	0	0	0	0	0	0	0.5	1

loss uncertainty recommended by the JCSS (COV 30%). However, the introduced reduction reflects the variability of losses explicitly introduced by random quantities used for the evaluation of losses (such as E_c , f_c , prestressing force, etc.). The utilised complete stochastic model is summarised within Table 2, which displays random quantities and their stochastic parameters. The employed variables are E – Young’s modulus (E - concrete, E_s - steel reinf., E_t - tendons), f_t - tensile strength, f_c - compressive strength, G_f - fracture energy, ρ - density of the concrete mixture, f_{ys} - yield strength of steel reinforcement, f_{yt} - yield strength of tendons, IL – model uncertainty for immediate losses of prestress, LTL – model uncertainty for long term losses of prestressing and P – initial prestressing force. The mean value of prestressing force was defined by the producer, while the variability and distribution function were defined according to [50]. The geometrical uncertainties are minimal due to the applied manufacturing procedure, and their effect can be neglected.

Also, statistical correlations were considered. The simulated annealing optimisation method [38] was utilised to introduce the required statistical correlations. The employed correlation matrix is shown in Table 3. The correlation of the material parameters of the concrete was set based on data combined from multiple sources. The

outcomes from the experimental campaign described in Section 4 led to the results summarised in [59]. The acquired data, however, might not represent a convincing set in terms of the number of performed experiments. The utilised correlation coefficients were therefore adjusted based on data from other sources [60]. The correlation among the material parameters of concrete is the subject of much debate, and it requires further experimental research. The correlation of other parameters, such as the E modulus and yield strength of the reinforcement, was considered according to JCSS recommendations contained in [50]. Within the utilised analytical models [12], both immediate and long-term losses of prestressing are dependent on the material parameters of the concrete and the initial prestressing force. This dependency should also be reflected in the uncertainties applied for model of prestressing losses. Therefore, it was decided that correlation would be introduced between $I.L.$ and $L.T.L.$ (see Table 3).

6.1. Results of statistical analysis

First of all, numerical simulation with mean values of input random variables was calculated, and the obtained result is compared to design value determined by a standard approach according to EN 1992 (127

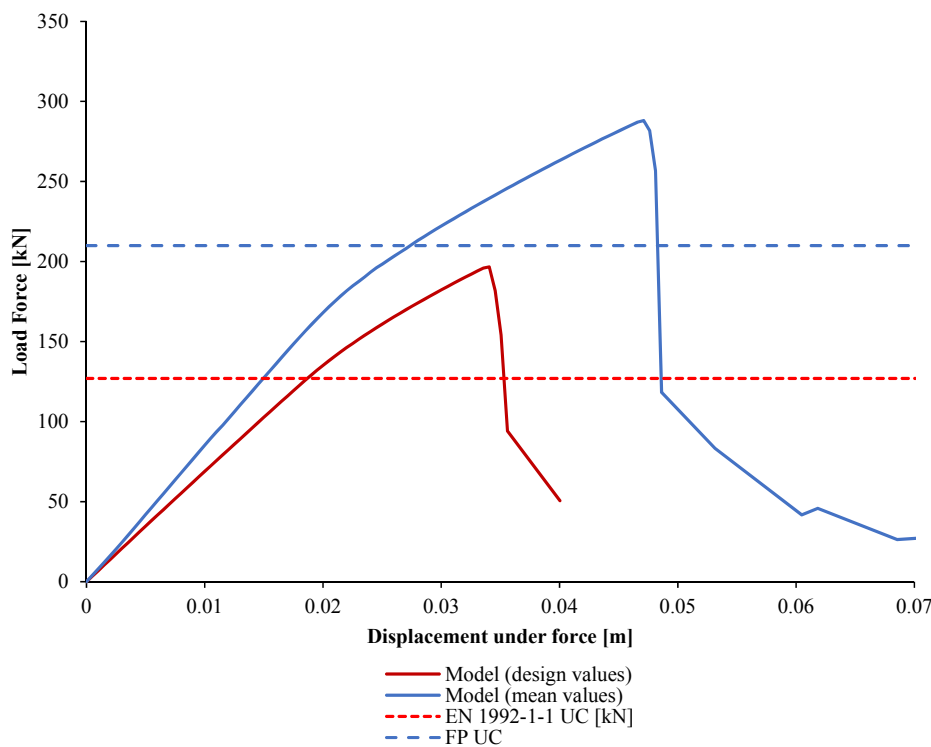


Fig. 9. EN 1992-1-1 ultimate capacity design value versus mean values-based NLFEA.

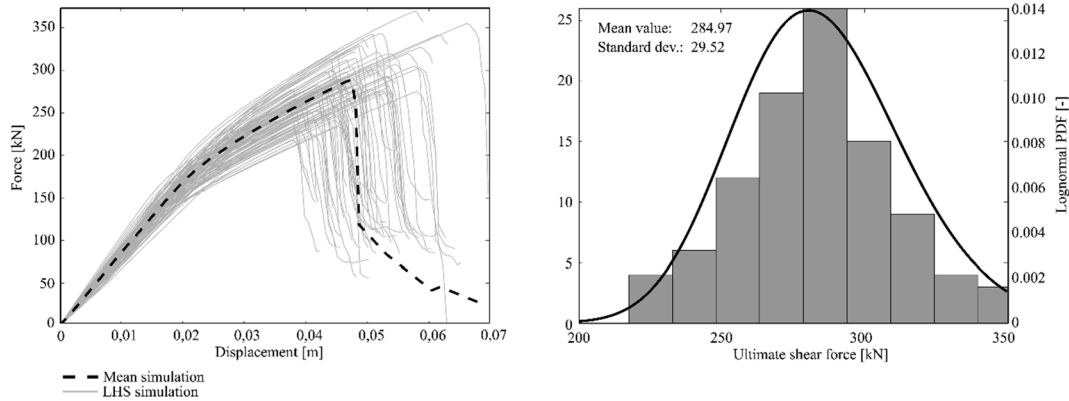


Fig. 10. LD curves: output from 100 NLFEA simulations.

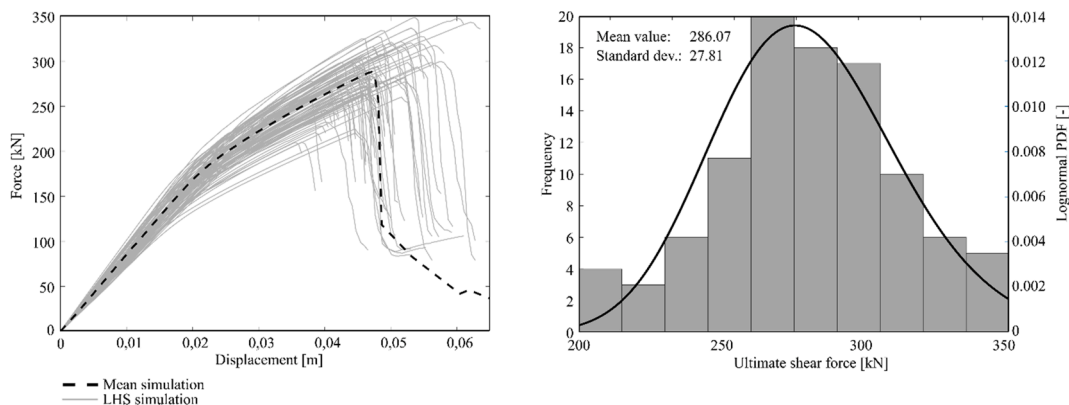


Fig. 11. LD curves: output from 100 NLFEA simulations.

kN) in Fig. 9. The presented comparison shows there is significant unused capacity within the nonlinear branch of the calculated LD diagram. Note that unused capacity can be taken into account just up to a design value derived from the Fully Probabilistic approach (hereinafter FP) according to the recommendation in [11] (see Section 6.3).

It is necessary to assume correlated random material characteristics in order to represent real material, especially in the case of concrete. However, probabilistic analysis becomes much more complicated in such cases. The very first problem is sampling from a joint probability distribution described by marginal distributions and a correlation matrix, which is not a complete set of information [46]. There are two possible solutions for practical analysis: the assumption of a specific copula (Nataf transformation), or combinatorial optimisation. Since the choice is not easy, and this paper is intended to demonstrate and examine the real application of the probabilistic design of structures, it was decided that both methods would be used, and the results compared. Note that the evaluation of a single NLFEA run took about 10 h and thus it was decided to generate a set of 100 simulations using the small-sample LHS mean technique with input random variables correlated by combinatorial optimisation to conduct sensitivity analysis and subsequently create efficient surrogate models to be utilised for further research purposes [61]. Fig. 10 shows the LD curves of the generated simulations used to construct a surrogate model based on polynomial chaos expansion [61].

For comparison, a traditional approach consisting of LHS mean and Nataf transformation was employed to generate a set of 100 correlated input random vector realisations. The obtained results (depicted in Fig. 11) are in agreement with the results of the alternative combinatorial optimisation approach and the statistical moments are identical for both methods. Therefore, it can be concluded that the combinatorial optimisation approach is an efficient alternative for the small-sample

stochastic analysis of computationally demanding mathematical models and it can be recommended especially in cases with complicated joint probability distribution function of input random variables, where traditional approach might fail to create a correlated sample. On the other hand, in case of lognormally or normally distributed random variables, it is beneficial to use Nataf's transformation due to the possibility of backward transformation to uncorrelated space. This might be crucial for sensitivity analysis, as is described in the following subsection.

6.2. Results of sensitivity analysis

The traditional sensitivity analysis method in statistics is represented by the correlation between an input variable and the quantity of interest [62,63]. Although standard measurement via the Pearson correlation coefficient is simple and efficient for linear monotonic dependency, it is necessary to utilise a generalised measure for non-linear monotonic relationship called non-parametric Spearman rank-order correlation technique. This method only works with ranks of input and output realisations as follows:

$$r_{s,i} = \frac{\sum_{j=1}^{N_{sim}} x_{rj} y_{rj} - N_{sim} \bar{x}_r \bar{y}_r}{(N_{sim} - 1) \sigma_{x_r} \sigma_{y_r}}, r_{s,i} \in \langle -1; 1 \rangle \quad (16)$$

where x_r and y_r are the two ranks of each observation sorted in ascending order, N_{sim} is the number of performed simulations \bar{x}_r and \bar{y}_r are the arithmetical mean of obtained ranks and σ_{x_r} and σ_{y_r} are standard deviations of mean. In case of simulation within the continual design where the probability of occurrence of two simulations with an equal value of some parameter is 0 might be Spearman rank-order correlation evaluated as:

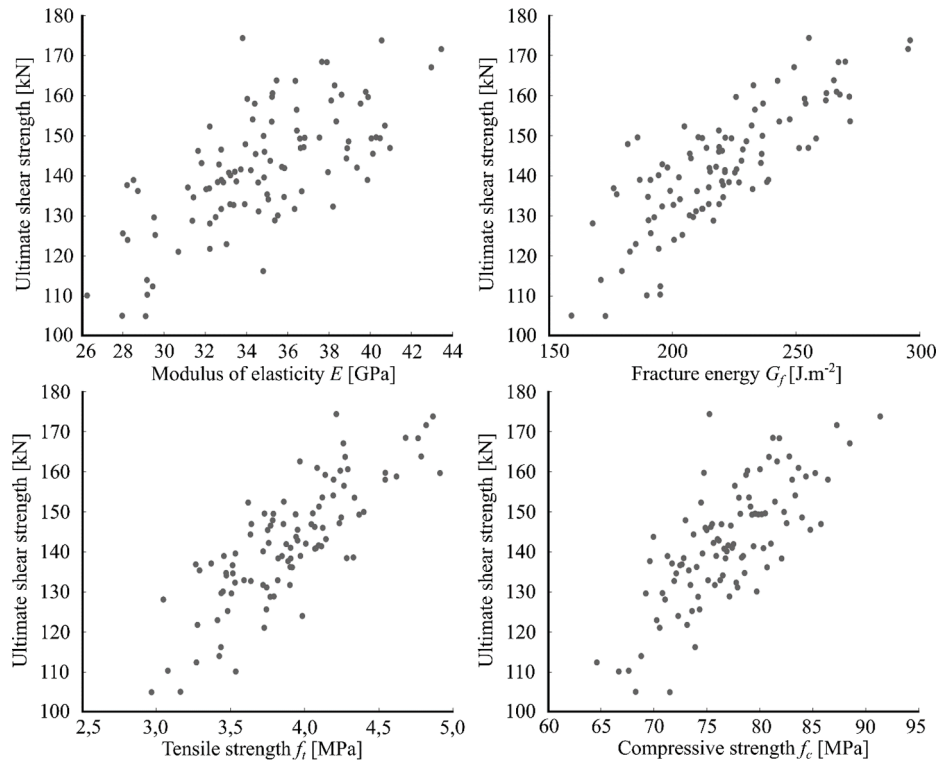


Fig. 12. Random material characteristics of concrete versus ultimate shear strength.

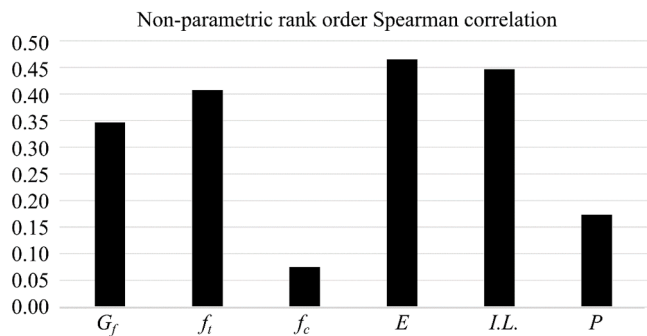


Fig. 13. Spearman rank-order correlation between input random variables and the ultimate shear strength of precast prestressed concrete roof girders for correlated space.

$$\rho_s = 1 - \frac{6 \sum d_i^2}{n(n^2 - 1)} \tag{17}$$

where n is the number of realisations, and d_i is the difference between paired ranks. The input-result diagrams are depicted in Fig. 12. This technique gives essential information about the strength and direction of dependence between input variables and the result of the mathematical model. The advantage of Spearman rank-order correlation is that results are naturally obtained as a by-product of LHS simulation and no additional demanding computation is needed.

Sensitivity analysis may be profoundly affected by the correlation among input random variables. The correlation among variables might be understood as a stochastic description of the complex natural relations which are not directly involved within a numerical model. Sensitivity analysis of the correlated model captures the cumulative effects of interdependent parameters. Such analysis corresponds to real-life behaviour of the modelled entity, but it does not provide objective information of the influence of numerical model parameters to the

observed output. Thus, it is necessary to analyse uncorrelated space as well to identify the actual role of input random variables. The obtained results for correlated space are depicted in Fig. 13 and for uncorrelated space in Fig. 14. In both cases, the essential material characteristics of concrete are apparent. It is possible to see the significant difference between correlated and uncorrelated space. Generally, in correlated space, there is a high correlation among concrete material characteristics, and thus their influence is together dominant in comparison to other variables. For correct interpretation of such results, correlated variables must be assumed as a group of variables. Note that, information about sensitivity in correlated space is valid only for this one stochastic model, including the given dependency structure. The mutual influence of concrete material parameters observed in model with correlation was verified by analysis of model without correlation showing that introduced uncertainty has a significant influence on immediate losses of prestressing. According to expectation, the compressive strength of concrete does not influence the model's performance (for given limit state). The significant influence of Young's modulus of concrete might be explained by the fact that it is involved within the utilised model for evaluation of prestressing losses. The assumption of uncorrelated material characteristics is not realistic, but such information may be crucial for the reduction of the stochastic model and further work possibly utilising different dependency structures etc.

The computational requirements of many available probabilistic methods, safety formats and surrogate models are strongly dependent on the size of the stochastic model. Thus, it is crucial to reduce the stochastic model as much as possible for further research. The reduced stochastic model contains only concrete material characteristics and uncertainty for immediate losses of prestressing in agreement with the sensitivity analysis described above. The stochastic model of concrete is fully described by the data available in Table 1. Note that the full stochastic model corresponds to the one described in Table 2. Random variables of concrete characteristics are statistically correlated according to the correlation among concrete parameters in Table 3. The correlation among concrete parameters is based on the results of laboratory experiments and information provided by the manufacturer.

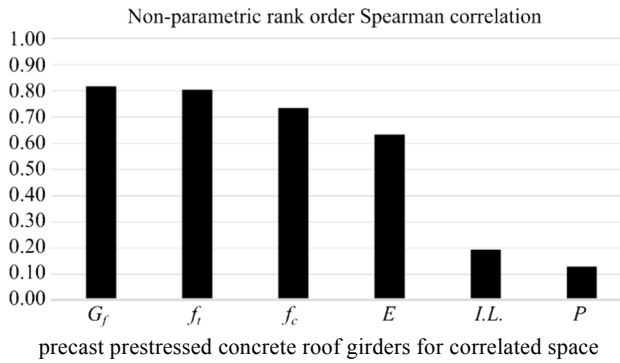


Fig. 14. Spearman rank-order correlation between input random variables and the ultimate shear strength of precast prestressed concrete roof girders for uncorrelated space.

The motivation for the performed sensitivity analysis was to reduce the stochastic model of the LDE7 roof girder utilised for the subsequent reliability-based optimisation of the LDE7 girder's structure. The performed sensitivity analysis helped to increase the accuracy of the surrogate models utilised within the reliability-based optimisation and to reduce the otherwise huge computational burden.

6.3. Probabilistic design of girders

In compliance with the semi-probabilistic approach implemented in the Eurocodes, the CoV of resistance v_R should generally consist of three parts: geometrical uncertainties v_g , modelling uncertainties v_m , and the uncertainty of the resistance due to material variability v_f . The geometrical uncertainties are minimal due to the applied manufacturing procedure, and their effect can be neglected. Modelling uncertainties are included in the stochastic model by IL and LTL - uncertainty for immediate or long-term losses of prestress. Therefore, the total CoV v_R is reduced to v_f , which can be obtained directly from statistically processed LHS results, as mentioned (for example) in [64,65], in this specific application. Nonetheless, note that the estimation of the modelling uncertainty of NLFEA has been a topic of high interest for the last decade and is not connected to the estimation of v_f . As a result, it is generally possible to use the additional safety factor γ_{Rd} associated with model uncertainty, which can be based on additional information (i.e. recommendations from scientific papers which are usually focused on specific structures, e.g. [66]), or on additional analysis, which is typically based on Bayesian calibration, as described in [67]. The design value of

resistance can then be further reduced to:

$$R_d = \frac{\mu_R \exp(-\alpha_R \beta_n v_f)}{\gamma_{Rd}} \tag{18}$$

As was already discussed, in order to estimate a design value for resistance which satisfies the given safety requirements, it is necessary to calculate the percentile of shear resistance corresponding to the target failure probability $p_f = 0.0012$ according to recommendations included in [11] (the nominator of the above equation). The procedure is based on the separation of resistance and the load action variables under the assumption of the lognormal distribution of R . Thus, one only needs the first two statistical moments of R . Therefore, the mean and variance obtained from LHS samples were used for the estimation of the given percentile. It is interesting that Nataf's transformation and combinatorial optimisation lead to identical results (the difference between the mean value and standard deviation is around 1kN). Thus, the results of the small-sample approach implemented in FRoET (FP) were assumed for the estimation of the design value depicted in Fig. 15, and the result is compared to that of normative methods found in Eurocode EN 1992-1-1, the global safety factor (GSF) method stated in EN 1992-2 for the non-linear analysis of concrete structures, and the standard partial safety factor (PSF) method laid down in EN 1990. PSF and GSF are simplified probabilistic methods based on FORM and thus can be compared to the general FP method, even though PSF and GSF assume conservative generally applicable values for the material or modelling uncertainties, which are different from the FP of a specific structure. Of course, FP is much more time-consuming, and it needs additional information about the stochastic model. Due to this, it is usually used for the calibration of the PSF for specific types of structures, such as membranes [68], or it can be beneficially employed for precast structural members, as described in this paper.

As can be seen, the design value determined by FP method is significantly higher in comparison to normative methods. Analytical approach, according to EN 1992-1-1 leads to lower design value due to the linearization of a real problem. Nevertheless, PSF and EN 1992-2 should generally lead to similar results as FP, and such differences might be interesting for practice. Note that our mathematical model is represented by the non-linear finite element method with the complex stochastic model including dependency structure of concrete material characteristics and thus it is not generally recommended to apply PSF due to non-linearity of the model. Last normative approach EN-1992 is recommended only for the compressive type of failure, and thus it should not be applied for general structures. Moreover, none of these methods is able to take correlation among input variables into account.

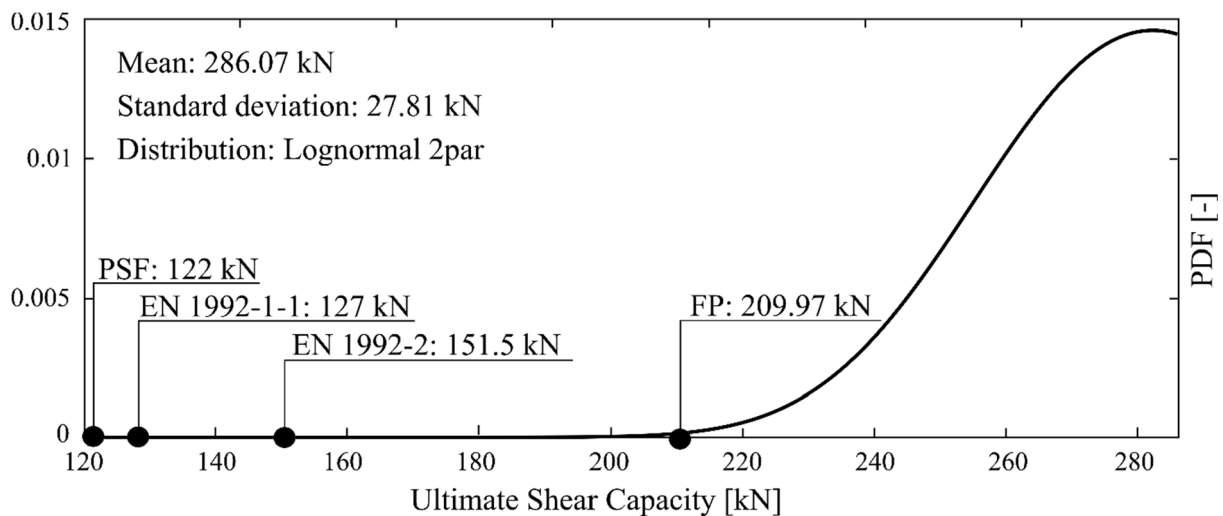


Fig. 15. Estimated structural response statistic and left tail of PDF of ultimate shear capacity.

Considering FP as the most advanced reference method (209,97 kN = 100%), we observe a significant drop of design ultimate shear capacity in case of normative conservative approaches: EN 1992-2 - decrease 28%, EN 1992-1-1 - 40% and PSF - 42%. Although normative methods are regularly used for design and analysis of structures represented by non-linear FEM, the FP method is the only solution, which is advanced and not extremely conservative, applicable for complex problems as the one presented herein. Future research will be focused on advanced and simplified methods for estimation of the coefficient of variation to determine design capacity, which is beyond the scope of this paper.

7. Conclusion

The paper describes the integration/application of the modelling of nonlinearity and uncertainty to predict the shear failure behaviour of prestressed concrete girders in the light of advanced statistical simulation and probabilistic-based design. The approach is complex, going from fracture-mechanical parameter determination through the advanced deterministic 3D computational modelling of girders up to stochastic modelling. The aim was to estimate the mean value and variability of ultimate shear capacity, and subsequently to present and verify the probabilistic design.

The complex stochastic modelling and design of precast prestressed concrete girders failing in shear involved several key steps: First, experimental studies were performed on scaled elements as well as on full-scale girders. These tests served as the basis for developing the deterministic nonlinear model and for the subsequent probabilistic assessment of structural resistance. Sensitivity analyses were performed, and a surrogate model was also used. Finally, the fully probabilistic design method was performed and compared with rather conservative normative approaches.

State-of-the-art methods were used to perform this practical industry-oriented research: For the preparation of the stochastic model, fracture-mechanics parameter identification was carried out based on an experimental/computational method using an ANN, while advanced NLFEA analysis was utilised for the nonlinearity modelling and small-sample simulation with correlation control was employed for the stochastic modelling. The degree of complexity that was used for this industrial application is, in a certain sense, unique.

The paper mainly describes stochastic modelling as part of a complex approach using a full-scale TT shaped roof girder as a benchmark. The mean value and variance of ultimate shear capacity were estimated with high accuracy. It was found that probabilistic design leads to a significantly higher design shear capacity (210 kN) in comparison to conservative design according to EN methods. This finding contributed to cost savings during girder production, while ensuring the manufactured structural elements exhibited the required level of reliability.

Generally, the developed procedures can be routinely applied for the modelling of other precast products. Future research will be based on the developed deterministic and stochastic models of girders and focused on the utilisation of alternative semi-probabilistic approaches for the design of these concrete elements. A further goal is to perform the reliability-based optimisation of a LDE7 girder element in order to increase capacity and to reduce the cost of production further.

Declaration of Competing Interest

The authors declare that they have no known competing financial interests or personal relationships that could have appeared to influence the work reported in this paper.

Acknowledgements

The authors would like to express their gratitude for the valuable data provided by Mr. Bernhard Krug and company Franz Oberndorfer GmbH & Co KG of and for the financial support from the PROMOSS

project, No. 17-02862S, which was awarded by the Czech Science Foundation.

Funding

This work was supported by the Czech Science Foundation under Grant PROMOSS, No. 17-02862S.

Author Contributions

Ondřej Slowik wrote first draft of this paper, create described numerical models, develop necessary software utilized for stochastic analysis and perform pilot stochastic simulations. Drahomír Novák provided crucial information and remarks to state of the art within given research field. He was responsible for data interpretation and team management. Lukáš Novák wrote Sections 1.3, 1.4, 4.2 and 4.3. He performed and evaluate presented sensitivity analysis and extended stochastic simulation. Alfred Strauss and Bernhard Krug were responsible for acquisition of initial data and communication with industrial partner. Alfred Straus provided valuable remarks helping to improve formal descriptions and information within the paper.

References

- [1] Bairan Garcia JM, Mari Bernat AR. Coupled model for the non-linear analysis of anisotropic sections subjected to general 3D loading. Part 1: Theoretical formulation. *Comput Struct* 2006;84(31–32):2254–63.
- [2] Bažant ZP, Yu Q. Designing against size effect on shear strength of reinforced concrete beams without stirrups. *Struct. Eng. Report*, No. 03-02/A466s, 2003.
- [3] Bažant ZP, Planas J. *Fracture and size effect in concrete and other quasibrittle materials*. Boca Raton: CRC Press LLC; 1998.
- [4] Ceresa P, Petrini L, Pinho R. Flexure-shear fiber beam-column elements for modeling frame structures under seismic loading - State of the art. *J Earthquake Eng* 2007;11(SUPPL. 1):46–88.
- [5] Mari A, Bairan J, Cladera A, Oller E, Ribas C. Shear-flexural strength mechanical model for the design and assessment of reinforced concrete beams. *Struct Infrastruct Eng* 2015;11(11):1399–419.
- [6] Russo G, Somma G, Mitri D. Shear strength analysis and prediction for reinforced concrete beams without stirrups. *J Struct Eng* 2005;131(1):66–74.
- [7] Kim C, Park HG, Hong G, Lee H, Suh JI. Shear strength of RC-composite beams with prestressed concrete and non-prestressed concrete. *ACI Struct J* 2018;115:917–30. <https://doi.org/10.14359/51702224>.
- [8] Collins MP, Bentz EC, Sherwood EG. Where is shear reinforcement required? Review of research results and design procedures. *ACI Struct J* 2008;105(5):590–600.
- [9] Červenka V, Jendele L, Červenka J. *ATENA Program Documentation – Part 1: Theory*. Cervenka Consulting; Prague, Czech Republic; 2016.
- [10] Resan, K., Hussien, Z.Y. Steps of ANSYS (Added new material and fatigue properties), 2019, 10.13140/RG.2.2.26295.78241.
- [11] CEN. Eurocode 2: Design of concrete structures - Part 1-1: General rules and rules for buildings. Vol. BS EN 1992-1-1:2004. 2004.
- [12] CEB-FIP Model Code 2010: "Design Code". Comité Euro-International Du Béton (HRSG.), 2).
- [13] Strauss A, Krug B, Slowik O, Novak D. Combined shear and flexure performance of prestressing concrete T-shaped beams: Experiment and deterministic modeling. *Structural Concrete* 2017;2017(1–20). <https://doi.org/10.1002/suco.201700079>.
- [14] Hendriks MAN, de Boer A, Belletti B. *Guidelines for Nonlinear Finite Element Analysis of Concrete Structures*, Rijkswaterstaat Centre for Infrastructure. Report RTD 2017;1016–1:2017.
- [15] Lemaire M, Chateaufneuf A, Mitteau J-C. Probability of failure, 2010.10.1002/9780470611708.ch7.
- [16] McKay MD, Conover WJ, Beckman RJ. A comparison of three methods for selecting values of input variables in the analysis of output from a computer code. *Echnometrics* 1979;21:239–45.
- [17] Novák D, Vořechovský M, Rusina R. Small-Sample Probabilistic Assessment – Software FREET. In: Proc. of 9th Int. Conf. on Applications of Statistics and Probability in Civil Engineering – ICASP 9, San Francisco, USA, Rotterdam Millpress, 2003, p. 91–96.
- [18] Schuëller GI, Bucher CG, Bourgund U, Ouyornprasert AW. On efficient computational schemes to calculate structural failure probabilities. *Probab Eng Mech* 1989;8.
- [19] Schuëller GI, Stix R. A critical appraisal of methods to determine failure probabilities. *Struct Saf* 1987;5:8.
- [20] Bourgund U, Bucher CG. A Code for importance sampling procedure using design points – ISPUD: A user manual. Inst. Eng. Mech., Innsbruck University, Report No. 8; 1986.
- [21] Hasofer AM, Lind NC. Exact and invariant second-moment code format. *J Eng Mech Division* 1974;100:ASCE.

- [22] Geyskens P, der Kiureghian A, De Roeck G. SORM analysis using quasi-newton optimization; 1991. doi:10.1007/978-94-011-3692-1_9.
- [23] Bucher C. Asymptotic sampling for high-dimensional reliability analysis. *Probabilistic Eng Mech* 2009;6.
- [24] Thompson SK, Seber G. Adaptive sampling. New York: Wiley; 1996.
- [25] Melchers RE. Structural system reliability assessment using directional simulation. *Struct Saf* 1994;16.
- [26] Bucher CG., Bourgund U. Efficient use of Response surface methods. Inst. Eng. Mech., Innsbruck University, report No. 9, 1987.
- [27] Sudret B, Blatman G, Berveiller M. Response surfaces based on polynomial chaos expansions, 2011. doi:10.1002/9781118601099.ch8.
- [28] Lehký D, Slowik O, Novák D. Reliability-based design: Artificial neural networks and double-loop reliability-based optimisation approaches. *Adv Eng Softw* 2018. ISSN 0965-9978.
- [29] Lehký D, Šomodíková M. Small-sample artificial neural network based response surface method for reliability analysis of concrete bridges. In: Proceedings of the Fourth International Symposium on Life-Cycle Civil Engineering (IALCCE 2014) – Life-Cycle of Structural Systems: Design, Assessment, Maintenance and Management. London, UK: Taylor & Francis Group; 2015, ISBN 978-1-138-00120-6.
- [30] Lehký D, Šomodíková M. Reliability calculation of time-consuming problems using a small-sample artificial neural network-based response surface method. *Neural Comput Appl* 2017. ISSN 0941-0643.
- [31] Novák L, Novák D. Polynomial chaos expansion for surrogate modelling: Theory and software. *Beton und Stahlbetonbau* 2018;113:27–32.
- [32] Görtz S, Hegger J, Walraven JC, Sherif A. Shear-cracking behaviour of prestressed and nonprestressed beams made of normal- and high-performance concrete. In: 5th International PhD Symposium in Civil Engineering - Proceedings of the 5th International PhD Symposium in Civil Engineering; 2004. p. 1213–21.
- [33] Ferreira D, Bairán J, Marí A. Numerical simulation of shear-strengthened RC beams. *Eng Struct* 2013;46:359–74.
- [34] Hegger J, Görtz S. Querkraftmodell für Bauteile aus Normalbeton und Hochleistungsbeton. *BBeton- Stahlbetonbau* 2006;101:695–705.
- [35] Hegger J, Görtz S, Beutel R, et al. Überprüfung und Vereinheitlichung der Bemessungsansätze für querkraftbeanspruchte Stahlbeton- und Spannbetonbauteile aus normalfestem und hochfestem Beton nach DIN 1045-1. Abschlussbericht für das DIBT-Forschungsvorhaben IV 1-5-876/98; DE-89 TIB/UB Hannover: RWTH Aachen; 1999.
- [36] Reineck K-H. Hintergründe zur Querkraftbemessung in DIN 1045-1 für Bauteile aus Konstruktionsbeton mit Querkraftbewehrung. *Bauing* 2001;76:168–79.
- [37] Routil L, Lehký D, Šimonová H, Kucharczyková B, Keršner Z, et al. Experimental-computational determination of mechanical fracture parameters of concrete for probabilistic life-cycle assessment. In: Proceedings of IALCCE 2014, Tokyo, Japan, 2014.
- [38] Strauss A, Zimmermann T, Lehký D, Novák D, Keršner Z. Stochastic fracture-mechanical parameters for the performance-based design of concrete structures. *Struct Concr* 2014;15(3):380–94.
- [39] Stoerzel J, Randl N, Strauss A. Monitoring shear degradation of reinforced and pre-tensioned concrete members. IABSE Conference 2015: Structural Engineering. Geneva: International Association for Bridge and Structural Engineering; 2015.
- [40] Elices M, Guinea GV, Planas J. Measurement of the fracture energy using three-point bend tests: Part 3—Influence of cutting the P- δ tail. *Mater Struct* 1992;25(6):327–34.
- [41] Lehký D, Keršner Z, Novák D. FraMePID-3PB software for material parameters identification using fracture test and inverse analysis. *Adv Eng Softw* 2013.
- [42] Vořechovský M, Novák D. Correlation control in small sample Monte Carlo type simulations I: A Simulated Annealing approach. *Probab Eng Mech* 2009;24(3):452–62.
- [43] Lebrun R, Dutfoy A. Do Rosenblatt and Nataf isoprobabilistic transformation really differ? *Probabilistic Eng Mech - Probabilistic Eng Mech* 2009;24:577–84. <https://doi.org/10.1016/j.probenmech.2009.04.006>.
- [44] Rosenblatt M. Remarks on a multivariate transformation. *Ann Math Stat* 1952;23(3):470–2.
- [45] Der Kiureghian A, Liu PL. Structural reliability under incomplete probability information. *J Eng Mech* 1986;112(1):85–104.
- [46] Lebrun R, Dutfoy A. B. An innovating analysis of the Nataf transformation from the copula viewpoint. *Probab Eng Mech* 2009;24(3):312–20.
- [47] Nataf A. Détermination des distributions de probabilité dont les marges sont données. *Comptes Rendus de l'Académie des Sciences* 1962:42–3.
- [48] Vořechovský M. Hierarchical refinement of Latin Hypercube Samples. *Comput-Aided Civil Infrastruct Eng (Wiley)* 2015. <https://doi.org/10.1111/mice.12088> 30:394–411.
- [49] JCSS. JCSS Probabilistic Model Code. Joint Committee on Structural Safety. ISBN 978-3-909386-79-6, 2001.
- [50] Červenka V, Červenka J, Pukl R, Sajdlova T. Prediction of shear failure of large beam based on fracture mechanics. In: Saouma V, Bolander J, Landis E, Editors, 9th international conference on fracture mechanics of concrete and concrete structures and concrete structures FraMCoS-9, Berkeley, California, USA, vol. 8, 2016.
- [51] Novák D, Vořechovský M, Teplý B. FREt: Software for the statistical and reliability analysis of engineering problems and FREt-D: Degradation module. *Advances in engineering software*, 2014, pp. 179–192. ISSN: 0965-9978.
- [52] Havlásek P, Pukl R. SARA Studio – User's Manual. Červenka Consulting s.r.o., 2015.
- [53] Slowik O, Novák D. Node based software concept for general purpose reliability-based optimisation tool. In: Proc. of 2019 International Conference on Quality, Reliability, Risk, Maintenance, and Safety Engineering (QR2MSE 2019), Zhangjiajie, Hunan, China, 2019.
- [54] Lehký D, Novák D. Inverse reliability problem solved by artificial neural networks. Paper presented at: Safety, Reliability, Risk and Life-Cycle Performance of Structures and Infrastructures—Proceedings of the 11th International Conference on Structural Safety and Reliability, ICOSAR 2013 [Internet], 2013, p. 5303–10. <https://www.crcpress.com/Safety-Reliability-Risk-and-Life-Cycle-Performance-of-Structures-and-Deodatis-Ellingwood-Frangopol/p/book/9781138000865>.
- [55] Hordijk D, Reinhardt H. Numerical and experimental investigation into the fatigue behavior of plain concrete. *Exp Mech* 1993;33(4):278–85.
- [56] Červenka J, Papanikolaou VK. (2008) Three dimensional combined fracture–plastic material model for concrete. *Int J Plasticity* 2008;24(12):2192–220. <https://doi.org/10.1016/j.ijplas.01.004>.
- [57] Torrent RJ. The log-normal distribution: A better fitness for the results of mechanical testing of materials. *Mat Constr* 1978;11:235. <https://doi.org/10.1007/BF02551768>.
- [58] Zimmermann T, Lehký D, Strauss A. Correlation among selected fracture-mechanical parameters of concrete obtained from experiments and inverse analyses. *Struct Concr* 2016;17(6):1094–103. ISSN: 1751-7648.
- [59] Trautwein L, Sanabria R, Sarmiento S, Almeida L. Reliability analysis of shear strength of reinforced concrete deep beams using NLFEA. *Eng Struct* 2019;203. <https://doi.org/10.1016/j.engstruct.2019.109760>.
- [60] Novák L, Novák D. Surrogate modelling in the stochastic analysis of concrete girders failing in shear. In: Proceedings of the fib Symposium 2019: Concrete - Innovations in Materials, Design and Structures. International Federation for Structural Concrete; 2019. p. 1741–7. ISBN: 9782940643004.
- [61] Borogonovo E, Plišchke E. Sensitivity analysis: A review of recent advances. *Eur J Oper Res* 2016;248:869–87. ISSN: 0377–2217.
- [62] Novák D, Teplý B, Shirashi N. Sensitivity analysis of structures: a review. In: Proceedings of the 5th international conference on civil and structural engineering computing, Edinburgh, Scotland; 1993. p. 201–7.
- [63] Allaix DL, Carbone VI, Mancini G. Global safety format for non-linear analysis of reinforced concrete structures. *Struct Concr* 2013;14:29–42. <https://doi.org/10.1002/suco.201200017>.
- [64] Castaldo Paolo, Gino Diego, Mancini Giuseppe. Safety formats for non-linear finite element analysis of reinforced concrete structures: discussion, comparison and proposals, *Engineering Structures*, Volume 193. ISSN 2019;136–153:0141–296. <https://doi.org/10.1016/j.engstruct.2019.05.029>.
- [65] Castaldo P, Gino D, Bertagnoli G, Mancini G. Resistance model uncertainty in non-linear finite element analyses of cyclically loaded reinforced concrete systems. *Eng Struct* 2020;211. <https://doi.org/10.1016/j.engstruct.2020.110496>.
- [66] Engen Morten, Hendriks Max AN, Köhler Jochen, Øverli Jan Arve, Åldstedt Erik. A quantification of the modelling uncertainty of non-linear finite element analyses of large concrete structures. *Struct Saf* 2017;64:1–8. <https://doi.org/10.1016/j.strusafe.2016.08.003>.
- [67] De Smedt Elien, Mollaert Marijke, Caspele Robby, Botte Wouter, Pyl Lincy. Reliability-based calibration of partial factors for the design of membrane structures. *Eng Struct* 2020;214:110632. <https://doi.org/10.1016/j.engstruct.2020.110632>. ISSN 0141-0296.

E Estimation of Coefficient of Variation for Structural Analysis: The Correlation Interval Approach

DOI: 10.1016/j.strusafe.2021.102101

E.1 Description

The paper is focused on the development of a novel method for Estimation of the Coefficient of Variation (ECoV) utilized for semi-probabilistic design and the assessment of structures and it also contains a short review of the existing ECoV methods with their limitations and assumptions. A special attention is given to the cases with dependent input random variables (material characteristics) solved by the non-linear finite element method. The novel method Eigen ECoV is proposed for an efficient estimation of statistical moments under the simplifying assumption of fully correlated input random variables. The Eigen ECoV is based on Taylor Series Expansion and the differencing scheme proposed by the authors in their previous work (Annex B). Specifically, the three variants of Eigen ECoV are derived, which differ in computational cost and accuracy. It is shown that Eigen ECoV generally leads to more accurate results in comparison with the commonly used ECoV method implemented in Model Code 2010 [20]. Moreover, thanks to the solid theoretical background, simplifying assumptions are clearly defined in contrast to some other existing methods. Finally, the correlation interval approach is presented, which is based on the combination of TSE and Eigen ECoV for the estimation of the lower and upper bound of variance.

E.2 Role of the Ph.D. Candidate

Percentage of contribution: 90%

Lukáš Novák is the main author of this paper responsible for the concept, the methodology and the numerical results of the presented research. Furthermore, he prepared the original draft of the paper which was later reviewed in cooperation with his supervisor, Drahomír Novák.



Estimation of coefficient of variation for structural analysis: The correlation interval approach

Lukáš Novák^{*}, Drahomír Novák

Faculty of Civil Engineering, Brno University of Technology, Veverí 331/95, Brno 60200, Czech Republic

ARTICLE INFO

Keywords:

Semi-probabilistic approach
 Estimation of coefficient of variation
 Taylor series expansion
 Correlation among random variables
 Nataf transformation

ABSTRACT

The paper is focused on the efficient estimation of the coefficient of variation for functions of correlated and uncorrelated random variables. Specifically, the paper deals with time-consuming functions solved by the non-linear finite element method. In this case, the semi-probabilistic methods must reduce the number of simulations as much as possible under several simplifying assumptions while preserving the accuracy of the obtained results. The selected commonly used methods are reviewed with the intent of investigating their theoretical background, assumptions and limitations. It is shown, that Taylor series expansion can be modified for fully correlated random variables, which leads to a significant reduction in the number of simulations independent of the dimension of the stochastic model (the number of input random variables). The concept of the interval estimation of the coefficient of variation using Taylor series expansion is proposed and applied to numerical examples of increasing complexity. It is shown that the obtained results correspond to the theoretical conclusions of the proposed method.

1. Introduction

Today, non-linear finite element analysis (NLFEA) is employed ever more frequently for the design and assessment of structures, especially concrete structures with significant non-linear behaviour. Moreover in the last decade, it has become more common to use reliability analysis of real structures. This trend reflects the higher economical and safety requirements placed on engineering in today's society. Therefore, it is natural to connect NLFEA and reliability analysis in order to obtain accurate results [1–4]. Although the combination of NLFEA and reliability analysis is a strong tool for the realistic modelling of structures, it is also still highly time consuming to perform the reliability analysis of large non-linear mathematical models with many input random variables.

This paper is focused on the semi-probabilistic approach, which is well known from EN 1990 and partial safety factors [5]. This approach is able to greatly reduce the number of non-linear calculations necessary in order to estimate the design value of resistance satisfying the target reliability when the approach is used instead of the direct calculation of failure probability. However, it is still challenging to apply the semi-probabilistic approach to non-linear mathematical models solved by finite element software, when one deals with the non-linearity of functions combined with highly computationally demanding calculations.

Assuming a mathematical model of input random vector \mathbf{X} described by a specific joint probability distribution, the basic reliability

concept is given as $Z(\mathbf{X}) = R - E$, where $Z(\mathbf{X})$ represents safety margin, which is defined as the difference between structural resistance R and action effect E . Failure of the structure is represented by condition $Z(\mathbf{X}) < 0$. In the semi-probabilistic approach, the resistance of structure R is separated and the design value of resistance R_d that satisfies safety requirements is evaluated, instead of the direct calculation of failure probability $p_f = P(Z(\mathbf{X}) < 0)$. The typical formula for the estimation of R_d , assuming a lognormal distribution of R , is

$$R_d = \mu_R \cdot \exp(-\alpha_R \beta v_R), \quad (1)$$

where μ_R is the mean value, v_R is the coefficient of variation (CoV) and α_R represents sensitivity factor derived from First Order Reliability Method (FORM) [6,7]; the recommended value is $\alpha_R = 0.8$ according to [5]. The target reliability index β for the ultimate limit state, moderate consequences of failure and a reference period of 50 years is set at $\beta = 3.8$ according to the Eurocode. Note that, from a probabilistic point of view, the whole process represents the estimation of a quantile satisfying the given safety requirements under the prescribed assumption of lognormal distribution.

Obviously, for the determination of a design value by a semi-probabilistic approach, it is crucial to estimate the mean value and variance of structural resistance $R = r(\mathbf{X})$ accurately. This can be done via various techniques, such as numerical quadrature [8], simplified

^{*} Corresponding author.

E-mail addresses: novak.l@fce.vutbr.cz (L. Novák), novak.d@fce.vutbr.cz (D. Novák).

methods for the estimation of the coefficient of variation (ECoV methods) [9], or stratified sampling [10]. Although simplified ECoV methods are often discussed at conferences, e.g. [11–14], and recommendations already exists in *fib* Model Code 2010 [15] and such methods are expected to be included in the Eurocode and *fib* Model Code 2020, there are still no significant scientific publications presenting the theoretical background and more importantly the limitations of the existing methods. Therefore, this paper contains a brief review of commonly used methods and also an investigation of the theoretical background of selected methods and their connection to well-known mathematical concepts.

ECoV methods offer a balance between computational cost and accuracy. However ECoV methods also have several limitations due to the assumed simplifications. Therefore besides an overview of ECoV methodology, this paper presents a novel generalization of ECoV methods for correlated random variables, since material characteristics (especially in the case of concrete structures) are correlated and this may play a crucial role in probabilistic analysis. In most cases, there is a lack of information on statistical correlation. Therefore, it is useful to examine two extreme cases (uncorrelated and fully correlated random variables). The interval ECoV approach and novel Eigen ECoV for fully correlated case are thus proposed in this paper.

2. Safety formats for NLFEA

The safety formats that include ECoV methods can be sorted by type of simplification into three levels as will be described in this section. Since non-linear mathematical models are generally not proportional, the standard quantile-based approach (level I) may lead to incorrect results. Accurate results are only guaranteed if the probability distribution of resistance f_R is identified together with statistical moments (Level III methods), which might not be a simple matter in general cases and is definitely time-consuming. Therefore, it is beneficial to assume several simplifications and employ Level II methods representing a compromise between accuracy and efficiency.

2.1. Level I: Quantile-based methods

Quantile-based methods are based on the very strict assumption that $r(\mathbf{X}_d) = R_d$, i.e. a numerical simulation with input variables set to a generally desired quantile (e.g. design \mathbf{X}_d) leads to a result corresponding to the identical desired quantile of response distribution R . Of course, this might be a severe problem in case of NLFEA, where a simulation with extreme input variable values may lead to the unrealistic behaviour of the computational model, which is usually verified within a specific range of input variables. However, such an approach can still be acceptable for simple structural members with a single almost linear failure mode and low v_R , e.g. the bending of a simple beam.

2.1.1. Partial safety factors

According to Partial Safety Factors (PSF) method proposed in EN 1990 [5], NLFEA is computed with design values of input random variables and it is assumed that the obtained result corresponds to the design value of resistance R_d [16]. The design values of input variables are typically derived from characteristic values using normative coefficients γ_M , which consider material and model uncertainty:

$$R_d = r(X_1/\gamma_M, X_2/\gamma_M, \dots). \quad (2)$$

Note that, the design values in the partial safety factors method are extremely low, thus possibly leading to the unrealistic redistribution of internal forces and even to different structural failure modes. One solution might be the calibration of partial safety factors based on laboratory experiments involving material and structural measurements [17].

2.1.2. Global safety factor according to EN 1992-2

In the global safety factor concept according to EN 1992-2 [18], the design value is estimated as follows:

$$R_d = \frac{r(f_{ym}, \tilde{f}_{cm}, \dots)}{\gamma_R}, \quad (3)$$

where $f_{ym} = 1.1f_{yk}$ is the mean value of the yield strength of steel reinforcement and f_{yk} represents its characteristic value (5% quantile), \tilde{f}_{cm} is the reduced mean value of concrete because of its higher variability and the idea shown in Eq. (4) that design values should correspond to the same probability and reflect the safety of normative material partial safety factors $\gamma_s = 1.15$ and $\gamma_c = 1.5$. The global safety factor for resistance is set as $\gamma_R = 1.27$ including model uncertainty.

$$\tilde{f}_{cm} = \gamma_s \cdot 1.1 \frac{f_{ck}}{\gamma_c} \approx 0.85 f_{ck}. \quad (4)$$

It is assumed that design values of concrete and steel should correspond to an identical quantile of probability. Furthermore, it is assumed that the mean value of steel can be obtained as $f_{ym} = 1.1f_{yk}$, and thus $f_{yd} = f_{ym}/1.27$.

Therefore, \tilde{f}_{cm} , according to Eq. (4), reflects the partial safety factors by virtue of the presented rationale. Note that \tilde{f}_{cm} does not represent the mean value of concrete material characteristics and it is lower than the characteristic values. As a result, it includes additional safety due to the higher variability of concrete. Also note that for concrete characteristics, Eurocode 2 allows only the compressive type of failure.

2.2. Level II: Simplified probabilistic methods

The task of Level II methods is reduced to the estimation of the mean value μ_R and variance of R , represented by the coefficient of variation v_R , which can be further decomposed as:

$$v_R = \sqrt{v_g^2 + v_m^2 + v_f^2}, \quad (5)$$

where v_g or v_m represents the coefficient of variation caused by geometrical or model uncertainties and the v_f coefficient of variation caused by the material. There are several studies dealing with model uncertainties and it is necessary to adopt v_g or v_m for specific structures [16, 19, 20]. Therefore for the sake of generality, the paper is focused only on the estimation of the coefficient of variation of mathematical model caused by the uncertainty of material parameters v_f .

2.2.1. Numerical quadrature

A classic method to estimate moments of function R , was proposed in 1975 by Rosenblueth [8]. This point estimate method is simple and direct, thus the method can be easily employed in practical applications. Moreover, Christian and Baecher [21] have shown its robustness and mathematical background in numerical quadrature. The expected value of the m -th moment of function $r(\mathbf{X})$ can be estimated as:

$$\mathbb{E}[R^m] \approx \sum_{i=1}^{2^N} P_i \cdot r_i^m, \quad (6)$$

where $P_i = \frac{1}{2^N}$ are weighting factors and r_i is a result of mathematical model. Since the function $r(\mathbf{X})$ is computed in 2^N points with coordinates plus/minus one standard deviation σ_{X_i} for the i -th random variable, the computational requirements increase rapidly with the number of input random variables – 2^N simulations are needed to estimate the statistical moments of R and thus it cannot be recommended for typical engineering applications.

2.2.2. ECoV by Červenka

The computationally efficient ECoV method was proposed in 2008 by Červenka [22]. The method is based on a simplified formula for the estimation of a characteristic value corresponding to a lognormal variable with the mean value μ_R and v_f :

$$R_k = \mu_R \exp(-1.645 v_f), \quad (7)$$

where -1.645 corresponds to the 5% quantile of standardized Gaussian distribution $\Phi(0.05)$. After simple mathematical operations and under the assumption that $R_m \approx \mu_R$, the coefficient of variation of R associated with material uncertainties v_f can be estimated as:

$$v_f = \frac{1}{1.645} \ln \left(\frac{R_m}{R_k} \right), \quad (8)$$

and the global resistance safety factor is calculated as:

$$\gamma_R = \exp(\alpha_R \beta v_f). \quad (9)$$

Note that, just 2 NLFEA simulations are needed in this approach independent of the size of the stochastic model – $R_m \approx r(\mu_X)$ with mean values of input random variables and R_k using characteristic values (5% percentile) of input variables. Obviously, there is the strong assumption that $R_k \approx r(X_k)$. However there is significant advantage in comparison to previous methods, since it estimates v_f and thus the design value R_d corresponds to target safety requirements and the specific distribution of R . Moreover the characteristic values of material parameters are not as extremely low as in the case of PSF and may not lead to structural system or material model exhibiting unrealistic behaviour, which can be considered as a significant advantage. Note that, the described concept was adopted in the *fib* Model Code 2010 [15] and is widely accepted in the engineering community today [23]. However, in spite of the success of this method, its theoretical background has not yet been sufficiently investigated. In this paper an attempt to fill this gap has been made, primarily in Section 4.1.

2.2.3. Taylor series expansion

Let us assume the mathematical model $r(\mathbf{X})$ is infinitely differentiable in an open interval around the mean values. Under this assumption, it is possible to expand the original model into an infinite Taylor series:

$$R = r(\mathbf{X}) = r(\mu_X) + \nabla r(\mu_X) \cdot (\mathbf{X} - \mu_X) + \frac{1}{2} (\mathbf{X} - \mu_X) \cdot \nabla \nabla r(\mu_X) \cdot (\mathbf{X} - \mu_X) + \dots \quad (10)$$

where the derivatives are evaluated at μ_X . In engineering applications, it is common to assume that the terms of TSE are only linear and that input random variables are independent. For the sake of clarity, the commonly known analytical expressions for the estimation of the expected value $\mathbb{E}[R]$ and variance $\text{VAR}[R]$ of a function $r(\mathbf{X})$ of N independent random variables, approximated by linear terms of the TSE, are as follows:

$$\mathbb{E}[R] \approx r(\mu_{X_1}, \mu_{X_2}, \dots, \mu_{X_n}), \quad (11)$$

and

$$\text{VAR}[R] \approx \sum_{i=1}^N \left(\frac{\partial r(X)}{\partial X_i} \right)^2 \sigma_{X_i}^2, \quad (12)$$

As can be seen from the equations, the efficiency and accuracy of TSE depends on the number of used terms and the differencing scheme for the practical computation of derivatives. A practical example of TSE utilization is the ECoV method proposed by Schlune et al. [24], which can be seen as a TSE in which, derivatives are approximated by one-sided differencing as:

$$\frac{\partial r(X)}{\partial X_i} = \frac{R_m - R_{X_i \Delta}}{\Delta X_i}. \quad (13)$$

where the response of mathematical model R_m is determined by a calculation with mean values, and $R_{X_i \Delta}$ is the result of a model using mean values of input random variables and a value of the i -th random variable which has been reduced by ΔX_i . This differencing scheme has been adapted for structural design according to Schlune et al. using step size parameter $c = (\alpha_R \beta) / \sqrt{2}$ and $X_{i \Delta} = F_i^{-1}(\Phi(-c))$, where F_i^{-1} is an inverse cumulative distribution function of the i -th variable and Φ is the cumulative distribution function of the standardized Gaussian distribution. For the sake of clarity, the difference is calculated as $\Delta X_i = \mu_{X_i} - X_{i \Delta}$.

Schlune et al. thus proposed a simple formula [24] for the coefficient of variation caused by material uncertainty v_f if material parameters are not correlated as:

$$v_f \approx \frac{1}{R_m} \sqrt{\sum_{i=1}^N \left(\frac{R_m - R_{X_i \Delta}}{\Delta X_i} \sigma_{X_i} \right)^2}. \quad (14)$$

Note that this approach requires $N + 1$ simulations of NLFEA, where N is the number of random variables. However, all simulations act as a parametric study of a numerical model, which is usually performed during the development of a model in industrial applications. As a result, TSE can be recommended due to its medium computational cost and strong theoretical background.

Of course, one can use various differencing schemes instead of Eq. (13) depending on ones computational possibilities, as was proposed by the authors of this paper in [25]. Assuming linear TSE, one of the most promising advanced differencing schemes using $n_{sim} = 2N + 1$ simulations is defined as:

$$\frac{\partial r(X)}{\partial X_i} = \frac{3R_m - 4R_{X_i \frac{\Delta}{2}} + R_{X_i \Delta}}{\Delta X_i}, \quad (15)$$

where the middle additional term $R_{X_i \frac{\Delta}{2}}$ is obtained via the evaluation of the original mathematical model with mean values and a reduced i -th variable $X_{i \frac{\Delta}{2}} = \mu_{X_i} - \Delta X_i / 2$.

2.3. Level III: Monte Carlo methods

Monte Carlo (MC) type sampling methods are the only general tools available for reliability or statistical analysis. However, it is necessary to perform large number of calculations if they are used. Nonetheless, the number of simulations is still lower than in the case of Level II methods for large stochastic models and thus Level III for ECoV [10] is recommended for large stochastic models or computationally cheap computational models.

The main feature of MC techniques is their use of pseudo-random sampling and the statistical analysis of performed deterministic simulations. Crude Monte Carlo is not efficient because thousands of simulations are needed and the use of this approach in combination with NLFEA, is not feasible in industrial applications. A stratified sampling technique called Latin Hypercube Sampling (LHS) was developed for the efficient estimation of statistical moments [26,27]. It drastically reduces the number of needed simulations. LHS is not dependent on the size of the stochastic model, and thus it is recommended for extensive stochastic models. The cumulative distribution function of the input variable is divided into n_{sim} equal intervals, where n_{sim} is the number of simulations. Every value is picked within each segment. There are several ways to choose the probability of picked value — mean value of interval, median or random value. Once the values are chosen, the random permutation of realizations is performed and random vectors of input variables are generated. The described approach leads to uniform distribution within a design domain. Additionally, MC type simulation techniques are able to take the correlation among input random variables into account. Several methods have been developed for this purpose, e.g. generalized Nataf transformation [28] and optimization techniques [29,30].

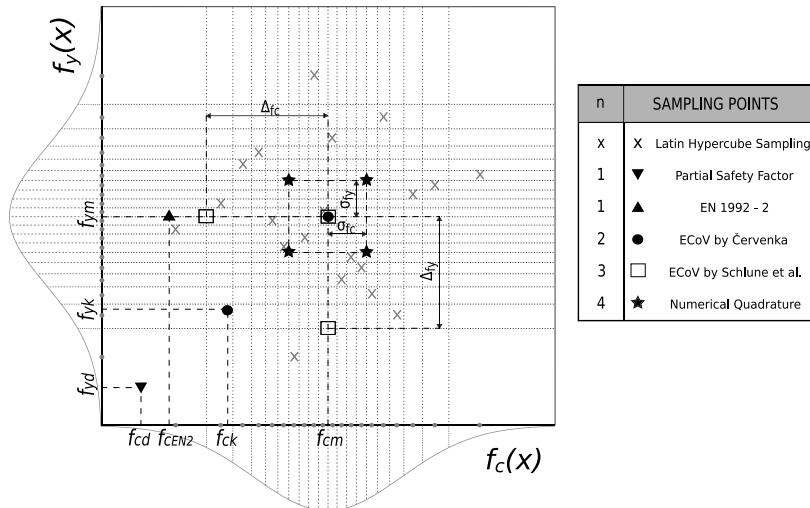


Fig. 1. The presented semi-probabilistic methods together with their computational cost n are depicted in 2-dimensional space (figure adapted from [31]).

2.4. Graphical comparison of safety formats

As was already shown by Pimentel et al. [31], each NLFEA simulation can be represented by a point in N -dimensional space called the design domain. The design domain is considered to be the domain of sampling probabilities, where coordinates of sampling points are described by an input random vector. The 2-dimensional case can be seen in Fig. 1 together with the sampling points used for the presented safety formats. The stochastic model contains only 2 typical input material characteristics – the yield strength of reinforcement f_y and the compressive strength of concrete f_c , which are considered to be random variables described by specific probability distributions.

Level I: The PSF and the EN-1992 methods represented by triangles are very efficient from the computational point of view — only one simulation is needed but CoV is not estimated. Although quantile-based methods are sufficient for a linear mathematical model, they may lead to severe problems depending on the degree of non-linearity of mathematical models solved by the NLFEA. Moreover, design values of input random variables are defined only for selected material parameters (excluding e.g. fracture energy).

Level II: ECoV by Červenka (represented in Fig. 1 by circles) always works with 2 simulations — the mean and the characteristic values of input random variables. On the other hand, TSE with differencing according to Schlune et al. (represented in Fig. 1 by squares) is linearly dependent ($n_{sim} = N + 1$), and the Numerical Quadrature (stars) is exponentially dependent ($n_{sim} = 2^N$) on the number of input random variables. Although such dependency is not a problem for low dimensional space, it can play a crucial role in industrial applications with many input variables and thus it might be more efficient to employ Monte Carlo type methods. The level III Monte Carlo type method is represented by LHS (crosses) in the figure. LHS can be used for general stochastic models and will be employed in this paper as a reference solution.

3. Correlation among random variables

The presented ECoV methods are recommended for the practical assessment of structures assuming that material characteristics are independent, which is usually incorrect. This is especially true in the case of concrete structures, where a correlation among compressive strength, tensile strength and fracture energy is usually assumed [3, 32]. Therefore, the paper is focused on the generalization of ECoV methods for structures with dependent input material characteristics, which are typically obtained from laboratory experiments or assumed according to the literature. General transformation between correlated and uncorrelated space is briefly described in this section.

3.1. Nataf transformation

In a general case involving non-normal correlated random variables, it is necessary to utilize what is known as the Rosenblatt transformation [33]. However, in practical applications only the marginal distributions and the correlation matrix are usually known, which does not provide complete information about the joint probability distribution [34]. Therefore, it is necessary to assume a specific copula [35] or construct an arbitrary joint distribution using vine copulas [36], which is beyond the scope of this paper. A special case of Rosenblatt transformation that assumes Gaussian copula [37] is also known as the Nataf transformation [38], which is usually utilized in reliability applications. Nataf transformation to ξ space is composed of three steps:

$$\xi = T_{Nataf}(\mathbf{X}) = T_3 \circ T_2 \circ T_1(\mathbf{X}). \quad (16)$$

The first two steps are commonly known as iso-probabilistic transformation, which uses the cumulative distribution function of variables F_x and the Gaussian inverse cumulative distribution function Φ^{-1} as follows:

$$T_2 \circ T_1(\mathbf{X}) : \mathbf{X} \mapsto \mathbf{Z} = \Phi^{-1}(F_x(\mathbf{X})). \quad (17)$$

The last step represents a transformation to uncorrelated space using linear transformation. For this procedure, we can use the Cholesky decomposition or the Eigen decomposition of the fictive correlation matrix \mathbf{R}_Z . Using Cholesky decomposition, the decomposition is

$$\mathbf{R}_Z = \mathbf{L}\mathbf{L}^T, \quad (18)$$

and final transformation using $\Gamma = \mathbf{L}^{-1}$ thus reads

$$T_3 : \mathbf{Z} \mapsto \xi = \Gamma\mathbf{Z}. \quad (19)$$

The Nataf transformation, can be easily inverted in order to transform $\xi \mapsto \mathbf{X}$. Note that the transformation matrix \mathbf{L} is a lower triangular matrix with a unit on the first entry of the main diagonal and therefore the first coordinate x_1 remains unchanged. This complication can be circumvented by using Eigen decomposition instead of Cholesky decomposition. The target covariance matrix Σ can be decomposed using Eigen decomposition as:

$$\Sigma = \Theta \lambda^{\frac{1}{2}} \lambda^{\frac{1}{2}} \Theta^T, \quad (20)$$

where λ is the diagonal matrix of eigenvalues of Σ and Θ is the eigenvector matrix associated with the eigenvalues. Instead of the transformation matrix \mathbf{L} , one can then use $\Theta \lambda^{\frac{1}{2}}$.

3.2. Fictive correlation matrix

A critical task for Nataf transformation is the determination of \mathbf{R}_Z . The fictive correlation matrix \mathbf{R}_Z is a square symmetric positive-definite matrix, and thus it is possible to perform Cholesky decomposition. The assumed Gaussian copula is parametrized by elements ρ_{zij} of \mathbf{R}_Z . Note that $\rho_z = 0 \leftrightarrow \rho_x = 0$ and $|\rho_x| \leq |\rho_z|$ as was shown in [34]. The relationship between fictive correlation coefficients ρ_{zij} and ρ_{xij} determined for \mathbf{X} is defined by the following integral equation:

$$\rho_{xij} = \frac{1}{\sigma_i \sigma_j} \iint_{\mathbb{R}^2} \{F_i^{-1}[\Phi(z_i) - \mu_i] F_j^{-1}[\Phi(z_j) - \mu_j] \times \phi_2(z_i, z_j, \rho_{zij})\}, \quad (21)$$

where μ is the mean value, σ is the standard deviation and ϕ_2 is the bivariate standard normal probability density function parametrized by fictive correlation coefficients ρ_{zij} . The computation of Eq. (21) might be complicated for practical usage. Moreover, for specific combinations of input parameters there is not a guaranteed solution (more details about the limitations of Nataf transformation can be found in [35]). Generally, a simplification of Eq. (21) according to Liu & Kiureghian [39] can be in the form $\rho_z = t \cdot \rho_x$, where t is known for several combinations of probability distributions of random variables. The material characteristics are often assumed to be lognormally distributed with coefficient of variation $v \leq 0.5$ in practical applications. Assuming both random variables to be lognormally distributed, Liu & Kiureghian derived t in the following form:

$$t = \frac{\ln(1 + \rho_x v_1 v_2)}{\rho_x \sqrt{\ln(1 + v_1^2) \ln(1 + v_2^2)}}, \quad (22)$$

where v_1 and v_2 are coefficients of variation of the first and second random variable respectively. As can be found in [39], the derived formula is exact in this specific case. Additionally, in common practical applications, one can assume there is a positive correlation among material characteristics which leads to negligible differences between ρ_z and ρ_x [34].

4. ECoV for functions of correlated random variables

Besides the general probabilistic methods in level III, it is also possible to extend Level II of safety formats for correlated random variables. The numerical quadrature can be easily extended for correlated variables via the modification of weighting factors P_i as follows [21]:

$$P_{(s_1, s_2, \dots, s_n)} = \frac{1}{2^n} \left[1 + \sum_{i=1}^{n-1} \sum_{j=i+1}^n (s_i)(s_j) \rho_{ij} \right], \quad (23)$$

where s_i is a positive sign when the value of the i -th variable is the mean plus the standard deviation σ and negative for points with a coordinate mean value minus the standard deviation. Although it is generally possible to use numerical quadrature, it is highly computationally demanding ($n_{sim} = 2^N$) and thus its potential for industrial applications is limited, and it will not be employed in numerical examples.

The next presented Level II method – TSE – is more interesting for industrial applications, since it is not highly computationally demanding. It is possible to generalize the TSE for correlated variables using additional terms of the expansion. Specifically, an extension of the method for dependent random variables can generally be obtained from a first order TSE assuming correlation among random variables represented by the correlation coefficient ρ in analytical form as

$$\text{VAR}[R] \approx \sum_{i=1}^N \left(\frac{\partial r(\mathbf{X})}{\partial X_i} \right)^2 \sigma_{X_i}^2 + \sum_{i,j=1, \dots, N, i \neq j} \rho_{i,j} \sigma_{X_i} \sigma_{X_j} \frac{\partial r(\mathbf{X})}{\partial X_i} \frac{\partial r(\mathbf{X})}{\partial X_j}. \quad (24)$$

However, higher terms of the TSE or more accurate approximations of derivatives should be considered for the correct estimation of variance in the case of dependent input random variables and non-linear

functions. The authors of this paper recently proposed a methodology consisting of three levels of increasing accuracy and complexity described from the mathematical point of view in [25]. This methodology can be used for an arbitrary correlation matrix.

There is no theoretical background available in literature for the second presented Level II method (ECoV by Červenka), and thus it is not possible to directly generalize it for any correlation matrix. Therefore, the TSE for functions of fully correlated random variables and its connection to ECoV by Červenka are investigated in the next subsection.

4.1. Special case: ECoV for fully correlated random variables

There is often a strong assumption of fully correlated input random variables in industrial applications, which will be adopted for the further investigation of TSE. Without loss of generality, let us investigate the situation in Gaussian space. Similarly as in the case of Eq. (7) for lognormal distribution, ECoV by Červenka, which assumes Gaussian distribution, is based on the following formula:

$$R_k = \mu_R (1 - 1.645 v_f), \quad (25)$$

and v_f is therefore obtained as:

$$v_f = \frac{R_m - R_k}{1.645 R_m}, \quad (26)$$

where $R_k = r(\mathbf{X}_k)$ and $R_m = r(\mathbf{X}_m) \approx \mu_R$.

For further comparisons, let us set up the step size parameter of TSE as $c = -\Phi(0.05) \approx 1.645$, which corresponds to the same quantile as in ECoV by Červenka. The differencing scheme defined for the uncorrelated case in Eq. (13) can be transformed by a Nataf transformation which has been parametrized by arbitrary correlation coefficients, as can be seen in Fig. 2 (left).

The N -dimensional ellipsoid corresponding to σ -distance is described by eigenvectors $(\theta_1, \dots, \theta_N)$ and eigenvalues $(\lambda_1, \dots, \lambda_N)$ obtained from the Eigen decomposition of a covariance matrix. Note that in the limit case $\lim_{\rho \rightarrow 1} \lambda_1 = \text{tr}(\Sigma) = \sigma_\theta^2$ and $\lim_{\rho \rightarrow 1} \lambda_i = 0 \forall i > 1$. In other words, the N -dimensional joint probability distribution is reduced to a 1-dimensional projection with the distribution $X_\theta \sim \mathcal{N}(\mu_\theta, \lambda_1)$. The Nataf transformation of $\mathbf{X}_{i\Delta}$ is depicted in standardized Gaussian space ξ for a 2D case with increasing positive $\rho \in (0, 1)$ together with isolines of bivariate Gaussian distribution in $c \cdot \sigma$ -distance. As can be seen in Fig. 2 (left), with increasing $\rho \rightarrow 1$ the coordinates of $\mathbf{X}_{i\Delta}$ transform to \mathbf{X}_k and $\mathbf{X}_{i\Delta} \forall i > 1$ to \mathbf{X}_m , and thus:

$$\frac{\partial r(\mathbf{X})}{\partial X_i} = \frac{R_m - R_{\mathbf{X}_{i\Delta}}}{\Delta X_i} = 0 \forall i > 1. \quad (27)$$

The limit cases $\rho = 0$ and $\rho = 1$ are compared in Fig. 2 (right). As can be seen, the iso-lines of bivariate Gaussian distribution in σ -distance (grey) and $c \cdot \sigma$ -distance (red) are reduced to a single line. From the simple geometry, one can derive the following expressions:

$$A_\theta = c \cdot \sqrt{\lambda_1} = \sqrt{\sum_{i=1}^N (\mu_{X_i} - X_{i\Delta})^2}. \quad (28)$$

Finally, the variance estimated by linear TSE for fully correlated input variables can be estimated as:

$$\text{VAR}[R] = \left(\frac{\partial r(\mathbf{X})}{\partial X_\theta} \right)^2 \lambda_1, \quad (29)$$

where the derivative is obtained from two simulations $R_m = r(\mathbf{X}_m)$ and $R_{\theta\Delta} = R_k = r(\mathbf{X}_{i\Delta})$ as

$$\frac{\partial r(\mathbf{X})}{\partial X_\theta} = \frac{R_m - R_{\theta\Delta}}{\Delta_\theta}. \quad (30)$$

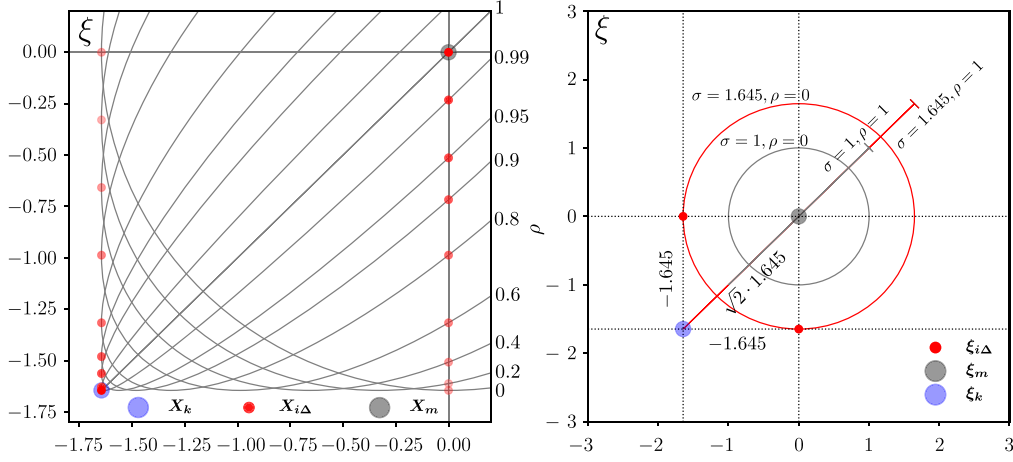


Fig. 2. Nataf transformation of a TSE in standardized Gaussian space. Transformation of $X_{i\Delta}$ with increasing ρ together with isolines of bivariate Gaussian distribution (left). Comparison of limit cases for $\rho=0$ and $\rho=1$ (right). (For interpretation of the references to colour in this figure legend, the reader is referred to the web version of this article.)

For a direct comparison with ECoV by Červenka, v_f from the equation above is obtained as:

$$v_f = \frac{\sigma_R}{\mu_R} = \sqrt{\left(\frac{R_m - R_{\theta\Delta}}{c \cdot \sqrt{\lambda_1}}\right)^2} \lambda_1 \frac{1}{\mu_R} = \frac{R_m - R_k}{1.645 R_m}. \quad (31)$$

Therefore, ECoV by Červenka (see Eq. (26)) can be seen as a special case of the TSE for fully correlated random variables that assumes linearity of the mathematical model together with a specific distribution of R (typically lognormal). If these assumptions are fulfilled ECoV by Červenka is a highly efficient method. In the opposite case, it may lead to inaccurate results. Note that this method is widely used without knowledge of assumed fully correlated input random variables, which usually increases the variance of the function in practical applications and thus obtains conservative results.

As significant disadvantage of ECoV by Červenka is its theoretical background based on the simplified formula Eq. (7), which is only accurate for low v_R . Moreover, it cannot be easily generalized and thus more complex ECoV formulas using different derivative schemes are derived from the TSE for fully correlated variables in the following section.

4.2. Eigen ECoV

Using differencing schemes proposed by the authors of this paper in [25], one can create several formulas similar to ECoV by Červenka directly from a TSE transformed by Nataf transformation for fully correlated random variables, which is depicted in Fig. 3 for Gaussian input random variables. In the special case that $\rho \rightarrow 1$, the joint probability distribution is reduced to the 1D distribution $X_{\theta} \sim \mathcal{N}(\mu_{\theta}, \lambda_1)$, which can be expanded by the TSE.

If there is no assumption of Gaussian input random variables, one has to use a corresponding probability distribution of input random variables, i.e. $X_{i\Delta} = F_i^{-1}(\Phi(-c))$. Moreover, the geometrical properties become more complex and thus one has to assume a specific distribution of X_{θ} in order to calculate Δ_{θ} in physical space. Typically, one can assume lognormal distribution and thus Δ_{θ} can be estimated as follows:

$$\Delta_{\theta} = \mu_{\theta} - \mu_{\theta} \cdot \exp(-c \cdot \frac{\sqrt{\lambda_1}}{\mu_{\theta}}), \quad (32)$$

where μ_{θ} is calculated as:

$$\mu_{\theta} = \sqrt{\sum_{i=1}^N (\mu_{X_i})^2}. \quad (33)$$

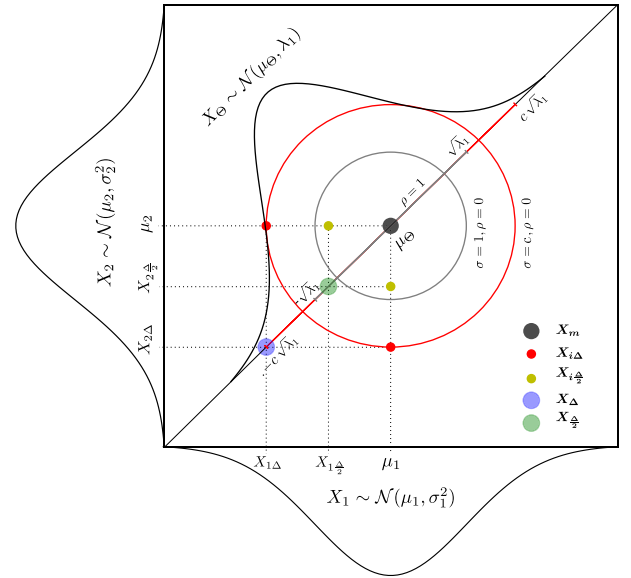


Fig. 3. Graphical interpretation of Eigen ECoV.

The first order TSE leads to well known expressions for the variance (Eq. (29)) and mean value $R_m \approx r(X_m)$ of structural resistance R . Furthermore, one can use an arbitrary differencing scheme and step-size parameter c . As was shown, simple backward differencing is used with different c by Schlune et al. [24] ($c = (\alpha_R \beta) / \sqrt{2}$) and Červenka [22] ($c = 1.645$). Note that $c = 1.645$ is assumed in Fig. 3. For the sake of clarity, let us recall the following notation: $R_{\theta\Delta} = r(X_{\theta\Delta})$ and $X_{\theta\Delta} = (X_{1\Delta}, \dots, X_{N\Delta})$. The input vector consists of reduced values of input random variables $X_{i\Delta} = F_i^{-1}(\Phi(-c))$. The Δ_{θ} is calculated according to Eq. (32) under the assumption of lognormally distributed X_{θ} or Eq. (28) under the assumption of Gaussian X_{θ} (Gaussian input random variables). The variance of 1D Eigen distribution is $\lambda_1 = \text{tr}(\Sigma) = \sum_{i=1}^N \sigma_{X_i}^2$. Based on the presented theory and notation, the following variants of Eigen ECoV are proposed:

- (a) The Eigen ECoV derived from the first order TSE using simple backward differencing leads to the following expression for the expected value, variance and CoV using two simulations:

$$\mathbb{E}[R] = R_m \approx r(X_m), \quad (34)$$

$$\text{VAR}[R] \approx \left(\frac{R_m - R_{\theta\Delta}}{\Delta_{\theta}}\right)^2 \cdot \lambda_1, \quad (35)$$

$$v_f \approx \frac{R_m - R_{\theta\Delta}}{\Delta_\theta} \cdot \frac{\sqrt{\lambda_1}}{R_m}. \quad (36)$$

(b) Furthermore the Eigen ECoV derived from the first order TSE using advanced backward differencing leads to the following expression for mean, variance and CoV using three simulations:

$$\mathbb{E}[R] = R_m \approx r(\mathbf{X}_m), \quad (37)$$

$$\text{VAR}[R] \approx \left(\frac{3R_m - 4R_{\theta\frac{\Delta}{2}} + R_{\theta\Delta}}{\Delta_\theta} \right)^2 \cdot \lambda_1, \quad (38)$$

$$v_f \approx \frac{3R_m - 4R_{\theta\frac{\Delta}{2}} + R_{\theta\Delta}}{\Delta_\theta} \cdot \frac{\sqrt{\lambda_1}}{R_m}, \quad (39)$$

where $R_{\theta\frac{\Delta}{2}} = r(\mathbf{X}_{\theta\frac{\Delta}{2}})$ and position of $\mathbf{X}_{\theta\frac{\Delta}{2}} = (X_{1\frac{\Delta}{2}}, \dots, X_{N\frac{\Delta}{2}})$ is depicted in Fig. 3. The input vector consists of reduced values of input random variables:

$$X_{i\frac{\Delta}{2}} = \mu_{X_i} - \frac{\mu_{X_i} - X_{i\Delta}}{2} = \mu_{X_i} - \frac{\Delta X_i}{2}. \quad (40)$$

(c) Additionally, using three identical simulations to those used in case (b), one can derive the Eigen ECoV from the second order TSE and thus obtain more accurate expressions. However it is necessary to include the information of higher statistical moments into the expression for variance in the case that X_θ has an assumed lognormal distribution (lognormally distributed input random variables). The following expressions are derived:

$$\mathbb{E}[R] \approx R_m + \frac{R_m - 2R_{\theta\frac{\Delta}{2}} + R_{\theta\Delta}}{\Delta_\theta^2} \cdot \frac{\lambda_1}{2}, \quad (41)$$

$$v_f \approx \frac{\sqrt{\text{VAR}[R]}}{\mathbb{E}[R]}. \quad (42)$$

- Assuming Gaussian X_θ , the third central moment $\mu_3 = 0$ and the fourth central moment $\mu_4 \approx 3\lambda_1^2$, and thus the variance is obtained via the following expression:

$$\text{VAR}[R] \approx \left(\frac{3R_m - 4R_{\theta\frac{\Delta}{2}} + R_{\theta\Delta}}{\Delta_\theta} \right)^2 \lambda_1 + \left(\frac{R_m - 2R_{\theta\frac{\Delta}{2}} + R_{\theta\Delta}}{\Delta_\theta^2} \right)^2 \frac{\lambda_1^2}{2}. \quad (43)$$

- Assuming lognormally distributed X_θ , higher central moments must be included in the expression as follows:

$$\text{VAR}[R] \approx \left(\frac{3R_m - 4R_{\theta\frac{\Delta}{2}} + R_{\theta\Delta}}{\Delta_\theta} \right)^2 \lambda_1 + \left(\frac{R_m - 2R_{\theta\frac{\Delta}{2}} + R_{\theta\Delta}}{\Delta_\theta^2} \right)^2 \frac{\mu_{4\theta} - \lambda_1^2}{4} + \mu_{3\theta} \left(\frac{3R_m - 4R_{\theta\frac{\Delta}{2}} + R_{\theta\Delta}}{\Delta_\theta} \right) \left(\frac{R_m - 2R_{\theta\frac{\Delta}{2}} + R_{\theta\Delta}}{\Delta_\theta^2} \right). \quad (44)$$

The third and fourth central moments can be derived for lognormal distribution $X_\theta \sim \mathcal{LN}(\mu_{LN}, \sigma_{LN})$ directly from the shape parameter $\sigma_{LN}^2 = \ln(1 + \frac{\lambda_1}{\mu_\theta^2})$ as:

$$\mu_{3\theta} = \left[\left(e^{\sigma_{LN}^2} + 2 \right) \sqrt{e^{\sigma_{LN}^2} - 1} \right] \lambda_1^{\frac{3}{2}}, \quad (45)$$

$$\mu_{4\theta} = \left[\left(e^{4\sigma_{LN}^2} \right) + 2 \left(e^{3\sigma_{LN}^2} \right) + 3 \left(e^{2\sigma_{LN}^2} \right) - 3 \right] \lambda_1^2. \quad (46)$$

4.3. Correlation interval ECoV

Since the information about correlation among input random variables is often vague and usually based on expert judgement, it is beneficial to study two limit cases: uncorrelated variables and fully correlated variables. The obtained results can be used for the reliable estimation of variance or CoV. Moreover, an analyst can clearly see

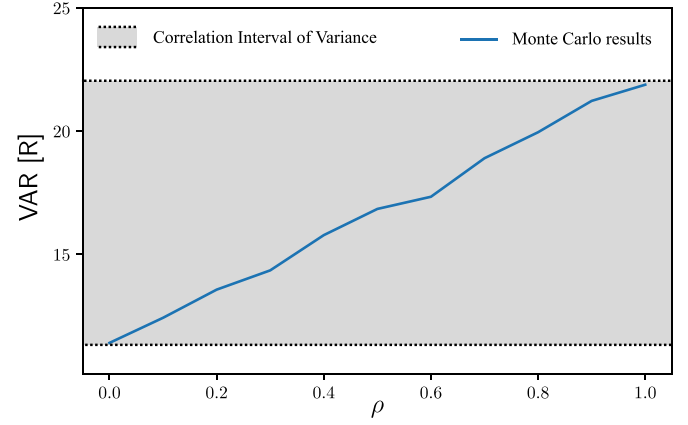


Fig. 4. Interval ECoV approach assuming identical increasing ρ among all variables. (For interpretation of the references to colour in this figure legend, the reader is referred to the web version of this article.)

the consequences of the imprecise determination of correlation matrix, which is often neglected. In the case of uncorrelated input random variables, TSE with simple ($n_{sim} = N + 1$) and advanced ($n_{sim} = 2N + 1$) differencing can be used according to the TSE methodology presented in [25]. The fully correlated case is examined via the proposed Eigen ECoV methods in three variants together with ECoV by Červenka. This methods are utilized in numerical examples in order to compare and show the limitations of the existing and proposed ECoV methods. From the practical point of view, it is beneficial to estimate variance while assuming fully correlated random variables in the case of a limited computational budget (large mathematical models) and only make further use of the TSE in order to obtain an accurate estimate of the role of correlation.

5. Numerical examples

The results of the numerical examples in this section are presented for two variants of stochastic models: under the assumption of Gaussian input variables and under the assumption of lognormal input variables. The reference solution is obtained by LHS with $n_{sim} = 10^4$ for uncorrelated random variables and also for increasing $\rho = (0, 1)$ with step 0.1 (identical ρ is assumed among all input variables). The two extremes (fully correlated and uncorrelated) define the boundaries for the interval of variance as can be seen in Fig. 4, where the blue line represents the reference solution obtained by a Monte Carlo type simulation technique for increasing ρ , and the interval is highlighted in grey. The depicted results correspond to Example 3, though the approach was used for all examples.

The variance of the uncorrelated case is estimated via a linear TSE with a simple derivative scheme (Eq. (13)) represented in the figures by a dashed line, and with an advanced differencing scheme (Eq. (15)) in figures represented by a dot-and-dash line. Note that these two methods represent the first and second order of the methodology proposed in [25]. The estimation of variance for a fully correlated limit case is obtained by the proposed Eigen ECoV and ECoV by Červenka, which is equal to Eigen ECoV (a) in Gaussian space, though there is a difference due to the approximation of lognormal distribution by Eq. (8).

5.1. Example 1: Ultimate bending moment

The very first example is a classical mathematical model of the ultimate bending moment of a reinforced section taken from Ditlevsen [40]:

$$R = r(\mathbf{X}) = X_1 X_2 X_3 - X_4 \frac{X_1^2 X_2^2}{X_5 X_6}, \quad (47)$$

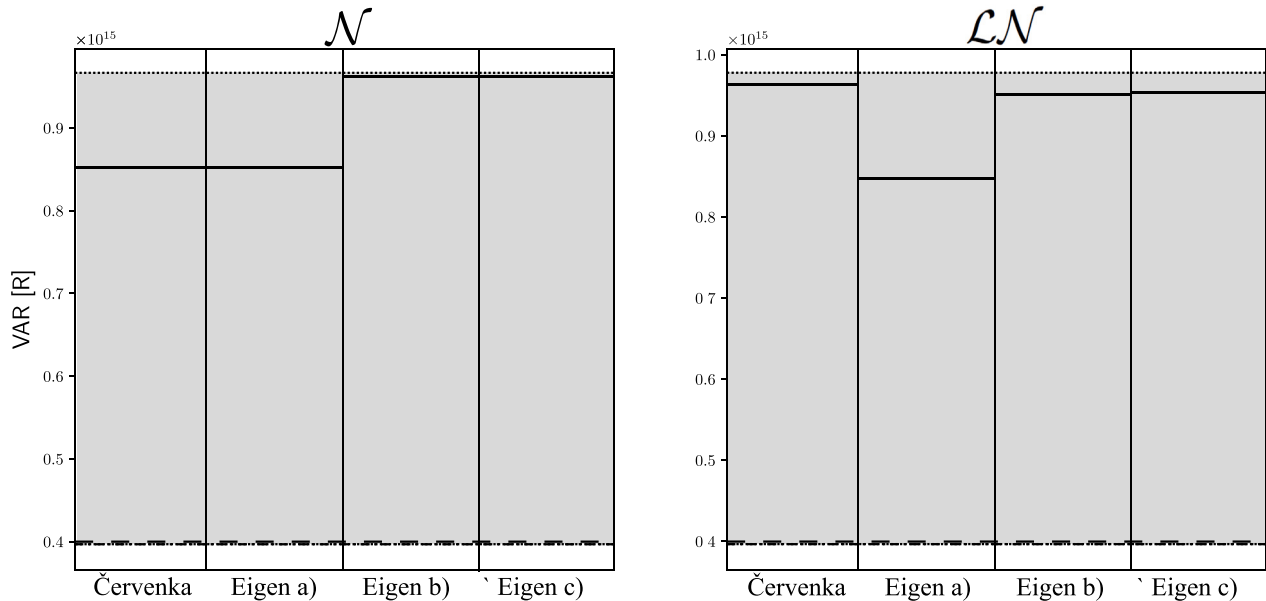


Fig. 5. Results of example 1 assuming Normal (left) and Lognormal (right) distribution of input variables. The variance of the uncorrelated case is estimated by the TSE with simple (dashed) and advanced (dot-and-dash) differencing. The variance of the correlated case is estimated by ECoV methods, which are depicted in the corresponding columns by solid lines. The reference solution (grey interval) is estimated by LHS.

Table 1

Stochastic model of the first example described by the first and the second statistical moments of input random variables.

Variable	X_1	X_2	X_3	X_4	X_5	X_6
Mean value	1260 mm ²	250 N/mm	770 mm	0.55	30 N/mm ²	250 mm
Standard deviation	63 mm ²	17.5 N/mm	10 mm	0.055	4.5 N/mm ²	5 mm

and the stochastic model contains six input random variables summarized in Table 1.

The results are compared in Fig. 5. The X-axis is divided into four columns representing the results of the ECoV methods used for the estimation of variance for fully correlated variables, and the Y-axis represents VAR [R]. Note that the grey colour corresponds to the variance interval determined by LHS (for the sake of clarity, results for intermediate ρ are not depicted). The TSE with both differencing schemes for uncorrelated random variables estimated almost identical variance, which reflects the linearity of the mathematical model. From the obtained results for fully correlated variables it is clear that ECoV by Červenka provided a very good estimate of the variance of the lognormal case, since this case fulfils both assumptions of the method: that the mathematical model is almost linear and the distribution of R is close to lognormal. In such cases, ECoV by Červenka represents the most efficient method. However, if the stochastic model contains Gaussian distribution, ECoV by Červenka fails. Note that ECoV (a) leads to inaccurate results in both cases due to the simple derivative scheme employed. However, using one more simulation ($n_{sim} = 3$) and expressions (b) and (c) of Eigen ECoV leads to accurate results that are independent of the distribution of input variables.

5.2. Example 2: Approximation of an industrial example

The second example is motivated by the industrial applications in civil engineering that are often represented by non-linear finite element models — typically the ultimate resistance given by the peak of the load-deflection curve of a concrete structural element. The behaviour of such physical system is often monotone with a slightly non-linear progression. A typical function solved by the FEM can be found for example in [24], and due to the computational demands of FEM, its

shape was replicated by the following artificial function suitable for the purposes of our tests:

$$R = r(\mathbf{X}) = X_1 X_2 - X_1^2 - \left(\frac{X_2^2}{30}\right) - (X_1 - 30)(X_2 - 200). \quad (48)$$

This function is significantly non-linear, and the stochastic model contains two input variables with the vector of mean values $\mu = [40, 300]$ and the corresponding vector $\mathbf{CoV} = [0.10, 0.15]$.

The non-linearity of the second mathematical model can be clearly seen from the difference between both TSE approximations used for the uncorrelated case. Generally, the difference between the two results is more significant with increasing non-linearity of the mathematical model, which is additionally highlighted by non-Gaussian distribution. Of course, Eigen ECoV (a) leads to a value identical to that obtained by ECoV by Červenka in Gaussian space, and a similar result is gained in lognormal space. With only one additional calculation, the results obtained by Eigen ECoV (b) and (c) are far more accurate. The superiority of these two methods is obvious from Fig. 6. In Gaussian space the results are almost exact and identical to each other, since higher central moments have negligible influence. However, in the lognormal case there is an obvious difference between both methods using identical calculations of the original mathematical model.

5.3. Example 3: Truss structure 2D NLFEA

The third example is represented by the 2D truss structure shown in Fig. 7. The ultimate load F for the allowed midspan deflection (the blue point in the figure) of $v = 10$ cm is obtained by NLFEA implemented in OpenSeesPy [41]. Uniaxial Giuffrè–Menegotto–Pinto steel material with isotropic strain hardening is used to represent all structural members. The stochastic model contains six random variables: yield strength f_y and initial elastic tangent E for the top chords (1), web members (2) and bottom chords (3), with the mean values $\mu_{f_y} = 255$ MPa, $\mu_E = 210$ GPa and CoVs: $CoV_{f_y} = 0.10$, $CoV_E = 0.05$.

The reference solution was obtained by LHS with $n_{sim} = 10^4$ simulations for each ρ and both variants (Gaussian and lognormal). The results gained by TSE and Eigen ECoV for this NLFEA are depicted in Fig. 8. Note that the function exhibits significant non-linearity, since the variance estimated by the linear TSE with simple differencing is

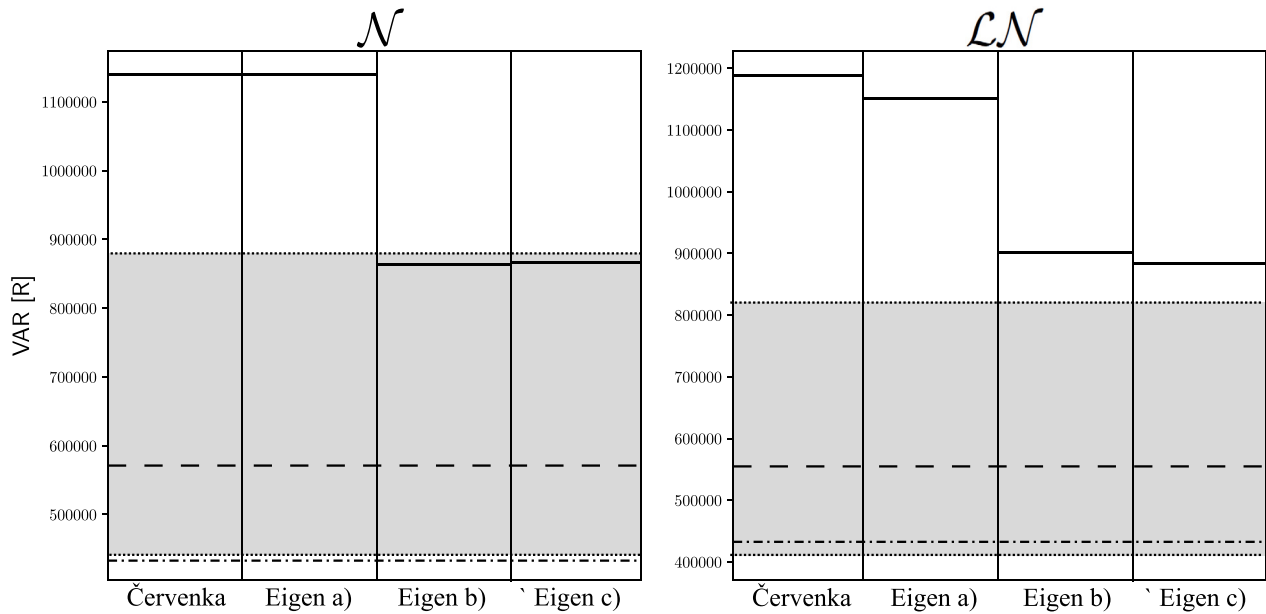


Fig. 6. Results of example 2 assuming Normal (left) and Lognormal (right) distribution of input variables. The variance of the uncorrelated case is estimated by the TSE with simple (dashed) and advanced (dot-and-dash) differencing. The variance of the correlated case is estimated by ECoV methods, which are depicted in the corresponding columns by solid lines. The reference solution (grey interval) is estimated by LHS.

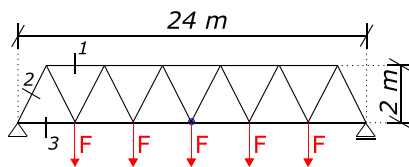


Fig. 7. Scheme of 2D truss structure. (For interpretation of the references to colour in this figure legend, the reader is referred to the web version of this article.)

significantly different from the reference solution and thus simple linear differencing is not able to approximate the function. On the other hand, the TSE with advanced differencing is very accurate, especially for the Gaussian variant. For the fully correlated random variables, Eigen ECoV (b) and (c) with $n_{sim} = 3$ calculations lead to very accurate results in both the Gaussian and the lognormal case. Moreover, Eigen ECoV is not limited to lognormal distribution but works generally for arbitrary distributions of response in similar manner to TSE.

6. Discussion

The proposed Eigen ECoV is derived directly from TSE, which is in compliance with PSF defined in Eurocode [7,42] and therefore can be recommended for the design and assessment of structures. Moreover, it is a general method that works without assumptions about the probability distribution of R , which stands in contrast to the widely used ECoV by Červenka implemented in Model Code 2010, which assumes Gaussian or lognormal distribution (with $v_R < 0.2$) of R . On the other hand, if these assumptions are fulfilled and the mathematical model is nearly linear, ECoV by Červenka is highly efficient.

The significant advantage of Eigen ECoV is its adaptivity using various differencing schemes. Eigen ECoV (a) represents an equivalent method to ECoV by Červenka. It is derived from the first order TSE with simple backward differencing and thus leads to identical results in Gaussian space. However, it has been shown that it is not suitable for non-linear mathematical models. Eigen ECoV (b) is derived from the first order TSE with advanced backward differencing, which leads to more accurate estimates and preserves the simplicity of the formulas for variance. Therefore, it can be easily used by civil engineers in industrial

Table 2

Comparison of estimated variance for example 2 assuming increasing uncertainty of input random variables.

CoV	LHS	Eigen ECoV b)	Eigen ECoV c)	ϵ
[0.10, 0.15]	$0.82 \cdot 10^6$	$0.90 \cdot 10^6$	$0.88 \cdot 10^6$	2%
[0.30, 0.35]	$4.63 \cdot 10^6$	$6.47 \cdot 10^6$	$5.82 \cdot 10^6$	14%
[0.40, 0.45]	$7.14 \cdot 10^6$	$11.15 \cdot 10^6$	$9.32 \cdot 10^6$	26%

applications using NLFEA. Although Eigen ECoV (c) is derived from the second order TSE, it uses identical numerical calculations of the original mathematical model to those employed by Eigen ECoV (b). It typically leads to slightly improved estimates of variance and expected values of R , taking higher moments of probability distributions of input random variables into account. However, the ECoV formula is much more complicated and should be implemented into a software application.

The difference between proposed Eigen ECoV (b) and (c) is higher with growing skewness and kurtosis of X_θ . Naturally, this plays significant role in case of lognormal distribution of X_θ with high CoV as can be clearly seen in Eq. (44). In order to amplify this difference, let us artificially increase the uncertainty of both input random variables in Example 2 as follows: $CoV = [0.30, 0.35]$ and $CoV = [0.40, 0.45]$. The estimated $VAR[R]$ assuming both input random variables lognormally distributed and fully correlated are summarized in the Table 2. Note that the percentual difference ϵ is defined as an absolute value of a difference between variance estimated by Eigen ECoV (b) and (c) divided by the reference solution estimated by LHS. We would like to note that, such high uncertainty of input variable is not common in industrial applications and thus the difference between both solutions is typically much lower.

In practical application of the correlation interval approach, one should start with Eigen ECoV for the estimation of the variance of fully correlated cases and then use standard TSE in order to obtain the variance of uncorrelated cases if necessary. The difference between variances is a direct measure of the impact of the vagueness of available information about the dependency structure among input random variables. Higher correlation among random variables typically leads to higher variance of R , and thus one can assume Eigen ECoV as a conservative estimate. However, analysts might need more accurate

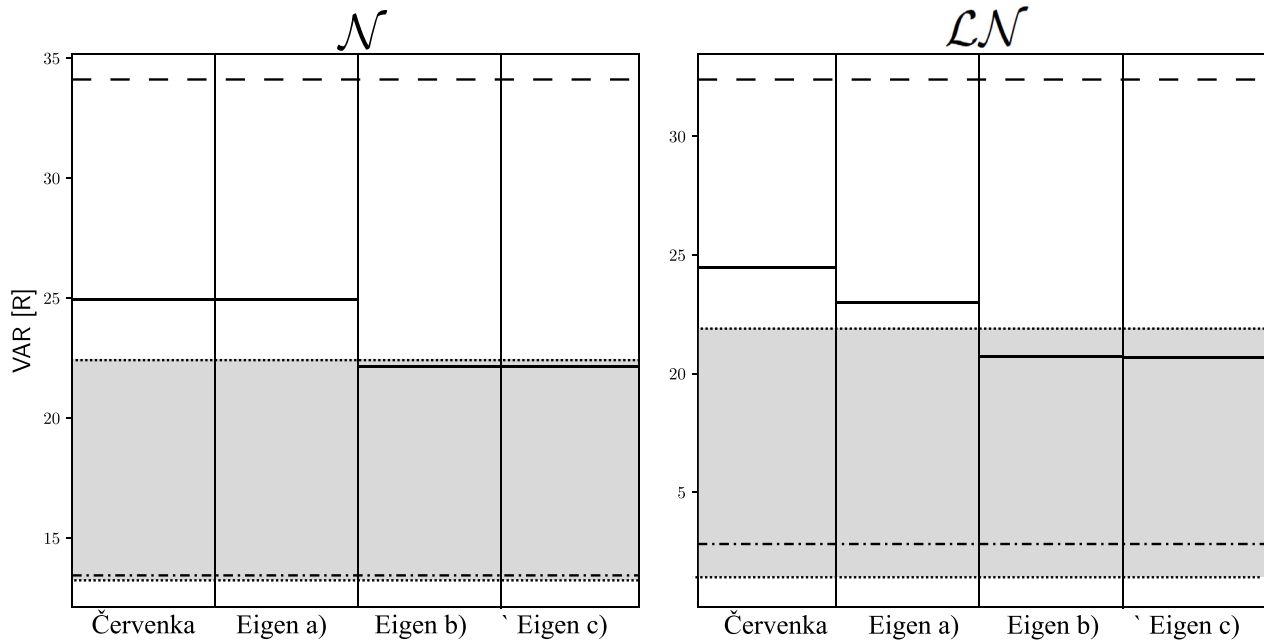


Fig. 8. Results of example 3 assuming Normal (left) and Lognormal (right) distribution of input variables. The variance of the uncorrelated case is estimated by the TSE with simple (dashed) and advanced (dot-and-dash) differencing. The variance of the correlated case is estimated by ECoV methods, which are depicted in the corresponding columns by solid lines. The reference solution (grey interval) is estimated by LHS.

results, and thus the standard TSE with simple or advanced differencing should be employed. More accurate results are especially important in case of existing structures, since the economic impact of unnecessary interventions could be significant. It naturally leads to more advanced structural analysis by NLFEA but it should be also reflected in semi-probabilistic analysis [31]. Note that for the practical design and assessment of structures, it is necessary to additionally include model uncertainty and geometrical uncertainty according to Eq. (5). The correlation interval ECoV approach then leads to minimal or maximal v_R and thus to the maximal (unsafe) design value R_d or the minimal (safe) design value R_d obtained as a corresponding quantile of the structural resistance.

7. Conclusions

The paper is focused on estimation of coefficient of variation methods for NLFEA. ECoV methods are the basis for the semi-probabilistic approach for the design and assessment of structures and thus it is crucial to use accurate and efficient methods for industrial applications. The review of existing methods and three levels of assumed simplifications is presented with attention to the theoretical mathematical background of each method. Furthermore, the influence of correlation among random variables and Nataf transformation is briefly described. Finally, the general Eigen ECoV method for functions of fully correlated random variables and the interval ECoV approach are proposed. The Eigen ECoV is analytically compared to the existing well known ECoV method by Červenka. It is shown that Eigen ECoV represents a special case of the general Taylor Series Expansion and can be directly compared to the ECoV method by Červenka in Gaussian space. However, it is a general method without any assumption regarding the probability distribution of structural resistance, which is in contrast to existing methods. The presented methods are applied for three numerical examples, and the expected behaviour of Eigen ECoV is proved. The most efficient method for industrial applications is Eigen ECoV (b) using three numerical calculations of the original mathematical model since it leads to the accurate estimation of variance, preserving the simplicity of analytical formulas that are easily applicable in industrial practice.

Acknowledgements

This research was funded by Czech Science Foundation, Czech Republic under project No. 20-01781S. The first author is Brno Ph.D. Talent Scholarship Holder - Funded by the Brno City Municipality, Czech Republic.

References

- [1] Bagge N. Demonstration and examination of a procedure for successively improved structural assessment of concrete bridges. *Structural Concrete* 2020;21(4):1321–44. <http://dx.doi.org/10.1002/suco.201900265>.
- [2] Casas JR, Wisniewski D. Safety requirements and probabilistic models of resistance in the assessment of existing railway bridges. *Structure and Infrastructure Engineering* 2013;9(6):529–45. <http://dx.doi.org/10.1080/15732479.2011.581673>.
- [3] Strauss A, Hoffmann S, Wendner R, Bergmeister K. Structural assessment and reliability analysis for existing engineering structures, applications for real structures. *Structure and Infrastructure Engineering* 2009;5(4):277–86. <http://dx.doi.org/10.1080/15732470601185638>.
- [4] Val D, Bljuzer F, Yankelevsky D. Reliability evaluation in nonlinear analysis of reinforced concrete structures. *Structural Safety* 1997;19(2):203–17. [http://dx.doi.org/10.1016/S0167-4730\(96\)00025-2](http://dx.doi.org/10.1016/S0167-4730(96)00025-2).
- [5] Comité Européen de Normalisation (CEN), Brussels, Belgium, EN 1990: Eurocode: Basis Of structural design. 2002.
- [6] Hasofer AM, Lind NC. Exact and invariant second-moment code format. *Journal of Engineering Mechanics-asce* 1974;100(EM1):111–21.
- [7] Melchers RE, Beck AT. *Second-moment and transformation methods*. John Wiley & Sons, Ltd; 2017, p. 95–130 (Ch. 4).
- [8] Rosenblueth E. Point estimates for probability moments. *Proc Natl Acad Sci* 1975;72(10):3812–4. <http://dx.doi.org/10.1073/pnas.72.10.3812>.
- [9] Castaldo P, Gino D, Mancini G. Safety formats for non-linear finite element analysis of reinforced concrete structures: discussion, comparison and proposals. *Eng Struct* 2019;193:136–53. <http://dx.doi.org/10.1016/j.engstruct.2019.05.029>.
- [10] Allaix DL, Carbone VI, Mancini G. Global safety format for non-linear analysis of reinforced concrete structures. *Structural Concrete* 2013;14(1):29–42. <http://dx.doi.org/10.1002/suco.201200017>.
- [11] Allaix DL, Carbone VI, Mancini G. Global resistance factor for reinforced concrete beams. In: *Proceedings of the 5th international probabilistic workshop*. Ghent, Belgium: ACCO; 2007, p. 195–208.
- [12] Šýkora M, Červenka J, Červenka V, Mlčoch J, Novák D, Novák L. Pilot comparison of safety formats for reliability assessment of rc structures. In: *Proceedings of the fib symposium 2019: concrete - Innovations in materials, design and structures*. 2019. p. 2076–83.

- [13] Novák L, Novák D, Pukl R. Probabilistic and semi-probabilistic design of large concrete beams failing in shear. In: *Advances in engineering materials, structures and systems: innovations, mechanics and applications*. Taylor and Francis Group CRC Press; 2019.
- [14] Novák D, Novák L, Slowik O, Strauss A. Prestressed concrete roof girders: Part iii – semi-probabilistic design. In: *Proceedings of the sixth international symposium on life-cycle civil engineering*. CRC Press, Taylor and Francis Group; 2018, p. 510–7.
- [15] Fib federation internationale du beton. In: *Fib model code for concrete structures 2010*. Berlin, Heidelberg: John Wiley & Sons; 2013.
- [16] Castaldo P, Gino D, Bertagnoli G, Mancini G. Partial safety factor for resistance model uncertainties in 2d non-linear finite element analysis of reinforced concrete structures. *Eng Struct* 2018;176:746–62. <http://dx.doi.org/10.1016/j.engstruct.2018.09.041>.
- [17] Gino D, Castaldo P, Bertagnoli G, Giordano L, Mancini G. Partial factor methods for existing structures according to fib bulletin 80: Assessment of an existing prestressed concrete bridge. *Structural Concrete* 2020;21(1):15–31. <http://dx.doi.org/10.1002/suco.201900231>.
- [18] Comité Européen de Normalisation (CEN), Brussels, Belgium, EN 1992: Eurocode 2: Design of concrete structures. 2004.
- [19] Engen M, Hendriks MA, Kohler J, Øverli JA, Åldstedt E. A quantification of the modelling uncertainty of non-linear finite element analyses of large concrete structures. *Structural Safety* 2017;64:1–8. <http://dx.doi.org/10.1016/j.strusafe.2016.08.003>.
- [20] Holický M, Retief JV, Sýkora M. Assessment of model uncertainties for structural resistance. *Probabilistic Engineering Mechanics* 2016;45:188–97. <http://dx.doi.org/10.1016/j.probengmech.2015.09.008>.
- [21] Christian JT, Baecher GB. Point-estimate method as numerical quadrature. *Journal of Geotechnical and Geoenvironmental Engineering* 1999;125(9):779–86. [http://dx.doi.org/10.1061/\(ASCE\)1090-0241\(1999\)125:9\(779\)](http://dx.doi.org/10.1061/(ASCE)1090-0241(1999)125:9(779)).
- [22] Červenka V. Global safety format for nonlinear calculation of reinforced concrete. *Beton- und Stahlbetonbau* 2008;103(S1):37–42. <http://dx.doi.org/10.1002/best.200810117>.
- [23] Červenka V. Reliability-based non-linear analysis according to fib model code 2010. *Structural Concrete* 2013;14(1):19–28. <http://dx.doi.org/10.1002/suco.201200022>.
- [24] Schlune H, Plos M, Gylltoft K. Safety formats for nonlinear analysis tested on concrete beams subjected to shear forces and bending moments. *Eng Struct* 2011;33(8):2350–6.
- [25] Novák L, Novák D. On Taylor series expansion for statistical moments of functions of correlated random variables. *Symmetry* 2020;12:1379. <http://dx.doi.org/10.3390/sym12081379>.
- [26] McKay MD. Latin hypercube sampling as a tool in uncertainty analysis of computer models. In: *Proceedings of the 24th conference on winter simulation*. New York, NY, USA: 1992. p. 557–64.
- [27] Iman RL, Conover W. Small sample sensitivity analysis techniques for computer models. with an application to risk assessment. *Comm Statist Theory Methods* 1980;9(17):1749–842.
- [28] Lebrun R, Dutfoy A. A generalization of the Nataf transformation to distribution with elliptical copula. *Probabilistic Engineering Mechanics* 2009;24(2):172–8. <http://dx.doi.org/10.1016/j.probengmech.2008.05.001>.
- [29] Vořechovský M, Eliáš J. Modification of the maximin and ϕ_p (ϕ) criteria to achieve statistically uniform distribution of sampling points. *Technometrics* 2020;62(3):371–86. <http://dx.doi.org/10.1080/00401706.2019.1639550>.
- [30] Vořechovský M, Novák D. Correlation control in small-sample Monte Carlo type simulations i: A simulated annealing approach. *Probabilistic Engineering Mechanics* 2009;24(3):452–62. <http://dx.doi.org/10.1016/j.probengmech.2009.01.004>.
- [31] Pimentel M, Brühwiler E, Figueiras J. Safety examination of existing concrete structures using the global resistance safety factor concept. *Eng Struct* 2014;70:130–43. <http://dx.doi.org/10.1016/j.engstruct.2014.04.005>.
- [32] Zimmermann T, Lehký D, Strauss A. Correlation among selected fracture-mechanical parameters of concrete obtained from experiments and inverse analyses. *Structural Concrete* 2016;17(6):1094–103. <http://dx.doi.org/10.1002/suco.201500147>.
- [33] Rosenblatt M. Remarks on a multivariate transformation. *Ann Math Stat* 1952;23(3):470–2.
- [34] Kiureghian AD, Liu P. Structural reliability under incomplete probability information. *J Eng Mech* 1986;112(1):85–104. [http://dx.doi.org/10.1061/\(ASCE\)0733-9399\(1986\)112:1\(85\)](http://dx.doi.org/10.1061/(ASCE)0733-9399(1986)112:1(85)).
- [35] Lebrun R, Dutfoy A. An innovating analysis of the Nataf transformation from the copula viewpoint. *Probabilistic Engineering Mechanics* 2009;24(3):312–20. <http://dx.doi.org/10.1016/j.probengmech.2008.08.001>.
- [36] Torre E, Marelli S, Embrechts P, Sudret B. A general framework for data-driven uncertainty quantification under complex input dependencies using vine copulas. *Probabilistic Engineering Mechanics* 2019;55:1–16. <http://dx.doi.org/10.1016/j.probengmech.2018.08.001>.
- [37] Lebrun R, Dutfoy A. Do Rosenblatt and Nataf isoprobabilistic transformations really differ? *Probabilistic Engineering Mechanics* 2009;24(4):577–84. <http://dx.doi.org/10.1016/j.probengmech.2009.04.006>.
- [38] Nataf A. Determination des distributions de probabilités dont les marges sont données. *C R Acad Sci* 1962;225:42–3.
- [39] Liu P-L, Der Kiureghian A. Multivariate distribution models with prescribed marginals and covariances. *Probabilistic Engineering Mechanics* 1986;1(2):105–12. [http://dx.doi.org/10.1016/0266-8920\(86\)90033-0](http://dx.doi.org/10.1016/0266-8920(86)90033-0).
- [40] Ditlevsen O. *Uncertainty modeling with applications to multidimensional civil engineering systems*. Advanced Book Program, McGraw-Hill International Book Company; 1981.
- [41] Zhu M, McKenna F, Scott MH. *Openseespy: Python library for the opensees finite element framework*. SoftwareX 2018;7:6–11.
- [42] Cornell CA. A probability based structural code. *J Amer Concr Inst* 1969;66(12):974–85.

F Variance-based Adaptive Sequential Sampling for Polynomial Chaos Expansion

DOI: 10.1016/j.cma.2021.114105

F.1 Description

The paper is focused on the adaptive sequential sampling method for building Polynomial Chaos Expansion (PCE). The proposed technique enables one-by-one extension of an experimental design while trying to obtain an optimal sample at each stage of the adaptive sequential surrogate model construction process. The proposed criterion for the sample selection balances both exploitation of the surrogate model and the exploration of the design domain. The original idea comes from Koksma-Hlawka inequality (which predicts an upper bound of MC integration error) and its utilization for sequential Monte Carlo sampling. In this paper, the proposed criterion consists of two parts: a local contribution to variance (directly derived from PCE basis functions), and a geometrical term assuring uniform coverage of the whole design domain and that the algorithm does not get stuck in local minima. It can be seen from the numerical results that the proposed sequential sampling leads to a higher accuracy of the PCE in all the tested examples (including the study in high dimensions). Additionally, it was shown in the paper that the proposed adaptive sequential sampling technique can be used in tandem with any user-defined sampling method.

F.2 Role of the Ph.D. Candidate

Percentage of contribution: 60%

Lukáš Novák is the main author of this paper responsible for the concept, the methodology and the numerical results of the presented research. He created the theoretical background of the proposed sequential sampling in collaboration with Miroslav Vořechovský and Michael D. Shields. The theoretical algorithm was implemented into a Python package by Lukáš Novák with a significant help from Václav Sadílek in order to perform an extensive numerical investigation.



ELSEVIER



Available online at www.sciencedirect.com

ScienceDirect

Comput. Methods Appl. Mech. Engrg. 386 (2021) 114105

**Computer methods
in applied
mechanics and
engineering**

www.elsevier.com/locate/cma

Variance-based adaptive sequential sampling for Polynomial Chaos Expansion

Lukáš Novák^{a,*}, Miroslav Vořechovský^a, Václav Sadílek^a, Michael D. Shields^b

^a Brno University of Technology, Brno, Czech Republic

^b Johns Hopkins University, Baltimore, USA

Received 27 March 2021; received in revised form 5 August 2021; accepted 8 August 2021

Available online xxxx

Abstract

This paper presents a novel adaptive sequential sampling method for building Polynomial Chaos Expansion surrogate models. The technique enables one-by-one extension of an experimental design while trying to obtain an optimal sample at each stage of the adaptive sequential surrogate model construction process. The proposed sequential sampling strategy selects from a pool of candidate points by trying to cover the design domain proportionally to their local variance contribution. The proposed criterion for the sample selection balances both *exploitation* of the surrogate model and *exploration* of the design domain. The adaptive sequential sampling technique can be used in tandem with any user-defined sampling method, and here was coupled with commonly used Latin Hypercube Sampling and advanced Coherence D-optimal sampling in order to present its general performance. The obtained numerical results confirm its superiority over standard non-sequential approaches in terms of surrogate model accuracy and estimation of the output variance.

© 2021 Elsevier B.V. All rights reserved.

Keywords: Polynomial Chaos Expansion; Adaptive sampling; Sequential sampling; Coherence optimal sampling

1. Introduction

The Polynomial Chaos Expansion (PCE), originally proposed by Norbert Wiener [1] and further investigated in the context of engineering problems by many researchers, e.g. [2,3], represents a spectral expansion of the original *stochastic problem* in a polynomial basis. PCE approximation represents very efficient method for sensitivity analysis, uncertainty quantification or reliability analysis [4]. Moreover, once the PCE is available, it is possible to investigate the constructed explicit function in order to estimate additional information about the original problem including its statistical moments, output probability distribution or sensitivity indices without additional sampling [5], which is especially beneficial in industrial applications [6,7]. PCE can be generally formulated in intrusive or non-intrusive form. Despite the recent progress in research on the intrusive approach [8], it is still rarely employed in practical applications since it requires redesign of the mathematical model solver.

On the other hand, the non-intrusive approach offers a convenient way to perform probabilistic analysis of any black-box model. There are generally two types of non-intrusive methods for calculation of deterministic

* Corresponding author.

E-mail addresses: novak.l@fce.vutbr.cz (L. Novák), vorechovsky.m@vut.cz (M. Vořechovský), sadilek.v@fce.vutbr.cz (V. Sadílek), michael.shields@jhu.edu (M.D. Shields).

<https://doi.org/10.1016/j.cma.2021.114105>

0045-7825/© 2021 Elsevier B.V. All rights reserved.

coefficients: spectral projection and linear regression. The spectral projection approach utilizes the orthogonality of multivariate polynomials and calculates the coefficients using inner products. Although the integrals in spectral projection can be calculated by traditional tensor-product quadrature rules, the number of collocation points grows exponentially with the number of input random variables which is called *curse of dimensionality* and thus computationally far more efficient sparse grids [9,10] should be employed. The second type of the non-intrusive approach is based on linear regression. Although it is typically less expensive than spectral projection (the number of samples should be at least $\mathcal{O}(P \ln(P))$, where P is the number of terms in PCE [11,12]) it suffers from the curse of dimensionality as well, since number of PCE terms is extremely large for high dimensions and high polynomial orders. Therefore, it is necessary to employ advanced adaptive techniques for construction of sparse PCE in order to obtain efficient solutions for real-life physical systems. Moreover, the regression based PCE can be significantly affected by sampling schemes as was recently shown in extensive review paper [13]. Therefore, this paper is focused on the combination of PCE adaptivity with a sequential sampling strategy designed for the non-intrusive approach based on linear regression.

Since each evaluation of a computer model representing the engineering problem is typically highly time-consuming (e.g. non-linear finite element method), it is necessary to reduce the number of model evaluations as much as possible in the process of training the surrogate model, while maintaining the accuracy of the approximation. The balance between accuracy and computational requirements is strongly connected to the selection of the support points in the *design domain* of input variables — a computational design of experiments (DoE). Besides the commonly used crude Monte Carlo sampling, there are several advanced techniques developed in the fields of statistical/numerical estimation of integrals which improve the efficiency and accuracy of the DoE. One of the most widely used techniques is Latin Hypercube Sampling (LHS) [14], a variance reduction technique that uses stratified selection of sampling points. Another popular strategy for DoE is to uniformly fill the design domain according to some *space-filling* criteria such as miniMax, Maximin [15] or generalized versions of distance-based criteria [16,17], or to decrease the *discrepancy* of the point set. Low discrepancy designs can be obtained either by direct algorithmic minimization of selected discrepancy measure or as Quasi Monte Carlo sequences (known also as low-discrepancy sequences, or number-theoretical designs; see e.g. the sequence due to Halton [18,19], Sobol' [20,21], Niederreiter [22–24], Faure [25], the generalization of the Faure sequences by Tezuka [26], and others). These techniques for DoE can be used for general probabilistic analysis (=numerical integration) without any knowledge about the specific mathematical model or surrogate model.

Further it is often beneficial to include additional information into the DoE stemming from the specific type of the surrogate model at hand. The coherence-based sampling was proposed specifically for PCE constructed by ordinary least squares regression (OLS) [27] and it leads to higher stability in estimation of PCE coefficients in comparison to general sampling methods such as LHS, which is commonly used in combination with PCE. Another method developed specifically for OLS is induced sampling [28], which has been proved to be optimal for weighted least-squares methods.

Methods for DoE construction usually need to specify the number of simulations *a priori*. It is however much more efficient and practical to sample additional points one-by-one until desired accuracy of the approximation is reached. Such methodology for sample size extension is referred to as sequential sampling and it is especially beneficial in practical engineering applications. Sequential sampling schemes are often driven by a defined criterion to compare candidates for sample size extension. The concept of adaptive experimental design for learning surrogate models is often termed *active learning*. This approach is a common approach when the goal is reliability analysis with a surrogate: an initial experimental design is iteratively updated based on the current estimation of the limit-state surface in an active learning algorithm [29–31]. Active learning approach involving PCE in the context of reliability analysis was used e.g. in [32–34].

Although there are recent studies focused on general sequential sampling based on space-filling criteria or alphabetical optimality used for PCE [35,36], it is beneficial to use both *exploitation* (leveraging model behavior) criteria and *exploration* (space filling) criteria for definition of an optimally balanced criterion [37]. Such sequential sampling for sparse Bayesian learning PCE combining both aspects — epistemic uncertainty of the statistical inference (exploration) together with quadratic loss function (local exploitation) was recently proposed [38]. However, its application is limited to PCE build by sparse Bayesian learning only. This paper presents a novel adaptive sequential sampling technique with such a balanced criterion. The technique presented in this paper can be coupled with any sparse regression solver and common methods for DoE such as LHS and thus can be easily

implemented into the existing software solutions for PCE construction (e.g. [39–43]). Additionally, in order to increase the efficiency of the proposed scheme, the developed technique is coupled with coherence D-optimal sampling created specifically for non-intrusive PCE solved by OLS and thus all parts of the method are designed in order to increase the efficiency and accuracy of this particular type of surrogate model.

2. Polynomial Chaos expansion

Assume a probability space $(\Omega, \mathcal{F}, \mathcal{P})$, where Ω is an event space, \mathcal{F} is a σ -algebra on Ω (collection of subsets closed under complementation and countable unions) and \mathcal{P} is a probability measure on \mathcal{F} . If the input variable of a mathematical model, $Y = g(X)$, is a random variable $X(\omega)$, $\omega \in \Omega$, the model response $Y(\omega)$ is also a random variable. Assuming that Y has a finite variance, PCE represents the output variable Y as a function of an another random variable ξ called the *germ* with given distribution

$$Y = g(X) = g^{\text{PCE}}(\xi), \quad (1)$$

and representing the function $g(X)$ via polynomial expansion in a manner similar to the Fourier series of a periodic signal. A set of polynomials, orthogonal with respect to the distribution of the germ, is used as a basis of the Hilbert space $L^2(\Omega, \mathcal{F}, \mathcal{P})$ of all real-valued random variables of finite variance, where \mathcal{P} takes over the meaning of the probability distribution. The orthogonality condition for all $j \neq k$ is given by the inner product of $L^2(\Omega, \mathcal{F}, \mathcal{P})$ defined for any two functions ψ_j and ψ_k with respect to the weight function p_ξ (probability density function of ξ) as:

$$\langle \psi_j, \psi_k \rangle = \int \psi_j(\xi) \psi_k(\xi) p_\xi(\xi) d\xi = 0. \quad (2)$$

This means that there are specific orthogonal polynomials associated with the corresponding distribution of the germ via its weighting function. For example, Hermite polynomials orthogonal to the Gaussian measure are associated with normally distributed germs. Orthogonal polynomials corresponding to other distributions can be chosen according to Wiener–Askey scheme [44]. For further processing, it is beneficial to use normalized polynomials (orthonormal), where the inner product is equal to the Kronecker delta δ_{jk} , i.e. $\delta_{jk} = 1$ if and only if $j = k$, and $\delta_{jk} = 0$ otherwise

$$\langle \psi_j, \psi_k \rangle = \delta_{jk}. \quad (3)$$

In the case of \mathbf{X} and $\boldsymbol{\xi}$ being vectors containing M independent random variables, the polynomial $\Psi(\boldsymbol{\xi})$ is multivariate and it is built up as a tensor product of univariate orthogonal polynomials as

$$\Psi_\alpha(\boldsymbol{\xi}) = \prod_{i=1}^M \psi_{\alpha_i}(\xi_i), \quad (4)$$

where $\boldsymbol{\alpha} \in \mathbb{N}^M$ is a set of integers called the *multi-index*. The quantity of interest (QoI), i.e. the response of the mathematical model $Y = g(\mathbf{X})$, can then be represented, according to Ghanem and Spanos [3], as

$$Y = g(\mathbf{X}) = \sum_{\boldsymbol{\alpha} \in \mathbb{N}^M} \beta_\alpha \Psi_\alpha(\boldsymbol{\xi}), \quad (5)$$

where β_α are deterministic coefficients and Ψ_α are multivariate orthogonal polynomials.

2.1. Non-intrusive computation of PCE coefficients

For practical computation, PCE expressed in Eq. (5) must be truncated to a finite number of terms P . The truncation is commonly achieved by retaining only terms whose total degree $|\boldsymbol{\alpha}|$ is less than or equal to a given p . Therefore, the truncated set of PCE terms is then defined as

$$\mathcal{A}^{M,p} = \left\{ \boldsymbol{\alpha} \in \mathbb{N}^M : |\boldsymbol{\alpha}| = \sum_{i=1}^M \alpha_i \leq p \right\}. \quad (6)$$

The cardinality of the truncated *index set* $\mathcal{A}^{M,p}$ is given by

$$\text{card } \mathcal{A}^{M,p} = \frac{(M+p)!}{M! p!}. \quad (7)$$

Moreover, in practical applications, it is beneficial to prefer only basis functions with lower number of interaction terms. Therefore, it was proposed by Blatman and Sudret [2] to create a PCE basis by a “hyperbolic” truncation scheme:

$$\mathcal{A}^{M,p,q} = \left\{ \boldsymbol{\alpha} \in \mathbb{N}^M : \|\boldsymbol{\alpha}\|_q \equiv \left(\sum_{i=1}^M \alpha_i^q \right)^{1/q} \leq p \right\}. \quad (8)$$

Note that selection of $q = 1$ corresponds to the standard truncation scheme according to Eq. (6) and, for $q < 1$, terms representing higher-order interactions are eliminated. Such an approach leads to a dramatic reduction in the cardinality of the truncated set for high total polynomial orders p and high dimensions M .

When PCE is truncated to a finite number of terms, there is an error ε of the approximation such that

$$Y = g(\mathbf{X}) = \sum_{\boldsymbol{\alpha} \in \mathcal{A}} \beta_{\boldsymbol{\alpha}} \Psi_{\boldsymbol{\alpha}}(\boldsymbol{\xi}) + \varepsilon.$$

From a statistical point of view, PCE is a simple linear regression model with intercept. Therefore, it is possible to use *ordinary least square* (OLS) regression to minimize the error ε

$$\boldsymbol{\beta} = \arg \min_{\boldsymbol{\beta} \in \mathbb{R}^P} \frac{1}{n_{\text{sim}}} \sum_{i=1}^{n_{\text{sim}}} [\boldsymbol{\beta}^T \boldsymbol{\Psi}(\boldsymbol{\xi}^{(i)}) - g(\mathbf{x}^{(i)})]^2. \quad (9)$$

Knowledge of vector $\boldsymbol{\beta}$ fully characterizes the approximation via PCE. To solve for $\boldsymbol{\beta}$, first it is necessary to create n_{sim} realizations of the input random vector \mathbf{X} and the corresponding results of the original mathematical model \mathcal{Y} , together called the experimental design (ED). Then, the vector of P deterministic coefficients $\boldsymbol{\beta}$ is calculated as

$$\boldsymbol{\beta} = (\boldsymbol{\Psi}^T \boldsymbol{\Psi})^{-1} \boldsymbol{\Psi}^T \mathcal{Y}, \quad (10)$$

where $\boldsymbol{\Psi}$ is the data matrix

$$\boldsymbol{\Psi} = \{ \Psi_{ij} = \Psi_j(\boldsymbol{\xi}^{(i)}), i = 1, \dots, n_{\text{sim}}, j = 0, \dots, P - 1 \}. \quad (11)$$

Note that the number of terms P is highly dependent on the number of input random variables M and the maximum total degree of polynomials p . Estimation of $\boldsymbol{\beta}$ by regression then needs at least the number of samples $\mathcal{O}(P \ln(P))$ for stable solution [11,12]. Therefore, in case of a large stochastic model, the problem can become computationally highly demanding. However, one can utilize advanced model selection algorithms such as Least Angle Regression (LAR) [45] to find an optimal set of PCE terms and thus reduce the number of samples needed to compute the unknown coefficients if the true coefficient vector is sparse or compressible as proposed by Blatman and Sudret [2]. Note that beside LAR, there are other best model selection algorithms such as orthogonal matching pursuit [46] or Bayesian compressive sensing [47] with comparable numerical results. The sparse set of basis functions obtained by any adaptive algorithm is further denoted for the sake of clarity as \mathcal{A} .

2.2. Estimation of approximation error

Once the PCE is constructed, it is crucial to estimate its accuracy. Further, the accuracy of PCE can be used for the direct comparison among several PCEs in order to choose the best surrogate model. Therefore it is beneficial to use methods which do not need any additional sampling of the original mathematical model. A common choice is the coefficient of determination R^2 , which is well known from machine learning. However, R^2 may lead to overfitting and thus advanced methods should be used. One of the most utilized methods for measuring the performance of the learning algorithm in recent years is the leave-one-out cross validation error Q^2 . This statistic is based on residuals between the original surrogate model and the surrogate model built with the ED while excluding one realization. This approach is repeated for all realizations in the ED and the average error is estimated. Although the calculation of Q^2 is typically highly time-consuming, it is possible to obtain results analytically from a single PCE as follows [48]

$$Q^2 = 1 - \frac{\frac{1}{n_{\text{sim}}} \sum_{i=1}^{n_{\text{sim}}} \left[\frac{g(\mathbf{x}^{(i)}) - g^{\text{PCE}}(\mathbf{x}^{(i)})}{1 - h_i} \right]^2}{\sigma_{Y, \text{ED}}^2}, \quad (12)$$

where $\sigma_{Y,ED}^2$ is a variance of experimental design calculated using the original mathematical model and h_i represents the i th diagonal term of matrix $\mathbf{H} = \Psi (\Psi^T \Psi)^{-1} \Psi^T$.

2.3. Statistical moments derived from PCE

The specific form of PCE together with the orthogonality of the polynomials allows for a powerful and efficient post-processing. Once a PCE approximation is created, it is possible to obtain statistical moments of the QoI. Generally, its raw statistical moment of the m th order is defined as

$$\begin{aligned} \langle Y^m \rangle &= \int [g(X)]^m p_X(X) dX = \int \left[\sum_{\alpha \in \mathbb{N}^M} \beta_\alpha \Psi_\alpha(\xi) \right]^m p_\xi(\xi) d\xi \\ &= \int \sum_{\alpha_1 \in \mathbb{N}^M} \dots \sum_{\alpha_m \in \mathbb{N}^M} \beta_{\alpha_1} \dots \beta_{\alpha_m} \Psi_{\alpha_1}(\xi) \dots \Psi_{\alpha_m}(\xi) p_\xi(\xi) d\xi \\ &= \sum_{\alpha_1 \in \mathbb{N}^M} \dots \sum_{\alpha_m \in \mathbb{N}^M} \beta_{\alpha_1} \dots \beta_{\alpha_m} \int \Psi_{\alpha_1}(\xi) \dots \Psi_{\alpha_m}(\xi) p_\xi(\xi) d\xi. \end{aligned} \quad (13)$$

As can be seen from the final part of the formula, in case of PCE, it is necessary to integrate only over the basis functions (orthonormal polynomials), which leads to a dramatic simplification in comparison to the integration of the original mathematical function. Moreover, it is also possible to write an analytical expression of the integral in several cases. Specifically, the first statistical moment (mean value) is obtained as

$$\mu_Y = \langle Y^1 \rangle = \int \left[\sum_{\alpha \in \mathbb{N}^M} \beta_\alpha \Psi_\alpha(\xi) \right] p_\xi(\xi) d\xi = \sum_{\alpha \in \mathbb{N}^M} \beta_\alpha \int \Psi_\alpha(\xi) p_\xi(\xi) d\xi. \quad (14)$$

Considering the orthonormality of the polynomials

$$\int \Psi_\alpha(\xi) p_\xi(\xi) d\xi = 0 \quad \forall \alpha \neq 0, \quad \Psi_0 \equiv 1,$$

it is possible to obtain the mean value directly from the PCE deterministic coefficients. Namely, the mean value is equal to the first deterministic coefficient of the expansion

$$\mu_Y = \langle Y^1 \rangle = \beta_0. \quad (15)$$

The second raw statistical moment, $\langle Y^2 \rangle$, is written as

$$\begin{aligned} \langle Y^2 \rangle &= \int \left[\sum_{\alpha \in \mathcal{A}} \beta_\alpha \Psi_\alpha(\xi) \right]^2 p_\xi(\xi) d\xi = \sum_{\alpha_1 \in \mathcal{A}} \sum_{\alpha_2 \in \mathcal{A}} \beta_{\alpha_1} \beta_{\alpha_2} \int \Psi_{\alpha_1}(\xi) \Psi_{\alpha_2}(\xi) p_\xi(\xi) d\xi \\ &= \sum_{\alpha \in \mathcal{A}} \beta_\alpha^2 \int \Psi_\alpha(\xi)^2 p_\xi(\xi) d\xi = \sum_{\alpha \in \mathcal{A}} \beta_\alpha^2 \langle \Psi_\alpha, \Psi_\alpha \rangle. \end{aligned} \quad (16)$$

Considering again the orthonormality of the polynomials, defined by the inner product in Eq. (3), it is possible to obtain the variance $\sigma_Y^2 = \langle Y^2 \rangle - \mu_Y^2$ as the sum of all squared deterministic coefficients except the intercept (which represents the mean value), i.e.

$$\sigma_Y^2 = \sum_{\substack{\alpha \in \mathcal{A} \\ \alpha \neq 0}} \beta_\alpha^2. \quad (17)$$

Note that, higher statistical central moments skewness γ_Y (3rd moment) and kurtosis κ_Y (4th moment) need precomputing of the triple and quadruple products.

In the following, we select the variance of the output variable, i.e. σ_Y^2 in Eq. (17), as the *target characteristic* of Y and we focus on development of the sequential sampling strategy in order to estimate this variance as accurately as possible at any stage of PCE build. The reason for selection of variance is that we expect a monotonic relationship between function *variation* in the sense of Hardy and Krause [49] and its *variance*. As will be shown below, Eq. (16) can be modified in order to obtain the local contribution to variance. We conjecture that it is therefore

important to place samples densely in regions of large local variance and sparsely in regions of small local variance, in order to obtain a near-optimal sample [37]. This arrangement of samples may decrease the error of the function approximation and its integral.

3. Sampling methods

Assuming a non-intrusive approach for calculation of the PCE coefficients using OLS defined in Eq. (9), it is necessary to create an ED containing n_{sim} realizations of the input random vector and the vector of corresponding results of the original mathematical model. Typically we consider sampling of ξ using its density f_{ξ} , which represents the distribution according to the Wiener–Askey scheme. For the M -dimensional Legendre polynomials this means sampling uniformly from the M -dimensional hypercube $[-1, 1]^M$ and for M -dimensional Hermite polynomials, it corresponds to sampling from the M -dimensional Gaussian distribution with independent standardized Gaussian marginal distributions. Naturally, it is crucial to use an efficient sampling scheme for the DoE of ξ in order to obtain accurate results for a given computational budget.

DoE has been an area of interest for many researchers since the beginning of uncertainty quantification and structural reliability. The most simple but generally applicable method is crude Monte Carlo Sampling (MC), i.e. a method associated especially with robust (and inefficient) numerical integration. In standard Monte Carlo integration, the important condition of integration being unbiased is that the sample is selected *uniformly* and *independently* with respect to the target density. In MC the sampling points are selected independently of each other and therefore, clusters of points emerge randomly as well as regions which are not covered by any point.

There has been considerable effort spent on improving the spatial arrangement of points in a sample. The Koksma–Hlawka inequality [49], which was developed to predict an upper bound of integration error, motivates the decrease in *discrepancy* of the sample set (ED). Discrepancy in a way measures *uniformity* of a point set, i.e. the difference between the desired uniform distribution and the empirical distribution of the point set. Such uniformity of point distribution may be useful also for initial screening or building a surrogate model. Low discrepancy can be achieved either by direct minimization of a suitable discrepancy measure [17,50–52] or simply by using various Quasi Monte Carlo sequences mentioned in the Introduction section. Quasi Monte Carlo sequences are deterministic point sets and they allow for sequential addition of points one-by-one while retaining an optimal rate of star discrepancy decrease with increasing sample size [53].

Another branch of research focuses on variance reduction techniques such as *importance sampling* which place points according to a predefined or adaptively adjusted *sampling* density which can be different from the target density or methods of stratified selection of sampling points that improve spatial arrangement of the sampling points. One of the most widely used techniques is Latin Hypercube Sampling (LHS) first suggested by Conover [14]; see also [54]. LHS specifically has the effect of reducing variance associated with the additive components of a transformation. Hence, for functions that are dominated by the main effects of the individual variables, LHS will significantly reduce variance. For functions with significant variable interactions, it is less effective. [55–58].

Another important aspect of sample selection for DOE is the uniformity of filling of the design domain. This aspect is important for *function approximation* and resulted in the seminal works on *space-filling* criteria based on mutual distances among points: the Maximin and miniMax criteria [15]. These criteria prefer designs without point clusters or without large empty areas. A generalization of the Maximin criterion to the phi-criterion [16] was presented along with a heuristic construction algorithm that can be combined with the LHS strategy. Similarly, the miniMax criterion can be generalized [59]. Moreover, the recently developed *periodic* versions of the whole class of distance-based criteria [17,60] guarantee *statistically uniform* distribution of points along with *even point distribution* within each single design. These distance-based criteria can be employed for direct design optimization.

Uniformity of ED and space-filling criteria are important characteristics to obtain a quality ED for PCE. The LHS thus typically leads to more accurate estimation of β in comparison to crude MC [61,62]. Sampling for PCE, however, might be motivated by additional criteria of optimality than the space-filling property, discrepancy or statistical uniformity with respect to the target distribution. The optimality criterion should consider aspects related to the particular method of identification of the polynomial modes and their coefficients.

This naturally leads to sampling from a probability measure different from the input distributions, which minimize a selected characteristic of the ED. Moreover, it is also necessary to modify the basis functions in order to preserve orthonormality of the data matrix. Minimizing the coherence parameter of a PCE basis functions [63] leads to the coherence optimal and related asymptotic sampling [27], which is theoretically more efficient in comparison

to standard sampling based on the input distribution. Similarly the Christoffel sparse approximation [64] was derived using a different definition of the coherence parameter. Note that these sampling strategies are derived for a specific purpose (non-intrusive PCE) and thus their efficiency in general probabilistic analysis might be unsatisfying. Although coherence optimal sampling is more computationally demanding, it is not a crucial problem in engineering, where the calculation of mathematical models takes the largest part of the whole process.

Also, it would be optimal if the PCE that has been set at any stage of sampling based on the available information about the samples and the corresponding function values $g(\mathbf{x})$, can propose the new sampling point (sample size extension). With such an algorithm at hand, one can build the PCE approximation incrementally while exploiting all the knowledge available so far. For efficient accurate exploitation, it is necessary to use an adaptive algorithm for PCE construction (by *adaptive* we mean selection of the most important combinations of modes in the index set \mathcal{A}). There are several methods for adaptive selection of the optimal PCE basis functions such as LAR [45] employed in numerical experiments. The selected basis functions are further used for the process of exploitation and thus it is crucial to identify new basis functions in every iteration of the sequential sampling in order to obtain the best possible location for a new sampling point. Moreover, the adaptivity of the basis functions is important for the accurate coherence optimal sampling briefly described in the following paragraphs.

3.1. Coherence-optimal sampling

Generally, it is beneficial to take all pieces of information about the given mathematical task into account in order to choose a correct methodology. Although standard sampling based on the input distribution is suitable for any probabilistic analysis, there are more efficient methods developed specifically for PCE solved by over-determined OLS [27], which is employed in this paper.

Coherence-optimal sampling constructs a new sampling measure minimizing a coherence parameter associated with stability and convergence of the PCE solved by OLS. The coherence parameter $\mu(Y)$ is defined as [65]

$$\mu(Y) := \sup_{\xi} \sum_{j=1}^P |w(\xi)\psi_j(\xi)|^2, \quad (18)$$

where the weight function $w(\xi)$ is

$$w(\xi) := \frac{P}{B(\xi)}. \quad (19)$$

The analytical expression of $B(\xi)$ is generally not available, but it is possible to evaluate its value for arbitrary ξ as

$$B(\xi) = \sqrt{\sum_{j=1}^P |\psi_j(\xi)|^2}. \quad (20)$$

Finally, the coherence-optimal probability measure is defined as

$$f_{\text{coh}}(\xi) := P^{-1} f(\xi) B^2(\xi). \quad (21)$$

In order to sample from $f_{\text{coh}}(\xi)$ one may use Markov Chain Monte Carlo (MCMC) [65]. The proposal distribution for MCMC is suggested for case when $p \leq M$ where one should use standard sampling from distributions naturally orthogonal to the employed polynomial basis as already described for standard sampling. If $p \geq M$, samples should be independently drawn from a uniform distribution on a M -dimensional ball of radius $\sqrt{2}\sqrt{2p+1}$ for Hermite polynomials, and a M -dimensional Chebyshev distribution for Legendre polynomials.

Note that the coherence-optimal sampling does not generally lead to the orthonormal columns of the data matrix and the deviation $\langle \Psi_{\alpha_1}, \Psi_{\alpha_2} \rangle - \delta_{\alpha_1\alpha_2}$ may be significant. Therefore, one has to apply a weight function $w(\xi)$ to the basis functions and use weighted least squares in order to estimate β using coherence-optimal sampling as described in previous paragraphs. Weighted least squares method is a special case of generalized least squares containing only diagonal members of the correlation matrix of residuals. Optimal values of the deterministic coefficients is then obtained by solution of the following system of equations:

$$\mathbf{W} \Psi \beta \approx \mathbf{W} \mathcal{Y}, \quad (22)$$

where matrix \mathbf{W} is a diagonal matrix with $W_{i,i} = w(\xi^{(i)})$.

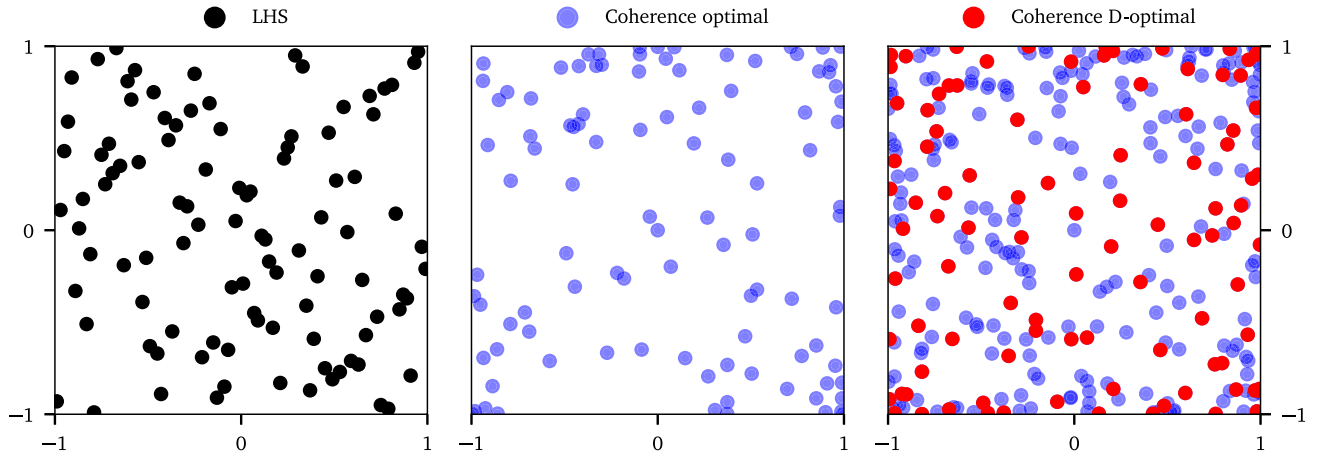


Fig. 1. An ED containing 100 samples generated by LHS, coherence-optimal sampling and coherence D-optimal sampling for Legendre polynomials.

3.2. D-optimal experimental design

Optimality of the ED for OLS can also be measured by the so-called alphabetic criteria of the information matrix $\mathcal{I} := \frac{1}{n_{\text{sim}}} \Psi^T \Psi$, which is crucial for stability of OLS. There are several types of criteria focused on various characteristics of the information matrix; see [62] for a review of criteria in the context of PCE. Although one of the most promising is the S-optimal criterion [35], it is also highly computationally demanding especially for large M . Therefore, in this paper we use the following cheaper and well known estimation-oriented criterion D-optimal design, which is focused on accurate estimation of β .

Since the PCE basis functions are orthonormal, \mathcal{I} is on average identity, but for finite sample size n_{sim} there is a deviation from the identity matrix

$$\|\mathcal{I} - \mathbf{I}\| > 0. \quad (23)$$

The D-optimal design, obtained by maximizing the determinant of the information matrix, leads to small deviation and thus stable estimation of β . For the practical construction of D-optimal ED, it is possible to employ Fedorov exchange algorithm [66], greedy algorithm [67] or rank revealing QR decomposition [68] to find an optimal information matrix containing n_{sim} rows out of a candidate pool containing $n_{\text{pool}} \gg n_{\text{sim}}$ rows.

3.3. Coherence D-optimal experimental design

As originally proposed together with coherence optimal sampling [68], it is beneficial to merge the previous two techniques in order to obtain a *Coherence D-optimal* (Coh D-opt) ED for the stable and accurate solution of WLS. Although Coh D-opt was originally proposed for compressed sensing in the context of PCE [68], D-optimality was already employed in combination with standard sampling (LHS and MC) for OLS and LAR in [35]. Therefore, Coh D-opt can similarly be used also for the non-intrusive approach based on WLS and LAR as employed in this paper. The pool of candidates is generated by coherence optimal sampling and further reduced by D-optimality criterion which leads to uniform ED without clusters of samples as can be seen in Fig. 1.

4. Adaptive sequential sampling

In industrial applications, it is often not feasible to perform a large number of evaluations of the original mathematical model (e.g. FEM) and thus it is important to reduce the number of simulations as much as possible. An efficient approach therefore is *adaptive sequential sampling*, which uses iterative selection of the new sampling points according to specific criteria while exploiting the already available information. Although general sequential sampling is an area of interest for many researchers [69–72], there is still a lack of studies focused specifically on PCE. The recent study [35] compared several simple sequential sampling methods based on D/S-optimality of samples or maximin criterion of samples.

Note that there are two different strategies for sequential sampling. The first is to enrich the initial ED according to a space-filling criterion (exploration) without assuming any knowledge of the mathematical model or PCE form; see e.g. [71,73]. The motivation is clear: we do not want to locate an augmented point very close to an existing point to avoid getting redundant information in the nearby region. However, by obtaining data sequentially, it is possible to learn from the early stages to inform subsequent data collection, minimize wasted resources, and provide answers for various objectives (exploitation). Therefore, the second strategy works with the structure of the PCE (basis functions) in order to identify an optimal sample. Unfortunately, in situations when the initial screening overlooks a globally important region, the exploitation criterion may continue refinement of some other, locally important region that was detected, and there is a risk of never discovering a globally important region. Therefore, it is beneficial to include a balance between both criteria in search for a suitable candidate. Note that, such approach was employed e.g. in [37] in a different context: a criterion motivated by the Koksma–Hlawka inequality [49] was proposed and coupled with stratified sampling in order to improve the efficiency of statistical integration.

As discussed above, the *adaptivity* feature of the PCE surrogate model can be ensured by any model selection algorithm. Moreover, it can be combined also with hyperbolic truncation according to Eq. (8), which is efficient for high P . A general adaptive sequential algorithm thus should adaptively reconstruct the PCE using model selection algorithms in order to identify a sparse set of basis functions \mathcal{A} in each iteration.

The *sequential* feature can be added by using a comparison criterion for selection of the best candidate from a pool of candidates while balancing between exploration and exploitation. *Exploitation* of the local areas of the design domain is focused on identification of sub-domains associated with a defined characteristic of the mathematical model such as high gradient, local maxima etc. The candidates from the identified sub-domains are further preferred. Another typical example can be identification of sub-domains associated with high variation of the mathematical model. Although exploitation is a powerful technique for identification of the best candidate, it is typically based on a built surrogate model and thus it is highly dependent on the quality of a given ED. On the other hand, *exploration* assures uniform coverage of the whole design domain, possibly with respect to specific characteristic as in case of alphabetical optimality [74], and it assures that the algorithm does not get stuck in local minima. It opens the door to detection and exploration of important areas in design domain, where the behavior of the studied function $g(\mathbf{x})$ might be significantly different from possibly incorrect expectation based on the surrogate.

4.1. The proposed Θ criterion for sequential sampling

We propose an adaptive sequential sampling strategy accompanied by a criterion designed for efficient and accurate estimation of β using least squares. Consider a pool of candidates containing n_{pool} realizations of the random vector ξ generated by an arbitrary sampling technique. Once the pool of candidates conditioned by the selected PCE basis is generated, it is necessary to construct a criterion for the selection of the best candidate balancing between the exploitation and exploration of the design domain. Such criterion, called the Θ criterion from here on, is proposed as follows

$$\Theta(\xi^{(c)}) \equiv \Theta_c = \underbrace{\sqrt{\sigma_{\mathcal{A}}^2(\xi^{(c)}) \cdot \sigma_{\mathcal{A}}^2(\xi^{(s)})}}_{\text{ave variance density}} \underbrace{l_{c,s}^M}_{\text{vol.}} \equiv \sqrt{\sigma_c^2 \cdot \sigma_s^2} l_{c,s}^M. \quad (24)$$

where we introduce an abbreviated notation by dropping the point designation $\xi^{(c)}$ and using simply the lower index instead and also by dropping the set of basic functions, \mathcal{A} , which is selected for every instant of the algorithm and thus may differ as the sample size increases. The criterion has an intuitive meaning and also has units of *variance* and is a product of two parts: the exploitation part (denoted as “ave variance density”) and the exploration part (the distance term $l_{c,s}$ raised to the domain dimension). Multiplication of these two independent contributions maintains the optimal balance between exploration and exploitation.

The *exploration* aspect is maintained by accounting for the distance $l_{c,s}$ between a candidate $\xi^{(c)}$ and its nearest neighboring point from the existing ED, $\xi^{(s)}$. For the distance term a suitable metric must be selected. In this paper, we select the Euclidean distance between the candidate and its nearest neighbor as

$$l_{c,s} = \sqrt{\sum_{i=1}^M |\xi_i^{(c)} - \xi_i^{(s)}|^2}, \quad (25)$$

although other distances can be considered, particularly in high dimension.

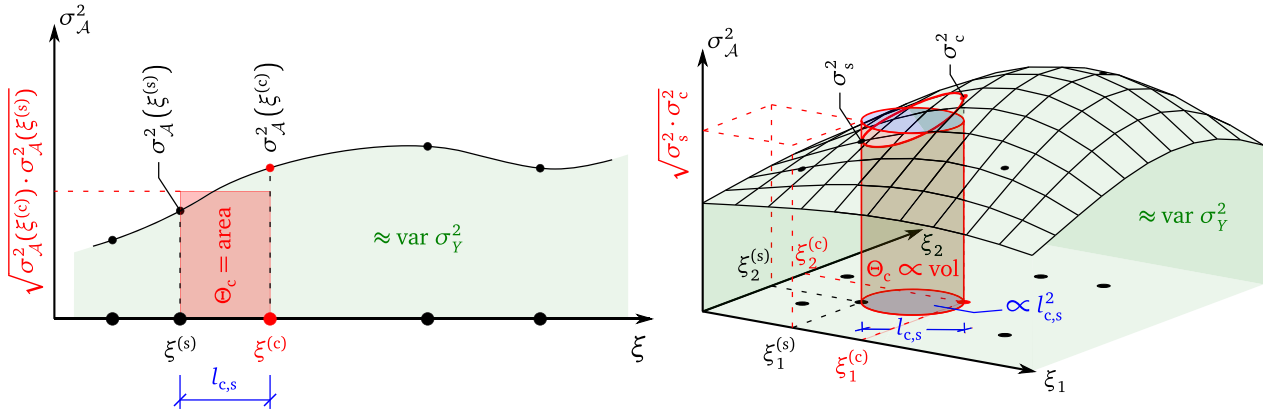


Fig. 2. Geometrical meaning of the proposed Θ criterion for a candidate “c” in two and three dimensions. Black solid circles are existing points and point “s” is the nearest neighbor to candidate “c”. The solid thin curve/surface represents the current estimation of variance density over the design domain.

The *exploitation* in candidate selection is motivated by our desire to *uniformly cover local contributions to the total variance*, σ_Y^2 . By recalling Eq. (17), we know that σ_Y^2 can be estimated simply as the sum of all squared deterministic coefficients except the intercept. The mean square can be obtained as the integral featuring the selected polynomial basis over the design domain; see Eq. (16). This means that the variance can be thought of as an integral of local contributions over the design domain indexed by coordinates ξ . In other words, we need to integrate a local *variance density* $\sigma_A^2(\xi)$. Once the PCE has been established at any given stage of the algorithm, the variance density is computationally cheap to evaluate for any location ξ as

$$\sigma_A^2(\xi) = \left[\sum_{\substack{\alpha \in \mathcal{A} \\ \alpha \neq 0}} \beta_\alpha w(\xi) \Psi_\alpha(\xi) \right]^2 p_\xi(\xi). \tag{26}$$

The local variance is therefore estimated based on the basis functions and coefficients β of the PCE. Depending on technique utilized for sampling of candidates, one should apply the weight $w(\xi)$ (also used in weighted least squares) to basis functions in order to reflect influence of sampling from a probability measure different from the input distribution. Specifically in this paper, $w(\xi)$ is defined for Coh D-opt according to Eq. (19) and $w(\xi) = 1$ for LHS. When considering a candidate “c”, one might think about the variance contribution of the region between the candidate and its nearest neighbor. A rough estimation may be obtained by considering an average of local variance densities between the candidate and its nearest neighbor, “s”. This average is represented by the *geometric mean* between the two numbers. The geometric mean between n numbers x_i is defined as $(\prod_{i=1}^n x_i)^{1/n}$ and therefore, we take the geometric mean of two local variance densities simply as the square root of the local variance densities of the candidate and its nearest neighbor, see the first term in Eq. (24). When this geometric mean is multiplied by the M th power of the distance between the two points, $l_{c,s}^M$, the volume (variance contribution) of a neighborhood between them is estimated; see the sketch in Fig. 2. In other words, the criterion estimates the amount of variance in a “bite” by the candidate. Note that Eq. (24) defines the bite as a hypercube of side-length $l_{c,s}$. However, other geometric entities may be considered without practical impact on the algorithm. The reason is that all the geometric volumes for various candidates under comparison would have the same positive multiplier of $l_{c,s}^M$ which can be dropped as it does not change the ranking of the compared candidates. Therefore, we can say that the proposed criterion helps to select a candidate with roughly the largest amount variance being refined. The balance between exploration and exploitation is maintained: a candidate which is close to an existing point can only be selected if the corresponding variance density is large. Similarly, when a region with low contribution is being detected by the PCE, candidates from such regions are ignored.

In situations when the variance density is a constant function, the criterion collapses to a simple space-filling criterion (a form of miniMax criterion); [15,60]. Such criterion ensures the preference of candidates filling the largest empty regions in the design domain and thus leading to uniform distribution of points in the sense of miniMax design criterion. We remark that miniMax design is a preferable choice for the construction of emulators because it minimizes the worst case prediction variance.

A question may arise: why do we propose to use the geometrical mean instead of arithmetical mean? The reason is that the criterion may also be used for infinite design domains (for example in conjunction with Gaussian germ). In such situation, the pool of candidates may contain points $\xi^{(c)}$ that are very far from the mean value and such a point may have (almost) zero variance density. Yet, the criterion would prioritize it due to the large distance from the nearest neighbor $\xi^{(s)}$ as the arithmetical average with its variance density would equal one half of the two local densities. In other words, infinitely distant candidate points would always win the comparison, despite a vanishing contribution of one of them. Using the geometrical mean prevents unimportant distant points with zero density from being selected.

Maximization of the criterion leads to the best candidate, which is added to active ED. As can be seen, the proposed criterion prefers candidate points in parts of multidimensional space associated with higher contribution to the variance of the mathematical model. This idea is similar to the sequential sampling proposed in [37] based on Koksma–Hlawka inequality respecting both variation of the function and discrepancy of realizations, however the proposed criterion is constructed specifically for PCE and thus it can use the PCE basis functions in order to increase the efficiency of the computation. The significant advantage of the proposed method is the ability to add candidates into existing ED one-by-one and thus it can be employed at any moment of the PCE construction process and it can be combined with any sampling algorithm for construction of initial ED marked with subscript as ξ_{ED} , \mathbf{W}_{ED} , \mathcal{Y}_{ED} .

4.2. Adaptive sequential sampling with LHS-based candidates

LHS represents perhaps the most common sampling technique in surrogate modeling and it can be easily coupled with the proposed sequential sampling in a simple manner. The pool of candidates is generated by LHS and the proposed criterion is employed for the selection of the best candidate. This process is repeated at every iteration of the sequential sampling (with the pool being either regenerated or reused from the preceding step). In order to illustrate the proposed sequential adaptive algorithm, we selected five iterations and depict the corresponding states in Fig. 3. The initial ED is represented by solid black circles and the sequentially selected realizations are plotted using solid red circles. The color maps represent the value of the proposed criterion (right column) and also its individual components (the preceding columns). Since the generation of the pool of candidates by LHS is simple and fast, LHS-based adaptive sequential sampling represents an efficient extension to non-sequential LHS and it could be easily implemented into existing software tools.

4.3. Adaptive sequential sampling with coherence-based candidates

The proposed criterion can generally be coupled with any sampling technique. However, since coherence-based sampling is highly affected by the set \mathcal{A} , it might be ideal if the pool of candidates is generated by coherence-based sampling. Further, in order to obtain stable estimates of β , the pool of candidates should be reduced using D-optimality criterion calculated by QR factorization with column pivoting [68] also called rank revealing QR factorization (RRQR). Note that it is necessary to evaluate the proposed criterion for every candidate and thus it might be computationally demanding for large n_{pool} . Therefore, we propose to generate the pool of candidates by coherence D-optimal sampling in every loop of sequential sampling instead of a single large pool generated before the start of the iteration process. Smaller pools for every iteration are not only computationally efficient but such approach reflects the actual sparse set of basis functions of PCE obtained by LAR in each iteration. This might be crucial for the candidate set generated by coherence-based sampling, since it is optimized for the selected basis functions in each step. Moreover, the proposed criterion gives higher importance to basis functions associated to higher β , which is important for identification of functional extremes.

Algorithm 1 thus reflects all pieces of information about the stochastic model (probabilistic distribution of input variables), investigated mathematical model (sparse set of basis functions) and even type of solver for PCE construction (weighted least squares) in order to obtain accurate and stable estimates of the deterministic PCE coefficients β . Combination of all techniques used in the algorithm thus leads to superior performance as will be shown in the numerical examples. However, generation of the pool of candidates is much more computationally demanding in comparison to the LHS-based adaptive sequential sampling.

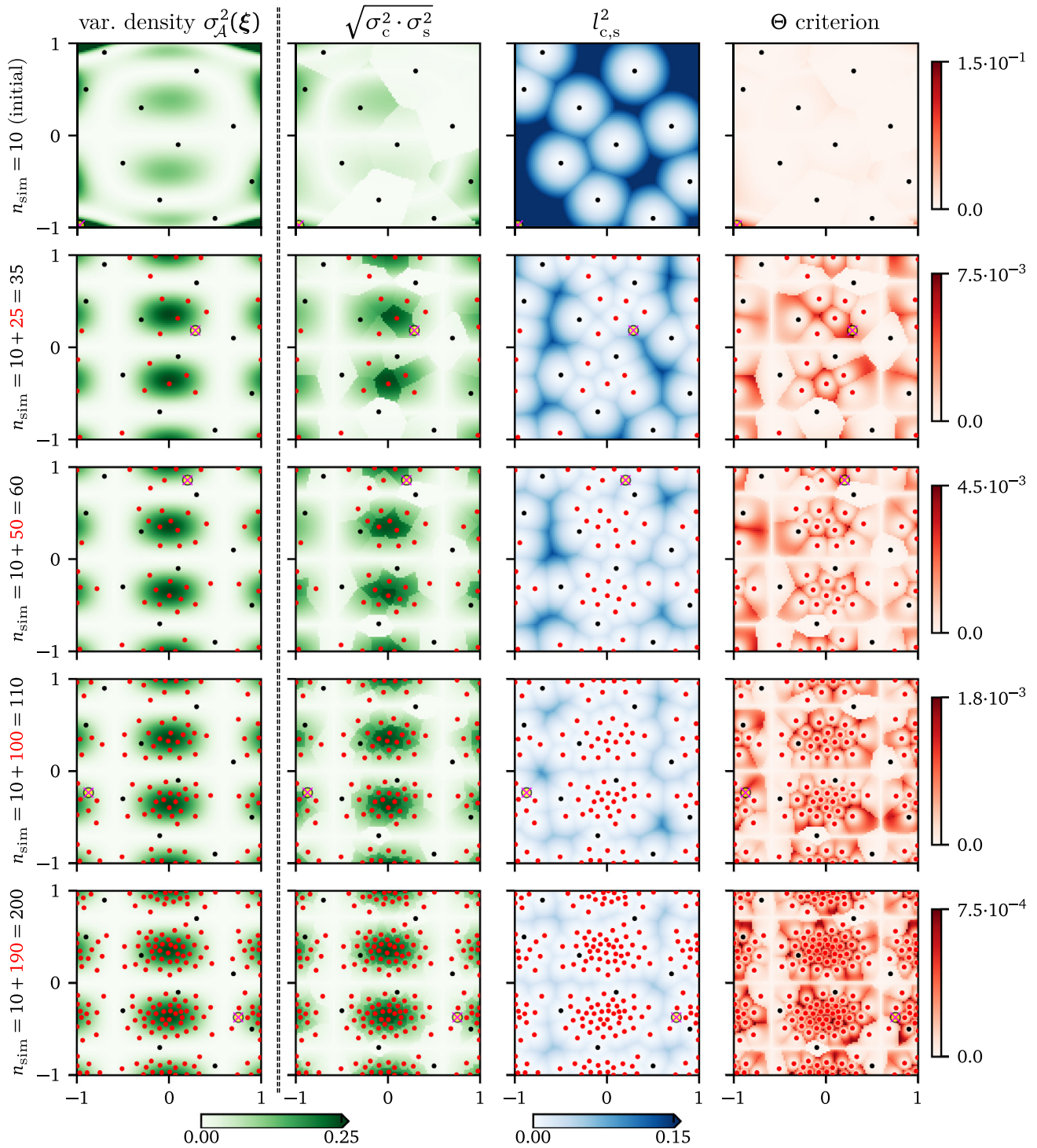


Fig. 3. Illustration of five stages during the proposed sequential sampling. Black solid circles: initial design. Red circles: extended sample. Crossed empty circle: the best candidate. The value of the proposed criterion and its components are depicted using the underlying color maps. (For interpretation of the references to color in this figure legend, the reader is referred to the web version of this article.)

5. Numerical experiments

The proposed algorithm was numerically tested on several examples of increasing complexity. The setup common to all examples was as follows: PCE is solved by non-intrusive OLS (LHS) or WLS (Coh D-opt), a sparse set of the basis functions \mathcal{A} is obtained by LAR with maximum total polynomial order $p = 10$, if not said otherwise.

Algorithm 1 Coherence-Based Adaptive Sequential Sampling — one iteration

Input: $\xi_{ED}, \mathbf{W}_{ED}, \mathcal{Y}_{ED}, \mathcal{A}, \beta, (n_{sim})$ 1: $n = 5P, n_{pool} = 3P$ 2: $\xi_{coh} \leftarrow n$ samples from $f_{coh}(\xi)$ using MCMC (Eq. (21)) 3: $\mathbf{W}_{coh} \leftarrow$ weights corresponding to ξ_{coh} (Eq. (22)) 4: $\xi_{pool}, \mathbf{W}_{pool} \leftarrow n_{pool}$ D-optimal samples & weights 5: for all $\xi^{(c)} \in \xi_{pool}$ do 6: $\xi^{(s)} \leftarrow \arg \min_{\xi \in \xi_{ED}} l_{c,s}(\xi^{(c)}, \xi)$ 7: $\theta_c = \theta(\xi^{(c)}, \xi^{(s)})$ 8: end for 9: $\xi^{(new)} \leftarrow \arg \max_{\xi^{(c)}} \theta_c$ Output: $\xi^{(new)}, w(\xi^{(new)})$	current Experimental Design and the corresponding PCE set the pool sizes based on the p and M draw points from the coherence density calculate the corresponding weights preselect the final pool of candidates loop thru all candidates find the nearest neighbor compute the criterion (Eq. (24)) select the best candidate return the best candidate and the corresponding weight
--	---

Identical p for all examples simulates a possible engineering situation with a black-box function (e.g. finite element analysis) where it is not possible to select the best p a priori. The initial ED for the PCE construction before the first step of the proposed iterative algorithm is generated by LHS and it contains an initial screening design with $n_{sim} = 10$ realizations of the input random vector for the first three examples and $n_{sim} = 20$ for the last example.

Although the proposed criterion can be coupled with any sampling technique for ED generation, only two selected techniques (LHS and Coh D-opt) were employed and compared in the numerical examples. LHS was selected for this study as it is the most common sampling technique for surrogate modeling due to its efficiency and simplicity. Existing software applications and packages for PCE construction (e.g. [39–43]) usually contain implementation of LHS and thus the process can be easily extended by proposed selection criterion. On the other hand, Coh D-opt is not a common approach, thus it is representative of advanced sampling methods suited specifically for least-squares PCE. Coh D-opt EDs usually achieve higher accuracy but their implementation is not straightforward.

Each example is solved by three types of strategies:

- non-sequential approach (non-seq) with ED generated via LHS for each sample size at once — this represents the most common approach employed in surrogate modeling,
- the proposed sequential sampling with candidates generated by LHS, and
- the proposed sequential sampling with candidates generated by Coh D-opt.

The sample size in the first (LHS) strategy is fixed and we study the PCE behavior for a range of these sample sizes selected a priori.

The two sequential sampling strategies differ in the way the pool of candidates is proposed. For the sake of clarity, the pool of candidates obtained by Coh D-opt for sequential sampling contains $3P$ D-optimal samples, which are selected from a greater pool of $5P$ Coh-optimal samples; for LHS sequential sampling, it contains $3P$ samples generated by LHS.

The results are compared in terms of the (i) *relative error in variance* of QoI

$$\epsilon = \frac{|\sigma^2 - \sigma_Y^2|}{\sigma_Y^2}, \quad (27)$$

defined as the absolute deviation of the estimated variance σ^2 from the exact value σ_Y^2 divided by the exact variance, and the (ii) *leave-one-out error* of PCE approximation Q^2 according to Eq. (12). In order to get a picture about reproducibility of the results, the calculations were repeated 100 times for each set of settings. The averages of $\log_{10}(\epsilon)$ (the order of relative error in variance) and $\log_{10}(1 - Q^2)$ are depicted by solid-lines and the scatters represent $\pm \sigma$ confidence intervals.

5.1. Toy 2D function

Consider a simple 2D function in which the two independent input random variables are uniformly distributed, $\mathbf{X} \sim \mathcal{U}$, with the mean values $\boldsymbol{\mu} = \{0, 0\}$ and variances $\boldsymbol{\sigma}^2 = \{6, 6\}$. The design domain is thus a square $[-\sqrt{18}; \sqrt{18}]^2$. The output variable (symmetrical and highly non-normal with zero mean value and skewness) is the following transformation

$$Y = \cos\left(\frac{X_1\pi}{5}\right) \sin\left(\frac{X_2\pi}{3}\right), \quad [\sigma_Y^2 \approx 0.199\,575\,434] \quad (28)$$

which should be easily approximated by all employed methods and the whole process is easily tractable.

Non-sequential LHS was calculated for 10 increasing sample sizes in range (24, 150). The supposedly uniform distribution of LH-samples is compared with the proposed algorithm for sequential selection of 140 candidates (to reach the same final sample size of 150 points). The rows in Fig. 3 show selected iterations of the sequential algorithm. The color maps show the local variance density (left column), and then spatial distribution of the two components of the proposed criterion: the average variance computed using the geometrical mean with the nearest neighbor and the squared distance to the nearest neighbor. The maps on the right hand side finally present the spatial distribution of the proposed Θ criterion. A relatively large pool of LHS candidates was generated and the color maps were computed on a fine grid of coordinates. The scale of Θ in the rightmost column is proportional to the amount of variance associated with individual candidates. It can be seen that the value Θ of the best candidate also indicates how much gain in the variance accuracy can be expected by adding one point. This information can be incorporated as a kind of “stopping criterion”. The scales in Fig. 3 show that refining from $n_{\text{sim}} = 10$ to $n_{\text{sim}} = 35$ decreases the variance bites from 10^{-1} to roughly $7.5 \cdot 10^{-3}$. However, further increase in sample size (and the associated time spent on evaluation of the $g(\mathbf{x})$ function) leads only to minor decrease in Θ criterion for the best candidate and this improvement may not be deemed as worth the expense.

This reasoning is well supported by the plots of variance error in Fig. 4 (left column). One can see that from the ED with $n_{\text{sim}} \approx 25$ points, further decreases in variance error are obtained at low rates. This is emphasized by a thin vertical dashed line showing that the available polynomial basis is saturated as the maximum polynomial order is exhausted. The decision to consider is either (i) stop the algorithm: the accuracy is acceptable or computing resources are too expensive (ii) increase the maximum polynomial order p with a chance to improve the convergence rate for further size extensions. Indeed, one can see in Fig. 4 (left column, bottom plot) that after adding about 15 points to the initial design with 10 points, the maximum polynomial degree of $p = 10$ gets almost always fully exploited and the error almost stabilizes (both the error in variance estimation and also the Q^2). When the experiment is repeated with $p = 20$ (see the middle column in Fig. 4), the saturation is postponed and both errors quickly decrease until the design reaches about $n_{\text{sim}} = 120$ points. This fact documents that the adaptivity feature should also increase the polynomial degree if higher accuracy is requested.

To conclude, the proposed sequential sampling clearly outperforms standard non-sequential sampling in error in estimated variance. Although difference in the approximation error Q^2 between non-seq and sequential LHS is not significant for $p = 10$, its sequential variant leads to the most accurate estimation of variance. In case of $p = 20$, the superiority of the sequential sampling is even more significant.

For the sake of completeness, the adaptivity of p was coupled with the proposed sequential sampling (see the right column in Fig. 4). Although there exist advanced adaptive algorithms such as adaptive Coh-D opt [75], the simplest algorithm with iterative increment of p was employed for both sampling schemes, i.e. p was iteratively increased from $p = 5$ to $p = 20$ and PCE was built for a given ED and finally p yielding the lowest approximation error measured by Q^2 was selected. The obtained results show the similar behavior of the sequential technique as in case of $p = 20$, as can be expected. Note that, techniques for p -adaptivity and many other advanced sampling techniques are beyond the scope of this paper. This research is focused on the proposed sequential sampling and for the possibility of direct comparison, such type of adaptivity is excluded in the following examples in order to show purely the role of Θ criterion, though they can generally lead to more accurate approximations.

5.2. Ishigami function

Consider now a three-dimensional Ishigami function [76]. The function is strongly nonlinear, non-monotonic and presents strong interactions. We set the coefficients as in [77]. Let $\mathbf{X} \sim \mathcal{U}[-\pi, \pi]^3$ and the mathematical model

$$Y = \sin(X_1) + 7 \sin^2(X_2) + 0.1 X_3^4 \sin(X_1). \quad [\sigma_Y^2 \approx 13.844\,587\,940] \quad (29)$$

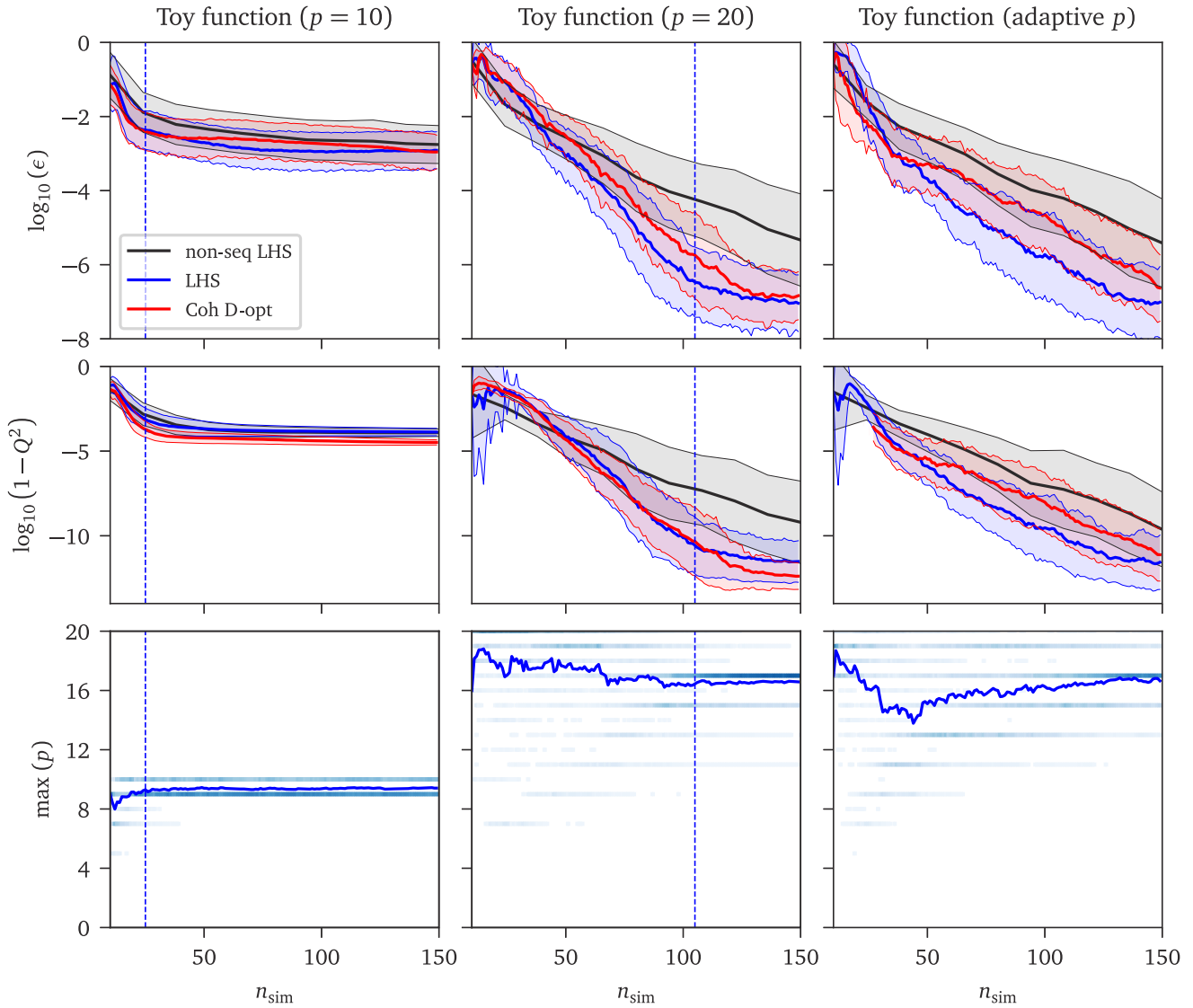


Fig. 4. Results for Toy 2D function obtained with maximum polynomial order $p = 10$ (left), $p = 20$ (middle) and adaptive p (right). The first two rows represent the accuracy measured by ϵ and Q^2 . The last row shows the mean value (solid blue line) and the empirical probability mass function (blue points) of the maximum order p in active \mathcal{A} for LHS. (For interpretation of the references to color in this figure legend, the reader is referred to the web version of this article.)

The Ishigami function represents a well-known benchmark function for surrogate modeling and sensitivity analysis and thus additional analysis with a very large pool size was performed in order to show additional results discussed extensively in Section 6. First of all, non-sequential PCE based on Coh-D optimal sampling was created for the direct comparison. The obtained results for standard setting are summarized in Fig. 5 (left column).

The non-sequential Coherence-D optimal ED leads to unsatisfactory results both in variance estimation and Q^2 . Although the convergence rate is lower for our purpose (low number of samples), note that it is significantly more efficient with increasing number of samples. As can be seen, the proposed sequential sampling clearly outperforms the non-seq standard approach. Moreover, the convergence rate is significantly higher, until the polynomial chaos gets saturated by reaching the maximum order $p = 10$ as can be seen in Fig. 5 (left column, bottom plot). Naturally, non-sequential technique converges to identical accuracy with increasing number of samples.

Since the Ishigami function is a low-dimensional and inexpensive example, it was also possible to perform calculation with ED pool containing a large number $n_{\text{pool}} = 5000$ of simulations and 100 repetitions in order to

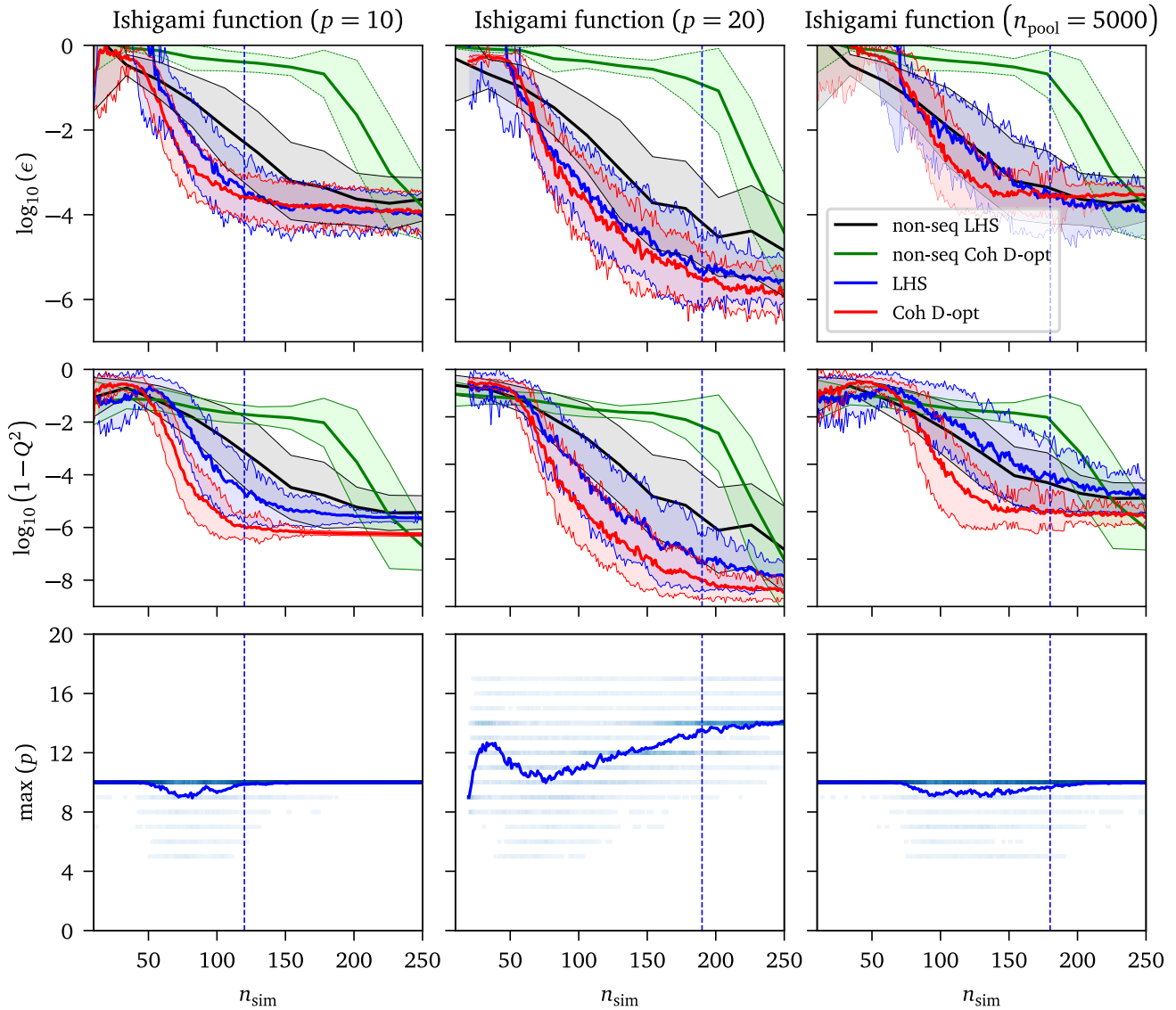


Fig. 5. Results for the Ishigami function. The first two rows represent the accuracy measured by ϵ and Q^2 . The last row shows the mean value (solid blue line) and the empirical probability mass function (blue points) of the maximum order p in active \mathcal{A} for LHS. The maximum polynomial order is $p = 10$ for the left ($n_{\text{pool}} = 858$) and right columns. The pool size for the middle column is $n_{\text{pool}} = 3P = 5313$ candidate points. (For interpretation of the references to color in this figure legend, the reader is referred to the web version of this article.)

obtain statistical estimates. Note that the pool for Coh-D opt was obtained by D-optimal reduction from larger pool generated by coherence optimal sampling as in the previous examples.

The obtained results, for the case of an extremely large pool of candidates, depicted in Fig. 5 (right column) are slightly worse in comparison to the moderate size of the pool. This phenomenon is extensively discussed in Section 6. Additionally, note that the presented results are obtained for the fixed maximum polynomial order $p = 10$, which imposes a strong limit on achievable accuracy for $n_{\text{sim}} \gtrsim 120$. Similarly to the previous numerical example, allowing a higher p leads to higher accuracy of the PCE, which can be seen in Fig. 5 (middle column) using $p = 20$ (the saturation is postponed to about $n_{\text{sim}} \approx 200$).

5.3. 2D mirror line singularities

The 2D line singularities function is a mirrored version of a function used in [37]. The true surface of this function is studied for three different values of the parameter δ ; see Fig. 6. In order to document the effectiveness

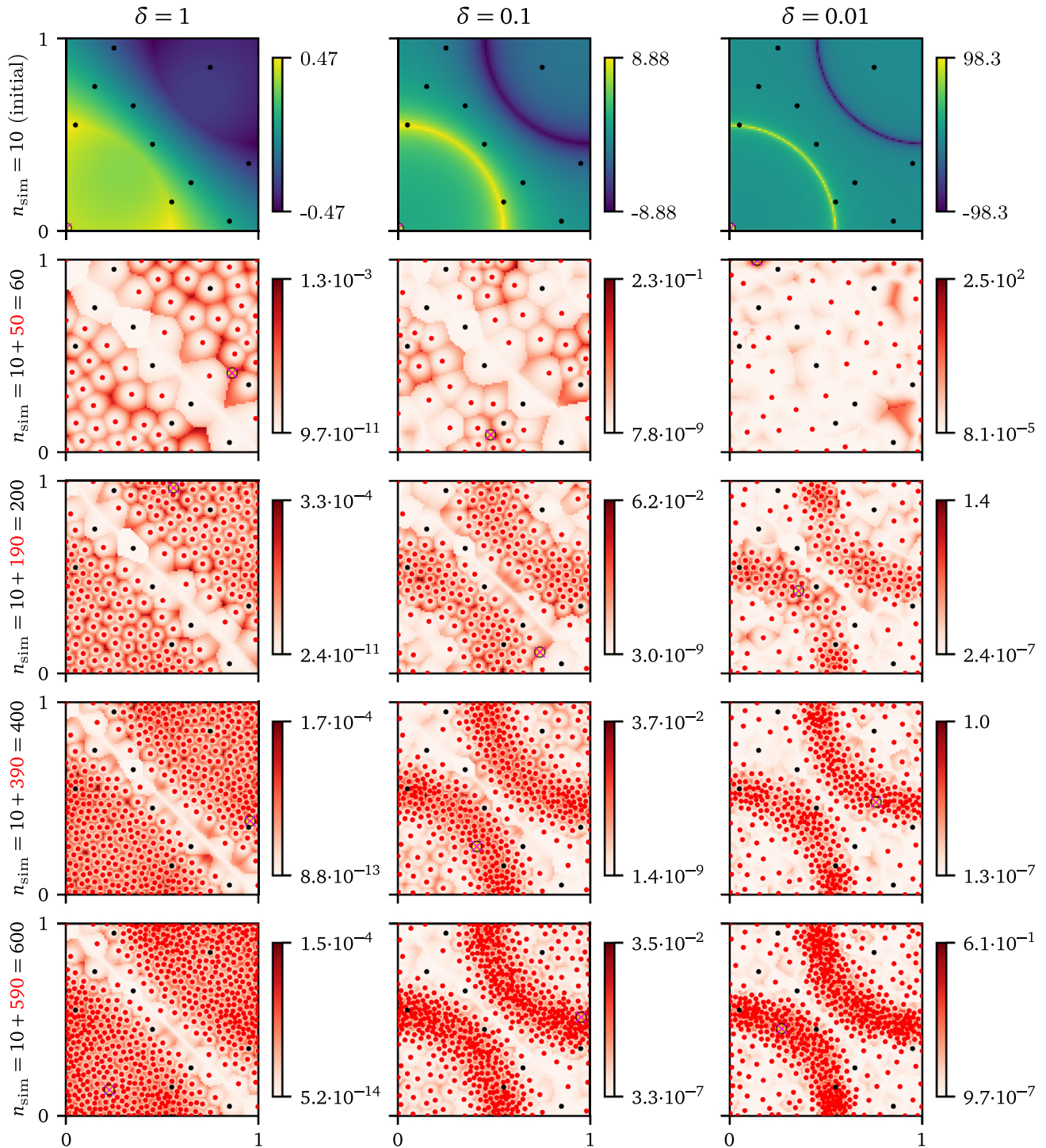


Fig. 6. 2D mirror line singularities: underlying map shows function values (the top row) and Θ criterion (others). Points represent the initial design ED (black points) and selected four iterations of algorithm adding candidates to the existing ED. Mathematical model for different parameters δ : $\delta = 1$ (left), $\delta = 0.1$ (middle), $\delta = 0.01$ (right). The maximum polynomial degree was $p = 12$ and therefore the ability of PCE to mimic a sharp singularity was limited.

of the proposed sequential sampling in the convergence plots, we selected the case of $\delta = 0.1$. Let $\mathbf{X} \sim \mathcal{U}[0, 1]^2$ and the mathematical model be in the following form

$$Y = \frac{1}{|0.3 - X_1^2 - X_2^2| + \delta} - \frac{1}{|0.3 - (1 - X_1)^2 - (1 - X_2)^2| + \delta}. \quad [\delta = 0.1 : \sigma_Y^2 \approx 13.070477042] \quad (30)$$

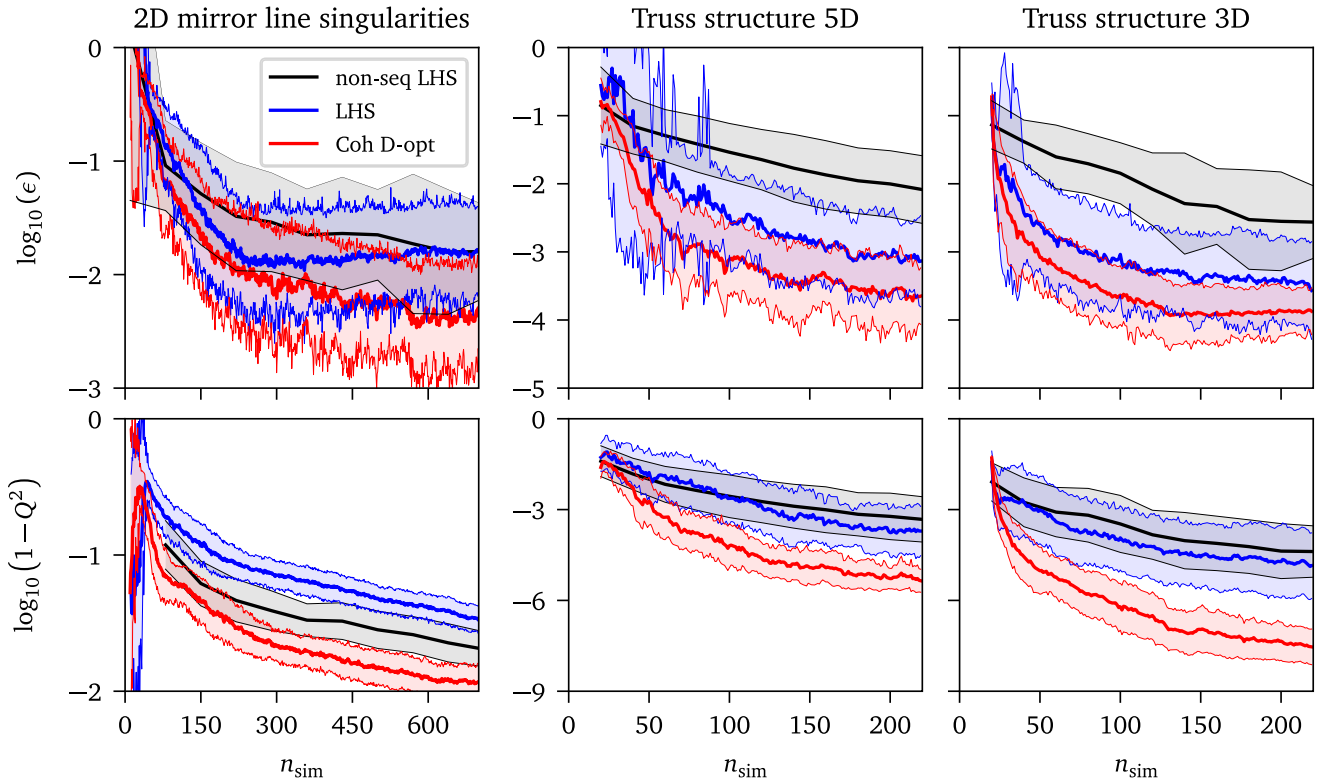


Fig. 7. Numerical results for Example 3 (left), Example 4 (middle) and Example 5 (right). The rows represent the accuracy measured via ϵ and Q^2 . (For interpretation of the references to color in this figure legend, the reader is referred to the web version of this article.)

Note that, this example represents a challenging task for PCE especially for low values of δ . There are curved singularities located in a narrow vicinity of two circular arcs and thus it is crucial to identify the location of the singularity and use high-degree interacting polynomials for approximation. The values of the function range between its extremes of roughly $\pm\delta^{-1}$. We remark that the results of non-seq Coh D-opt are out of the graph range and thus this technique is not depicted in Fig. 7. Fig. 7 (top-left) shows a typical comparison of sequential and non-sequential LHS techniques. Sequential sampling is significantly better for mid-size ED, while the differences are reduced for large sample sizes when the polynomial chaos gets saturated. We remark that the high convergence rate for small to medium sample size is the practical range for which the proposed method is developed. Coh-D opt sequential strategy shows the best accuracy in Q^2 as well as in estimated variance. On the other hand, as can be seen in Fig. 7 (bottom-left) sequential LHS leads to low accuracy measured by Q^2 .

5.4. Truss structure (Hermite polynomials)

This problem involves nonuniform input variables and thus the selected set of polynomials is composed of Hermite polynomials. The design domain becomes open: \mathbb{R}^M . The mathematical model represents deflection of the truss structure depicted in Fig. 8. The deflection can be computed using the method of virtual work (unit load method). This method results in the following expression for the mid-span deflection

$$Y = F \left(\frac{552}{A_h E_h} + \frac{50.9117}{A_d E_d} \right). \quad [\sigma_Y^2 \approx 0.0002373] \quad (31)$$

The input random vector of the model, \mathbf{X} , consists of five independent random variables: the properties of the horizontal bars (Young's modulus E_h and cross-section area A_h), the properties of the diagonal bars (Young's modulus E_d and cross-section area A_d), and the magnitude of the loading forces F on the top joints. The properties of the input random variables are summarized in Table 1.

First of all, in order to construct PCE, the input random vector is transformed to standardized Gaussian random space by Nataf transformation [78,79] corresponding to Hermite germs. Further full set of polynomial basis functions

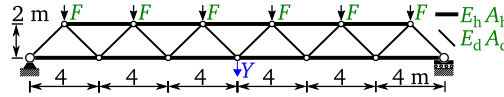


Fig. 8. Truss structure constructed from two types of bars.

Table 1

Five random variables featured in the truss example.

Variable	Distribution	Mean	Units	CoV
E_h, E_d	Log-normal	210	GPa	0.10
A_h	Log-normal	2000	mm ²	0.10
A_d	Log-normal	1000	mm ²	0.10
F	Gumbel-Max	50	kN	0.15

P is reduced by hyperbolic truncation with $q = 0.5$ according to Eq. (8). The initial ED contains $n_{sim} = 20$ realizations of X generated by LHS. We remark that Nataf transformation might increase the polynomial degree required to compute the PCE approximation of a function. To avoid the increase in nonlinearity of the problem by using the Nataf transformation, one could also compute the polynomials numerically in practical applications [80].

Obtained results can be seen in Fig. 7 (middle column). Similar to the previous example, sequential LHS leads to higher accuracy in estimated variance but the approximation error Q^2 is comparable to non-sequential LHS. The proposed sequential Coh D-opt method is clearly the most accurate and convergence rate is significantly faster both in Q^2 and variance estimation. The Coh-D sequential sampling converges to errors several orders of magnitude smaller than commonly used non-sequential LHS.

5.5. Truss structure (Hermite polynomials) — Reduced dimension

Adaptivity of the proposed algorithm is provided by the best model selection algorithm (LAR in this paper), which should be able to select the best possible set of basis functions \mathcal{A} . In order to examine this feature in the context of the proposed adaptive sequential sampling, the results of the previous example are compared to a manually reduced stochastic model of the previous example (Truss structure) preserving identical mathematical model as follows [81]:

$$Y = F \left(\frac{552}{\mathcal{A}_h} + \frac{50.9117}{\mathcal{A}_d} \right), \quad [\sigma_Y^2 \approx 0.0002373] \tag{32}$$

where \mathcal{A}_h is a Log-normal random variable with mean of 420 MN and \mathcal{A}_d is a Log-normal random variable with mean of 210 MN, CoV of both random variables equals 0.14177. The results obtained from the sequential sampling are summarized in Fig. 7 (right). As can be seen, the final accuracy of this example measured by relative error in variance ϵ is similar to the 5D formulation of the $g(X)$ when the size of ED reaches the final $n_{sim} = 220$, although the convergence of the reduced model to this value is significantly faster for lower n_{sim} . This is in compliance with the theoretical behavior of the model selection algorithm, which becomes more efficient with greater samples size. The faster convergence also affects the final accuracy of Coh D-opt measured by Q^2 , which is able to converge to lower values for the final n_{sim} .

6. Discussion

6.1. Optimal pool size and the maximum polynomial order p

As already briefly mentioned above, the selection of fixed maximum polynomial order p may impose a lower bound on achievable accuracy. This phenomenon was visible in the first “Toy” example (see Fig. 4) as well as for the “Ishigami function”, see Fig. 5. In these examples, the initial guess on $p = 10$ was found insufficient and selection of $p = 20$ allowed for much higher accuracy of the surrogate. This is documented by examination of the set \mathcal{A} , specifically maximum p in the active set of basis functions \mathcal{A} chosen by LAR depicted by blue color in the bottom rows of Figs. 4 and 5. It can be seen, that convergence rate is very low once the maximum order p in

active \mathcal{A} achieves its prescribed maximum of $p = 10$ since there are no additional possibilities for improvement of the approximation (the space of basis functions is out of suitable candidates). Therefore, if one extends the space of basis functions by sufficiently incrementing p , the decrease in error does not stop and ϵ for maximum n_{sim} is significantly lower. Unfortunately, the ideal p is not known a priori and thus one should adaptively increase it with growing active ED. However, as discussed already in [2], it is possible to employ an adaptive selection of the best p for each iteration. Such a feature might play a significant role in some cases. Such approach was deliberately not employed in this paper because the influence of the proposed sampling scheme might not be clearly separable from the model selection.

The proposed sequential technique achieved higher accuracy of estimated variance for lower number of samples in comparison to non-sequential sampling in all presented numerical examples. However, as can be seen from numerical results of the Ishigami function, increasing the pool size does not generally lead to higher accuracy or faster convergence rate. In fact, a very large number of candidates might cause slower convergence (comparable to non-sequential sampling). After detailed examination of this example, one can see the different structure of \mathcal{A} for the large set of candidates depicted in Fig. 5 (rightmost column). During the initial phase of the adaptive sequential sampling, LAR algorithm typically selects high-order polynomials since there is not enough information about a mathematical model, which leads to *overfitting*. Further increasing the sample size enables the adaptive algorithm to identify more appropriate low-order basis functions ($n_{\text{sim}} \approx 50$ for Ishigami function). Sequential sampling in the following steps of algorithm selects the candidates with respect to the current \mathcal{A} and exploration aspect. Note that high-order basis functions are selected by adaptive algorithm once the new regions associated to high local variance are discovered (peaks of the given mathematical model). However, such regions are not preferred by the selection criterion since low-order basis functions ignore the currently unknown extremes. Therefore, the convergence rate of the adaptive sequential sampling can be significantly affected by the number of candidates, since if there are no candidates in regions favored by low-order basis functions, the exploration part of the proposed criterion could investigate new functional extremes and adapt \mathcal{A} to a set of high-order basis functions. This phenomenon is illustrated by blue color in numerical results in Fig. 5 (left). In the first case with $n_{\text{pool}} = 3P$ (and $p = 10$), one can see a fast convergence for n_{sim} ranging between 50 and 150 (associated to lower maximum p in active \mathcal{A}) until the space of basis functions is out of suitable candidates as described in the paragraph above. On the other hand, for the second case with $n_{\text{pool}} = 5\,000$ (and $p = 10$ again; see Fig. 5 right), an active \mathcal{A} contains low-order basis functions for a range of significantly greater n_{sim} , which leads to a slower convergence of accuracy ultimately leading to the identical final error.

In summary, the achievable accuracy of the adaptive sequential sampling is limited by the maximum polynomial order p used. Simply, the flexibility of the polynomial approximation may not be sufficient to approximate the original function at a given precision level. In practical applications, a sufficient polynomial order is not known a priori and therefore p should be adaptively increased with increasing n_{sim} in order to achieve the best performance of the proposed algorithm. On the other hand, the convergence rate is significantly affected by n_{pool} and extremely large pool leads to slow convergence, since a selection of high-order basis functions is postponed to higher n_{sim} . Therefore the heuristic rule $n_{\text{pool}} = 3P$ is recommended for practical applications.

6.2. High dimensions

What remains an open question is the behavior of the proposed criterion in high dimensions. In particular, we need to understand the effect of the exploration part $l_{c,s}^M$ in Eq. (24). Generally, in high-dimensional space with independent and identically distributed (iid) components, the Minkowski distance of order $\mathcal{P} > 0$ (sometimes referred to as the \mathcal{P} -norm) concentrates, i.e. the coefficient of variation of the norm decreases with increasing dimension, M . This effect on \mathcal{P} -norm of letting M go large is well known in the computational learning literature. A discussion in the context of iid Gaussian distribution can be found e.g. in [82]. The asymptotic behavior of \mathcal{P} -norm and its convergence rates have been studied in [83].

The role of the distance term must be discussed especially in the case of uniform distribution of the germ which is defined over a hypercube. It is known that Euclidean distances (a special case of Minkowski distance with $\mathcal{P} = 2$) of any pair of points inside a hypercube tend to concentrate around its mean value when the dimension is high. It is known that the standard deviation of the Euclidean distance between any two randomly picked points stays approximately constant with increasing dimension while the mean value keeps growing proportionally to

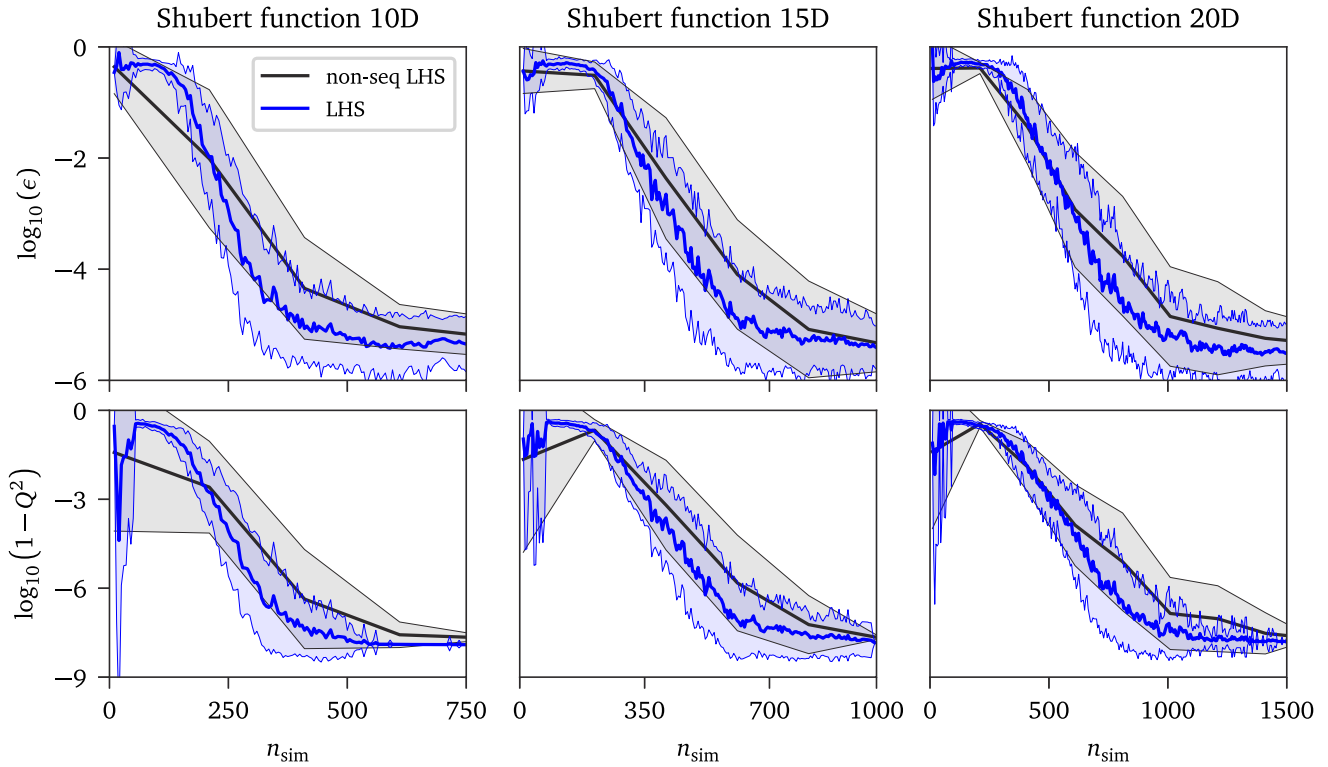


Fig. 9. Results for the Shubert function in 10 (left), 15 (middle) and 20 (right) dimensions. The first row represents the accuracy of estimated variance measured by ϵ and the second row shows the approximation accuracy measured by Q^2 .

\sqrt{M} [84,85]. Therefore, the coefficient of variation of a random distance is asymptotically proportional to $1/\sqrt{M}$. In such a case the distance contrast decreases and it is said that the distances concentrate [86,87]. The same holds also for the squared Euclidean distance l^2 between points picked at random: the squared distance has Gaussian distribution with the mean value of $M/6$ and variance $7M/180$. In order to obtain the hypervolume of a region in between a pair of points, the squared distance must be raised to $M/2$. We have found that the coefficient of variation of such volume quickly increases as the problem dimension grows high. Therefore, there is no problem with insufficient contrast as the proposed Θ criterion sufficiently varies even in domains of high dimension.

Although it will be necessary to perform extensive study with advanced sampling schemes in order to investigate the efficiency of the proposed criterion in high dimensions, the general behavior of the Θ criterion is demonstrated in the following simple example with input random vector $X \sim \mathcal{U}[-1, 1]^M$ — Shubert function No. 4 [88]:

$$Y = \sum_{i=1}^M \sum_{j=1}^5 j \cos((j+1)X_i + j). \quad [\sigma_Y^2 \approx M \cdot 45.266\,621\,664] \quad (33)$$

This function can be easily utilized as a benchmark for an arbitrary number of input random variables; in our study we use $M = \{10, 15, 20\}$. The maximum polynomial order $p = 12$ and hyperbolic truncation parameter $q = 0.3$ were used for construction of surrogate model, and the initial ED contains $n_{\text{sim}} = 10$ realizations of X generated by LHS. Since the hyperbolic truncation significantly reduces the P in high dimensions, we increased the pool size to $n_{\text{pool}} = 5P$. Note that, this study is focused only on stability of the proposed Θ criterion in higher dimensions and thus only the sequential and the non-sequential LHS were employed for direct comparison. From the obtained results depicted in Fig. 9, it can be seen that the proposed criterion enabling one-by-one extension of ED achieves higher accuracy in comparison to non-sequential approach independently of dimension M and thus the theoretical discussion in the previous paragraph was presented also numerically. Naturally, the absolute value of accuracy is highly dependent on the investigated function and on the particular sampling scheme coupled with Θ criterion, however this study demonstrates the applicability of the proposed criterion in high dimensions.

6.3. Further work

Since the DoE is usually not a bottleneck in probabilistic analysis and sequential sampling offers several advantages in comparison to non-sequential sampling, it can be recommended to employ the proposed algorithm for the construction of PCE despite higher computational requirements of repetitive DoE in each step. Although the choice of the sampling technique coupled with the proposed criterion for the sequential selection of the best candidate is arbitrary, it can be seen from the numerical examples, that LHS is efficient for low dimensional mathematical models. On the other hand, coherence D-optimal sampling achieved significantly higher accuracy in more complex examples. Therefore further work will be focused on an improvement of effectiveness by using advanced optimized space-filling designs for the generating of a pool of candidates and a comparative study of existing advanced sampling techniques coupled with the proposed criterion will be performed. Employment of designs generated from the target distribution that additionally avoids clustering [17,81,89] or empty regions [60] while maintaining true statistical homogeneity via periodic distance-based criteria has the potential to further improve the effectiveness of the proposed method, especially in high-dimensional space. Moreover, it was shown that fixed p represents a significant limitation for the proposed method and thus further work will be also focused on adaptive basis strategies [75,90], which have the potential to dramatically improve the final accuracy of PCE and solve the problem with LAR and with a large size of the pool of candidates.

7. Conclusion

A novel adaptive sequential sampling technique for accurate and efficient construction of a non-intrusive PCE was proposed in this paper and its performance was validated on several numerical examples of increasing complexity and dimensionality. The proposed technique selects the best candidate sample from a large pool maintaining the balance between exploration of the design domain and exploitation of the current characteristics of the PCE. The criterion driving the selection of the best candidate was successfully coupled with LHS and Coh-D optimal sampling and both variants were used in numerical examples. From the obtained results, it can be concluded that the proposed technique leads to higher accuracy of the constructed PCE in comparison to non-sequential sampling. The difference in accuracy between sequential and non-sequential sampling is especially significant for a low-size ED. However, it can be expected that the accuracy of sequential sampling converges to identical results as a non-sequential sampling for a very large ED in which the PCE is saturated. Comparing both sequential sampling techniques, superior performance was achieved by sequential adaptive Coh-D optimal sampling due to its adaptivity of the candidate sample in each iteration.

Declaration of competing interest

The authors declare that they have no known competing financial interests or personal relationships that could have appeared to influence the work reported in this paper.

Acknowledgments

The authors acknowledge financial support provided by the Ministry of Education, Youth and Sports of the Czech Republic under Project No. LTAUSA19058. Additionally, the first author is also supported by the Ministry of Education, Youth and Sports of the Czech Republic under Project No. FAST-J-21-7209.

References

- [1] N. Wiener, The homogeneous chaos, *Amer. J. Math.* 60 (4) (1938) 897–936, <http://dx.doi.org/10.2307/2371268>.
- [2] G. Blatman, B. Sudret, Adaptive sparse polynomial chaos expansion based on least angle regression, *J. Comput. Phys.* 230 (6) (2011) 2345–2367, <http://dx.doi.org/10.1016/j.jcp.2010.12.021>.
- [3] R.G. Ghanem, P.D. Spanos, *Stochastic Finite Elements: A Spectral Approach*, Springer, New York, 1991, <http://dx.doi.org/10.1007/978-1-4612-3094-6>.
- [4] T. Crestaux, O.L. Maître, J.-M. Martinez, Polynomial chaos expansion for sensitivity analysis, *Reliab. Eng. Syst. Saf.* 94 (7) (2009) 1161–1172, <http://dx.doi.org/10.1016/j.res.2008.10.008>.
- [5] B. Sudret, Global sensitivity analysis using polynomial chaos expansions, *Reliab. Eng. Syst. Saf.* 93 (7) (2008) 964–979, <http://dx.doi.org/10.1016/j.res.2007.04.002>.

- [6] N.-Z. Chen, C. Guedes Soares, Spectral stochastic finite element analysis for laminated composite plates, *Comput. Methods Appl. Mech. Eng.* 197 (51) (2008) 4830–4839, <http://dx.doi.org/10.1016/j.cma.2008.07.003>.
- [7] L. Novak, D. Novak, Surrogate modelling in the stochastic analysis of concrete girders failing in shear, in: *Proc. of the Fib Symposium 2019: Concrete - Innovations in Materials, Design and Structures*, 2019, pp. 1741–1747.
- [8] M. Chatzimanolakis, K.-D. Kantarakias, V. Asouti, K. Giannakoglou, A painless intrusive polynomial chaos method with RANS-based applications, *Comput. Methods Appl. Mech. Eng.* 348 (2019) 207–221, <http://dx.doi.org/10.1016/j.cma.2019.01.018>.
- [9] G.T. Buzzard, Global sensitivity analysis using sparse grid interpolation and polynomial chaos, *Reliab. Eng. Syst. Saf.* 107 (2012) 82–89, <http://dx.doi.org/10.1016/j.ress.2011.07.011>, SAMO 2010.
- [10] Z. Perko, L. Gilli, D. Lathouwers, J.L. Kloosterman, Grid and basis adaptive polynomial chaos techniques for sensitivity and uncertainty analysis, *J. Comput. Phys.* 260 (2014) 54–84, <http://dx.doi.org/10.1016/j.jcp.2013.12.025>.
- [11] A. Cohen, G. Migliorati, Optimal weighted least-squares methods, *SMAI J. Comput. Math.* 3 (2017) 181–203, <http://dx.doi.org/10.5802/smai-jcm.24>.
- [12] A.C. Narayan, J. Jakeman, T. Zhou, A christoffel function weighted least squares algorithm for collocation approximations, *Math. Comp.* 86 (2017) 1913–1947, <http://dx.doi.org/10.1090/mcom/3192>.
- [13] N. Lüthen, S. Marelli, B. Sudret, Sparse polynomial chaos expansions: Literature survey and benchmark, *SIAM/ASA J. Uncertain. Quantif.* 9 (2) (2021) 593–649, <http://dx.doi.org/10.1137/20M1315774>.
- [14] W. Conover, On a better method for selecting input variables, 1975, unpublished Los Alamos National Laboratories manuscript, reproduced as Appendix A of “Latin Hypercube Sampling and the Propagation of Uncertainty in Analyses of Complex Systems” by J.C. Helton and F.J. Davis, Sandia National Laboratories report SAND2001-0417, printed November 2002. URL <https://prod-ng.sandia.gov/techlib-noauth/access-control.cgi/2001/010417.pdf>.
- [15] M. Johnson, L. Moore, D. Ylvisaker, Minimax and maximin distance designs, *J. Statist. Plann. Inference* 2 (26) (1990) 131–148, [http://dx.doi.org/10.1016/0378-3758\(90\)90122-B](http://dx.doi.org/10.1016/0378-3758(90)90122-B).
- [16] M.D. Morris, T.J. Mitchell, Exploratory designs for computational experiments, *J. Statist. Plann. Inference* 43 (3) (1995) 381–402, [http://dx.doi.org/10.1016/0378-3758\(94\)00035-T](http://dx.doi.org/10.1016/0378-3758(94)00035-T).
- [17] M. Vořechovský, J. Eliáš, Modification of the Maximin and ϕ_p (phi) criteria to achieve statistically uniform distribution of sampling points, *Technometrics* 62 (3) (2020) 371–386, <http://dx.doi.org/10.1080/00401706.2019.1639550>.
- [18] J. Halton, On the efficiency of certain quasi-random sequences of points in evaluating multi-dimensional integrals, *Numer. Math.* 2 (1) (1960) 84–90, <http://dx.doi.org/10.1007/BF01386213>.
- [19] H. Faure, C. Lemieux, Generalized Halton sequences in 2008: A comparative study, *ACM Trans. Model. Comput. Simul.* 19 (4) (2009) 15:1–15:31, <http://dx.doi.org/10.1145/1596519.1596520>.
- [20] I. Sobol’, On the distribution of points in a cube and the approximate evaluation of integrals, *USSR Comput. Math. Math. Phys.* 7 (1967) [http://dx.doi.org/10.1016/0041-5553\(67\)90144-9](http://dx.doi.org/10.1016/0041-5553(67)90144-9).
- [21] I.M. Sobol’, Uniformly distributed sequences with an additional uniform property, *USSR Comput. Math. Math. Phys.* 16 (5) (1976) 236–242, [http://dx.doi.org/10.1016/0041-5553\(76\)90154-3](http://dx.doi.org/10.1016/0041-5553(76)90154-3), Short communication.
- [22] H. Niederreiter, Point sets and sequences with small discrepancy, *Monatsh. Math.* 104 (4) (1987) 273–337, <http://dx.doi.org/10.1007/BF01294651>.
- [23] H. Niederreiter, Low-discrepancy and low-dispersion sequences, *J. Number Theory* 30 (1) (1988) 51–70, [http://dx.doi.org/10.1016/0022-314X\(88\)90025-X](http://dx.doi.org/10.1016/0022-314X(88)90025-X).
- [24] H. Niederreiter, Random Number Generation and Quasi-Monte Carlo Methods, in: *CBMS-NSF Regional Conference Series in Applied Mathematics*, Society for Industrial and Applied Mathematics (SIAM), Philadelphia, Pennsylvania, 1992, <http://dx.doi.org/10.1137/1.9781611970081>.
- [25] H. Faure, *Discrèpances de suites associées à un système de numération (en dimension un)* [Discrepancy of sequences associated with a number system (in dimension one)], *Bull. Soc. Math. France* 109 (1981).
- [26] S. Tezuka, Uniform Random Numbers: Theory and Practice, in: *The Springer International Series in Engineering and Computer Science* 315, Springer, Boston, MA, 1995, <http://dx.doi.org/10.1007/978-1-4615-2317-8>.
- [27] J. Hampton, A. Doostan, Compressive sampling of polynomial chaos expansions: Convergence analysis and sampling strategies, *J. Comput. Phys.* 280 (2015) 363–386, <http://dx.doi.org/10.1016/j.jcp.2014.09.019>.
- [28] A. Cohen, G. Migliorati, Optimal weighted least-squares methods, *SMAI J. Comput. Math.* 3 (2017) 181–203, <http://dx.doi.org/10.5802/smai-jcm.24>.
- [29] B. Echard, N. Gayton, M. Lemaire, AK-MCS: An active learning reliability method combining Kriging and Monte Carlo simulation, *Struct. Saf.* 33 (2) (2011) 145–154, <http://dx.doi.org/10.1016/j.strusafe.2011.01.002>.
- [30] L. Shi, B. Sun, D.S. Ibrahim, An active learning reliability method with multiple kernel functions based on radial basis function, *Struct. Multidiscip. Optim.* 60 (1) (2019) 211–229, <http://dx.doi.org/10.1007/s00158-019-02210-0>.
- [31] X. Yang, X. Cheng, Active learning method combining Kriging model and multimodal-optimization-based importance sampling for the estimation of small failure probability, *Internat. J. Numer. Methods Engrg.* 121 (21) (2020) 4843–4864, <http://dx.doi.org/10.1002/nme.6495>.
- [32] S. Marelli, B. Sudret, An active-learning algorithm that combines sparse polynomial chaos expansions and bootstrap for structural reliability analysis, *Struct. Saf.* 75 (2018) 67–74, <http://dx.doi.org/10.1016/j.strusafe.2018.06.003>.
- [33] Y. Zhou, Z. Lu, W. Yun, Active sparse polynomial chaos expansion for system reliability analysis, *Reliab. Eng. Syst. Saf.* 202 (2020) 107025, <http://dx.doi.org/10.1016/j.ress.2020.107025>.
- [34] K. Cheng, Z. Lu, Active learning polynomial chaos expansion for reliability analysis by maximizing expected indicator function prediction error, *Internat. J. Numer. Methods Engrg.* 121 (14) (2020) 3159–3177, <http://dx.doi.org/10.1002/nme.6351>.

- [35] N. Fajraoui, S. Marelli, B. Sudret, Sequential design of experiment for sparse polynomial chaos expansions, *SIAM/ASA J. Uncertain. Quantif.* 5 (1) (2017) 1061–1085, <http://dx.doi.org/10.1137/16m1103488>.
- [36] M. Thapa, S.B. Mulani, R.W. Walters, Adaptive weighted least-squares polynomial chaos expansion with basis adaptivity and sequential adaptive sampling, *Comput. Methods Appl. Mech. Eng.* 360 (2020) 112759, <http://dx.doi.org/10.1016/j.cma.2019.112759>.
- [37] M.D. Shields, Adaptive Monte Carlo analysis for strongly nonlinear stochastic systems, *Reliab. Eng. Syst. Saf.* 175 (2018) 207–224, <http://dx.doi.org/10.1016/j.ress.2018.03.018>.
- [38] Y. Zhou, Z. Lu, K. Cheng, C. Ling, An efficient and robust adaptive sampling method for polynomial chaos expansion in sparse Bayesian learning framework, *Comput. Methods Appl. Mech. Engrg.* 352 (2019) 654–674, <http://dx.doi.org/10.1016/j.cma.2019.04.046>.
- [39] S. Marelli, B. Sudret, UQLab: A framework for uncertainty quantification in matlab, in: *Vulnerability, Uncertainty, and Risk*, 2014, pp. 2554–2563, <http://dx.doi.org/10.1061/9780784413609.257>.
- [40] E. Patelli, S. Tolo, H. George-Williams, J. Sadeghi, R. Rocchetta, M. de Angelis, M. Broggi, OpenCossan 2.0: an efficient computational toolbox for risk, reliability and resilience analysis, in: *Proceedings of the Joint ICVRAM ISUMA UNCERTAINTIES Conference*, 2018, pp. 1–8, URL <http://icvramisuma2018.org/cd/web/PDF/ICVRAMISUMA2018-0022.PDF>.
- [41] L. Novak, D. Novak, Polynomial chaos expansion for surrogate modelling: Theory and software, *Beton- Stahlbetonbau* 113 (2018) 27–32, <http://dx.doi.org/10.1002/best.201800048>.
- [42] J. Feinberg, H.P. Langtangen, Chaospy: An open source tool for designing methods of uncertainty quantification, *J. Comput. Sci.* 11 (2015) 46–57, <http://dx.doi.org/10.1016/j.jocs.2015.08.008>.
- [43] A. Olivier, D. Giovanis, B. Aakash, M. Chauhan, L. Vandanapu, M.D. Shields, UQpy: A general purpose Python package and development environment for uncertainty quantification, *J. Comput. Sci.* 47 (2020) 101204.
- [44] D. Xiu, G.E. Karniadakis, The Wiener–Askey polynomial chaos for stochastic differential equations, *SIAM J. Sci. Comput.* 24 (2) (2002) 619–644, <http://dx.doi.org/10.1137/s1064827501387826>.
- [45] B. Efron, T. Hastie, I. Johnstone, R. Tibshirani, Least angle regression, *Ann. Statist.* 32 (2) (2004) 407–451, <http://dx.doi.org/10.2307/3448465>.
- [46] J.A. Tropp, A.C. Gilbert, Signal recovery from random measurements via orthogonal matching pursuit, *IEEE Trans. Inf. Theory* 53 (12) (2007) 4655–4666, <http://dx.doi.org/10.1109/tit.2007.909108>.
- [47] S. Ji, Y. Xue, L. Carin, Bayesian compressive sensing, *IEEE Trans. Signal Process.* 56 (6) (2008) 2346–2356, <http://dx.doi.org/10.1109/TSP.2007.914345>.
- [48] G. Blatman, B. Sudret, An adaptive algorithm to build up sparse polynomial chaos expansions for stochastic finite element analysis, *Probab. Eng. Mech.* 25 (2) (2010) 183–197, <http://dx.doi.org/10.1016/j.probengmech.2009.10.003>.
- [49] J.F. Koksma, Een algemeene stelling uit de theorie der gelijkmatige verdeling modulo 1, *Math. B* 11 (1942/1943) 7–11.
- [50] K.-T. Fang, Y. Wang, *Number-Theoretic Methods in Statistics*, first ed., Chapman and Hall/CRC, London; New York, 1993.
- [51] F.J. Hickernell, A generalized discrepancy and quadrature error bound, *Math. Comp.* 67 (221) (1998) 299–322, <http://dx.doi.org/10.1090/S0025-5718-98-00894-1>.
- [52] F.J. Hickernell, Lattice rules: How well do they measure up? in: P. Hellekalek, G. Larcher (Eds.), *Random and Quasi-Random Point Sets*, Springer New York, New York, NY, 1998, pp. 109–166, http://dx.doi.org/10.1007/978-1-4612-1702-2_3, Ch. Lattice Rules: How Well Do They Measure Up?.
- [53] J. Dick, F. Pillichshammer, *Digital Nets and Sequences: Discrepancy Theory and Quasi-Monte Carlo Integration*, Cambridge University Press, 2010, <http://dx.doi.org/10.1017/cbo9780511761188>.
- [54] M.D. McKay, W.J. Conover, R.J. Beckman, A comparison of three methods for selecting values of input variables in the analysis of output from a computer code, *Technometrics* 21 (1979) 239–245, <http://dx.doi.org/10.1080/00401706.1979.10489755>.
- [55] M. Stein, Large sample properties of simulations using Latin hypercube sampling, *Technometrics* 29 (2) (1987) 143–151, <http://dx.doi.org/10.1080/00401706.1987.10488205>.
- [56] A.B. Owen, A central limit theorem for Latin hypercube sampling, *J. R. Stat. Soc. Ser. B Stat. Methodol.* 54 (2) (1992) 541–551, <http://dx.doi.org/10.2307/2346140>.
- [57] A.B. Owen, Controlling correlations in latin hypercube samples, *J. Amer. Statist. Assoc. (Theory Methods)* 89 (428) (1994) 1517–1522.
- [58] M.D. Shields, J. Zhang, The generalization of Latin hypercube sampling, *Reliab. Eng. Syst. Saf.* 148 (2016) 96–108, <http://dx.doi.org/10.1016/j.ress.2015.12.002>.
- [59] L. Pronzato, Minimax and maximin space-filling designs: some properties and methods for construction, *J. Soc. Fr. Stat.* 158 (1) (2017) 7–36.
- [60] J. Eliáš, M. Vořechovský, V. Sadílek, Periodic version of the minimax distance criterion for Monte Carlo integration, *Adv. Eng. Softw.* 149 (2020) 102900, <http://dx.doi.org/10.1016/j.advengsoft.2020.102900>.
- [61] S.-K. Choi, R.V. Grandhi, R.A. Canfield, C.L. Pettit, Polynomial chaos expansion with latin hypercube sampling for estimating response variability, *AIAA J.* 42 (6) (2004) 1191–1198, <http://dx.doi.org/10.2514/1.2220>.
- [62] M. Hadigol, A. Doostan, Least squares polynomial chaos expansion: A review of sampling strategies, *Comput. Methods Appl. Mech. Eng.* 332 (2018) 382–407, <http://dx.doi.org/10.1016/j.cma.2017.12.019>.
- [63] E.J. Candes, Y. Plan, A probabilistic and RIPless theory of compressed sensing, *IEEE Trans. Inf. Theory* 57 (11) (2011) 7235–7254, <http://dx.doi.org/10.1109/tit.2011.2161794>.
- [64] J.D. Jakeman, A. Narayan, T. Zhou, A generalized sampling and preconditioning scheme for sparse approximation of polynomial chaos expansions, *SIAM J. Sci. Comput.* 39 (3) (2017) A1114–A1144, <http://dx.doi.org/10.1137/16M1063885>.
- [65] J. Hampton, A. Doostan, Coherence motivated sampling and convergence analysis of least squares polynomial chaos regression, *Comput. Methods Appl. Mech. Eng.* 290 (2015) 73–97, <http://dx.doi.org/10.1016/j.cma.2015.02.006>.
- [66] A.J. Miller, N.-K. Nguyen, Algorithm AS 295: A fedorov exchange algorithm for D-optimal design, *J. R. Stat. Soc. Ser. C (Appl. Stat.)* 43 (4) (1994) 669–677, <http://dx.doi.org/10.2307/2986264>.

- [67] O. Dykstra, The augmentation of experimental data to maximize [X'X], *Technometrics* 13 (3) (1971) 682–688, <http://dx.doi.org/10.1080/00401706.1971.10488830>.
- [68] P. Diaz, A. Doostan, J. Hampton, Sparse polynomial chaos expansions via compressed sensing and D-optimal design, *Comput. Methods Appl. Mech. Eng.* 336 (2018) 640–666, <http://dx.doi.org/10.1016/j.cma.2018.03.020>.
- [69] Z. Wu, D. Wang, P.N. Okolo, K. Zhao, W. Zhang, Efficient space-filling and near-orthogonality sequential latin hypercube for computer experiments, *Comput. Methods Appl. Mech. Eng.* 324 (2017) 348–365, <http://dx.doi.org/10.1016/j.cma.2017.05.020>.
- [70] C. Tong, Refinement strategies for stratified sampling methods, *Reliab. Eng. Syst. Saf.* 91 (10) (2006) 1257–1265, <http://dx.doi.org/10.1016/j.ress.2005.11.027>.
- [71] M. Vořechovský, Hierarchical refinement of Latin Hypercube Samples, *Comput.-Aided Civ. Infrastruct. Eng.* 30 (5) (2015) 394–411, <http://dx.doi.org/10.1111/mice.12088>.
- [72] M. Shields, Refined latinized stratified sampling: a robust sequential sample size extension methodology for high-dimensional latin hypercube and stratified designs, *Int. J. Uncertain. Quantif.* 6 (2016) 79–97.
- [73] M.D. Shields, K. Teferra, A. Hapij, R.P. Daddazio, Refined stratified sampling for efficient Monte Carlo based uncertainty quantification, *Reliab. Eng. Syst. Saf.* 142 (2015) 310–325.
- [74] J.J. Borkowski, E.S. Valeroso, Comparison of design optimality criteria of reduced models for response surface designs in the hypercube, *Technometrics* 43 (4) (2001) 468–477, <http://dx.doi.org/10.1198/00401700152672564>.
- [75] J. Hampton, A. Doostan, Basis adaptive sample efficient polynomial chaos (BASE-PC), *J. Comput. Phys.* 371 (2018) 20–49, <http://dx.doi.org/10.1016/j.jcp.2018.03.035>.
- [76] T. Ishigami, T. Homma, An importance quantification technique in uncertainty analysis for computer models, in: *Proceedings. First International Symposium on Uncertainty Modeling and Analysis*, IEEE Comput. Soc. Press, 1990, pp. 398–403, <http://dx.doi.org/10.1109/isuma.1990.151285>.
- [77] A. Marrel, B. Iooss, B. Laurent, O. Roustant, Calculations of Sobol indices for the Gaussian process metamodel, *Reliab. Eng. Syst. Saf.* 94 (3) (2009) 742–751, <http://dx.doi.org/10.1016/j.ress.2008.07.008>.
- [78] A. Nataf, Détermination des distributions de probabilité dont les marges sont données, *C. R. Acad. Sci.* 225 (1962) 42–43.
- [79] R. Lebrun, A. Dutfoy, An innovating analysis of the Nataf transformation from the copula viewpoint, *Probab. Eng. Mech.* 24 (3) (2009) 312–320, <http://dx.doi.org/10.1016/j.probengmech.2008.08.001>.
- [80] J.D. Jakeman, F. Franzelin, A. Narayan, M. Eldred, D. Pflüger, Polynomial chaos expansions for dependent random variables, *Comput. Methods Appl. Mech. Engrg.* 351 (2019) 643–666, <http://dx.doi.org/10.1016/j.cma.2019.03.049>.
- [81] M. Vořechovský, J. Mašek, J. Eliáš, Distance-based optimal sampling in a hypercube: Analogies to N-body systems, *Adv. Eng. Softw.* 137 (2019) 102709, <http://dx.doi.org/10.1016/j.advengsoft.2019.102709>.
- [82] L. Katafygiotis, K. Zuev, Geometric insight into the challenges of solving high-dimensional reliability problems, *Probab. Eng. Mech.* 23 (2–3) (2008) 208–218, <http://dx.doi.org/10.1016/j.probengmech.2007.12.026>.
- [83] G. Biau, D.M. Mason, High-dimensional p -norms, in: *Mathematical Statistics and Limit Theorems*, Springer International Publishing, 2015, pp. 21–40, http://dx.doi.org/10.1007/978-3-319-12442-1_3.
- [84] R.S. Anderssen, R.P. Brent, D.J. Daley, P.A.P. Moran, Concerning $\int_0^1 \dots \int_0^1 (x_1^2 + \dots + x_k^2)^{1/2} dx_1 \dots dx_k$ and a Taylor series method, *SIAM J. Appl. Math.* 30 (1) (1976) 22–30, <http://dx.doi.org/10.1137/0130003>.
- [85] V. Sadílek, M. Vořechovský, Evaluation of pairwise distances among points forming a regular orthogonal grid in a hypercube, *J. Civ. Eng. Manage.* 24 (5) (2018) 410–523, <http://dx.doi.org/10.3846/jcem.2018.5189>.
- [86] C.C. Aggarwal, A. Hinneburg, D.A. Keim, On the surprising behavior of distance metrics in high dimensional space, in: *Database Theory — ICDT 2001*, Springer Berlin Heidelberg, 2001, pp. 420–434, http://dx.doi.org/10.1007/3-540-44503-x_27.
- [87] A. Flexer, D. Schnitzer, Choosing ℓ^p norms in high-dimensional spaces based on hub analysis, *Neurocomputing* 169 (2015) 281–287, <http://dx.doi.org/10.1016/j.neucom.2014.11.084>.
- [88] M. Jamil, X. Yang, A literature survey of benchmark functions for global optimisation problems, *Int. J. Math. Model. Numer. Optim.* 4 (2013) 150–194, <http://dx.doi.org/10.1504/IJMMNO.2013.055204>.
- [89] M. Vořechovský, J. Mašek, Distance-based optimal sampling in a hypercube: Energy potentials for high-dimensional and low-saturation designs, *Adv. Eng. Softw.* 149 (2020) 102880, <http://dx.doi.org/10.1016/j.advengsoft.2020.102880>.
- [90] G. Migliorati, Adaptive approximation by optimal weighted least-squares methods, *SIAM J. Numer. Anal.* 57 (5) (2019) 2217–2245, <http://dx.doi.org/10.1137/18M1198387>.

Confirmation of the stated contribution for the Appendix C and Appendix D

On behalf of all authors, the supervisor of main authors Lixia Pan and Ondřej Slowik, hereby confirms that stated “Role of the Ph.D. candidate” and percentual contribution of Lukáš Novák are correct and in accordance with real situation. This confirmation is provided for the following journal papers:

1. Lixia Pan, **Lukáš Novák**, David Lehký, Drahomír Novák, and Maosen Cao. Neural network ensemble-based sensitivity analysis in structural engineering: Comparison of selected methods and the influence of statistical correlation. *Computers & Structures*, 242:106376, 2021. doi: <https://doi.org/10.1016/j.compstruc.2020.106376>
2. Ondřej Slowik, Drahomír Novák, **Lukáš Novák**, and Alfred Strauss. Stochastic modelling and assessment of long-span precast pre-stressed concrete elements failing in shear. *Engineering Structures*, 228:111500, 2021. doi: <https://doi.org/10.1016/j.engstruct.2020.111500>

Brno, 20.09.2021

Prof. Ing. Drahomír Novák, DrSc.

Curriculum vitæ

Personal information



Name and surname: Ing. Lukáš Novák
Date of birth: 30.01.1993
Place of birth: Hustopeče
Address: Čápkova 22/15, Brno 60200
Phone number: +420 608 511 448
E-mail: novak.l@fce.vutbr.cz
Website: <https://www.fce.vutbr.cz/STM/novak.l>

Discipline and the start date of doctoral studies

Institution: Brno University of Technology, Faculty of Civil Engineering

Field of study: Civil engineering, Structures and Traffic Constructions

Topic: Effective probabilistic design of concrete structures using safety formats and response surface

Supervisor: Prof. Ing. Drahomír Novák, DrSc.

Date of admission & inscription: 7.2.2018 & 9.2.2018

Education and qualification

Brno University of Technology, Faculty of Civil Engineering
Civil Engineering, Building Constructions, Structural mechanics

Master's thesis (supervisor prof. Ing. Drahomír Novák, DrSc.):

Probabilistic Modeling of Shear Strength of Prestressed Concrete Beams: Sensitivity Analysis and Semi-Probabilistic Design Methods (grade: A/A)

Bachelor's thesis (supervisor prof. Ing. Drahomír Novák, DrSc.):

Software of Fracture-Mechanical Parameters and Probabilistic Analysis Support Used for Statistical Analysis of Roof Prestressed Girders (grade: A/A)

Relevant courses:

Scia Engineer Certificate (FEM)	30.11.2015
Atena Červenka Consulting Advanced (NLFEM)	13-15.11.2017
JCSS: Structural reliability (South Africa)	3-12.4.2018
Reliability of structures (organizer , BUT)	20.6.2018
Modeling and Numerical Methods for UQ (France)	2-6.9.2019

Teaching experience:

CD004 Structural Reliability (Czech)
BD004 Structural Analysis II (Czech)

Scientific activities and academic awards

\mathcal{H} -index / citations: 3 (4) / 21 (34) according to WoS (Scopus)

Journal ISI papers J_{imp} / conference papers D : 6 / 11 according to Scopus

Academic awards

Medal SIGNUM PROSPERITATIS (FCE BUT)	22.11.2017
Award of dean of Faculty of Civil Engineering	19.02.2018
Czech Concrete Society award for master thesis	19.02.2018
Diploma thesis Award (BUT)	19.02.2018
Josef Hlavka Award	17.11.2018
Brno Ph.D. talent scholarship	01.01.2019

Organizations and committee memberships:

fib Task Group 3.1: Reliability of existing structures

fib Action Group 8: Non-linear finite element modelling

scientific committee of International Probabilistic Workshop 2022

Invited lectures:

Hohai University, China	29.08.2019
FCE, BUT, Brno	19.11.2019

Research positions and selected scientific projects

Brno University of Technology: Student researcher 1.1.2015- 1.1.2018

Brno University of Technology: Researcher since 1.1.2017

Advanced Materials, Technologies and Structures Center: Researcher since 1.1.2018

2020-2022 Co-Investigator	<i>Development of theory and advanced algorithms for UNCertainty analyses in Engineering PROblems (UNCEPRO) INTER-Action CZ-USA project funded by Ministry of Education, Youth and Sports of Czech Republic under project No. LTAUSA19058.</i>
2019-2021 Investigator	<i>Highly Efficient Reliability Analysis (HERA) Brno Ph.D. talent project and scholarship funded by Brno City Municipality</i>
2019 Investigator	<i>Moment-independent sensitivity analysis using polynomial chaos expansion funded by Ministry of Education, Youth and Sports of Czech Republic under project No. FAST-J-19-5780</i>
2018 Investigator	<i>Using polynomial chaos expansion as surrogate model funded by Ministry of Education, Youth and Sports of Czech Republic under project No. FAST-J8-5309</i>
2018-2020 Co-investigator	<i>Response surface and sensitivity analysis methods in stochastic computational mechanics (RESUS) granted by Czech science foundation under project No. 18-13212S</i>

Selected scientific publications

L. NOVÁK, M. VOŘECHOVSKÝ, V. SADÍLEK, M. D. SHIELDS, Variance-based Adaptive Sequential Sampling for Polynomial Chaos Expansion. *Computer Methods in Applied Mechanics and Engineering*, 2021, vol. 386, 114105. ISSN: 0045-7825.

DOI: 10.1016/j.cma.2021.114105 [IF/AIS: 6.756 (D1)/1.805 (D1)]

L. NOVÁK, D. NOVÁK, Estimation of Coefficient of Variation for Structural Analysis: The Correlation Interval Approach. *Structural Safety*, 2021, vol. 92, 102101. ISSN: 0167-4730.

DOI: 10.1016/j.strusafe.2021.102101 [IF/AIS: 5.047 (Q1)/1.461 (D1)]

L. Pan, **L. NOVÁK**, D. NOVÁK, D. LEHKÝ, M. CAO, Neural Network Ensemble-Based Sensitivity Analysis in Structural Engineering: Comparison of Selected Methods and the Influence of Statistical Correlation. *Computers & Structures*, 2021, vol. 242, 106376. ISSN: 0045-7949.

DOI: 10.1016/j.compstruc.2020.106376 [IF/AIS: 4.578 (Q1)/1.131 (D1)]

O. SLOWIK, D. NOVÁK, **L. NOVÁK**, A. STRAUSS, Stochastic Modelling and Assessment of Long-Span Precast Prestressed Concrete Elements Failing in Shear. *Engineering Structures*, 2021, vol. 228, 111500. ISSN: 0141-0296.

DOI: 10.1016/j.engstruct.2020.111500 [IF/AIS: 4.471 (Q1)/0.927 (Q1)]

L. NOVÁK, D. NOVÁK, On Taylor Series Expansion for Statistical Moments of Functions of Correlated Random Variables †. *Symmetry*, 2020, vol. 12, issue 8, p. 1-14. ISSN: 2073-8994.

DOI: 10.3390/sym12081379 [IF/AIS: 2.645 (Q2)/0.304 (Q3)]

L. NOVÁK, D. NOVÁK, Surrogate Modelling in the Stochastic Analysis of Concrete Girders Failing in Shear. In *Proceedings of the fib Symposium 2019: Concrete - Innovations in Materials, Design and Structures*. International Federation for Structural Concrete, 2019. p. 1741-1747. ISBN: 9782940643004.

L. NOVÁK, D. NOVÁK, R. PUKL, Probabilistic and Semi-Probabilistic Design of Large Concrete Beams Failing in Shear. In *Advances in Engineering Materials, Structures and Systems: Innovations, Mechanics and Applications*. London: Taylor and Francis Group CRC Press, 2019. ISBN: 9781138386969.

L. NOVÁK, D. NOVÁK, Polynomial Chaos Expansion for Surrogate Modelling: Theory and Software, *Beton und Stahlbeton* volume 113, ISSN:1437-1006, Austria, 2018

DOI: 10.1002/best.201800048 [IF/AIS: 0.966 (Q3)/0.179 (Q4)]

L. NOVÁK, D. NOVÁK; O. SLOWIK, Application of Polynomial Chaos Expansion to Reliability Analysis of Prestressed Concrete Roof Girders. In *Proceedings of Engineering Mechanics 2018*, ISBN 978-80-86246-88-8, Svratka, Czech Republic, 2018

L. NOVÁK, M. VOŘECHOVSKÝ, Generalization of Coloring Linear Transformation. In *Proceedings of Modelování v mechanice 2018*, Ostrava, Czech Republic, 2018

L. NOVÁK, L. PAN; O. SLOWIK; D. NOVÁK, Advanced Reliability and Sensitivity Analysis of Prestressed Concrete Girders Failing in Shear. In *Proceedings of fib Ph.D. symposium 2018*, Praha, Czech Republic, 2018

D. NOVÁK; **L. NOVÁK**, O. SLOWIK; A. STRAUSS, Prestressed Concrete Roof Girders: Part III – Semi-Probabilistic Design. In *Proceedings of the Sixth International Symposium on Life-Cycle Civil Engineering (IALCCE 2018)*. London: CRC press, Taylor and Francis group, 2018. ISBN: 9781138626331.

Complete list of author's publications:

<https://www.vutbr.cz/en/people/lukas-novak-154284/publikace>

Practical research

Lukáš Novák is an active member of the practical research team cooperating with several national and international industrial partners. His task is mainly the implementation of developed advanced theoretical methods into software tools for design and the assessment of concrete structures in the following projects:

- 2019-2022
Co-Investigator *Efficient semi-probabilistic methods for design and assessment of structures* funded by Technology agency of the Czech Republic under project No. TH04010138.
- 2019-2021
Co-Investigator *Advanced system for monitoring, diagnosis and reliability assessment of large-scale concrete infrastructures CZ-CHINA DELTA* project funded by Technology agency of the Czech Republic under project No. TF06000016
- 2018-2021
Co-Investigator *INTERREG SAFEBRIDGE project*, awarded by the European Regional Development Fund within the European Union program Interreg Austria–Czech Republic under project No. ATCZ190

Developed software tools

Theoretical methods applied during practical research were implemented into standalone software tools in order to be easily employed in future applications by industrial partners:

PCE-UQ

NOVÁK, L. and NOVÁK D.

<http://www.fce.vutbr.cz/stm/novak.l/pce-uq/pce-uq.html>

Comment: Lukáš Novák was the leading person in research and development of the state-of-the-art advanced software tool based on theory of Polynomial Chaos Expansion for complex reliability analysis. More details about the algorithm can be found in the following journal paper:

L. NOVÁK; D. NOVÁK, Polynomial Chaos Expansion for Surrogate Modelling: Theory and Software, Beton und Stahlbeton volume 113, ISSN:1437-1006, Austria, 2018.

SEMIP

NOVÁK, L. and NOVÁK D.

<https://www.fce.vutbr.cz/STM/novak.l/semip/semip.html>

Comment: Lukáš Novák was the leading person in research and development of the state-of-the-art advanced software tool focused on semi-probabilistic design and assessment of structures. More details about the implemented theoretical methods can be found in the following journal paper:

L. NOVÁK, D. NOVÁK, Estimation of Coefficient of Variation for Structural Analysis: The Correlation Interval Approach. Structural Safety, 2021, vol. 92, 102101. ISSN: 0167-4730.